EUROPEAN SOUTHERN OBSERVATORY

Scientific Report

No. 11 – November 1991

Low Mass Star Formation in Southern Molecular Clouds

Edited by Bo Reipurth

Published by
EUROPEAN SOUTHERN OBSERVATORY
Karl-Schwarzschild-Straße 2, D-8046 Garching bei München
Germany

Low Mass Star Formation in Southern Molecular Clouds

Edited by
Bo Reipurth

ESO Scientific Report No. 11
November 1991

Table of Contents

Low Mass Star Formation in Orion 1
J. Brand and J.G.A. Wouterloot

The Canis Majoris OB1 Association 59
G.H. Herbig

Low Mass Star Formation in Puppis and Vela 69
B. Pettersson

The Chamaeleon Dark Clouds and T–Associations 93
R.D. Schwartz

The Southern Coalsack – Where are all the Young Stars? 119
L.-Å Nyman

The Star Forming Region in Lupus 127
J. Krautter

Young Low Mass Stars in the Norma Cloud 149
B. Reipurth and J.A. Graham

Star Formation in the Ophiuchus Molecular Cloud Complex 159
B.A. Wilking

Star Formation in the Corona Australis Region 185
J.A. Graham

The Serpens Molecular Cloud 197
C. Eiroa

Foreword and Acknowledgements

In July 1989 an ESO Workshop on "Low Mass Star Formation and Pre-Main Sequence Objects" was held in Garching near Munich, Germany. The papers presented were published as ESO Conference and Workshop Proceedings No. 33.

As part of the scientific activities of the workshop, a special poster session was held in which all the major southern star forming regions were described one by one by researchers with extensive experience in each. The purpose of this mini poster session was to attract attention to the richness of the southern star forming regions. Four out of five of the nearest star forming cloud complexes are in the southern sky, and yet, for geographical reasons, most of the observational work on the formation of stars has been performed in the northern sky. With the growth in the number of large southern optical/infrared telescopes and in the sophistication of their instrumentation, and the advent of southern radio telescopes like the Swedish-ESO-Sub-Millimeter Telescope and the Australia Telescope, the situation is fortunately improving. The poster session was well received, and it was decided to compile the information in the form of a small book, thus disseminating it to a larger audience.

The present book is the result of the efforts of the ten colleagues whose collaboration I asked for, and I would like to express to them my sincere thanks for the care and dedication they have put into this project. The book gives an overview of each of the most important southern regions of low mass star formation, and lists extensive references to the literature, with the aim to facilitate and encourage observers to obtain new data and add to our growing understanding of these regions and of the star formation processes in general. While the authors and the editor have gone to great pains to ensure that all important papers up to about mid-1991 are mentioned, the sheer vastness of the literature makes it unavoidable that we have missed some papers. Readers are welcome to send their comments, corrections or additions to either the editor or the individual authors. If we after some years feel that the book has had a useful impact, it is a possibility that we may prepare a later version, updated with the hopefully large amounts of studies which are going to be performed in these southern star forming clouds.

I am grateful to ESO for publishing this work, and to my colleagues who in various ways helped the project, in particular to Doris Leiva, who typed all the manuscripts.

Bo Reipurth

Low Mass Star Formation in Orion

J. Brand[1] and J.G.A. Wouterloot[2]

[1] Osservatorio Astrofisico di Arcetri,
Largo Enrico Fermi 5, I-50125 Firenze, Italy

[2] I. Physikalisches Institut, Universität Köln,
Zülpicker Str. 77, D-5000 Köln 41, Germany

Introduction

This contribution presents an overview of low-mass (i.e. less than several $M_\odot$) star formation in Orion, its accompanying phenomena, and the molecular environment in which it takes place. We tried to collect from the literature all relevant material, and to present it such that it can be used by observers to find their way around in this amazingly rich and very thoroughly studied complex.

We have restricted ourselves to the region between α=5^h24^m and α=5^h56^m, δ=$-11°$ and δ=$+4°$ (1950.0). In this area are located the large molecular complexes consisting of L1640, L1641, L1647, and L1617, L1627, L1630 (L1-62); see figure 1 (taken from Kutner *et al.*, K3-77).

Our literature search encompasses more than 130 years of observational work on Orion. From this, lists were compiled of Hα emission line stars (including T Tauri and Herbig Ae/Be stars), reflection nebulae, Herbig-Haro (HH) objects, molecular outflow-, IR-, and X-ray sources, H_2O masers, and the molecular clouds in which all these objects are embedded. Papers concerning observations of the above mentioned type of objects are included in our search; those that are directly related to observations of the ionized gas, or the exciting stars of the prominent HII regions NGC1976/1977 (Ori A) and NGC2024 (Ori B), or to the dense molecular cloud OMC1, are not. For these, see e.g. Goudis (G1-82) or Genzel and Stutzki (G4-89).

In the following, the information collected from the literature is presented in the form of tables, giving a.o. object identifications, coordinates, and a list of references in which these objects are discussed. The references are coded; note that references to papers published before 1900 are marked with an asterisk. Due to the sheer vastness of the material, no attempt has been made to either provide a historical context or to discuss the data collected here in the sense of reviewing and combining the various parts.

The literature search was carried out by going through all the Astronomy and Astrophysics Abstracts books (1969-1 up to and including 1990-1); for the major journals (AA, ApJ, AJ, MNRAS) the literature is complete up to December 1990. For the period before 1969, the volumes of the Astronomischer Jahresbericht were consulted. Very old references were

selected from cross-references in the papers themselves, and from Müller and Hartwig (M1-18), and Schneller (S1-52, S1-57, and S1-61). An extensive list of literature on variable stars has been prepared by Huth and Wenzel (H1-81).

A large number of papers are on phenomena associated with low-mass star formation in Orion in general, rather than about any specific object. Some of these are broad reviews, others discuss general aspects of HH-objects, young stellar objects, outflows etc., using the Orion region objects as examples. These references are included in our list, but will not always be found in any of the tables. Because these papers are useful, they are mentioned in the text, at the appropriate locations.

With reference to the tables, it is important to realize that not all parts of the region under consideration have been equally thoroughly studied. Most surveys of Hα emission line stars and variable stars, for instance, have concentrated on an area of a size of several square degrees centered on the Trapezium cluster, and not all were carried out to the same limiting magnitude. Likewise, surveys of NIR sources have been limited to small areas near some of the reflection nebulae, to IRAS sources in L1641, and to parts of L1630. Attempts at an unbiased search for Herbig-Haro objects are hampered by the strong optical emission of more extended objects in the region. This means that a statistical study, based on the material gathered here, of the relative frequency of the various types of objects is not a straightforward matter. With regards to the emission line stars, this situation is now improving, with the publication of the large-scale systematic survey being carried out at Kiso Observatory by Wiramihardja and collaborators (K2-89, W2-89, W1-91). The area immediately around the Trapezium cluster remains a problem, however: because of the large number of stars, and the intense nebulosity, distinguishing individual emission line stars is impossible in this type (objective prism) of survey (see also the remarks at the end of section 1).

1. Hα Emission Line Stars

A distinct class of low-mass pre-main sequence stars are the T Tau irregular variables. Apart from variability, one of their characteristics is Hα emission. In fact, searches for T Tau stars are mainly carried out by means of Hα objective prism surveys. If a star with Hα emission is found in a heavily obscured area (such as the Lynds clouds in Orion) it is almost certainly a T Tau star or a related object (Herbig, H2-62). The stars found in this way still have to be studied spectroscopically, in order to rule out the possibility of dMe or Be stars, supergiants, or symbiotic stars. This has to be kept in mind when using Table 1, which lists all Hα emission line stars in Orion, found in the literature (unless we found proof of their definite non-T Tauri nature). The presence of CaII emission, fluorescent FeI emission lines (at 4063, 4132 Å), and strong LiI absorption will confirm the T Tau nature (H2-62).

Surveys of Hα emission line stars have in most cases concentrated on the Trapezium region (in NGC1976 in L1640), and the region around the Horsehead Nebula (in IC434 in L1630). Most stars in the table have been taken from a number of well-known survey papers and

catalogues: Haro (H1-53), Haro and Moreno (H2-53), Herbig (H2-62), Herbig and Kuhi (H1-63), Herbig and Rao (H1-72), Parsamian and Chavira (P2-82), and Herbig and Bell (H1-88). Furthermore, we included stars from three recently published surveys of Orion Hα emission line stars, using the Kiso Schmidt telescope, in Kiso sky areas A-0903 (Kogure *et al.*, K2-89), A-0904 (Wiramihardja *et al.*, W2-89), A-0975, and A-0976 (Wiramihardja *et al.*, W1-91). Strom *et al.* (S7-89) present a list of optical counterparts of IRAS sources in L1641; those that have Hα emission were added to Table 1.

Strom *et al.* (S3-90) have identified optical counterparts to several *Einstein* X-ray sources, and obtained photometry and spectra for many of them. Among the optical candidates they found a number of late-type Hα emission line stars, which are included in Table 1. Finally, the table contains emission line stars found in a survey of a part of L1641 by Wouterloot and Brand (W2-91). In this last work, stellar spectra between 6300Å and 9000Å were obtained on a photographic plate. The ESO 3.6-m telescope was used in combination with the triplet corrector and a 1540Åmm^{-1} red grism. A circular field of diameter $\approx$1° was observed, centered at approximately α=5^{h}34^m, δ=−7°05' (1950.0), in which 112 Hα emission line stars were found, 87 of them new. The strength of the emission ranged from 1 (very weak and to be confirmed) to 4 (strong). Twenty two stars were found that coincided with known Hα emission line stars. Of 27 stars (13 of which newly found), spectra (at 114Åmm^{-1}) were later obtained with the ESO 2.2-m telescope. In a second region, centered at α=5^{h}38^{m}40^s, δ=−9°05' (1950.0; in L1647), three new emission line stars were found (W2-91). Unfortunately, due to bad weather the quality of this plate is not good. In total, W2-91 found 115 emission line stars, of which 90 are new.

Almost all of the surveys mentioned above provide finding charts; Herbig and Bell (H1-88) indicate for each star in their catalogue if and where charts can be found.

Herbig Ae/Be stars are included in Table 1. These stars belong to a class of pre-main sequence stars, originally defined by Herbig (H2-60). Herbig's list of 26 stars was selected following three criteria: the star should have spectral type A or earlier, it should lie in an obscured region, and illuminate a "fairly bright nebula" in its immediate vicinity. More recently Finkenzeller and Mundt (F2-84) have presented a list of 57 (candidate) Herbig Ae/Be stars, three of which (T, BF, and V380 Ori) are within the α, δ boundaries considered here (note that HD37490 (ω Ori) is just outside this region). In addition to these three, there are seven others that have at some point in time been marked as (possible) members of this class: HD37411, HD37357, HD38238, HD37806, Nk81, V350 Ori, and V599 Ori; they are therefore also included in Table 1. Early type emission line stars, that are not identified as Herbig Ae/Be stars were excluded.

Many (especially weak line-) T Tauri stars are sources of X-ray emission (see e.g. the review by Appenzeller and Mundt, A4-89). Most X-ray observations have been made with a relatively low angular resolution, and confusion can occur when identifying a particular star as the origin of the radiation. Where X-ray sources were found to be associated with stars from our list of Hα emission line stars (Table 1), the reference was put in the appropriate column. Some papers give results of X-ray observations of individual objects (e.g. K2-79, P5-

81, K3-82, C1-86, S3-90), but most papers deal with X-ray emission from Orion in general. These are the following: G1-72 M1-72 G2-74 M4-76 W4-77 C4-78 D1-78 F1-78 B3-79 K2-79 C1-81 B6-82 S10-83 G2-85 G1-86 M6-87 C1-89 C1-90.

General references on variable (i.e. RW Aur-type) stars in Orion are: S1-57* B1-67* H1-82* V1-12 V1-19 B1-37 K1-53 P1-53 P2-54 K1-55 K2-59 W1-61 W2-61 G1-63 S1-64 V1-65 M1-69 S2-69 S1-72 M1-73 P1-73 B3-74 W1-74 G1-75 M2-75 S4-75 S5-75 P3-76 R2-77 W3-77 C1-79 Q1-79 Q2-79 S3-79 W2-80 A1-81 I1-81 P1-81 S4-81 S5-81 G1-82 H4-82 I1-82 K4-82 F3-84 H2-85 R6-85 W1-86 A4-89 S3-89 S8-89. The RW Aur-type variable stars include the Orion variables ("In" stars, of which T Tau stars are a subgroup), and rapid irregular variables ("Is").

Aggregates of T Tauri stars are called T-associations. General references on T-associations in Orion are: K1-55 K1-58 K1-59 K2-59 S2-69 D2-75 S3-79 S3-80.

In Table 1 we have not included flare-, flash-, and eruptive variables, *unless* they are specifically known also to be T Tauri - or at least Hα emission line stars. Hundreds of stars are known, which have exhibited a flare-up once or more, but for which nothing is known about their evolutionary status, although it is possible that some fraction of these stars are or have been T Tauri stars. The reference list does however contain the large flare star surveys as 'general references', for those who are interested in cross-checking Table 1 with those lists. References on flare stars: H2-64 H1-66 H1-68 A1-69 A2-69 A3-69 H1-69 H2-69 R2-69 R3-69 R4-69 S1-69 G3-70 S2-71 S5-71 A1-72 K1-72 G2-76 H1-76 P2-76 T1-76 C1-77 C3-78 K1-80 M2-80 N1-80 P1-80 P2-80 M3-81 N1-81 K1-82 E1-85 M5-86 C3-88 M3-88. Further reviews can be found in Gurzadyan (G3-80).

Table 1 is constructed as follows: columns 1 to 7 are reserved for the most used identifications: column 1 has the star number in the catalogues of Haro (H1-53) and Haro and Moreno (H2-53), column 2 lists the number of Parsamian and Chavira (P2-82; PC), column 3 gives the number in the Herbig and Bell - (H1-88; HBC) or the Herbig and Rao catalogue (H1-72; HRC), column 4 the Parenago number (P1-54; P), column 5 the variable star number (V) or name (Kukarkin and collaborators), column 6 the Brun number (B1-34), and in column 7 are listed identifications taken from various other sources (see footnote to Table 1). Columns 8 and 9 give the right ascension and declination for 1950.0. A number of papers give accurate coordinates (e.g. K2-89, S7-89, W2-89, W2-90, W1-91, W2-92). In the older papers, positions are usually given for 1900.0, and often only in decimal time- and arc minutes, but sometimes these are the only coordinates available. They were then precessed by us, and we always give the 1950-coordinates in (arc)seconds. Therefore, not all positions are claimed to have astrometric accuracy. In particular, the coordinates of PC-, Haro4- or Haro5-stars that have no other reference than P2-82, H1-53, or F1-60 can be off by as much as 5 arcmin, and should be treated with caution. In column 10 we give the references for each star. Only references are included that concern observations of the *stars themselves* (and the associated IRAS sources, if any); references on associated phenomena (masers, outflows, reflection nebulae, Herbig-Haro objects) are collected in other tables.

Much work on Hα emission line stars has been carried out by Haro and co-workers at the Tonantzintla and Tacubaya Observatories, and various lists have been prepared by these observers. Many stars therefore have a Tonantzintla number (see e.g. P2-82). The original list of Hα emission line stars in the Orion Trapezium region by Haro (H1-53) contains 255 stars. Parsamian and Chavira (P2-82), in their catalogue of Hα emission line stars in a 5° × 5° region around the Orion Nebula, have continued this numbering system. The original Haro numbering system for stars in the Trapezium region is usually referred to as Haro4-, while the stars in the survey of IC434 (H2-53) have Haro5- (sometimes called HM-) numbers. These prefixes were added by Herbig (H2-62) to distinguish stars in the different Tonantzintla Hα surveys. For the sake of consistency, we have added the prefix "Haro4-" also to all Tonantzintla numbers higher than 255 in the PC-catalogue. Thus, in Table 1, column 1, the stars with numbers 4-1 through 4-255 are the original (H1-53) Haro4-numbers. Note that *flare* stars found at Tonantzintla *also* have Ton-numbers, and individual stars should preferably be identified with one of the other designations, to avoid confusion. For clarity, we here give a list of the various Haro-numbers one may encounter in the literature (see H2-62 and H1-72):

Haro1-: Sco-Oph
Haro2-: Galactic Center
Haro3-: Galactic Center
Haro4-: Orion Nebula
Haro5-: IC434
Haro6-: Tau-Aur-Ori
Haro7-: Unpublished

Some confusion is unavoidable. For example, in the literature we frequently found references to an Hα emission line star Haro2-249, which according to the above, should lie in the Galactic Center region. This star is PC484 = HBC491; according to the finding charts, it is number 249 in Haro (H1-53), and must therefore be Haro4-249.

There are a number of other controversies, where the identifications of a certain star in the different catalogues do not agree:

- In Table 1, we identify WZ Ori with PC110 = Haro4-127 = P1424 = Brun234. These identifications are confirmed in the other catalogues, except in Brun (B1-34) who states that WZ Ori = Brun254. Even though the coordinates of PC110 are more consistent with those of Brun254, the finding charts show that PC110 = Brun234, and we assume Brun has erred in the identification of WZ Ori.
- A similar case is BS Ori: we use PC54 = Haro4-31 = P1204 = Brun104 = BS Ori, which is consistent with the identifications found in other catalogues, except B1-34. Brun has BS Ori = Brun76, although the coordinates of Brun76 differ from those of PC54 by 12sec. The coordinates of Brun104 are the same as those of PC54, and the

finding charts show that PC54 = Haro4-31 = Brun104, so we assumed Brun was in error here (as in fact was also noted by Haro (H1-53)).

- In P2-82 we find PC113 = Haro4-21 = P1435. Haro (H1-53) states that Haro4-21 = Brun222, but Parenago identifies Brun222 with P1415, and P1435 with Brun236. Also in Brück (B1-71) we find Brun222 = P1415 = Haro4-21. Finding charts show, that PC113 = Brun236, and PC113 = Haro4-21, while the coordinates of PC113 are those of P1435. Therefore, PC113 = Brun236 (which is also consistent with the star's magnitude). For a long time we used Haro's identification of Haro4-21 = Brun222, and did not look for Brun236 in those cases where only Brun numbers were given in the literature. Therefore, the references for this entry may be incomplete in Table 1.

- PC475 = V594 Ori (see e.g. A2-72), and *not* V592 Ori, as found in P2-82. In fact, V592 Ori = PC453; in Strom *et al.* (S3-90) the latter two are identified as two separate stars (Xray52c and d, respectively), but in Table 1 we have left them as a single star.

- In Brück (B2-72) we find Haro4-213 = P2388 = PR Ori. While the second part of this identification is correct, the first one is not. Haro4-213 = PC388 = V832 Ori (according to P2-82 and the finding charts), and this star is not in the Parenago catalogue (P1-54). Also, a star cannot have both a V-number and a name. The conclusion is, that Brück has erred with the Haro4-213 = PR Ori identification.

- In Table 1 we use PC233 = Haro4-194 = P1931 = Brun637 = HBC138, and PC234 = Haro4-193. Parenago (P1-54) confirms that P1931 = Brun637 = Bond659 (Bond, B1-67*), while Brun (B1-34) also says that Brun637 = Bond659. However Haro (H1-53) identifies Brun637 with Haro4-193, as does Brück (B2-72) who states that P1931 = Brun637 = Haro4-193. But the finding charts show that PC233 = Haro4-194, and PC234 = Haro4-193. The confusing agent here might have been the coordinates, which in the PC catalogue are identical for PC233 and PC234.

- In Strom *et al.* (S3-90), HBC487 = P2494 is erroneously identified as Brun1009. The correct identification is Brun1069. Likewise, in the same reference, Xray-source 25 should be PC323, instead of PC353. Note, that S3-90 do not consider this star to be a member of the L1641 dark cloud population, on the basis of the weakness of its Li lines.

- For the cross-identification of stars with BD-numbers, we have followed Parenago (P1-54). In two cases, Brun (B1-34) gives different BD-identifications: for Brun312 and Brun430. Also, B1-34 identifies Brun1069 (= P2494) with BD−6 1258, whereas in P1-54 this BD-number is for P2495 (= Brun1068), which is not in our Table 1.

- In the identification of stars in the survey of Kiso field 0976 (Wiramihardja *et al.*, W1-91), a number of errors were found: KiHa76-199 is Haro4-216, not Haro4-21; KiHa76-274 = PC410, but the BF Ori identification is wrong; KiHa76-386 = KiHa4-145, instead of KiHa4-45; KiHa76-401 is not PC517 (in fact, finding charts show that

PC517 = KiHa76-374, which is also found in W1-91); finally, the identification of KiHa76-263 with V380 Ori is correct, according to the coordinates, but W1-91 give a V-magnitude of 15.8 for this star, which seems to be too faint (Herbig and Bell (H1-88) quote a range of 10.0 to 10.5 for V). Wiramihardja *et al.* (W2-89) erroneously identify KiHa4-10 with St48 (S8-86): the confusion perhaps arises because the (1900) coordinates of St48 in S8-86 are approximately equal to the (1950) coordinates of KiHa4-10 in W2-89.

Figures 2 and 3 show the distribution of the stars from Table 1 in L1640/1641/L1647 and L1617/L1627/1630, respectively. The scales of the figures are identical. Next to these figures are reproductions from the POSS E-plates on the same scale. It is striking that, whereas the bulk of the Hα emission line stars in figure 2 are found within the boundaries of L1640/1641, in figure 3 the distribution of the stars is much more even, with only a slight concentration in the L1627/1630 clouds (see also K2-89, W2-89, W1-91). Most of the stars outside the cloud boundaries in figures 2 and 3 are from the Kiso sky survey (K2-89, W2-89, W1-91); no membership information for these stars is available, and it may be that there is a contamination here of background stars.

The region of the most recently formed massive stars, Ori OB1d (see e.g. Warren and Hesser, W2-77) forms part of the Trapezium cluster. Here, the spatial density of newborn stars (age less than 1 x 10^6 years) is about 2200 pc^{-3} (142 stars brighter than $M(I_C)$=+6.0 within a 9 $arcmin^2$ area; Herbig and Terndrup, H5-86), higher than in any known star forming region, and more than an order of magnitude higher than what is derived using the stars in Table 1. Most of these stars are of low mass ($< 1\ M_\odot$), and have not been studied spectroscopically. There are indications that also in other parts of the Orion complex star clusters are being formed (S6-89, L2-90). In reference to the Trapezium region, we note that Haro (H1-53) has remarked that the number of variable stars, possibly with emission characteristics, increases with decreasing distance to the Trapezium cluster, but that close to this cluster no emission lines could be detected (in his survey) due to strong interference of the nebula.

2. Reflection Nebulae

Reflection nebulae are nebulosities associated with stars of type B or later, and we have included all these objects in our search. The largest of these objects are among the first discovered phenomena associated with low-mass star formation; some of them were already found by Messier and the Herschels. The Orion region contains reflection nebulae of sizes ranging from several arcseconds to many arcminutes. They are listed in several catalogues, mainly Bernes (Bs; B1-77), van den Bergh (vdB; V1-66), Cohen (RNO; C4-80), Reipurth (Re; R3-85). These catalogues were not always compiled with the aim to find reflection nebulae and many (red nebulous) objects were later identified as Herbig-Haro objects (see R4-89) or HII regions instead. In addition there are reflection nebulae that contain a radio point source, possibly a compact HII region (e.g. NGC2071, B2-83).

Table 2 presents information concerning the known reflection nebulae. Included in this table are a number of very small, red objects (Re), that upon spectroscopic study could turn out to be HH-objects (Reipurth, personal communication; see also R4-89). Column 1 gives the principal name of the region. Columns 2 and 3 give the coordinates for 1950.0. Column 4 lists other names for the region, as well as the names of star(s) associated with the object. Column 5 gives references to literature about the objects. For convenience, a distinction has been made between references pertaining to optical (including UV), NIR, and FIR work, and observations of the molecular (including NIR H_2 measurements) and atomic constituents (all collected under "mol").

3. Herbig-Haro Objects, Molecular Outflows, and H_2O Masers

In the vicinity of young stars one often observes (bipolar) outflows, that may give rise to manifestations such as Herbig-Haro objects and water vapour masers.

Herbig-Haro objects are 'semi-stellar' patches of nebulosity, that were at one time thought to be either protostellar condensations (e.g. M1-65, H4-69), or reflection nebulae (e.g. S1-74, S2-74, S3-74). The now generally accepted interpretation is, that they are the result of the interaction of high-velocity stellar winds with the ambient molecular gas. The driving sources of the HH-objects are thought to be low- to intermediate mass T Tau-like stars (L1-85), and as such they are manifestations of low-mass star formation.

Typical properties of HH-objects are a rich emission spectrum with only a faint (blue) continuum, a small angular extent and a high radial or tangential velocity. The Orion region may contain two kinds of HH-objects. First, the classical ones such as HH1 and 2, which are related to a newly formed low-mass star. Second, the HH-like objects that are located close to the HII region M42 (e.g. M42-HH3 and M42-HH4). These show a high proper motion, but the place of origin, as traced back from their proper motions, is unclear (W2-88). Ogura and Walsh (O1-91) suggest that M42 HH1,2,5-10 are being excited by IRc2, however.

Catalogues with HH-objects are given by H1-74, and V3-88.

Reviews discussing HH-objects in Orion are: B1-75 B2-78 B3-78 B5-83 C1-83 J2-83 M6-83 S3-83 S4-83 C3-84 C4-84 C1-85 C2-85 M3-85 S4-85 S9-85 R4-87 S8-87 B6-89 R9-89.

L1641 contains the well-known HH-objects HH1,2,3 (H1-51,H1-52,H1-53). Most studies are limited to these objects and several others near M78 (=NGC2068) (HH19-27), that are grouped close together. Recently Reipurth and Graham (R5-88), Reipurth (R4-89, R5-89), Ogura and Walsh (O1-91), and Reipurth and Olberg (R1-91) found, on deep red Schmidt plates, many more HH-objects (HH58-71, HH83-95, HH110-113, HH126-130). A peculiar HH-object (HH131) was found by Ogura (O2-91); it lies *outside* the L1641 cloud, and appears not to be associated with any molecular material. In addition there are some objects that are little studied and can only be called candidate HH-objects (such as GGD- (Gyulbudagian *et al.*, G4-78) and HHL-objects (Gyulbudagian *et al.*, G5-87)). Ishida (I1-90) reports that on

deep red plates, made at Kiso Observatory, 900 candidate HH-objects were found in L1641, and 60 in L1630.

In Table 3 we have assembled information on all HH- (-like) objects in Orion, found in the literature. The format of the table is the same as that of table 2. There are objects, such as NGC1999 that are a reflection nebula, but also contain Herbig-Haro objects (see S9-86) as well as an Hα emission line star (in this case V380 Ori), and therefore for those objects references from Tables 1 and 2 are duplicated in Table 3. Many HH-objects consist of several components. In those cases Table 3 gives the average position. In the case of HH19-27 in NGC2068, the HH-objects are very close together, and are often considered as one group (for instance in molecular studies); the region is then referred to under various names, such as HH19-27, or HH24-26. Because this nomenclature is somewhat arbitrary, we listed references for e.g. HH19-27 only with HH19 and HH27 in Table 3.

HH-objects are possibly related to molecular outflows. Von Hippel *et al.* (V3-88) list some areas where both phenomena are found. The Orion North and South complexes contain 18 CO outflows listed by Fukui (F1-89), and presented here in Table 4. Some of the regions are complex and contain more than one outflow. Morgan and Bally (M1-91) carried out a systematic search for CO emission towards a large number of IRAS sources in L1641, and found lines with "definite wing profile" in 14 cases (7 of them new). This work was followed up by Morgan *et al.* (M2-91), who mapped a number of the sources from M1-91 in CO, and concluded that there are three new outflows in this sample. One of these (IRAS05339−0626) could however be part of L1641-N. On the other hand, no mapping was done of the sources found by Wouterloot *et al* (W4-89), so it is unknown how many of these are true outflows; they were therefore not included in Table 4. Recently a strongly collimated jet was found (in CO) near the center of the Orion Nebula (Schmid-Burgk *et al.*, S1-90), that may be related to the HH-like objects found in this region. Note that the references in Table 4 are only those, which concern observations of the molecular outflow material. Reviews with information on outflow sources in Orion are: S11-83 C3-84 B1-85 L1-85 M3-85 M4-85 S9-85 R3-86 S5-87 S8-87 L1-88.

Searches for (and observations of) H_2O maser emission in Orion have been made by: D1-74 L1-75 S2-75 M3-76 K2-76 C1-78 C2-78 G1-79 R1-80 T1-81 S1-81 L2-82 H2-83 R2-83 S2-85 W4-86 W5-86 Z3-87 G5-87 C4-88 B3-89 B8-89 C5-90. Positions of H_2O masers are given in Table 5. These objects are usually associated with FIR sources. Because of their intrinsic variability, there might be some potential masers that were off at the time they were observed (W5-86). In the table we included only those references that concern H_2O maser observations.

4. IR Sources

The Orion North and South complexes contain a large number of embedded objects which are observable through NIR and FIR measurements. Because the studies are rather incomplete

(especially in sky coverage) and the nature of the sources cannot easily be distinguished in all cases (i.e. not all of these IR sources are necessarily associated with low-mass star formation, or even with the Orion clouds), we do not give positions of all of these sources, but just the individual references (see below). The results of IRAS facilitate a rapid progress in our understanding of these embedded sources, and we list papers based on IRAS results separately. A number of IR sources are optically visible. If they have Hα emission, they are listed in Table 1. For those IR sources associated with reflection nebulae or HH-objects, references are given in tables 2 and 3, respectively. Recently, two series of papers (W5-86, W5-88, W4-89, H1-91 and S5-89, S6-89, S7-89, M4-90, S3-90, M1-91) were published, which together give a good insight in the properties of embedded (IRAS) sources in L1641.

- NIR: M1-69 M2-69 W1-71 A1-73 C1-73 C2-73 C1-74 G1-74 G3-74 S3-74 S6-75 S2-76 R2-77 C3-80 B2-81 M4-81 P1-81 L4-82 T2-82 L2-83 M5-83 S6-83 R1-83 A1-85 C5-85 K2-85 R2-85 S8-85 N1-86 B3-87 C1-87 E2-87 M14-87 T4-87 S5-89 S6-89 S7-89 L2-91
- FIR: E1-75 S2-81 H1-82 C5-84 C6-85 E2-85
- IRAS: B2-86 B3-86 R1-86 T1-86 W3-86 W4-86 W5-86 C5-87 M14-87 P2-87 Z3-87 P1-88 S3-88 S8-88 W3-88 W5-88 B4-89 B8-89 S6-89 S7-89 W4-89 C3-90 M4-90 T1-90 W2-90 H1-91 M1-91

5. Interstellar Medium

Star formation generally takes place in small molecular clumps, that form part of the large molecular complexes. The occurrence of low-mass star formation may be related to the properties of these giant molecular clouds. Observations of this gaseous environment are therefore of great importance. References about the small molecular clouds associated with HH-objects, reflection nebulae and IRAS sources are given in the relevant sections. There are however many papers that are concerned with the large-scale structure and distribution of the molecular and atomic constituents of the Orion region. These papers are also of importance for the understanding of star formation in general.

One can find data on

- HI in: M1-57 M1-58 G2-70 I1-73 C7-89
- CO in: T1-73 M4-75 M5-75 K1-76 K3-77 T1-77 M3-80 T1-82 S3-82 M1-86 M2-86 B1-87 T1-87 B1-89 B2-89 C5-89 C3-90 U1-91
- OH in: G3-76 B1-80 C3-83 J1-86 J5-90
- H_2CO in: D1-73 D1-75 F1-79 C3-83
- CS in: M1-75 L1-89 L1-90 L2-90 L1-91

A discussion of large-scale gas- and gamma ray emission is given by D2-83, B3-84, H3-85, M1-89, and F1-90.

Barnard's Loop, which may affect conditions in the molecular cloud, is discussed in A2-74, I1-78, and R1-78. Early references (photographs) to this emission nebula are found in Barnard (B1-94*), Pickering (P1-89*), Barnard (B1-03), and Roberts (R1-03).

Inside the Orion Nebula, small-scale structure is present (see e.g. B4-83, S6-88, and W2-85). Indications of density fluctuations in the Trapezium region were found by Isobe (I1-80), from observations of interstellar sodium absorption lines, and by Shore (S4-82). Laques and Vidal (L1-79; also V1-82) observed a number of very small (<few arcsec) nebular condensations, which they identify as partially ionized globules. These objects have also been observed with the VLA by Moran *et al.* (M4-82) and by Churchwell *et al.* (C3-87); for those condensations that are associated with stars, the latter authors favour an interpretation as low-mass stars with evaporating proto-stellar disks. Ammonia observations of small clouds of stellar mass in OMC1 are discussed by Matsakis *et al.* (M2-82) and Harris *et al.* (H1-83). Taylor *et al.* (T3-86) observed clumps of high velocity blue-shifted material in the core of the Nebula. Lada (L1-89, L1-90, L2-90, L1-91) discusses the clumpy structure in L1630, based on her CS observations of that cloud.

It is remarkable that the HH-objects in L1641 studied by Reipurth (R4-89) are approximately aligned in the same direction as the filaments found in ^{13}CO by Bally *et al.* (B1-87), which is along the magnetic field lines (see e.g. Vrba *et al.*, V4-88). Relevant references on the magnetic field in Orion in general are V1-69, M2-70, S2-80, T4-86, and H5-87; concerning the magnetic field in L1641 are A2-74 B3-74 H2-82 H3-83 H7-87 S8-88 V4-88 and T3-89; concerning L1630 are V1-76 V1-77 C4-83 and H4-86.

6. OMC2

Moderate-mass (about 2.5 $M_\odot$) star formation is going on in the molecular cloud OMC2, located to the north of M42. Since this region cannot be ascribed to the other categories of objects, and is usually not covered by reviews of OMC1, we give references to this cloud below:

- Mol: G1-74 M1-74 K3-76 M3-76 R1-77 C2-78 H1-79 F1-80 L1-80 S1-81 B3-82 K2-82 B4-83 R2-83 F2-85 B3-89 B4-90
- Radio: W2-74 W1-76
- NIR: G1-74 T2-82 W3-82 P1-86 H2-84 H1-85 R3-89 J6-90
- FIR: H2-76 M1-77 T2-78 M3-90
- Reviews: T2-78 G1-82

7. Request

We would appreciate it, if readers could inform us if they find any object in the tables that ought not to be there, or alternatively if we have not included a particular object or relevant reference from this period in our lists. We also welcome comments the reader may have on possible misidentifications of objects in the tables.

Acknowledgement

This work was in part supported by the Deutsche Forschungsgemeinschaft through grant SFB301. A cunning plan by Baldrick is gratefully acknowledged.

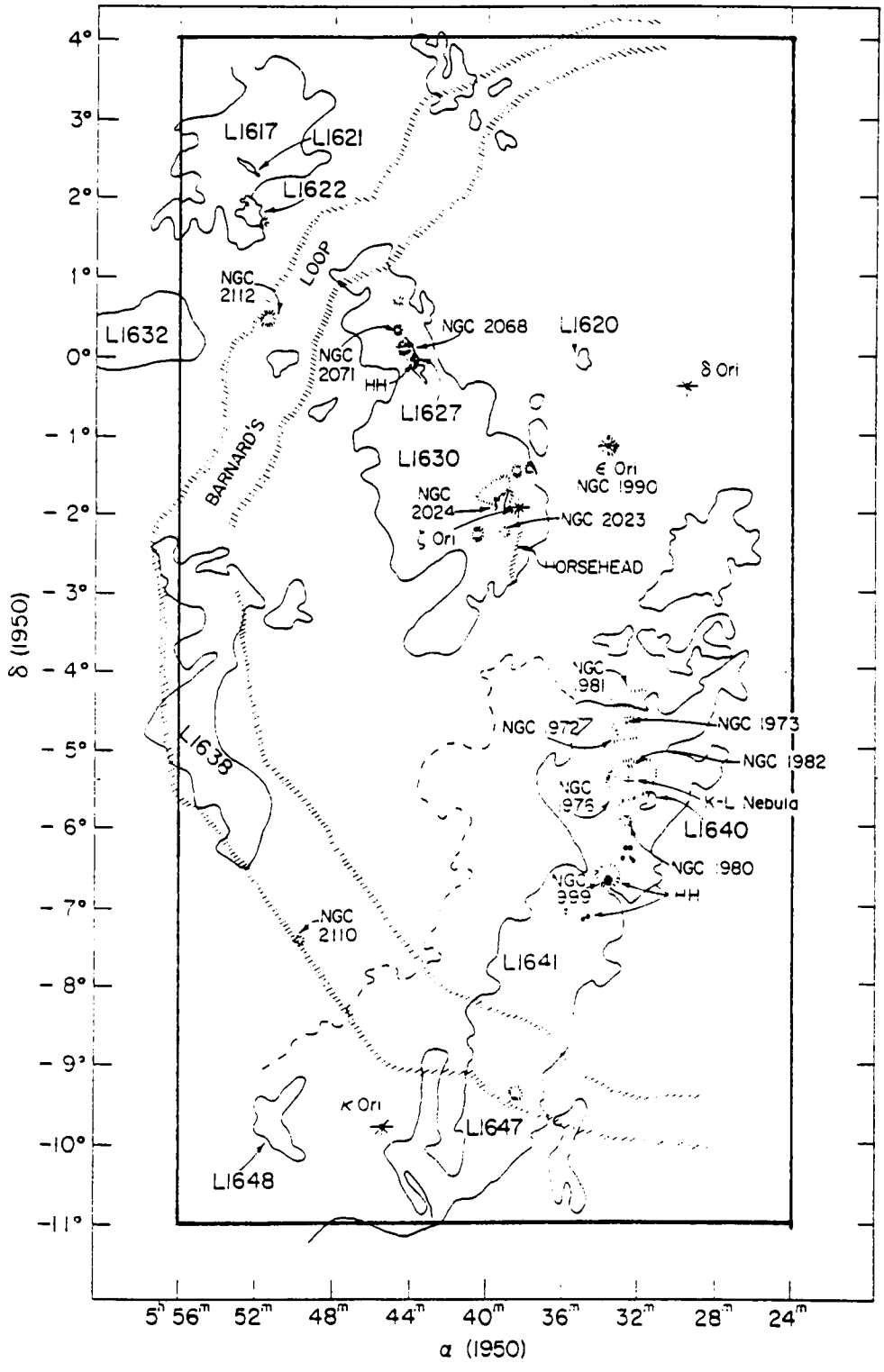

Figure 1. Sketch of the Orion region, showing the outlines of the Lynds clouds in the region (taken from Kutner *et al.*, K3-77). The area of investigation to which we have limited ourselves, is enclosed by the drawn lines.

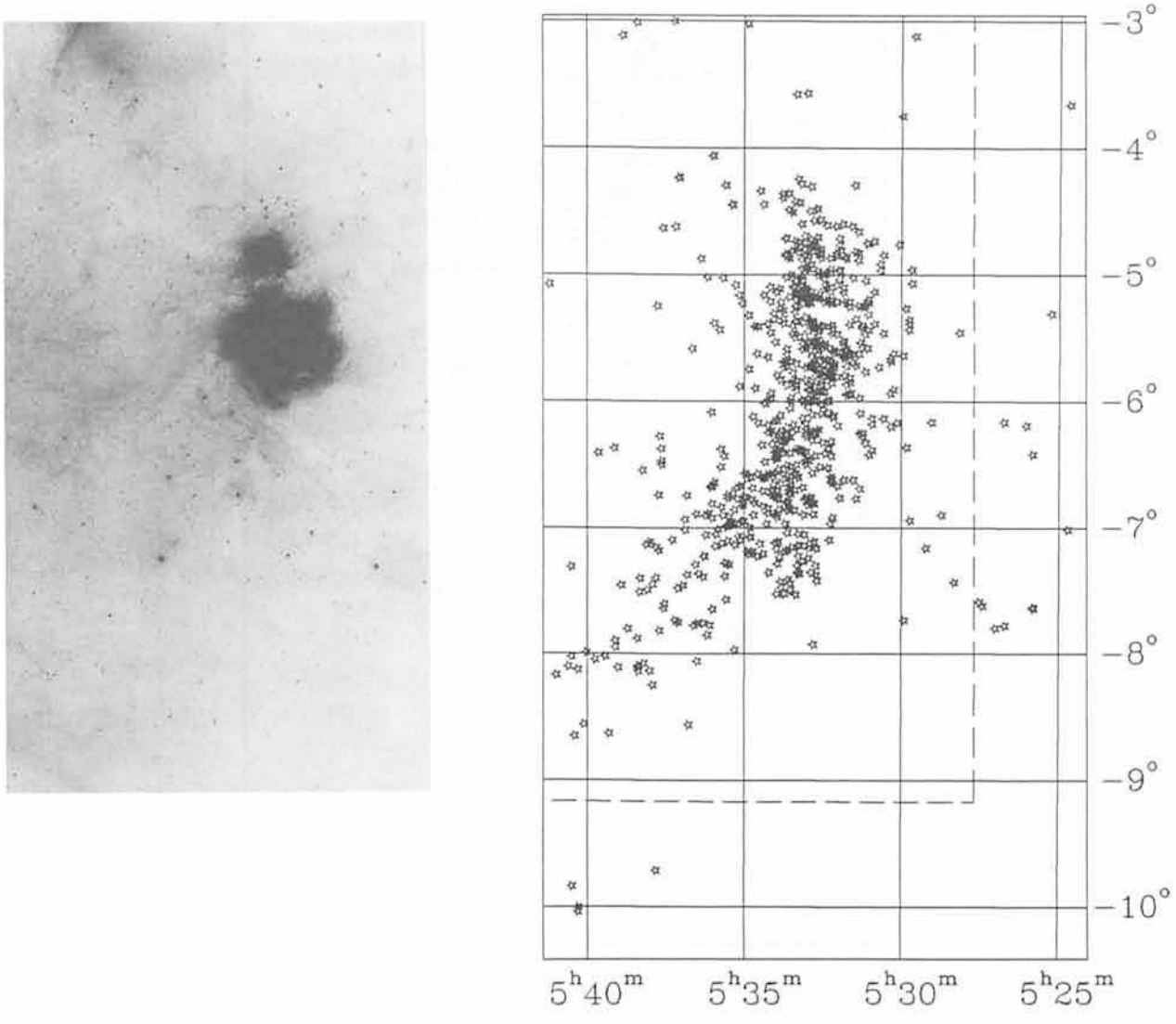

Figure 2. The distribution of the stars from Table 1 in the region of L1640/L1641/L1647, with a reproduction, on the same scale, of the POSS E-plate of the region. The boundaries of the POSS E-print are indicated by the dashed lines in the figure.

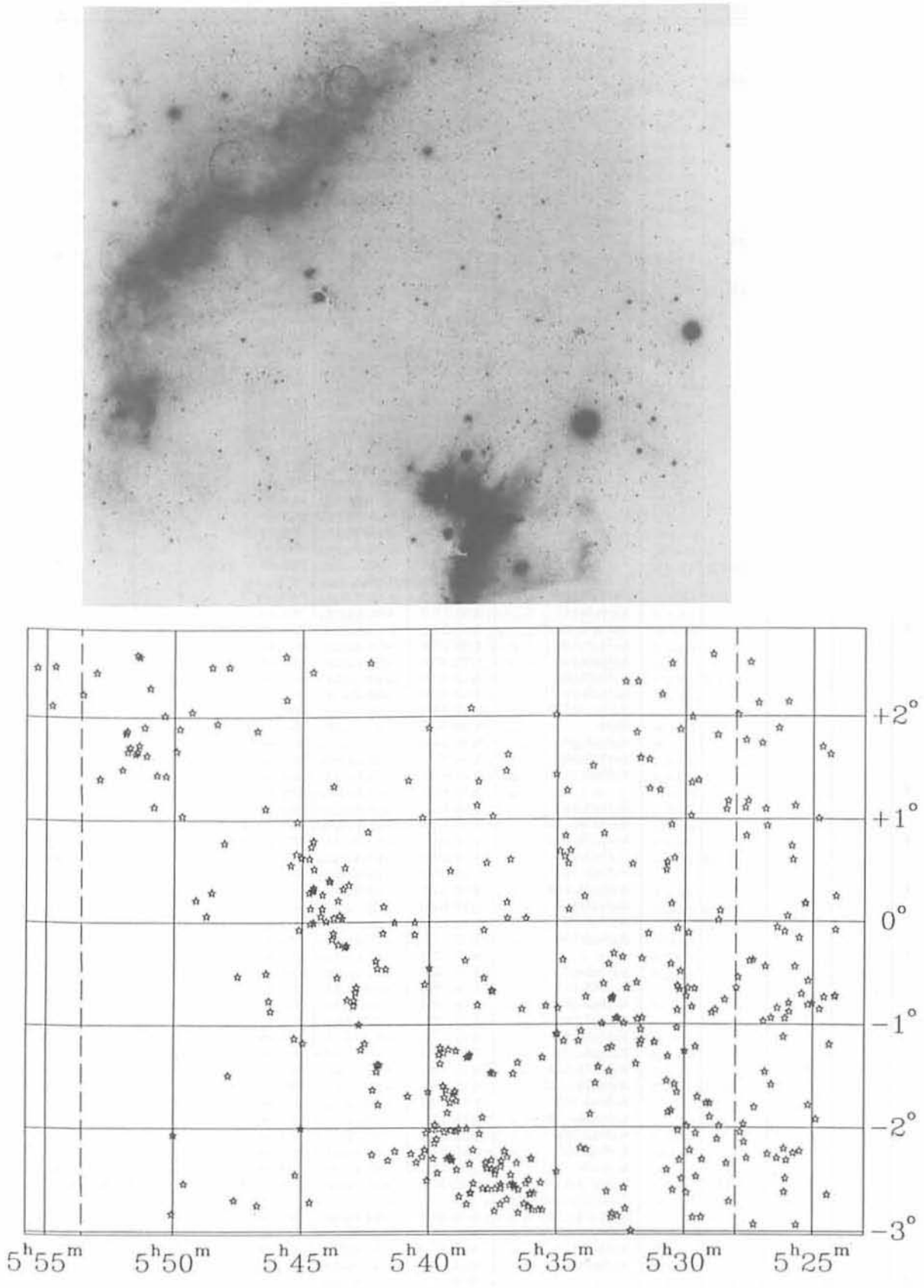

Figure 3. As figure 2, but for the region of L1617/L1627/L1630.

TABLE 1. Hα EMISSION LINE STARS IN ORION.

Haro (1)	PC (2)	HBC (3)	P (4)	Name (5)	Brun (6)	Other (7)	RA (1950) (8)	DEC (1950) (9)	References (10)
						KiHa75-92	5:24: 1.0	−04:54:56	W1-91
						KiHa75-93	5:24: 2.0	−03:25:28	W1-91
						KiHa3-130	5:24: 6.0	+00:14:57	K2-89
						KiHa3-131	5:24: 7.0	−00: 4:46	K2-89
						KiHa3-132	5:24: 8.0	−00:43:24	K2-89
						KiHa3-133	5:24: 9.0	−00:43:40	K2-89
						KiHa75-94	5:24:12.0	−03: 6: 8	W1-91
						KiHa75-95	5:24:14.0	−06:46:22	W1-91
						KiHa3-134	5:24:20.0	+01:37:52	K2-89
						KiHa3-135	5:24:21.0	−01:11:32	K2-89
						KiHa75-96	5:24:21.0	−05:55:32	W1-91
						KiHa3-136	5:24:26.0	−02:38:38	K2-89
						KiHa75-97	5:24:26.0	−06:38: 0	W1-91
						KiHa3-137	5:24:34.0	−00:44: 4	K2-89
						KiHa75-98	5:24:34.0	−02:56:52	W1-91
						KiHa75-99	5:24:35.0	−02:40:37	W1-91
						KiHa75-100	5:24:35.0	−07: 0:45	W1-91
						KiHa3-138	5:24:38.0	+01:42:12	K2-89
						KiHa75-102	5:24:40.0	−07: 4: 2	W1-91
						KiHa75-101	5:24:40.0	−07:51:11	W1-91
						KiHa3-139	5:24:44.0	−00:51: 0	K2-89
4-256	1					KiHa75-103	5:24:45.0	−03:39:30	P2-82 W1-91
4-257	2					KiHa75-104	5:24:46.0	−07: 2:23	P2-82 W1-91
						KiHa3-140	5:24:47.0	+01: 0:21	K2-89
						KiHa3-141	5:24:52.0	−01:55: 0	K2-89
						KiHa75-105	5:24:52.0	−05:20:50	W1-91
						KiHa75-106	5:24:57.0	−03:11: 4	W1-91
						KiHa3-142	5:25: 2.0	−00:47:51	K2-89
						KiHa75-107	5:25: 6.0	−07:20: 1	W1-91
						KiHa3-143	5:25:10.0	−01:46:48	K2-89
						KiHa3-144	5:25:11.0	−00:34:36	K2-89
						KiHa3-145	5:25:11.0	−00:48:30	K2-89
						KiHa75-108	5:25:13.0	−06:54:14	W1-91
						KiHa3-146	5:25:17.0	+00:10:52	K2-89
						KiHa75-110	5:25:18.0	−05:37:15	W1-91
						KiHa75-109	5:25:17.0	−06:27: 6	W1-91
						KiHa3-147	5:25:19.0	+00:10:36	K2-89
4-258	3					KiHa75-111	5:25:21.0	−05:18:58	P2-82 W1-91
						KiHa3-149	5:25:26.0	−00:42:10	K2-89
						KiHa3-148	5:25:30.0	−02:13:34	K2-89
						KiHa3-150	5:25:32.0	−00: 9:28	K2-89
						KiHa3-151	5:25:38.0	−02:56: 4	K2-89
						KiHa75-112	5:25:38.0	−06:17:44	W1-91
						St40	5:25:42.0	+01: 7:50	S8-86 D1-88
						KiHa3-152	5:25:42.0	−00:26:15	K2-89
						KiHa3-153	5:25:45.0	−02:14:40	K2-89
						KiHa3-154	5:25:47.0	+00:36:17	K2-89
4-261	6						5:25:48.7	−07:38:21	P2-82
						KiHa3-155	5:25:50.0	+00:44:22	K2-89
						KiHa75-113	5:25:52.0	−04: 2:32	W1-91
4-260	5					KiHa75-114	5:25:52.0	−07:39:28	P2-82 W1-91
						KiHa3-156	5:25:55.0	−00:52:31	K2-89
						KiHa3-157	5:25:56.0	−00:47:34	K2-89
4-259	4					KiHa75-115	5:25:56.0	−06:28:19	P2-82 W1-91
						KiHa3-158	5:25:58.0	+02: 8:15	K2-89
						KiHa3-159	5:25:59.0	+00: 3:18	K2-89
						KiHa3-160	5:26: 1.0	−02:18:46	K2-89
4-262	7						5:26: 2.4	−06:11:58	P2-82
						KiHa3-161	5:26: 3.0	−02:29:21	K2-89
						KiHa3-162	5:26: 5.0	−00:56:25	K2-89
						KiHa3-163	5:26: 6.0	−00: 5:45	K2-89
						KiHa3-164	5:26: 6.0	−02:37:15	K2-89
						KiHa3-165	5:26: 7.0	−02:12: 9	K2-89
						KiHa3-166	5:26: 8.0	−01: 7:13	K2-89
						KiHa75-116	5:26: 8.0	−03:27:43	W1-91
						KiHa75-117	5:26:18.0	−05:25:57	W1-91
						KiHa3-167	5:26:20.0	+01:53: 4	K2-89
						KiHa75-118	5:26:21.0	−04:48:56	W1-91
						KiHa3-168	5:26:23.0	−00: 3:17	K2-89
						KiHa3-169	5:26:23.0	−00:50:21	K2-89
						KiHa3-170	5:26:23.0	−02:17:39	K2-89
				RX		KiHa75-119 IRAS05264−0608	5:26:27.0	−06: 8:28	P3-04 H1-31 P1-52 P1-54 W1-91
						KiHa75-120	5:26:28.0	−04:53:46	W1-91
						KiHa3-171	5:26:36.0	−01:35: 0	K2-89
						KiHa3-172	5:26:37.0	−00:56:12	K2-89
						KiHa75-122	5:26:39.0	−06:37:52	W1-91
4-263	9						5:26:42.5	−07:47:13	P2-82
		432	P 102			St41, BD−6 1193, IRAS05267−0610	5:26:44.8	−06:10:25	P1-54 B1-67 M1-82 S8-86 D1-88 H1-88 W2-90
						KiHa3-173	5:26:45.0	−02:15:12	K2-89
						KiHa3-174	5:26:47.0	+00:56:11	K2-89
						KiHa3-175	5:26:51.0	+01: 6: 2	K2-89
						KiHa3-177	5:26:51.0	−00:26:16	K2-89
						KiHa3-176	5:26:51.0	−01:27:34	K2-89
						KiHa3-178	5:26:55.0	−00:58: 7	K2-89

TABLE 1. CONTINUED.

Haro	PC	HBC	P	Name	Brun	Other	RA (1950)	DEC (1950)	References
(1)	(2)	(3)	(4)	(5)	(6)	(7)	(8)	(9)	(10)
						KiHa75-123	5:26:58.0	−05:20:20	W1-91
						KiHa3-179	5:26:59.0	+01:44:17	K2-89
						KiHa75-124	5:26:59.0	−07:35: 4	W1-91
4-264	10					KiHa75-125	5:27: 4.0	−07:48:53	P2-82 W1-91
						KiHa75-126	5:27: 7.0	−03:48: 3	W1-91
						KiHa3-180	5:27: 8.0	+02: 7:40	K2-89
						KiHa75-127	5:27:12.0	−04:42:40	W1-91
						KiHa3-181	5:27:16.0	−01:48: 7	K2-89
						KiHa3-182	5:27:17.0	−02:55:49	K2-89
						KiHa3-183	5:27:20.0	−00:22:29	K2-89
						KiHa75-128	5:27:20.0	−06:56:32	W1-91
						KiHa3-184	5:27:27.0	+02:31: 2	K2-89
						KiHa3-185	5:27:28.0	−00:23: 2	K2-89
4-265	11					KiHa75-129	5:27:30.0	−07:39:23	P2-82 W1-91
4-266	12						5:27:30.8	−07:35:58	P2-82
						KiHa3-186	5:27:32.0	+01:10:42	K2-89
						KiHa3-187, KiHa75-130	5:27:34.0	−02:17:37	K2-89 W1-91
						KiHa3-188	5:27:36.0	+00:50:13	K2-89
						KiHa3-189	5:27:37.0	+01:46: 6	K2-89
						KiHa3-190	5:27:39.0	+01: 6:45	K2-89
						KiHa3-191	5:27:40.0	−02: 8:26	K2-89
						KiHa3-192	5:27:41.0	−01:57:57	K2-89
						KiHa75-131	5:27:46.0	−04:44:43	W1-91
						KiHa3-193	5:27:49.0	−02: 2:42	K2-89
						KiHa75-133	5:27:50.0	−02:28:45	W1-91
						KiHa75-132	5:27:50.0	−06: 8:50	W1-91
						KiHa75-134	5:27:54.0	−06:20:32	W1-91
						KiHa3-194	5:27:55.0	−00:32:36	K2-89
						KiHa3-195	5:27:56.0	+02: 0:50	K2-89
						KiHa3-196	5:27:59.0	−00:38:46	K2-89
						KiHa75-135	5:28: 8.0	−04:10:58	W1-91
						KiHa75-136	5:28:10.0	−05: 6:49	W1-91
	13			V538		KiHa75-137, KiHa76-1	5:28:11.0	−05:27:57	R1-62? P2-82 G1-85 W1-91
						KiHa75-138	5:28:14.0	−06:55:47	W1-91
						KiHa3-197	5:28:15.0	−02:42:38	K2-89
						KiHa75-139	5:28:15.0	−06:36:46	W1-91
						KiHa3-198	5:28:19.0	+01:10:34	K2-89
						KiHa3-199	5:28:21.0	−02:20:38	K2-89
4-267	14					KiHa75-140	5:28:21.0	−07:27:11	P2-82 W1-91
						KiHa3-200	5:28:23.0	+01: 5:46	K2-89
						KiHa3-201	5:28:26.0	−00:45:35	K2-89
						KiHa76-2	5:28:33.0	−05:44:20	W1-91
						KiHa76-3	5:28:35.0	−06:35:56	W1-91
						KiHa3-203	5:28:37.0	+00: 6:24	K2-89
						KiHa3-204	5:28:38.0	−01:58:59	K2-89
						KiHa75-141	5:28:38.0	−03:46:25	W1-91
						KiHa3-205	5:28:41.0	+00: 0:51	K2-89
						KiHa3-206	5:28:43.0	−02: 6:37	K2-89
4-268	15						5:28:43.0	−06:54:27	P2-82
4-269	16					KiHa75-142, KiHa76-4	5:28:43.0	−06:54:27	P2-82 W1-91
						KiHa3-207	5:28:44.0	+01:49: 0	K2-89
						KiHa4-1, KiHa3-208	5:28:47.8	−00:51:31	K2-89 W2-89
						KiHa75-143	5:28:54.0	−07:32:51	W1-91
						KiHa3-209	5:28:55.0	+02:35:25	K2-89
						KiHa3-210, IRAS05290−0053?	5:28:56.0	−00:53:12	K2-89
						KiHa75-145, IRAS05289−0430	5:28:58.0	−04:30: 9	W1-91
						KiHa75-144	5:28:58.0	−05: 7:25	W1-91
						KiHa3-211	5:29: 0.0	−01:53:40	K2-89
						KiHa3-212	5:29: 1.0	−01:45:46	K2-89
4-270	17					KiHa75-146, KiHa76-5	5:29: 4.0	−06:10:51	P2-82 G1-85 W1-91
						KiHa75-147	5:29: 5.0	−04:30: 4	W1-91
						KiHa3-213	5:29: 8.0	−01:45:44	K2-89
						KiHa76-6	5:29: 8.0	−06:22:12	W1-91
4-271	18						5:29:13.3	−07:10:17	P2-82
						KiHa3-214	5:29:18.0	−02:18:30	K2-89
						KiHa75-148	5:29:18.0	−02:49:58	W1-91
						KiHa3-215	5:29:20.0	−02:51:46	K2-89
						KiHa76-7	5:29:28.0	−02:49:24	W1-91
						KiHa76-9	5:29:28.0	−04: 8:43	W1-91
						KiHa76-8	5:29:28.0	−04:29: 0	W1-91
5-63						KiHa4-2, KiHa3-216	5:29:28.5	−01:42:19	H2-53 F1-60 G1-65 K2-89 W2-89
						KiHa3-217	5:29:29.0	+01:22:30	K2-89
						KiHa3-218	5:29:32.0	−02:28:23	K2-89
						KiHa3-219	5:29:33.0	−02: 3:24	K2-89
5-64						KiHa4-3, KiHa3-220	5:29:34.0	−01:13: 8	H2-53 F1-58 K1-59 F1-60 G1-65 K2-89 W2-89
	20	97				San1, KiHa75-149	5:29:34.4	−03: 7:38	S1-71 H1-72 C1-74 C2-79 M4-80 B10-82 P2-82 H2-86 H1-88 W1-91
						KiHa3-221	5:29:37.0	−00:39:20	K2-89

TABLE 1. CONTINUED.

Haro	PC	HBC	P	Name	Brun	Other	RA (1950)	DEC (1950)	References
(1)	(2)	(3)	(4)	(5)	(6)	(7)	(8)	(9)	(10)
						KiHa75-150	5:29:37.0	−06:52:11	W1-91
						KiHa76-10	5:29:38.0	−04:58:15	W1-91
						KiHa75-151	5:29:38.0	−07:31:26	W1-91
						KiHa75-152	5:29:39.0	−02:34:41	W1-91
5-82		436		RY		IRAS05296−0251	5:29:39.6	−02:51:56	P3-04 W1-06 G1-14 M1-29 H1-31 C1-38 H1-49 K1-50 H3-52 P2-52 H2-53 S1-53 F1-58 K1-59 F1-60 G1-65 C1-73 C3-73 G3-74 H1-88 W2-90
4-272	19			V695			5:29:39.8	−04:58: 7	P2-82
4-273	21		P 847	HP		KiHa75-153, KiHa76-11	5:29:41.0	−05: 4:38	P1-52 P1-54 K1-59 R1-62 M2-81 P2-82 M4-83 C1-86 M4-88 W1-91
4-277	25			V540		KiHa75-154, KiHa76-12	5:29:42.0	−06:57:44	R1-62? P2-82 G1-85 W1-91
						KiHa3-222	5:29:43.0	−00:49:50	K2-89
4-274	22					KiHa75-156, KiHa76-14	5:29:43.0	−05:21:42	P2-82 G1-85 W1-91
						KiHa75-155, KiHa76-13	5:29:43.0	−05:24:12	W1-91
						KiHa3-223	5:29:44.0	+01:59:23	K2-89
						KiHa76-15	5:29:44.0	−05:39:53	W1-91
						KiHa3-224	5:29:45.0	+01:21:10	K2-89
4-275	23						5:29:45.3	−05:23:50	P2-82
4-276	24						5:29:45.3	−05:26:38	P2-82 G1-85
						KiHa3-225	5:29:47.0	+01: 1:55	K2-89
						KiHa3-226	5:29:47.0	−02:13:13	K2-89
						KiHa75-157, KiHa76-16	5:29:48.0	−05:37: 7	W1-91
						KiHa76-17	5:29:48.0	−06: 3: 9	W1-91
4-278	26					KiHa75-158, KiHa76-18	5:29:48.0	−06:23: 1	P2-82 G1-85 W1-91
						KiHa3-227	5:29:51.0	−00: 6:42	K2-89
4-279	27					KiHa76-19	5:29:51.0	−05:15:43	P2-82 W1-91
4-282	30					KiHa75-159, KiHa76-20	5:29:52.0	−05:39: 0	P2-82 G1-85 W1-91
						KiHa4-4, KiHa3-228	5:29:52.6	−00:38:59	K2-89 W2-89
						KiHa3-229	5:29:54.0	−01:59:16	K2-89
5-65							5:29:55.0	−01:59: 2	H2-53 K1-59 F1-60 G1-65
						KiHa3-230	5:29:55.0	−02:37:44	K2-89
						KiHa3-231	5:29:56.0	−00:43:45	K2-89
4-280	28					KiHa75-161, KiHa76-22	5:29:56.0	−03:45:19	P2-82 W1-91
						KiHa76-21	5:29:56.0	−05: 0:28	W1-91
						KiHa75-160	5:29:56.0	−05: 7:29	W1-91
						KiHa75-162	5:29:58.0	−06:30:13	W1-91
5-66				V462		KiHa4-5, KiHa3-232	5:30: 0.0	−01:15:52	H2-53 F1-58 K1-59 F1-60 G1-65 K2-89 W2-89
4-281	29					KiHa75-163	5:30: 0.0	−07:42:56	P2-82 W1-91
						KiHa75-164	5:30: 1.0	−06:36:25	W1-91
4-283	31						5:30: 4.1	−04:46:15	P2-82 G1-85
						KiHa3-233	5:30: 6.0	−02:29:37	K2-89
4-284	32					KiHa75-165	5:30: 6.0	−06:10:59	P2-82 W1-91
						KiHa76-23	5:30: 9.0	−03:31:56	W1-91
						KiHa75-166	5:30:10.0	−03:55:46	W1-91
						SS2-28	5:30:10.4	−00:29:20	S2-77
						KiHa4-6, KiHa3-234	5:30:10.5	−00:29:20	K2-89 W2-89
						KiHa3-235	5:30:11.0	−02:18:57	K2-89
						KiHa76-24	5:30:11.0	−05:53:52	W1-91
						KiHa3-236	5:30:12.0	+01:52: 2	K2-89
						KiHa3-237	5:30:12.0	−00:39:53	K2-89
						KiHa3-238	5:30:15.0	−02: 1:44	K2-89
						KiHa75-167	5:30:15.0	−03:50:45	W1-91
4-145	33					KiHa75-168, KiHa76-25, IRAS05302−0537	5:30:16.0	−05:38: 2	H1-53 K1-59 A2-72 G1-76 P2-82 B3-89 H1-91 W1-91
						KiHa4-7	5:30:16.7	−00: 4: 0	W2-89
						KiHa3-240	5:30:17.0	−00:37:47	K2-89
						KiHa3-239	5:30:17.0	−00:51:48	K2-89
						KiHa75-169	5:30:17.0	−06:35:21	W1-91
						KiHa4-8	5:30:17.4	−01:39:30	W2-89
						KiHa3-241	5:30:18.0	−01: 2:11	K2-89
4-286	35					KiHa75-171, KiHa76-27	5:30:18.0	−05:40:19	P2-82 G1-85 W1-91
4-285	34					KiHa75-170, KiHa76-26	5:30:18.0	−05:55:28	P2-82 W1-91
						KiHa76-28	5:30:20.0	−04:43:49	W1-91
4-155	36		P1009	UZ	16	KiHa76-29	5:30:20.0	−05:41:46	P2-04 H1-23 B1-34 P1-52 H1-53 P1-54 K1-59 R1-62 B2-72 G1-76 P2-82 M2-83 P1-85 W1-91
						KiHa75-172	5:30:20.0	−07:17:22	W1-91
4-287	37						5:30:20.4	−06:12:40	P2-82 G1-85
						KiHa4-9	5:30:23.4	−01:34:54	W2-89
						KiHa76-30	5:30:24.0	−05:46:14	W1-91
						KiHa3-242	5:30:25.0	+00:37:13	K2-89
						KiHa75-174	5:30:25.0	−03:31:51	W1-91
4-288	38		P1041		22	KiHa75-173, KiHa76-31	5:30:25.0	−05:57: 6	B1-34 P1-54 A1-74 P2-82 M2-83 G1-85 W1-91
5-81							5:30:27.0	−02:36:10	H2-53 K1-59 F1-60 G1-65

TABLE 1. CONTINUED.

Haro	PC	HBC	P	Name	Brun	Other	RA (1950)	DEC (1950)	References
(1)	(2)	(3)	(4)	(5)	(6)	(7)	(8)	(9)	(10)
						KiHa4-10	5:30:27.6	−00:38:24	W2-89
						KiHa3-243	5:30:31.0	−01:50: 9	K2-89
						KiHa75-175	5:30:31.0	−06: 4:47	W1-91
						KiHa4-11	5:30:31.6	+00:10:25	W2-89
						KiHa3-244	5:30:32.0	+02:30: 8	K2-89
						KiHa4-12	5:30:32.2	+00:56:35	W2-89
						KiHa4-13, KiHa3-245	5:30:33.1	−00:24:58	K2-89 W2-89
4-46	39	98	P1066	HS		KiHa75-176, KiHa76-32	5:30:34.0	−04:51:17	P1-52 H1-53 P1-54 H2-55 K1-59 R1-62 W1-63 W1-66 H1-72 W1-72 G1-76 C2-79 C2-80 T1-81 P2-82 M2-83 H1-88 W1-91
		99	P1072	HT	39		5:30:34.3	−06: 8:53	B1-34 P1-52 P1-54 K1-59 R1-62 B1-67 W1-69 S3-71 H1-72 A1-74 O1-77 K1-78 C2-79 M2-83 W1-83 Y1-88 M3-89
4-124	40	100	P1076	V466	42	KiHa75-177, KiHa76-33	5:30:34.8	−05:28:29	B1-34 H1-53 P1-54 K1-57 K1-59 H2-62 F1-70 B1-71 S3-71 H1-72 A1-74 B2-76 G1-76 B4-77 K1-78 C2-79 M4-80 P2-82 M2-83 S7-83 H2-86 H1-88 M3-89 W1-91
						KiHa75-178	5:30:36.0	−05: 1:48	W1-91
						KiHa3-247	5:30:38.0	−01:51:12	K2-89
						KiHa3-248	5:30:39.0	−01:18:42	K2-89
4-290	42						5:30:39.8	−04:58:29	P2-82 G1-85
4-289	41						5:30:39.9	−04:55:35	P2-82 G1-85
						KiHa75-179	5:30:40.0	−03:19:29	W1-91
						KiHa3-249	5:30:41.0	−02:24:31	K2-89
						KiHa4-14	5:30:41.9	−01:33: 4	W2-89
						KiHa4-15	5:30:42.4	+00:34:48	W2-89
						KiHa75-181	5:30:43.0	−06: 9:31	W1-91
4-168	43	101		V384		Ton5?, KiHa76-34	5:30:43.4	−05:44:27	H1-53 H2-54 H1-55 R1-56 P1-58 K1-59 H1-62 R1-62 B2-72 H1-72 G1-76 C2-79 A1-81 P2-82 H1-88 W1-91
						KiHa3-250	5:30:44.0	+00:30:20	K2-89
						KiHa76-35	5:30:49.0	−04:24:47	W1-91
	45			V394			5:30:51.6	−05: 8:36	R1-56 P1-58 K1-59 R1-62 P2-82
						KiHa76-36	5:30:52.0	−06:52:17	W1-91
4-291	44						5:30:52.1	−04:44:48	P2-82 G1-85
						KiHa76-37	5:30:53.0	−07: 3:57	W1-91
4-116	46		P1157	VW	82	KiHa76-38	5:30:54.0	−05:23:37	P2-04 H1-23 B1-34 H1-50 P1-52 H1-53 P1-54 K1-59 G1-76 P2-82 M2-83 W1-91
						KiHa76-39	5:30:55.0	−05:34:35	W1-91
						KiHa4-16	5:30:55.2	+02:12:14	W2-89
4-292	47						5:30:56.4	−06:11:31	P2-82 G1-85
4-293	50						5:30:56.4	−06:11:31	P2-82
4-223	48			V542		KiHa76-40	5:30:57.0	−06:24:52	H1-53 P2-82 W1-91
						KiHa75-182	5:30:59.0	−04:39: 3	W1-91
						KiHa3-252	5:31: 0.0	+01:16:54	K2-89
4-108	51		P1190	V719	97	KiHa76-42, IRAS05310−0518	5:31: 1.0	−05:19:28	B1-34 H1-53 P1-54 K1-59 B2-72 A1-74 G1-76 P2-82 M2-83 W1-91
4-202	49					KiHa76-41	5:31: 1.0	−06: 9: 3	H1-53 G1-76 P2-82 W1-91
						KiHa76-43	5:31: 2.0	−05:29:36	W1-91
4-295	58						5:31: 2.1	−06:26:13	P2-82 G1-85
4-294	57						5:31: 3.5	−05:12:19	P2-82 G1-85
4-122	52					KiHa76-44	5:31: 4.0	−05:27:23	H1-53 B2-72 G1-76 P2-82 W1-91
4-31	54		P1204	BS	104	KiHa75-184, KiHa76-47	5:31: 4.1	−04:46:18	P2-04 S2-24 B1-34 H1-50 P1-52 H1-53 P1-54 R1-56 K1-59 B1-63 B1-71 A1-74 G1-76 P2-82 M2-83 W1-91
4-97	55		P1206	RZ	109	KiHa76-45	5:31: 5.0	−05:13:58	W1-03 P2-04 H1-23 S2-24 B1-34 H1-50 P1-52 H1-53 P1-54 K1-59 G1-76 P2-82 W1-91
4-136	56	102	P1207		108		5:31: 5.0	−05:35:34	B1-34 H1-53 P1-54 K1-57 K1-59 B1-71 A2-72 H1-72 A1-74 D1-75 G1-76 C2-79 P2-82 M2-83 H1-88 M3-89
		437	P1207/c				5:31: 5.0	−05:35:34	C2-79 H1-88
4-30	53	103	P1203	VX	106	KiHa75-183, KiHa76-46	5:31: 5.9	−04:45:47	P2-04 H1-23 S2-24 B1-34 H1-50 P1-52 H1-53 P1-54 H2-55 R1-56 R1-62 W1-66 B1-71 H1-72 W1-72 G1-76 C2-79 A1-81 P2-82 M2-83 H1-88 W1-91
						KiHa75-185	5:31: 7.0	−04:14:23	W1-91
4-217	61		P1221	SS		KiHa76-48	5:31: 7.0	−06:21:36	P2-04 H1-23 P1-52 H1-53 P1-54 R1-62 G1-76 P2-82 M2-83 W1-91
4-71	59	104	P1218	VY	112	KiHa76-50	5:31: 8.0	−05: 3:33	P2-04 H1-23 S2-24 B1-34 P1-52 H1-53 P1-54 H2-55 B1-57 R1-62 W1-63 K2-64 W1-66 W1-69 B1-71 S3-71 A2-72 B1-72 H1-72 W1-72 A1-74 K2-75 G1-76 C2-79 T1-81 P2-82 M2-83 H1-88 K3-88 W1-91
						KiHa76-49	5:31: 8.0	−06:49:33	W1-91
4-296	60						5:31: 8.9	−05:46:44	P2-82 G1-85
		438	P1229	HU	119		5:31: 9.9	−05:28:54	B1-34 P1-52 P1-54 F1-70 S3-71 A1-74 K2-79 A1-81 M2-83 S7-83 C1-86 H1-88 M3-89
						St42	5:31:10.0	−01:10:30	S8-86 D1-88
5-67		105				San2, KiHa4-17	5:31:11.0	−01:10:25	H2-53 F1-60 G1-65 S1-71 H1-72 C1-74 C2-79 M4-80 H1-88 W2-89
4-98	62					KiHa76-51	5:31:11.0	−05:15:14	H1-53 K1-59 A2-72 G1-76 P2-82 W1-91
4-121	63					KiHa76-52	5:31:14.0	−05:26: 5	H1-53 K1-59 A2-72 G1-76 P2-82 W1-91
4-297	65						5:31:14.3	−06:15:50	P2-82 G1-85
4-298	66						5:31:14.3	−06:17:38	P2-82
	64			V726			5:31:15.1	−05:35: 8	P2-82
4-101	67		P1254	V729	133	KiHa76-53	5:31:17.0	−05:16:10	B1-34 H1-53 P1-54 K1-57 K1-59 S3-71 B2-72

TABLE 1. CONTINUED.

Haro (1)	PC (2)	HBC (3)	P (4)	Name (5)	Brun (6)	Other (7)	RA (1950) (8)	DEC (1950) (9)	References (10)
4-101									A1-74 G1-76 P2-82 M2-83 W1-91
		107		V386		Ton7?	5:31:17.6	−05:33: 8	H2-54 H1-55 R1-56 P1-58 K1-59 H1-62 R1-62 H1-72 D1-75 C2-79 A1-81 C1-86 H1-88
4-131	69	106	P1260	VZ	136	KiHa76-54	5:31:18.0	−05:32:50	P1-95* P2-04 H1-23 B1-34 R1-46 H1-50 P1-52 H1-53 P1-54 R1-56 H2-62 B1-71 S3-71 H1-72 A1-74 D1-75 G1-76 C2-79 M4-80 P2-82 J1-83 M2-83 C1-86 H1-88 W1-91
						KiHa76-55	5:31:18.0	−05:38:31	W1-91
4-201	71	108	P1267	V1006	134	KiHa76-56	5:31:18.8	−06: 6:25	B1-34 H1-53 P1-54 H2-55 W1-63 W1-66 W1-69 B1-71 B1-72 H1-72 W1-72 A1-74 G1-76 C2-79 A1-81 P2-82 M2-83 H1-88 W1-91
4-118	68					KiHa76-57	5:31:19.0	−05:25:26	H1-53 P2-82 W1-91
4-238	76		P1277	ST		KiHa76-58	5:31:19.0	−06:42:35	P2-04 H1-23 H1-50 P1-52 H1-53 P1-54 R1-62 G1-76 P2-82 M2-83 W1-91
	74	109	P1270		141	KiHa76-60	5:31:19.7	−05:59:13	B1-34 P1-54 H2-62 W1-69 F1-70 B1-71 B1-72 H1-72 A1-74 M2-76 K1-78 C2-79 M4-80 P2-82 M2-83 C1-86 H2-86 H1-88 Y1-88 M3-89 W1-91
4-48	70			V731		KiHa76-59	5:31:20.0	−04:54: 8	H1-53 K1-59 B1-63 B2-72 G1-76 P2-82 W1-91
4-99	73					KiHa76-61	5:31:20.0	−05:15:25	H1-53 G1-76 P2-82 W1-91
4-299	72			V545			5:31:20.3	−06:15:56	R1-62? P2-82
4-39	77						5:31:22.0	−04:50:20	H1-53 K1-59 G1-76 P2-82
4-300	78		P1283	V354		KiHa76-63	5:31:22.0	−05:38:22	R1-46 P1-52 P1-54 R1-56 K1-59 P2-82 G1-85 W1-91
4-18	75		P1272	HX	140	KiHa75-186, KiHa76-62	5:31:22.2	−04:40:26	B1-34 P1-52 H1-53 P1-54 R1-56 K1-59 R1-62 B1-71 S3-71 A1-74 G1-76 P2-82 M2-83 W1-91
						KiHa76-64	5:31:23.0	−04:50:21	W1-91
						KiHa3-253	5:31:24.0	+01:17:40	K2-89
						KiHa76-65	5:31:24.0	−06:23:30	W1-91
						St43	5:31:25.0	+01:34:43	S8-86 D1-88
4-159	81		P1296	HY	160	KiHa76-66	5:31:25.0	−05:43:49	B1-34 R1-46 P1-52 H1-53 P1-54 R1-56 K1-59 B1-71 S3-71 A2-72 A1-74 G1-76 P2-82 M2-83 W1-91
4-3	79		P1292		150	KiHa75-187, KiHa76-67	5:31:26.0	−04:18:25	B1-34 H1-53 P1-54 B1-71 A1-74 G1-76 T1-80 P2-82 M2-83 C1-86 W1-91
						KiHa4-18	5:31:26.1	−00: 7: 6	W2-89
			P1309				5:31:26.7	−06:46:46	P1-54 S3-90
4-112	80		P1294	V468	154		5:31:27.4	−05:21:39	B1-34 H1-53 P1-54 K1-57 K1-59 S3-71 A2-72 B2-72 A1-74 G1-76 P2-82 M2-83 P1-85
4-34	82	110	P1301	SU	156		5:31:27.7	−04:49:49	W1-03 P2-04 H1-23 S2-24 B1-34 H1-50 P1-52 H1-53 P1-54 H2-55 R1-56 K1-59 H2-62 W1-63 W2-69 H1-72 W1-72 G1-76 A1-77 M4-77 C2-79 M4-80 T1-81 P2-82 M2-83 P1-85 H1-88
4-301	83					KiHa76-68	5:31:30.0	−05:42: 5	P2-82 G1-85 W1-91
4-302	84		P1323	SV			5:31:31.9	−06:38: 3	P2-04 H1-23 P1-52 P1-54 K1-59 R1-62 H1-69 P2-82 M2-83 G1-85 P1-85 C3-88
		439	P1319		166		5:31:32.0	−05: 2: 3	B1-34 P1-54 W1-69 B1-72 A1-74 A1-81 M2-83 S7-83 W1-83 C1-86 H1-88 M3-89 W1-90
4-303	87		P1333	II			5:31:33.0	−05:38:15	P1-52 P1-54 R1-56 K1-59 R1-69 R3-69 R4-69 S3-71 A1-74 P2-82 G1-85 P1-85 A1-88
						KiHa76-69	5:31:34.0	−02:54: 4	W1-91
4-15	85						5:31:34.2	−04:37:51	H1-53 G1-76 P2-82
4-14	86					KiHa75-188, KiHa76-70	5:31:35.0	−04:38: 4	H1-53 H2-55 K1-59 G1-76 P2-82 W1-91
4-148	88		P1341	WW	178	KiHa76-71	5:31:36.0	−05:38:56	P1-95* P2-04 H1-23 B1-34 R1-46 H1-50 P1-52 H1-53 P1-54 R1-56 B1-71 S3-71 G1-76 P2-82 M2-83 P1-85 C1-86 A1-88 W1-91
		440	P1347		179		5:31:36.4	−05:56:53	B1-34 P1-54 W1-69 M2-83 W1-83 H1-88
4-304	89						5:31:38.8	−05:49:40	P2-82 G1-85
4-305	90						5:31:38.8	−05:51:52	P2-82 G1-85
4-117	92						5:31:39.3	−05:24:16	H1-53 P2-82
4-100	91	111	P1352	WX	189	KiHa76-72	5:31:39.7	−05:15:44	P1-95* P2-04 H1-23 S1-24 B1-34 R1-46 P1-52 H1-53 P1-54 R1-56 H2-62 R1-62 K1-59 M1-66 M1-68 B1-71 S3-71 H1-72 C2-79 P2-82 M2-83 S7-83 H1-88 W1-91
		441				WX/c	5:31:39.7	−05:15:44	P1-54 C2-79 H1-88
5-69							5:31:40.0	−00:56:27	H2-53 K1-59 F1-60 G1-65
4-95	93		P1362		185	KiHa76-73	5:31:40.0	−05:13:40	B1-34 H1-53 P1-54 K1-57 K1-59 A2-72 B2-72 P2-82 M2-83 W1-91
5-68							5:31:41.0	−01: 9:21	H2-53 F1-60 G1-65
4-146	94			V396		KiHa76-74	5:31:41.0	−05:38:16	H1-53 R1-56 K1-59 P2-82 W1-91
4-190	95		P1367		197	KiHa76-75	5:31:41.0	−05:57:46	B1-34 H1-53 P1-54 K1-59 B1-71 G1-76 P2-82 M2-83 W1-91
						KiHa4-19	5:31:41.4	−00:21:49	W2-89
						KiHa75-189	5:31:42.0	−02:30:42	W1-91
						KiHa4-20	5:31:42.9	−01: 3: 2	W2-89
4-47	97			V546		KiHa75-190, KiHa76-76	5:31:43.0	−04:53:20	H1-53 H2-55 R1-62 B2-72 G1-76 P2-82 W1-91
4-45	98		P1373	BT	200	KiHa75-191, KiHa76-77	5:31:44.0	−04:52:22	P2-04 S2-24 H1-31 B1-34 R1-46 P1-52 H1-53 P1-54 R1-56 K1-59 G1-76 P2-82 M2-83 W1-91
						KiHa4-21	5:31:44.7	−01:11:33	W2-89
4-306	96						5:31:44.8	−05:52:40	P2-82 G1-85
4-307	99					KiHa76-78	5:31:45.0	−05:57:20	P2-82 G1-85 W1-91
4-308	101						5:31:45.1	−05:37:16	P2-82
						KiHa3-255	5:31:46.0	+01:35:46	K2-89
						KiHa3-254	5:31:46.0	+01:35:26	K2-89
4-135	100		P1386	IM	214	KiHa76-79	5:31:46.0	−05:35:52	B1-34 R1-46 P1-52 H1-53 P1-54 R1-56 K1-59 A2-72 G1-76 P2-82 M2-83 W1-91

TABLE 1. CONTINUED.

Haro	PC	HBC	P	Name	Brun	Other	RA (1950)	DEC (1950)	References
(1)	(2)	(3)	(4)	(5)	(6)	(7)	(8)	(9)	(10)
						KiHa76-82	5:31:47.0	−03:59:22	W1-91
						St45	5:31:47.0	−05:13:36	S8-86
		442	P1394		216	BD−5 1299, IRAS05317−0538	5:31:47.0	−05:38:52	B1-34 P1-54 S1-58 J1-65 B1-67 W1-69 F1-70 B1-72 S2-72 P2-73 B2-76 M1-76 M2-76 C1-77 W2-77 M2-83 H1-88 V1-88 M3-89 W2-90
4-167	102					KiHa76-81	5:31:47.0	−05:44:19	H1-53 K1-59 A2-72 G1-76 P2-82 W1-91
4-309	103			V742		KiHa76-80	5:31:47.0	−05:57:40	P2-82 G1-85 C1-86 M4-88 W1-91
		112	P1397		218		5:31:48.8	−05:48:32	B1-34 P1-54 B1-63 H1-72 P1-73 P2-73 D1-75 O1-77 C2-79 B2-81 M2-83
	104	113	P1404	V1044	220	KiHa76-83, IRAS05317−0538	5:31:49.3	−05:38:44	B1-34 R1-46 P1-54 S1-58 H2-62 W1-69 F1-70 B1-71 B1-72 H1-72 P2-73 D1-75 P1-75 B2-76 M1-76 M2-76 B4-77 C1-77 H1-77 K1-78 C2-79 P2-82 M2-83 S9-83 R2-84 H2-86 I1-87 H1-88 K3-88 V1-88 Y1-88 M3-89 W1-91
	108	115	P1412	SW		KiHa76-84, IRAS05317−0638	5:31:49.7	−06:38: 2	W1-03 P2-04 H1-23 P1-52 P1-54 H2-62 R1-62 M1-63 S3-71 B2-72 H1-72 D1-75 C2-79 M4-80 A1-81 P2-82 M2-83 P1-85 C3-88 H1-88 S7-89 S3-90 W2-90 M1-91 M2-91 W1-91 W2-91
						KiHa76-86	5:31:50.0	−02:59:47	W1-91
4-310	106		P1411	V470		KiHa76-87	5:31:50.0	−05:33:56	P1-54 R1-56? P2-82 W1-91
4-147	107					KiHa76-85	5:31:50.0	−05:40:15	H1-53 K1-59 A2-72 G1-76 P2-82 W1-91
	105	114	P1409	EZ	224	IRAS05318−0506	5:31:50.8	−05: 6:46	B1-34 R1-46 H2-50 P1-52 B1-54 P1-54 R1-56 K1-59 H2-62 K1-66 M1-66 K1-68 M1-68 M2-68 W1-69 F1-70 M3-70 S3-71 B1-72 B2-72 H1-72 K1-74 P1-75 B2-76 B4-77 C1-77 K1-78 W2-78 C2-79 U1-79 B2-81 B10-82 P2-82 M2-83 M3-83 S9-83 S10-83 W1-83 R2-84 C1-86 H1-88 Y1-88 M3-89 W1-90 W2-90
						St44	5:31:51.0	−00:57: 5	S8-86 D1-88
4-312	111					KiHa76-88	5:31:51.0	−05:39: 6	P2-82 W1-91
		444	P1410		223		5:31:51.1	−05: 9: 0	B1-34 P1-54 H3-69 W1-69 B2-72 P1-75 W1-83 H1-88
4-313	112		P1428	V746	241		5:31:51.1	−05:32:41	B1-34 P1-54 S1-58 B1-63 M1-76 P2-82 M2-83
						KiHa3-256	5:31:52.0	+02:19:44	K2-89
4-127	110		P1424	WZ	234	KiHa76-89	5:31:52.0	−05:32:18	P2-04 H1-23 B1-34 R1-46 H1-50 P1-52 H1-53 P1-54 R1-56 S1-58 K1-59 F1-70 B1-71 G1-76 P2-82 M2-83 W1-91
4-311	109						5:31:52.2	−04:36:47	P2-82 G1-85
						KiHa4-22	5:31:53.2	−00:35:49	W2-89
5-70				V469		KiHa4-23	5:31:53.6	−01:23: 4	H2-53 F1-58 F1-60 W2-89 B3-90
						KiHa3-257	5:31:55.0	+01:50:21	K2-89
4-21	113		P1435	V547	236	KiHa76-90	5:31:55.0	−04:43:38	B1-34 H1-53 P1-54 K1-59 R1-62 B1-71 G1-76 P2-82 M2-83 W1-91
		445	P1440		244		5:31:55.9	−04:49: 9	B1-34 P1-54 W1-69 B1-72 B2-76 M2-83 S7-83 W1-83 H1-88 M3-89
4-316	117		P1458		260		5:31:57.7	−05: 2:47	B1-34 P1-54 P2-82 G1-85
4-57	118		P1464	IR	258		5:31:57.8	−04:58:59	B1-34 R1-46 P1-52 H1-53 P1-54 H2-55 R1-56 R1-62 G1-76 P2-82 M2-83 A1-88
						Xray4	5:31:57.8	−06:46:25	S3-90
4-314	114		P1452	IP	248	KiHa76-92	5:31:58.0	−04:58:25	B1-34 R1-46 P1-52 P1-54 R1-56 K1-59 R1-62 S3-80 P2-82 G1-85 A1-88 W1-91
4-315	115		P1453				5:31:58.0	−04:58:53	P1-54 P2-82
4-58	116		P1454	IQ	249	KiHa76-91	5:31:58.0	−04:58:53	B1-34 R1-46 P1-52 H1-53 P1-54 R1-56 K1-59 R1-62 B2-72 S3-80 P2-82 M2-83 A1-88 W1-91
						KiHa76-93	5:32: 0.0	−04:13:10	W1-91
4-29	119		P1468	BV	256	KiHa76-94	5:32: 1.0	−04:47: 0	P2-04 H1-23 S2-24 B1-34 R1-46 H1-50 P1-52 H1-53 P1-54 H2-55 R1-56 K1-59 R1-62 R1-69 G1-76 P2-82 M2-83 P1-85 W1-91
		446	P1487		288		5:32: 1.8	−06:12:22	B1-34 P1-54 W1-69 M2-83 W1-83 C1-86 H1-88
4-13	120				264	KiHa76-96	5:32: 2.0	−04:37:49	B1-34 H1-53 G1-76 P2-82 W1-91
4-41	121		P1475		267	KiHa76-95	5:32: 2.0	−04:51:48	B1-34 H1-53 P1-54 G1-76 P2-82 M2-83 W1-91
4-94	124		P1481	IS	280	KiHa76-97	5:32: 2.0	−05:13:45	B1-34 R1-46 P1-52 H1-53 P1-54 R1-56 K1-59 A2-72 G1-76 P2-82 M2-83 J1-88 W1-91
4-321	128		P1502	V755			5:32: 2.6	−06:40:37	H1-04 P1-54 H1-69 P2-82 W2-91
4-319	125						5:32: 2.8	−05:49: 5	P2-82
						KiHa76-98, IRAS05320−0300	5:32: 3.0	−02:59:55	W1-91
4-141	126		P1497		301		5:32: 3.1	−05:37:17	B1-34 H1-53 P1-54 G1-76 P2-82 M2-83 J1-88
4-317	122						5:32: 3.2	−05:28:59	P2-82
						KiHa4-24	5:32: 3.5	+00:33:39	W2-89
4-318	123				276		5:32: 3.7	−05: 5:35	B1-34 W1-69 H1-76 P2-82 M1-85 M4-87 M2-90
4-320	127		P1501	IT	282		5:32: 4.0	−04:50:11	B1-34 P1-52 P1-54 R1-56 K1-59 P2-82 G1-85
5-83							5:32: 5.0	−02:59:35	H2-53 F1-60 G1-65
		116	P1519	IU	312	HD36884, BD−5 1303	5:32: 8.8	−05:43:21	B1-34 P1-52 P1-54 H2-62 S2-62 J1-65 B1-67 W1-69 F1-70 S3-71 B1-72 H1-72 E1-73 C1-74 B3-75 D1-75 P2-75 B2-76 M1-76 H1-77 K1-78 C2-79 B2-81 M2-83 W1-83 K2-86 O1-86 I1-87 I1-88 V1-88 M3-89
4-158	133		P1535	V980	327		5:32: 8.9	−05:43: 0	B1-34 H1-53 P1-54 K1-57 K1-59 B1-71 A2-72 P2-82 M2-83
4-171	134		P1536	V1000	316		5:32: 8.9	−05:44:54	B1-34 H1-53 P1-54 K1-59 A2-72 B2-72 P2-82 M2-83
4-142	130		P1524	V759	314	KiHa76-99	5:32: 9.0	−05:38:13	B1-34 H1-53 P1-54 K1-59 A2-72 G1-76 P2-82 M2-83 J1-88 W1-91
4-140	129		P1516		305		5:32: 9.1	−05:36:48	B1-34 H1-53 P1-54 K1-59 A2-72 G1-76 P2-82 M2-83 J1-88
4-200	132	117	P1530	XX	319	KiHa76-100	5:32: 9.5	−06: 7:31	R1-90* H1-04 P2-04 H1-23 S2-24 B1-34 H1-50

TABLE 1. CONTINUED.

Haro (1)	PC (2)	HBC (3)	P (4)	Name (5)	Brun (6)	Other (7)	RA (1950) (8)	DEC (1950) (9)	References (10)
4-200									P1-52 H1-53 P1-54 H2-55 R1-62 W1-63 W1-66 H3-69 W1-69 W2-69 B1-71 B1-72 H1-72 W1-72 A1-74 C1-74 G1-76 A1-77 M4-77 C2-79 M4-80 T1-81 P2-82 M2-83 P1-85 H1-88 W1-91
4-139	131		P1527	IV	321	KiHa76-101	5:32:10.0	−05:36:48	B1-34 R1-46 P1-52 H1-53 P1-54 R1-56 S1-58 K1-59 G1-76 P2-82 M2-83 J1-88 W1-91
			P1557				5:32:11.5	−06:55:52	P1-54 P3-76 S3-90
4-60	135				323	KiHa76-102	5:32:12.0	−04:59:36	B1-34 H1-53 G1-76 P2-82 W1-91
				V938			5:32:12.0	−06: 8:15	S3-90
		447	P1540		334		5:32:12.3	−05:26:22	B1-34 P1-54 S1-58 F1-70 P2-73 P1-75 B2-76 M1-76 M2-83 C1-86 H1-88 J1-88 M2-88 V1-88 M3-89 Z2-89
		448	P1541		335		5:32:12.5	−05:28:38	B1-34 P1-54 S1-58 W1-69 F1-70 M1-76 M2-83 W1-83 H1-88 J1-88 M3-89
						Xray7c	5:32:12.7	−06:37:52	S3-90
		449	P1554	IY	341		5:32:13.3	−05:52:12	B1-34 P1-52 P1-54 K1-59 W1-69 F1-70 S3-71 B2-76 M2-83 W1-83 C1-86 H1-88 M3-89
4-115	137	118	P1552	IX	340		5:32:13.4	−05:24:38	B1-34 R1-46 H2-50 P1-52 H1-53 B1-54 P1-54 H2-55 R1-56 S1-58 K1-59 H2-62 M1-66 F1-70 H1-72 C1-74 P1-75 M1-76 K2-79 M4-80 P2-82 M2-83 H1-88 J1-88 M3-89
4-323	140		P1564		348	KiHa76-104	5:32:14.0	−05:47:13	B1-34 P1-54 P2-82 M2-83 C1-86? W1-91
4-177	141		P1565	XY	364	KiHa76-105	5:32:14.0	−05:48: 8	P2-04 H1-23 B1-34 R1-46 H1-50 P1-52 H1-53 P1-54 R1-56 A2-72 B2-72 G1-76 P2-82 M2-83 P1-85 W1-91
4-222	145			V766		KiHa76-103	5:32:14.0	−06:27: 9	H1-53 G1-76 P2-82 W1-91
			P1578				5:32:14.7	−06:36:31	P1-54 P5-81 S3-90
4-322	136		P1543				5:32:14.8	−05:49:24	P1-54 P2-82
4-324	143		P1571		362		5:32:14.8	−05:49:48	B1-34 P1-54 P2-82
4-174	147		P1576	IZ			5:32:14.9	−05:46:36	R1-46? P1-52 H1-53 P1-54 R1-56 K1-59 R1-62 P2-82 M2-83 P1-85
4-93	139		P1563	V473	347	KiHa76-106	5:32:15.0	−05:14:15	B1-34 H1-53 P1-54 J1-57 K1-57 S1-58 K1-59 B1-63 F1-70 B1-71 S3-71 G1-76 M1-76 K2-79 P2-82 M2-83 C1-86 J1-88 M3-89 W1-91
4-154	138		P1553	V398	339		5:32:15.0	−05:42: 0	B1-34 H1-53 P1-54 R1-56 K1-57 K1-59 M1-68 M2-68 H3-69 F1-70 B1-71 S3-71 G1-76 K2-79 P2-82 M2-83 C1-86 M3-89
5-71				V472		KiHa4-25	5:32:15.7	−00:39:12	H2-53 F1-58 F1-60 G1-65 W2-89
4-56	142						5:32:15.8	−04:57:54	H1-53 P2-82
						WBHa 1	5:32:15.9	−06:58:53	W2-91
4-82	148		P1585		368	KiHa76-108	5:32:17.0	−05: 8:45	B1-34 H1-53 P1-54 R1-62? B1-71 P1-75 G1-76 P2-82 M2-83 W1-91
4-90	149		P1586	XZ	367	KiHa76-109	5:32:17.0	−05:12:44	P2-04 H1-23 S2-24 B1-34 R1-46 H1-50 P1-52 H1-53 P1-54 H2-55 R1-56 R1-62 K1-59 P1-75 K2-79 P2-82 M2-83 J1-88 W1-91
	144			V765		KiHa76-107	5:32:17.0	−06:18:59	P2-82 W1-91
				V1118		Chanal's object	5:32:17.4	−05:35:38	A2-84 H4-84 N1-84 P1-87 G2-89 G3-89 H2-89 G2-90 V1-90
						WBHa 2	5:32:17.8	−07: 6:32	W2-91
5-1							5:32:18.0	−02:46:54	H2-53 F1-60 G1-65
4-326	153			V771			5:32:18.7	−06:23: 3	P5-81 P2-82 C1-86 S3-90
4-151	152		P1601	V474	385	KiHa76-110	5:32:19.0	−05:41: 3	B1-34 H1-53 P1-54 K1-57 K1-59 B1-71 S3-71 A2-72 G1-76 K2-79 P2-82 M2-83 W1-91
		450	P1608		394		5:32:19.2	−06: 0:47	B1-34 P1-54 W1-69 A1-74 M2-83 S7-83 W1-83 C1-86 H1-88 M3-89
			P1609				5:32:19.3	−06:23:36	S3-90
4-44	146					KiHa76-112	5:32:20.0	−04:52:47	H1-53 P2-82 W1-91
4-78	151		P1599	V550	382	KiHa76-111	5:32:20.0	−05: 6:51	B1-34 H1-53 P1-54 R1-62 P2-82 M2-83 W1-91
4-325	150						5:32:20.2	−06:38:58	P2-82 W2-91
4-328	163						5:32:20.5	−06: 6: 7	P2-82 G1-85
						KiHa4-26	5:32:20.7	+02:19:43	W2-89
4-178	157		P1616	V774	409		5:32:20.8	−05:48:19	B1-34 H1-53 P1-54 K1-59 B2-72 G1-76 P2-82 M2-83
4-196	158	119	P1617	YY	408	KiHa76-113	5:32:20.8	−05:59:53	P1-95* P2-04 H1-23 S1-24 B1-34 R1-46 H1-50 P1-52 H1-53 P1-54 H2-55 K1-59 H2-62 R1-62 W1-63 W1-66 W1-69 B1-71 S3-71 H1-72 W1-72 A1-74 C1-74 D1-75 B2-76 G1-76 A1-77 B2-77 B4-77 H1-77 M4-77 W1-77 K2-78 W1-78 C2-79 G1-80 G2-80 M4-80 W1-80 T1-81 B5-82 P2-82 J1-83 M2-83 W1-83 A1-84 F1-85 K1-86 M10-87 H1-88 K3-88 M3-89 B3-90 W1-91
4-166	156		P1614	KK	404	KiHa76-114	5:32:21.0	−05:44:24	B1-34 R1-46 P1-52 H1-53 P1-54 R1-56 K1-59 R1-62? S3-71 B2-72 G1-76 S3-80 P2-82 M2-83 P1-85 A1-88 W1-91
						KiHa4-27	5:32:21.4	−02:34:50	W2-89
4-327	159		P1622		420		5:32:21.5	−05:13: 1	B1-34 P1-54 P2-82 J1-88
4-59	155						5:32:21.8	−04:59:49	H1-53 K1-59 P2-82
4-176	160		P1625	V400	423	KiHa76-115	5:32:22.0	−05:48: 0	B1-34 H1-53 P1-54 H2-55 R1-56 K1-59 R1-69 R3-69 R4-69 G1-76 P2-82 M2-83 P1-85 W1-91
4-228	162		P1635	V374		KiHa76-116	5:32:22.0	−06:32:22	P2-04 B2-37 P1-52 H1-53 P1-54 K1-59 R1-62 M1-63 A2-72 B2-72 G1-76 P2-82 M2-83 W1-91
						KiHa4-28	5:32:22.2	−00:59:26	W2-89
4-12	154		P1611	V773	392		5:32:22.2	−04:37:25	B1-34 H1-53 P1-54 K1-57 B1-71 A1-74 G1-76 P2-82 M2-83 C1-86
4-74	164	120	P1648	YZ	422	KiHa76-117	5:32:25.2	−05: 5:22	R1-90* P2-04 P4-04 H1-23 B1-34 R1-46 H1-50 H2-50 P1-52 H1-53 B1-54 P1-54 R1-56 K1-59 R1-62 B1-71 B2-72 H1-72 D1-75 G1-76 C2-79

TABLE 1. CONTINUED.

Haro	PC	HBC	P	Name	Brun	Other	RA (1950)	DEC (1950)	References
(1)	(2)	(3)	(4)	(5)	(6)	(7)	(8)	(9)	(10)
4-74									M4-80 P2-82 M2-83 P1-85 H1-88 W1-91
		121	P1649		430	BD−5 1307	5:32:26.0	−05:34:52	B1-34 P1-54 J1-57 S1-58 B1-60 L1-60 B1-68 W1-69 F1-70 B1-72 H1-72 P2-73 D1-75 B2-76 M1-76 C1-77 H1-77 K1-78 C2-79 B2-81 M2-83 J1-88 K3-88 V1-88 M3-89
						KiHa4-29	5:32:26.1	−00:20:55	W2-89
4-330	166						5:32:26.7	−05:56: 1	P2-82
4-329	165						5:32:27.0	−05:40:55	P2-82 G1-85
4-333	171		P1667	KO	448		5:32:27.1	−05:33:25	B1-34 P1-52 P1-54 R1-56 S1-58 K1-59 W1-69 F1-70 S3-71 B1-72 M1-76 K3-82 P2-82 M2-83 C1-86 A2-88 J1-88
4-332	169						5:32:27.6	−05: 7:25	P2-82 G1-85
4-331	167						5:32:27.7	−05: 2:49	P2-82
4-91	170	123	P1665	KN	445		5:32:28.0	−05:13:25	B1-34 R1-46 P1-52 H1-53 P1-54 R1-56 S1-58 K1-59 H2-62 F1-70 B1-71 S3-71 A2-72 H1-72 D1-75 G1-76 M1-76 C2-79 K2-79 P2-82 M2-83 B3-88 H1-88 J1-88 M3-89
4-179	168		P1661	ZZ	446	KiHa76-119	5:32:28.0	−05:48:39	R1-90* P1-95* W1-03 P2-04 P4-04 H1-23 B1-34 R1-46 P1-52 H1-53 P1-54 R1-56 K1-59 R1-62 G1-76 P2-82 M2-83 W1-91
4-219	173		P1669	BW		KiHa76-118	5:32:28.0	−06:25:46	P2-04 S1-24 S2-24 H1-31 H1-50 P1-52 H1-53 P1-54 K1-59 R1-62 M1-63 S3-71 B2-72 G1-76 P2-82 M2-83 P1-85 C3-88 C3-89 W1-91
		122	P1659	KM	443		5:32:28.5	−05:25: 8	R1-46 B1-34 P1-52 P1-54 R1-56 S1-58 K1-59 H2-62 F1-70 S3-71 H1-72 P2-73 M1-76 C1-77 K1-78 C2-79 K2-79 M4-80 K3-82 M2-83 B4-85 B4-86 C1-86 A1-88 B3-88 H1-88 J1-88 V1-88 Y1-88
4-157	172	124	P1668	KP	451	KiHa76-120	5:32:28.7	−05:43:21	B1-34 R1-46 P1-52 H1-53 P1-54 H2-55 R1-56 K1-59 W1-63 W1-66 B2-72 H1-72 W1-72 D1-75 G1-76 C2-79 P2-82 M2-83 H1-88 W1-91
						KiHa76-121	5:32:31.0	−04:52: 7	W1-91
4-188	177		P1688	BX	459	KiHa76-122	5:32:31.0	−05:56:24	P2-04 S2-24 B1-25 H1-31 B1-34 R1-46 H1-50 P1-52 H1-53 P1-54 K1-59 G1-76 P2-82 M2-83 W1-91
			P1691				5:32:31.1	−06:20:25	P1-54 R2-84 P5-81 S3-90
4-173	176		P1687	KT	473	KiHa76-124	5:32:32.0	−05:46:25	B1-34 R1-46 P1-52 H1-53 P1-54 K1-59 B2-72 G1-76 P2-82 M2-83 W1-91
4-197	178		P1689			KiHa76-123	5:32:32.0	−06: 1:54	H1-53 P1-54 B2-72 A1-74 P2-82 M2-83 W1-91
	175	125	P1684	KR	467		5:32:32.6	−05:24:57	B1-34 R1-46 H2-50 P1-52 B1-54 P1-54 R1-56 S1-58 K1-59 B1-61 H2-62 J1-65 F1-70 S3-71 H1-72 P2-73 D1-75 P1-75 M1-76 B1-79 C2-79 K3-82 P2-82 M2-83 C1-86 A1-88 H1-88 J1-88 S3-90
						Xray15a	5:32:32.7	−06: 6:31	
4-339	187						5:32:32.8	−05:51:20	P2-82
4-337	183						5:32:32.8	−05:52:44	P2-82
4-338	185					KiHa76-125	5:32:33.0	−04:34:48	P2-82 G1-85 W1-91
4-62	189		P1723	V554	496		5:32:33.8	−05: 0:14	B1-34 H1-53 P1-54 K1-59 R1-62 P3-76 P2-82 M2-83
4-334	174		P1682		461		5:32:34.0	−04:48:38	B1-34 P1-54 P2-82 G1-85
4-340	188		P1721		484		5:32:34.0	−04:51: 2	B1-34 P1-54 P2-82
4-335	179		P1692		463		5:32:34.0	−04:51: 2	B1-34 P1-54 P2-82
4-336	182						5:32:34.0	−04:51: 8	P2-82
4-199	184					KiHa76-126	5:32:34.0	−06: 3:18	H1-53 K1-59 P2-82 W1-91
4-36	180					KiHa76-127	5:32:35.0	−04:50:28	H1-53 G1-76 P2-82 W1-91
4-38	181		P1701		475	KiHa76-128	5:32:35.0	−04:51:16	B1-34 H1-53 P1-54 K1-57 K1-59 P2-82 M2-83 W1-91
				V789			5:32:35.7	−06:32: 7	P5-81 S3-90
5-2							5:32:36.0	−02:51: 8	H2-53 F1-60 G1-65
4-43	186		P1710	BY	469	KiHa76-129	5:32:36.0	−04:52:48	P2-04 S2-24 H1-31 B1-34 R1-46 P1-52 H1-53 P1-54 R1-56 P2-82 M2-83 W1-91
		452	P1724		490		5:32:36.5	−05:10: 7	B1-34 P1-54 S1-58 W1-69 F1-70 B1-72 P1-75 B2-76 M1-76 C1-77 B2-81 M2-83 C1-86 H1-88 J1-88 V1-88 M3-89
						St46	5:32:37.0	−00:56:27	S8-86
						KiHa76-130	5:32:38.0	−05:36:23	W1-91
	194	126	P1746	LL	510		5:32:38.1	−05:27:14	B1-34 R1-46 P1-52 P1-54 S1-58 K1-59 W1-60 H2-62 J1-65 K1-68 W1-69 F1-70 H1-72 P2-73 K1-74 D1-75 M1-76 U1-79 C2-79 B2-81 B10-82 K3-82 P2-82 M2-83 W1-83 C1-86 A1-88 H1-88 J1-88 V1-88 Y1-88
4-343	193						5:32:38.3	−06:14. 8	P2-82 G1-85
4-175	200		P1756	V482	514		5:32:38.9	−05:47:20	B1-34 H1-53 P1-54 K1-57 K1-59 A2-72 B2-72 G1-76 P2-82 M2-83 C1-86
4-143	207		P1767	LO	524		5:32:39.0	−05:38:56	B1-34 R1-46 P1-52 H1-53 P1-54 R1-56 K1-59 G1-76 K2-79 P2-82 M2-83 C1-86 J1-88
4-130	205		P1765	LM	533		5:32:39.1	−05:33:38	B1-34 R1-46 P1-52 H1-53 P1-54 R1-56 S1-58 K1-59 F1-70 P3-76 P2-82 M2-83 J1-88
4-134	199		P1755	V982	525		5:32:39.1	−05:35:26	B1-34 H1-53 P1-54 R1-56 S1-58 K1-59 G1-76 P2-82 M2-83 J1-88
	196			V408			5:32:39.1	−05:35:50	K1-59 R1-62 P2-82 P1-85
4-344	195		P1747		505		5:32:39.2	−05:29: 8	T1-31 B1-34 P1-54 P2-82 M2-83 J1-88
4-342	192		P1735		494		5:32:39.6	−05:11:26	B1-34 P1-54 P2-82 G1-85
4-341	191		P1734		503		5:32:39.8	−05: 0:44	B1-34 P1-54 P2-82 G1-85
4-7	197		P1752	V481	509	KiHa76-131	5:32:40.0	−04:29:46	B1-34 H1-53 P1-54 K1-57 K1-59 B1-71 A1-74 G1-76 P2-82 M2-83 M3-89 W1-91
4-28	198		P1753	V555	507	KiHa76-132	5:32:40.0	−04:48:47	B1-34 H1-53 P1-54 K1-59 R1-62 G1-76 P2-82

TABLE 1. CONTINUED.

Haro	PC	HBC	P	Name	Brun	Other	RA (1950)	DEC (1950)	References
(1)	(2)	(3)	(4)	(5)	(6)	(7)	(8)	(9)	(10)
4-28									M2-83 W1-91
	190		P1733		495		5:32:40.0	−04:50:32	B1-34 P1-54 R1-56 K1-59 P2-82
	202		P1761		513		5:32:40.1	−04:43: 2	B1-34 P1-54 P2-82
	206	128	P1766	LN	532		5:32:40.7	−05:34:38	B1-34 R1-46 H2-50 P1-52 P1-54 R1-56 K1-59 H1-72 D1-75 P2-82 M2-83 H1-88 J1-88
4-55	204			V556		KiHa76-134	5:32:41.0	−04:59: 6	H1-53 R1-62 G1-76 P2-82 W1-91
4-345	203					KiHa76-133	5:32:41.0	−05:55:37	P2-82 G1-85 W1-91
4-6	201	127	P1760	SY	515	KiHa76-135	5:32:41.6	−04:29:34	R1-90* P1-95* P2-04 P4-04 H1-23 S1-24 S2-24 B1-34 R1-46? H1-50 P1-52 H1-53 P1-54 H2-55 R1-56 K1-59 H2-62 R1-62 W1-63 W1-66 B1-71 H1-72 W1-72 A1-74 C1-74 G1-76 A1-77 M4-77 B1-79 C2-79 M4-80 T1-81 P2-82 H1-88 M3-89 W1-91
						KiHa4-30	5:32:41.7	−00:56:44	W2-89
	208	129	P1773	V356	522		5:32:41.7	−05:31:53	B1-34 R1-46 H2-50? P1-52 B1-54 P1-54 R1-56 K1-57 S1-58 K1-59 H2-62 F1-70 B1-71 S3-71 H1-72 M1-76 C2-79 K3-82 P2-82 M2-83 S7-83 A1-88 H1-88 J1-88 M3-89
						WBHa 3	5:32:41.7	−07:26:15	W2-91
4-346	210		P1788		539	KiHa76-136	5:32:42.0	−06: 0:11	B1-34 P1-54 A1-74 P2-82 W1-91
						WBHa 4	5:32:42.2	−07:10:42	W2-91
		453	P1784	LQ	536		5:32:43.2	−05:25:38	B1-34 P1-52 P1-54 S1-58 K1-59 F1-70 P2-73 M1-76 K3-82 M2-83 C1-86 H5-86 A1-88 H1-88 J1-88
4-180	209	130	P1787	AA	543	KiHa76-137	5:32:43.4	−05:48:28	R1-90* P1-95* W1-03 P2-04 P4-04 H1-23 B1-34 R1-46 H1-50 H2-50 P1-52 H1-53 P1-54 K1-59 H2-62 B1-71 A2-72 H1-72 D1-75 G1-76 C2-79 M4-80 P2-82 M2-83 S7-83 C1-86 H1-88 M3-89 W1-91
						WBHa 5	5:32:43.8	−07:23:26	W2-91
						WBHa 6	5:32:43.9	−07:18:56	W2-91
4-351	225						5:32:44.1	−06:26:39	P2-82
4-349	216						5:32:44.3	−06:15:21	P2-82 G1-85
4-350	223						5:32:44.3	−06:16:33	P2-82 G1-85
4-347	211		P1797		534	KiHa76-139	5:32:45.0	−04:44:52	B1-34 P1-54 R1-62? P2-82 W1-91
4-149	220		P1846	LY	572		5:32:45.0	−05:40:57	B1-34 P1-52 H1-53 P1-54 R1-56 K1-59 R1-62 B1-71 S3-80 P2-82 M2-83 C1-86 A1-88 J1-88
		454	P1807	LV	551		5:32:45.1	−05:25:38	B1-34 P1-52 P1-54 S1-58 K1-59 F1-70 M1-76 K3-82 M2-83 H5-84 C1-86 H5-86 A1-88 H1-88 J1-88
4-348	212		P1801		556		5:32:45.1	−05:33:45	B1-34 P1-54 S1-58 F1-70 M1-76 P2-82 M2-83 J1-88
4-126	214		P1809	LW			5:32:45.2	−05:32:21	R1-46? P1-52 H1-53 P1-54 R1-56 S1-58 K1-59 P2-82 A1-88 J1-88
4-170	215	131	P1811	V486	553	KiHa76-138	5:32:45.3	−05:45:13	B1-34 H1-53 P1-54 K1-57 K1-59 B1-71 S3-71 A2-72 H1-72 D1-75 G1-76 C2-79 P2-82 M2-83 S7-83 C1-86 H1-88 W1-91
4-85	213		P1805	V557	559		5:32:45.6	−05:11: 3	B1-34 H1-53 P1-54 K1-59 R1-62 A2-72 G1-76 P2-82 M2-83 P1-85 J1-88
4-150	219	133	P1828	LX	563	KiHa76-140	5:32:45.9	−05:41:29	B1-34 P1-52 H1-53 P1-54 K1-59 H2-62 B1-71 H1-72 P2-73 C1-74 D1-75 G1-76 K1-78 C2-79 M4-80 S3-80 P2-82 M2-83 A1-88 H1-88 Y1-88 M3-89 W1-91
4-128	218	134	P1827	V488	561	KiHa76-141	5:32:46.3	−05:32:51	B1-34 R1-46 H1-53 P1-54 J1-57 K1-57 S1-58 K1-59 H2-62 F1-70 B1-71 S3-71 H1-72 M1-76 M4-80 K3-82 P2-82 M2-83 A1-88 H1-88 J1-88 M3-89 W1-91
						KiHa4-31	5:32:46.5	−00:18:45	W2-89
						WBHa 7	5:32:46.8	−06:48:59	W2-91
		132	P1817		555		5:32:46.9	−04:46:37	B1-34 R1-46 P1-54 W1-69 F1-70 B1-72 H1-72 M2-76 K1-78 C2-79 M4-80 S9-83 S10-83 R2-84 C1-86 H1-88 Y1-88 M2-83 M3-89
4-10	217		P1816	V487	554	KiHa76-142, IRAS05328−0435	5:32:47.0	−04:35:20	B1-34 H1-53 P1-54 K1-57 B1-71 A1-74 G1-76 P2-82 M2-83 W1-91
4-186	222		P1850	BZ	586	KiHa76-143	5:32:47.0	−05:54: 2	P2-04 S2-24 B1-25 H1-31 B1-34 R1-46 H1-50 P1-52 H1-53 P1-54 K1-59 B1-71 P2-82 M2-83 W1-91
						WBHa 8	5:32:47.0	−07: 7:15	W2-91
5-72				V483		KiHa4-32	5:32:47.1	−00:44: 7	H2-53 F1-58 F1-60 G1-65 W2-89
4-169	221	135	P1848	AB	574	KiHa76-144	5:32:47.2	−05:45:11	P1-95* S1-98* P2-04 H1-23 B1-34 R1-46 H1-50 P1-52 H1-53 P1-54 K1-59 H2-62 R1-62 B1-71 S3-71 A2-72 H1-72 D1-75 G1-76 C2-79 M4-80 P2-82 M2-83 C1-86 M9-87 H1-88 W1-91
						WBHa 9	5:32:47.5	−06:49:15	W2-91
						WBHa10	5:32:48.3	−06:54:16	W2-91
4-353	237						5:32:48.3	−07:56:21	P2-82
			P1865/c		587/c	V1016/c, HD37020/c	5:32:48.4	−05:25: 8	I3-88 B7-89
		455	P1869		591		5:32:48.5	−05:25:43	B1-34 P1-54 S1-58 F1-70 M1-76 K3-82 M2-83 H5-84 H5-86 C3-87 H1-88 J1-88
	224	136	P1856	TT	558	KiHa76-145	5:32:48.6	−04:47:38	R1-90* P1-95* W1-03 P2-04 P4-04 H1-23 S1-24 B1-34 R1-46 P1-52 P1-54 R1-56 K1-59 H2-62 H1-72 S3-71 C2-79 K2-79 P2-82 M2-83 H1-88 M3-89 W1-91
			P1863/c		595/c	BM/c, HD37021/c	5:32:48.7	−05:25: 0	I2-88 A3-89
5-4							5:32:49.0	−02:49:45	H2-53 F1-58 K1-59 F1-60 G1-65

TABLE 1. CONTINUED.

Haro	PC	HBC	P	Name	Brun	Other	RA (1950)	DEC (1950)	References
(1)	(2)	(3)	(4)	(5)	(6)	(7)	(8)	(9)	(10)
4-23	226		P1882	V559	571	KiHa76-146	5:32:49.0	−04:46:46	B1-34 H1-53 P1-54 K1-59 R1-62 B1-71 K2-79 P2-82 M2-83 W1-91
		456	P1885	MR	604		5:32:49.4	−05:23:39	B1-34 G1-46 P1-52 P1-54 S1-58 K1-59 F1-70 P2-73 B2-76 M1-76 B2-81 M2-83 H5-86 A1-88 H1-88 J1-88
		457	P1884	AE	615		5:32:49.7	−05:23:25	H1-82* P1-95* P1-04 P3-04 P4-04 H1-23 B1-34 P1-52 P1-54 S1-58 K1-59 F1-70 M1-76 K3-82 M2-83 H5-86 A1-88 H1-88 J1-88
		137	P1909	AD	617		5:32:49.8	−05:24:29	H1-82* P1-95* P1-04 P4-04 B1-34 H2-50 P1-52 P1-54 S1-58 K1-59 F1-70 H1-72 C2-79 T1-81 K3-82 M2-83 C1-86 H5-86 A1-88 H1-88 J1-88
	243			V795			5:32:49.9	−06:34:45	P2-82
						WBHa11, KiHa76-147	5:32:49.9	−06:49: 9	W1-91 W2-91
						St47	5:32:50.0	−01:13:10	S8-86 D1-88
4-49	228					KiHa76-149	5:32:50.0	−04:55:39	H1-53 P2-82 W1-91
4-352	235						5:32:50.2	−06:19:21	P2-82
		458	P1910	MT	622		5:32:50.4	−05:24:39	B1-34 P1-52 P1-54 S1-58 F1-70 P2-73 P1-75 M1-76 K3-82 M2-83 C1-86 H5-86 C3-87 A1-88 H1-88 J1-88
						KiHa4-33	5:32:50.6	−00:45: 2	W2-89
4-191	227						5:32:50.6	−05:58:27	H1-53 P2-82
						Xray15d	5:32:50.6	−06: 7: 9	S3-90
		459	P1925		627		5:32:50.8	−05:24:31	B1-34 P1-54 S1-58 F1-70 M1-76 K3-82 M4-82 M2-83 H5-86 C3-87 H1-88 J1-88
4-156	229		P1916		611		5:32:50.9	−05:42:39	B1-34 H1-53 P1-54 P2-82 M2-83
4-161	230		P1917	V411	634		5:32:50.9	−05:44: 3	B1-34 H1-53 P1-54 H2-55 R1-56 K1-59 G1-76 P2-82 M2-83
4-165	231		P1929		635		5:32:50.9	−05:44:21	T1-31 B1-34 H1-53 P1-54 K1-57 K1-59 B1-71 A2-72 G1-76 P2-82 M2-83 M3-89
4-194	233	138	P1931		637	KiHa76-148, IRAS05328−0600	5:32:50.9	−06: 0:20	B1-34 H1-53 P1-54 W1-63 W1-66 W1-69 B1-72 B2-72 H1-72 A1-74 C1-74 D1-75 C2-79 M4-80 T1-81 P2-82 M2-83 H1-88 K3-88 W1-91
5-3						KiHa76-152?	5:32:51.0	−02:52: 3	H2-53 F1-60 G1-65 W1-91?
4-144	236		P1942	V412			5:32:51.0	−05:39:27	H1-53 P1-54 R1-56 K1-59 G1-76 P2-82 M2-83 J1-88
4-183	232		P1930	V793	640	KiHa76-151	5:32:51.0	−05:51:31	T1-31 B1-34 H1-53 P1-54 K1-59 B2-72 G1-76 P2-82 M2-83 W1-91
4-193	234					KiHa76-150	5:32:51.0	−06: 0:20	H1-53 H2-55 W1-72 P2-82 W1-91
		460	P1922	MV	628		5:32:51.1	−05:22:27	T1-31 B1-34 P1-52 P1-54 S1-58 F1-70 P2-73 M1-76 K3-82 M2-83 H5-86 A1-88 H1-88 J1-88
4-50	241		P1951	V414	654		5:32:51.9	−04:55:57	B1-34 H1-53 P1-54 R1-56 K1-59 B1-71 G1-76 K2-79 P2-82 M2-83
4-19	240		P1948	CD	648		5:32:52.1	−04:43:57	P2-04 H1-23 S2-24 B1-34 H1-50 P1-52 H1-53 P1-54 R1-56 K1-59 B1-71 S3-71 P2-82 M2-83
						KiHa4-34	5:32:52.2	−00:45:18	W2-89
						WBHa12	5:32:52.6	−07:22: 6	W2-91
		461	P1937	TU	643		5:32:52.7	−05:22:50	P1-95* H1-82* S1-98* P3-04 B1-10 H1-23 B1-34 G1-46 R1-46 H2-50 P1-52 P1-54 S1-58 K1-59 H2-62 J1-65 W1-69 F1-70 P2-73 M1-76 B2-81 K3-82 M2-83 C1-86 H5-86 J2-86 A1-88 H1-88 J1-88
4-224	248					KiHa76-153	5:32:53.0	−06:29:18	H1-53 K1-59 P2-82 W1-91
						WBHa13	5:32:53.3	−06:45:59	W2-91
		462	P1953	MX	653	BD−5 1317	5:32:53.5	−05:11: 9	B1-34 P1-52 P1-54 J1-57 S1-58 K1-59 L1-60 S2-62 J1-65 B1-68 W1-69 F1-70 B1-72 C1-73 C3-73 G3-74 P1-75 B2-76 M1-76 M2-76 C1-77 W2-77 S3-80 B2-81 M1-82 M2-83 W1-83 K1-85 A1-88 H1-88 J1-88 V1-88 M3-89
		463	P1955		656		5:32:53.6	−05:14: 6	B1-34 P1-54 J1-57 S1-58 B1-60 L1-60 B1-68 W1-69 F1-70 P2-73 M1-76 M2-76 C1-77 K3-82 M2-83 S9-83 S10-83 R2-84 C1-86 H1-88 J1-88 M3-89
4-79	242		P1952	V415	662	KiHa76-154, IRAS05329−0508	5:32:54.0	−05: 8:55	B1-34 H1-53 P1-54 R1-56 K1-57 K1-59 B1-71 S3-71 P1-75 G1-76 P2-82 M2-83 W1-91
						KiHa76-157	5:32:54.0	−05:36:53	W1-91
4-160	247		P1979	V416	680	KiHa76-155	5:32:54.0	−05:44: 6	B1-34 H1-53 P1-54 R1-56 K1-59 R1-62 G1-76 P2-82 M2-83 W1-91
4-8	239	139	P1946	V1007		KiHa76-156	5:32:54.3	−04:30:44	H1-53 P1-54 H2-55 K1-59 R1-62 W1-63 W1-66 H1-72 W1-72 A1-74 P2-82 M2-83 H1-88 W1-91
						WBHa14	5:32:54.3	−06:47:24	W2-91
						WBHa15	5:32:54.3	−06:49: 9	W2-91
4-137	246	140	P1977	AG	673	KiHa76-158	5:32:54.4	−05:36:40	W1-03 P2-04 H1-23 B1-34 R1-46 H1-50 H2-50 P1-52 H1-53 P1-54 R1-56 S1-58 K1-59 H2-62 F1-70 B1-71 H1-72 G1-76 C2-79 P2-82 M2-83 H1-88 J1-88 W1-91
4-2	238		P1945	V561	639	KiHa76-159	5:32:55.0	−04:19: 7	B1-34 H1-53 P1-54 R1-62 A1-74 P2-82 W1-91
						KiHa76-160	5:32:55.0	−05:54:30	W1-91
		465	P1996		684		5:32:55.1	−05:53: 0	B1-34 P1-54 B1-68 W1-69 F1-70 M1-76 M2-83 S7-83 S9-83 S10-83 R2-84 C1-86 H1-88 M3-89
						WBHa16	5:32:55.8	−07: 8: 9	W2-91
4-357	253						5:32:56.3	−06:14:51	P2-82 G1-85
						KiHa4-35	5:32:56.4	−01:27:23	W2-89
4-359	257						5:32:56.6	−05:59:33	P2-82
4-356	252						5:32:56.7	−05:54:51	P2-82
4-355	250		P1997				5:32:56.7	−05:55:39	P1-54 P2-82
4-42	249		P1987		675	KiHa76-163	5:32:57.0	−04:53:12	B1-34 H1-53 P1-54 P2-82 M2-83 W1-91

TABLE 1. CONTINUED.

Haro	PC	HBC	P	Name	Brun	Other	RA (1950)	DEC (1950)	References
(1)	(2)	(3)	(4)	(5)	(6)	(7)	(8)	(9)	(10)
4-92	251		P2000	NO	704	KiHa76-162	5:32:57.0	−05:13:51	B1-34 R1-46 P1-52 H1-53 P1-54 H2-55 R1-56 K1-59 B2-72 G1-76 K2-79 P2-82 M2-83 P1-85 W1-91
4-354	245		P1976	MZ	667		5:32:57.1	−05:33: 9	B1-34 R1-46 P1-52 P1-54 R1-56 S1-58 K1-59 F1-70 P2-82 M2-83 A1-88 J1-88
4-358	255		P2022	V417	706		5:32:57.2	−05:32: 9	B1-34 P1-54 R1-56 S1-58 K1-59 F1-70 M1-76 P2-82 C1-86 J1-88
						WBHa17	5:32:57.7	−07:10:27	W2-91
4-53	254		P2019	V563	699		5:32:57.8	−04:57:57	B1-34 H1-53 P1-54 K1-59 R1-62 B2-72 G1-76 P2-82 M2-83 P1-85 M4-88
4-198	258	142	P2039	NS	709		5:32:57.8	−06: 3:39	B1-34 R1-46 P1-52 H1-53 P1-54 H2-55 K1-59 R1-62 W1-63 W1-66 R1-69 R3-69 R4-69 B1-71 H1-72 W1-72 A1-74 D1-75 G1-76 A1-77 C2-79 M4-80 A1-81 P2-82 M2-83 P1-85 H1-88
4-33	244				668		5:32:58.0	−04:50:15	B1-34 H1-53 P2-82
		466	P2006	AH	696	IRAS05329−0512?	5:32:58.0	−05:11:42	P2-04 G1-20 H1-23 S1-24 B1-34 G1-46 R1-46 H2-50 P1-52 P1-54 R1-56 S1-58 K1-59 H2-62 R1-62 K1-64 J1-65 F1-70 S3-71 P1-75 M1-76 S3-80 M2-83 A1-88 H1-88 J1-88 M3-89 J6-90 W2-90
						KiHa76-165	5:32:58.0	−05:47:37	W1-91
						KiHa76-164	5:32:58.0	−06: 3:39	W1-91
						WBHa18	5:32:58.1	−07:15:19	W2-91
						KiHa4-36	5:32:58.4	−00:24:59	W2-89
		467	P2020	NP	698	IRAS05329−0512?	5:32:58.5	−05:10:33	B1-34 P1-52 P1-54 R1-56 S1-58 K1-59 R1-62 W1-69 F1-70 S3-71 B1-72 P1-75 M1-76 K2-79 M2-83 S7-83 W1-83 C1-86 H1-88 J1-88 M3-89 W2-90
		468	P2032	AK	715		5:32:58.9	−05:27:33	S1-98* H1-82* P2-04 B1-10 D1-14 G1-22 H1-23 B1-34 R1-46 H2-50 P1-52 P1-54 S1-58 K1-59 F1-70 S3-71 P2-73 M1-76 M2-83 C1-86 A1-88 H1-88 J1-88
4-89	256	141	P2029	AI	708	IRAS05329−0512?	5:32:59.1	−05:13: 0	P2-04 G1-20 H1-23 S1-24 T1-31 B1-34 R1-46 H2-50 P1-52 H1-53 P1-54 R1-56 S1-58 K1-59 H2-62 R1-62 F1-70 B1-71 S3-71 B2-72 H1-72 P2-73 C1-74 P1-75 M1-76 B2-81 P2-82 M2-83 H1-88 J1-88 M3-89 J6-90 W2-90
4-241	265		P2060	NT		KiHa76-166	5:32:59.2	−06:49:49	P1-52 H1-53 P1-54 K1-59 R1-62 M1-63 S3-71 A2-72 B2-72 G1-76 P5-81 P2-82 M2-83 P1-85 S3-90 W1-91 W2-91
4-360	259						5:32:59.4	−03:34:45	P2-82
						KiHa4-37	5:32:59.7	−01:13:56	W2-89
4-361	260		P2042	V418	705	KiHa76-168	5:33: 0.0	−04:50: 9	B1-34 P1-54 R1-56 K1-59 P2-82 W1-91
4-87	261		P2045	V419		KiHa76-167, IRAS05329−0512?	5:33: 0.0	−05:12: 7	H1-53 P1-54 R1-56 K1-59 B2-72 G1-76 S3-80 P2-82 M2-83 J1-88 J6-90 W1-91
				V801		IRAS05329−0628	5:33: 0.5	−06:28:40	T1-86 W5-86 W5-88 S5-89 S7-89 W4-89 M4-90 M1-91 M2-91
4-363	269			V564		KiHa76-170	5:33: 1.0	−06:11:31	R1-62? P2-82 W1-91
4-364	270			V798		KiHa76-171	5:33: 1.0	−06:16: 7	P2-82 G1-85 W1-91
						KiHa76-169	5:33: 1.0	−06:21:34	W1-91
		469	P2057		726		5:33: 1.3	−05: 7:57	B1-34 P1-54 W1-69 B1-72 M2-83 W1-83 H1-88
4-195	268					KiHa76-172	5:33: 1.5	−06: 1: 6	H1-53 K1-59 A2-72 G1-76 P2-82 S3-90 W1-91
						KiHa4-38	5:33: 1.8	−02:37: 0	W2-89
						KiHa76-173	5:33: 2.0	−05:51:41	W1-91
4-369	283						5:33: 2.0	−06:30:46	P2-82
4-368	282						5:33: 2.1	−06:24:46	P2-82 G1-85
4-362	264						5:33: 2.3	−06:17:28	P2-82 G1-85
4-366	275						5:33: 2.8	−06:45:57	P2-82 W2-91
4-51	266	143	P2066	AL	737	KiHa76-175	5:33: 2.9	−04:57:10	P2-04 H1-23 S2-24 B1-34 R1-46 P1-52 H1-53 P1-54 H2-55 R1-56 K1-59 R1-62 W1-66 W1-69 S3-71 B1-72 B2-72 H1-72 W1-72 G1-76 C2-79 K2-79 P2-82 M2-83 W1-83 H1-88 W1-91
4-164	263		P2059		758		5:33: 2.9	−05:44:40	B1-34 H1-53 P1-54 K1-59 A2-72 G1-76 P2-82 M2-83
4-365	274		P2078	V498	755	KiHa76-174	5:33: 3.0	−05:50:37	B1-34 P1-54 D1-58 H1-62 R1-62 M1-66 M1-68 H3-69 B1-71 S3-71 P2-82 M2-83 S7-83 W1-91
4-109	273		P2075		753		5:33: 3.4	−05:20:46	B1-34 H1-53 P1-54 K1-57 S1-58 K1-59 B1-63 W1-69 F1-70 M1-76 K3-82 P2-82 M2-83 W1-83 C1-86 J1-88
		470				HH34/source	5:33: 3.7	−06:28:53	R2-86 H1-88
4-54	267		P2067		743		5:33: 3.8	−04:59: 4	B1-34 H1-53 P1-54 K1-59 B2-72 G1-76 P2-82 M2-83
4-37	262		P2055		723		5:33: 3.9	−04:51:40	B1-34 H1-53 P1-54 B2-72 P2-82 M2-83
4-27	271		P2071	V565	739	KiHa76-179	5:33: 4.0	−04:48:50	B1-34 H1-53 P1-54 K1-59 R1-62 P2-82 M2-83 W1-91
4-77	272		P2072	V422	752	KiHa76-177	5:33: 4.0	−05: 6:54	B1-34 R1-46 H1-53 P1-54 H2-55 R1-56 K1-59 R2-69 G1-76 P2-82 M2-83 P1-85 W1-91
						KiHa76-178	5:33: 4.0	−05:20:49	W1-91
4-367	278					KiHa76-176	5:33: 4.0	−06:13:58	P2-82 W1-91
4-17	279						5:33: 4.1	−04:42:16	H1-53 K1-59 G1-76 P2-82
		471	P2086	NV	767	BD−5 1324	5:33: 4.1	−05:35: 1	S1-78* B1-34 P1-52 P1-54 J1-57 S1-58 K1-59 S1-62 S2-62 J1-65 B1-68 L1-68 W1-69 F1-70 S2-72 C1-73 C3-73 P2-73 G3-74 B2-76 M1-76 B4-77 C1-77 W2-77 B2-81 M2-83 H3-84 K1-85 H1-88 J1-88 V1-88 M3-89
4-84	277	144	P2084	V360	757	KiHa76-180	5:33: 4.2	−05:11:20	G1-22 B1-34 R1-46? P1-52 H1-53 P1-54 H2-55 R1-56 K1-57 S1-58 K1-59 H2-62 W1-69 F1-70

TABLE 1. CONTINUED.

Haro	PC	HBC	P	Name	Brun	Other	RA (1950)	DEC (1950)	References
(1)	(2)	(3)	(4)	(5)	(6)	(7)	(8)	(9)	(10)
4-84									B1-71 S3-71 A2-72 B1-72 H1-72 C1-74 D1-75 P1-75 B2-76 G1-76 M1-76 B4-77 K1-78 C2-79 M4-80 P2-82 M2-83 W1-83 I1-87 H1-88 J1-88 K3-88 M3-89 W1-91
		472				HH34/IRS5	5:33: 4.6	−06:28:37	R2-86 H1-88
4-22	276		P2081		756	KiHa76-181	5:33: 5.0	−04:45:52	B1-34 H1-53 P1-54 K1-57 B1-71 P2-82 M2-83 M3-89 W1-91
4-25	280		P2092		754	KiHa76-184	5:33: 5.0	−04:48:17	B1-34 H1-53 P1-54 K1-59 G1-76 P2-82 M2-83 W1-91
						KiHa76-182	5:33: 5.0	−05:33: 3	W1-91
4-239	286	145	P2105	TW		KiHa76-183	5:33: 5.2	−06:47:10	W1-03 H1-04 P2-04 H1-50 P1-52 H1-53 P1-54 K1-59 R1-62 M1-63 S3-71 A2-72 B2-72 H1-72 G1-76 C2-79 M4-80 A1-81 P2-82 M2-83 H1-88 W1-91 W2-91
						WBHa19	5:33: 5.3	−07: 3:55	W2-91
4-26	281		P2093	V423	768	KiHa76-185	5:33: 6.0	−04:48:47	B1-34 H1-53 P1-54 R1-56 K1-59 G1-76 P2-82 M2-83 W1-91
						KiHa76-186	5:33: 7.0	−06:16:24	W1-91
			P2127				5:33: 7.0	−06:54:30	P1-54 P5-81 S3-90
4-111	288	146	P2111	AM	789	KiHa76-188	5:33: 7.7	−05:23:19	P2-04 B1-10 H1-23 B1-34 R1-46 H1-50 H2-50 P1-52 H1-53 P1-54 R1-56 S1-58 K1-59 H2-62 F1-70 H1-72 M1-76 B1-79 C2-79 M4-80 P2-82 M2-83 H1-88 J1-88 W1-91
						WBHa20	5:33: 7.9	−06:41:24	W2-91
4-1	284					KiHa76-187	5:33: 8.0	−04:18:13	H1-53 K1-59 G1-76 P2-82 W1-91
4-371	287		P2109		781	KiHa76-190	5:33: 8.0	−04:53:13	B1-34 P1-54 P2-82 W1-91
	292	148	P2119	NY		KiHa76-189	5:33: 8.4	−05:14:16	H2-50 P1-52 P1-54 R1-56 S1-58 K1-59 F1-70 H1-72 P2-73 P2-82 M2-83 A1-88 H1-88 J1-88 H2-89 W1-91
4-370	285						5:33: 8.4	−06: 8:46	P2-82 G1-85
4-67	290	147	P2115	TV	785	KiHa76-191	5:33: 8.6	−05: 3: 8	P1-95* S1-98* W1-01 W1-03 P2-04 H1-23 H2-23 S1-24 B1-34 G1-46 R1-46 H1-50 P1-52 H1-53 P1-54 R1-56 K1-59 R1-62 J1-65 W1-69 B1-71 S3-71 H1-72 B2-76 G1-76 B4-77 K1-78 C2-79 M4-80 P2-82 M2-83 W1-83 H1-88 K3-88 Y1-88 M3-89 W1-91
4-372	289						5:33: 8.6	−06: 0:52	P2-82
						WBHa21	5:33: 8.9	−07:16:47	W2-91
4-133	295		P2123	V568	794	KiHa76-192	5:33: 9.0	−05:36: 3	B1-34 H1-53 P1-54 R1-62 P2-82 M2-83 J1-88 W1-91
4-129	294		P2122		821		5:33: 9.1	−05:33:28	B1-34 H1-53 P1-54 P2-82 M2-83 J1-88
4-73	291		P2116	V424	788		5:33: 9.7	−05: 6: 4	B1-34 H1-53 P1-54 R1-56 K1-59 G1-76 P2-82 M2-83
						KiHa4-39	5:33: 9.9	+00:51:28	W2-89
						St48	5:33:10.0	−00:36:24	S8-86
4-63	297					KiHa76-193	5:33:10.0	−05: 1:33	H1-53 G1-76 P2-82 W1-91
4-373	296					KiHa76-194	5:33:11.0	−06:25:18	P2-82 G1-85 W1-91
		473	P2143		808		5:33:11.3	−05:10:48	B1-34 P1-54 S1-58 J1-65 W1-69 F1-70 P1-75 M1-76 M2-83 W1-83 H1-88 J1-88
4-11	293					KiHa76-195, IRAS05332−0437	5:33:12.0	−04:37:10	H1-53 G1-76 P2-82 W1-91
4-52	298		P2141		800	KiHa76-196	5:33:12.0	−04:57:35	B1-34 H1-53 P1-54 P2-82 M2-83 W1-91
4-374	299					KiHa76-197	5:33:13.0	−05:59:55	P2-82 W1-91
5-73				V499		KiHa4-40	5:33:13.3	−00:59:44	H2-53 F1-58 F1-60 G1-65 W2-89
4-376	308						5:33:14.1	−06:23:35	P2-82 G1-85
						WBHa22	5:33:14.3	−07:22:27	W2-91
4-5	300	149	P2152	BO	810	San3, KiHa76-198	5:33:14.6	−04:26:47	B1-21 B1-34 H1-50 P1-52 H1-53 P1-54 R1-56 K1-59 W1-69 S1-71 S3-71 B1-72 B2-72 H1-72 G1-76 A1-77 M4-77 C2-79 M4-80 P2-82 M2-83 W1-83 C1-86 H1-88 K3-88 M3-89 W1-91
	301	150	P2167	AN	831		5:33:14.6	−05:30: 4	S1-78* P2-04 B1-10 G1-22 H1-23 C1-30 C2-31 B1-34 C2-35 C2-36 O1-40 G1-46 R1-46 J2-49 H2-50 P1-52 B1-54 P1-54 L1-56 S1-58 K1-59 H2-62 J1-65 K1-66 K1-68 F1-70 S3-71 H1-72 P2-73 M1-76 K1-78 M4-80 K3-82 P2-82 M2-83 M3-84 C1-86 I1-87 A1-88 H1-88 J1-88 V1-88
4-216	306	474	P2186	V571		KiHa76-199	5:33:14.7	−06:24:38	H1-53 P1-54 K1-59 R1-62 M1-63 A2-72 B2-72 G1-76 P2-82 M2-83 P1-85 R1-85 R2-85 H1-88 C2-90 S3-90 Y1-90 W1-91
						WBHa23	5:33:14.9	−07: 9:29	W2-91
		475	P2172	V569	834		5:33:15.5	−05:11: 9	B1-34 P1-54 S1-58 D1-61 R1-62 M1-66 M1-68 H3-69 W1-69 F1-70 B1-71 S3-71 P1-75 B2-76 M1-76 S3-80 M2-83 W1-83 A1-88 H1-88 J1-88
4-32	302		P2170	OP	842	KiHa76-201	5:33:16.0	−04:49:56	B1-34 R1-46 P1-52 H1-53 P1-54 H2-55 R1-56 K1-59 G1-76 P2-82 M2-83 W1-91
4-76	303		P2171	AO	839	KiHa76-200	5:33:16.0	−05: 7:33	P2-04 H1-23 S2-24 B1-34 R1-46 P1-52 H1-53 P1-54 R1-56 K1-59 R1-62 B1-71 P1-75 G1-76 K2-79 P2-82 M2-83 W1-91
4-375	304		P2177		825		5:33:16.1	−04:45:23	B1-34 P1-54 P2-82 G1-85
4-1a	307					KiHa76-205	5:33:16.6	−04:15:23	H1-53 P2-82 W1-91
						WBHa24	5:33:16.6	−07:14: 6	W2-91
4-231	312	151		V573		KiHa76-202, IRAS05332−0637	5:33:16.7	−06:36:43	H1-53 K1-59 R1-62 M1-63 A2-72 H1-72 D1-75 G1-76 C2-79 A1-81 P2-82 T1-86 H1-88 S7-89 W2-90 W1-91 W2-91
						Xray23	5:33:16.7	−07: 3:46	S3-90
4-81	305	476	P2181	V500	850		5:33:17.1	−05: 9: 9	B1-34 H1-53 P1-54 K1-57 W1-69 B1-72 B2-72 P1-75 G1-76 K2-79 P2-82 M2-83 W1-83 C1-86

TABLE 1. CONTINUED.

Haro (1)	PC (2)	HBC (3)	P (4)	Name (5)	Brun (6)	Other (7)	RA (1950) (8)	DEC (1950) (9)	References (10)
4-81									H1-88 M3-89
						WBHa25	5:33:17.4	−07: 8:56	W2-91
						WBHa26	5:33:17.5	−07:22:37	W2-91
4-377	309		P2199		852	KiHa76-204	5:33:18.0	−05:22:28	B1-34 P1-54 S1-58 P3-76 P2-82 J1-88 W1-91
4-378	310		P2201		859	KiHa76-203	5:33:18.0	−05:52:54	B1-34 P1-54 P2-82 M2-83 C1-86 M3-89 W1-91
						WBHa27	5:33:18.8	−07:22: 0	W2-91
						WBHa28	5:33:19.2	−07:18:42	W2-91
5-84							5:33:20.0	−03:35:11	H2-53 F1-60
4-86	314		P2205	V574	863	KiHa76-208	5:33:20.0	−05:12:21	B1-34 H1-53 P1-54 K1-57 S1-58 K1-59 R1-62 B2-72 M1-76 P2-82 M2-83 C1-86 J1-88 W1-91
4-96	315		P2207		869	KiHa76-206	5:33:20.0	−05:15: 9	B1-34 H1-53 P1-54 R1-56 K1-59 B2-72 G1-76 P2-82 M2-83 J1-88 W1-91
4-182	318		P2218	CF	877	KiHa76-207	5:33:20.0	−05:51:17	P2-04 H1-23 S2-24 B1-25 B1-34 R1-46 H1-50 P1-52 H1-53 P1-54 K1-59 B1-71 G1-76 P2-82 M2-83 W1-91
4-382	323			V988			5:33:20.0	−06:30:59	P2-82 S3-90
4-379	311						5:33:20.3	−06:14:11	P2-82
4-66	313	152	P2203	CE	856	KiHa76-209	5:33:20.4	−05: 3:20	P2-04 S2-24 B1-25 H1-31 B1-34 R1-46 H1-50 P1-52 H1-53 P1-54 H2-55 R1-56 R1-62 W1-66 H1-72 W1-72 G1-76 A1-77 M4-77 C2-79 M4-80 T1-80 A1-81 P2-82 M2-83 H1-88 W1-91
4-384	329		P2254	OU	897		5:33:20.7	−05:53:29	B1-34 P1-52 P1-54 K1-59 S3-71 P2-82 M2-83 S7-83
			P2210	V378	868	Ton1	5:33:20.9	−05:42:53	B1-34 H3-53 P1-54 R1-56 P1-58 R1-69 R3-69 R4-69
4-381	320		P2228	V812		KiHa76-210	5:33:21.0	−05:55:48	P1-54 P2-82 W1-91
4-215	322		P2236	V814		KiHa76-211	5:33:21.0	−06:23:27	H1-53 P1-54 M1-63 G1-76 P2-82 M2-83 W1-91
4-69	317	477	P2215	V1018	860	CE/c	5:33:21.1	−05: 3:30	B1-34 H1-53 P1-54 K1-59 G1-76 P3-76 C2-79 P2-82 M2-83 H1-88
						Xray26b	5:33:21.1	−06:35:14	S3-90
						KiHa4-41	5:33:21.3	−01:24:55	W2-89
4-110	321		P2234	V364	879		5:33:21.3	−05:23: 5	B1-34 R1-46 P1-52 H1-53 P1-54 R1-56 K1-59 P2-82 J1-88
			P2245	V379	886	Ton2	5:33:21.5	−05:15:53	B1-34 H3-53 P1-54 R1-56 P1-58 R1-69 R3-69 R4-69 J1-88
4-383	325		P2243	V575	883		5:33:21.6	−05: 8:53	B1-34 P1-54 R1-62 P1-75 P1-85 P2-82 M2-83
						WBHa29	5:33:21.8	−07:32:40	W2-91
						KiHa4-42	5:33:22.0	−01:24:56	W2-89
4-380	319		P2226				5:33:22.0	−04:48:17	P1-54 P2-82 G1-85
4-207	328		P2249	V1001	891	KiHa76-212	5:33:22.0	−06:13:58	B1-34 H1-53 P1-54 B1-71 A2-72 B2-72 G1-76 P2-82 M2-83 W1-91
	316		P2211	V389	853	Ton8?	5:33:22.4	−04:26:23	B1-34 H2-54 P1-54 H1-55 P1-58 K1-59 H1-62 R1-62 K1-64 H3-69 W1-69 B1-72 B2-72 A1-74 P2-82 M2-83
4-385	330			V989			5:33:22.9	−06:42:43	P2-82 M4-88 W2-91
4-104	326	153	P2246	OT	889	KiHa76-213	5:33:23.1	−05:18:20	B1-34 R1-46 P1-52 H1-53 P1-54 R1-56 K1-59 H1-62 H2-62 R1-62 R1-69 R3-69 R4-69 B2-72 H1-72 G1-76 C2-79 P2-82 P1-85 C1-86 H1-88 J1-88 W1-91
4-123	327	154	P2247	T	884	BD−5 1329	5:33:23.1	−05:30:26	S1-78* S1-82* S1-83* P1-93* P2-93* P1-95* W1-03 P2-04 B1-08 C1-12 C1-18 L1-19 H1-23 C1-24 C1-25 C1-26 C1-27 C2-27 C1-29 C2-30 J1-30 L1-30 C1-31 C1-32 Z1-32 C1-33 J1-33 B1-34 C1-34 C1-35 C1-36 C1-37 O1-40 S1-44 C1-46 G1-46 R1-46 H1-49 M2-49 P1-49 H1-50 L1-50 P1-50 L1-51 H2-52 H3-52 P1-52 H1-53 B1-54 P1-54 L1-56 S1-58 K1-59 H2-60 H2-62 K1-63 K1-64 J1-65 B1-68 W1-69 F1-70 G1-70 M3-70 W1-70 S3-71 H1-72 C2-73 C3-73 P2-73 B2-74 G3-74 B2-76 M1-76 C1-77 B3-77 B4-77 K1-77 W2-77 G2-78 C2-79 P1-79 V1-79 M4-80 B2-81 T1-81 F1-82 P2-82 L2-83 M2-83 F1-84 F2-84 H3-84 F1-85 K2-85 S7-85 H1-86 S7-86 B3-87 H6-87 I1-87 M9-87 I1-88 H1-88 J1-88 K1-88 K3-88 V1-88 Y1-88 I1-89 M3-89 D1-90 J3-90 J4-90 S2-90
		478	P2244		887		5:33:23.9	−05:10: 0	B1-34 P1-54 S1-58 W1-69 F1-70 B1-72 P1-75 M2-83 W1-83 H1-88 M3-89 W1-90
4-20	324		P2241		878	KiHa76-214	5:33:24.0	−04:44:56	B1-34 H1-53 P1-54 R1-56 K1-59 B1-71 G1-76 P2-82 M2-83 W1-91
						Xray26c	5:33:24.0	−06:35:26	S3-90
4-244	334		P2264	AT		KiHa76-215	5:33:24.2	−06:52:23	W1-03 P2-04 H1-23 P1-52 H1-53 P1-54 K1-59 R1-62 M1-63 A2-72 G1-76 P2-82 M2-83 W1-91 W2-91
				V813			5:33:24.3	−06:35: 8	S3-90
		479	P2252		892		5:33:24.8	−05: 6:57	B1-34 P1-54 W1-69 F1-70 B1-72 M1-76 P1-75 M2-83 S7-83 S9-83 S10-83 W1-83 R2-84 H1-88 V1-88 M3-89
						KiHa76-216	5:33:25.0	−04:11:48	W1-91
4-204	333					KiHa76-217, IRAS05334−0611	5:33:25.0	−06:11:52	H1-53 K1-59 A2-72 G1-76 P2-82 T1-86 W5-86 H1-91 W1-91
4-72	332	155	P2263	AR	901	KiHa76-218	5:33:26.2	−05: 6: 6	P2-04 H1-23 S1-24 B1-34 R1-46 H1-50 H2-50 P1-52 H1-53 P1-54 R1-56 K1-59 H2-62 B1-71 S3-71 H1-72 G1-76 B1-79 C2-79 P2-82 M2-83 C1-86 H1-88 W1-91
5-78						KiHa4-43	5:33:26.9	−01:34:15	H2-53 F1-60 G1-65 W2-89
4-172	338						5:33:26.9	−05:47:18	H1-53 P2-82

TABLE 1. CONTINUED.

Haro	PC	HBC	P	Name	Brun	Other	RA (1950)	DEC (1950)	References
(1)	(2)	(3)	(4)	(5)	(6)	(7)	(8)	(9)	(10)
4-120	335		P2269	OW	904	KiHa76-220	5:33:27.0	−05:28:35	B1-34 R1-46 P1-52 H1-53 P1-54 R1-56 K1-59 R1-62 G1-76 P2-82 J1-88 W1-91
			P2270	OX	905	Ton3	5:33:27.2	−05:28:54	B1-34 R1-46 P1-52 H3-53 P1-54 R1-56 K1-59 R1-62 J1-88
4-114	340		P2280	V428	919		5:33:27.3	−05:24:54	B1-34 H1-53 P1-54 R1-56 K1-59 G1-76 P2-82 M2-83 J1-88
4-24	331		P2255	AS	898		5:33:28.0	−04:49: 6	P2-04 W1-03 H1-04 H1-23 S2-24 B1-34 R1-46 P1-52 H1-53 P1-54 R1-56 K1-59 R1-62 G1-76 P2-82 M2-83
4-181	339					KiHa76-221	5:33:29.0	−05:51:20	H1-53 P2-82 W1-91
						WBHa30	5:33:29.3	−07:10: 4	W2-91
4-9	337					KiHa76-222	5:33:30.0	−04:31:15	H1-53 H2-55 K1-59 B2-72 G1-76 P2-82 W1-91
4-189	342	157	P2285	AU	927	KiHa76-224	5:33:30.9	−05:59: 9	P2-04 P4-04 H1-23 B1-34 R1-46 H1-50 P1-52 H1-53 P1-54 H2-55 K1-59 R1-62 W1-63 W1-66 A2-72 H1-72 W1-72 A1-74 D1-75 G1-76 C2-79 P2-82 M2-83 H1-88 W1-91
						KiHa76-225	5:33:31.0	−06:17:28	W1-91
4-225	344					KiHa76-223	5:33:31.0	−06:31:28	H1-53 M1-63 P2-82 W1-91
4-233	348			V576		KiHa76-226	5:33:31.1	−06:42: 8	H1-53 K1-59 R1-62 M1-63 A2-72 G1-76 P2-82 W1-91 W2-91
4-61	341	156	P2282	V390	918	Ton9?	5:33:31.2	−05: 0:37	B1-34 H1-53 H2-54 P1-54 H1-55 R1-56 P1-58 K1-59 H1-62 H2-62 R1-62 K1-64 B2-72 H1-72 G1-76 C2-79 A1-81 P2-82 M2-83 H1-88
4-237	349	158	P2299	V577		Nk34, KiHa76-227, IRAS05335−0645?	5:33:31.5	−06:44:32	H1-53 P1-54 K1-59 R1-62 M1-63 H1-72 S3-71 A2-72 D1-75 G1-76 C2-79 A1-81 P2-82 M2-83 N1-86 T1-86 W5-86 A1-88 H1-88 W5-88 S5-89 S7-89 M4-90 S3-90 W2-90 W1-91 W2-91
						WBHa31	5:33:31.5	−07:30:22	W2-91
4-387	347		P2298				5:33:31.6	−06:40: 3	P1-54 P5-81 P2-82 G1-85 S3-90 W2-91
		480	P2292		928		5:33:31.9	−05:41:50	B1-34 P1-54 W1-69 F1-70 B1-72 P2-73 A1-74 P1-75 B2-76 M1-76 M2-83 S9-83 W1-83 R2-84 M2-85 H1-88 V1-88
4-232	346		P2297	OY		KiHa76-230	5:33:31.9	−06:38:22	P1-52 H1-53 P1-54 K1-59 R1-62 M1-63 A2-72 G1-76 P2-82 M2-83 W1-91 W2-91
	345			V654		KiHa76-229	5:33:32.0	−06: 4:29	P2-82 W1-91
4-386	343					KiHa76-228	5:33:32.0	−06:25:34	P2-82 G1-85 W1-91
4-389	351		P2307				5:33:32.3	−06:17:54	P1-54 P2-82 M2-83
						WBHa32	5:33:32.3	−07:27:19	W2-91
4-388	350						5:33:32.6	−06: 0:48	P2-82 G1-85
						WBHa33	5:33:33.3	−06:51:34	W2-91
4-83	356		P2318	V655	947		5:33:33.6	−05:11:12	B1-34 H1-53 P1-54 K1-57 S1-58 K1-59 B1-71 S3-71 B2-72 A1-74 G1-76 M1-76 P2-82 M2-83
4-40	355		P2315		941		5:33:33.9	−04:52:48	B1-34 H1-53 P1-54 R1-56 K1-59 B2-72 G1-76 P2-82 M2-83
4-236	354	159	P2312	AV		Nk35, KiHa76-231, IRAS05335−0645?	5:33:34.2	−06:44:23	W1-03 P2-04 H1-50 P1-52 H1-53 P1-54 K1-59 R1-62 M1-63 S3-71 A2-72 B2-72 H1-72 D1-75 G1-76 C2-79 M4-80 A1-81 P2-82 M2-83 N1-86 T1-86 W5-86 A1-88 H1-88 W5-88 S5-89 S7-89 M4-90 S3-90 W2-90 W1-91 W2-91
		481				AV/c, IRAS05335−0645?	5:33:34.2	−06:44:23	P1-54 C2-79 T1-86 W5-86 H1-88 W5-88 S5-89 S7-89 M4-90 W2-90
4-390	353		P2309		931		5:33:34.4	−04:29:54	B1-34 P1-54 A1-74 P2-82 G1-85
						WBHa34	5:33:34.7	−06:42:40	W2-91
4-210	359			V393		Ton12, KiHa76-232	5:33:35.0	−06:17:21	H1-53 H1-54 H1-55 P1-58 K1-59 R1-62 M1-63 B2-72 G1-76 P2-82 W1-91
						WBHa35	5:33:35.6	−06:48:40	W2-91
						WBHa36	5:33:36.0	−07:25:28	W2-91
						KiHa4-44	5:33:36.2	+01:31: 7	W2-89
						WBHa37	5:33:37.0	−06:52:24	S3-90 W2-91
						WBHa38	5:33:37.9	−06:36:17	W2-91
4-4	352					KiHa76-234	5:33:38.0	−04:22:28	H1-53 K1-59 G1-76 P2-82 W1-91
4-391	357		P2322		934	KiHa76-233	5:33:38.0	−04:43:44	B1-34 P1-54 P2-82 G1-85 W1-91
						Xray31	5:33:38.0	−06:13:17	S3-90
						WBHa39	5:33:38.1	−07: 3:10	W2-91
						WBHa40	5:33:38.3	−07:11:28	W2-91
4-184	370						5:33:38.7	−05:52:54	H1-53 G1-76 P2-82
4-394	366		P2335			KiHa76-236	5:33:38.9	−06:48:22	P1-54 P2-82 G1-85 S3-90 W1-91 W2-91
4-393	365		P2334	AW		KiHa76-235	5:33:39.0	−06:31:22	P2-04 W1-06 H1-23 S1-24 P1-52 P1-54 K1-59 R1-62 M1-63 S3-71 B2-72 P2-82 M2-83 G1-85 W1-91
4-64	367		P2337	V580	964		5:33:39.7	−05: 1:54	B1-34 H1-53 P1-54 K1-59 R1-62 A1-74 G1-76 P2-82 M2-83
						KiHa4-45	5:33:39.8	−01:52:15	W2-89
4-16	360		P2326	CH	942	KiHa76-237	5:33:40.0	−04:43:11	P2-04 H1-23 S2-24 B1-34 R1-46 H1-50 P1-52 H1-53 P1-54 R1-56 K1-59 B2-72 G1-76 P2-82 M2-83 P1-85 W1-91
4-392	358		P2323		943		5:33:40.0	−04:50:42	B1-34 P1-54 P2-82 G1-85
4-132	362			V579		KiHa76-238	5:33:40.0	−05:36: 8	H1-53 K1-59 R1-62 G1-76 P2-82 W1-91
4-153	363		P2332		954	KiHa76-239	5:33:40.0	−05:42:12	B1-34 H1-53 P1-54 K1-59 A2-72 G1-76 P2-82 M2-83 W1-91
4-163	364		P2333	V501	953	KiHa76-240	5:33:40.0	−05:44:11	B1-34 R1-46 H1-53 P1-54 K1-57 K1-59 F1-70 B1-71 S3-71 A1-74 G1-76 M1-76 P2-82 M2-83 M3-89 W1-91
4-209	369		P2338	AX	955	KiHa76-241	5:33:40.0	−06:16:15	P2-04 H1-23 S1-24 B1-34 H1-50 P1-52 H1-53 P1-54 K1-59 R1-62 M1-63 S3-71 A2-72 B2-72 G1-76 P2-82 M2-83 W1-91
4-35	361		P2330		956	KiHa76-242	5:33:41.0	−04:51:51	B1-34 H1-53 P1-54 K1-59 G1-76 P2-82 M2-83

TABLE 1. CONTINUED.

Haro	PC	HBC	P	Name	Brun	Other	RA (1950)	DEC (1950)	References
(1)	(2)	(3)	(4)	(5)	(6)	(7)	(8)	(9)	(10)
4-35									W1-91
						WBHa41	5:33:41.4	−06:58:55	W2-91
4-395	368					KiHa76-243	5:33:42.0	−05:38:28	P2-82 W1-91
4-398	377		P2350	AY		KiHa76-244	5:33:42.3	−06:50:17	P2-04 P1-52 P1-54 K1-59 R1-62 M1-63 P2-82 M2-83 G1-85 W1-91 W2-91
						Xray34a	5:33:42.9	−06:19: 0	S3-90
4-106	371		P2347	V502	965	KiHa76-245	5:33:43.0	−05:21:34	B1-34 H1-53 P1-54 K1-57 S1-58 K1-59 M1-66 M1-68 H3-69 F1-70 B1-71 S3-71 A1-74 G1-76 M1-76 P2-82 M2-83 M3-89 W1-91
4-162	372					KiHa76-246	5:33:43.0	−05:44:16	H1-53 K1-59 A2-72 G1-76 P2-82 W1-91
				V825			5:33:43.0	−06:20:25	S3-90
						WBHa42	5:33:43.4	−07:32:19	W2-91
						WBHa43	5:33:43.6	−07:12:11	W2-91
4-152	376					KiHa76-247	5:33:44.0	−05:41:38	H1-53 G1-76 P2-82 W1-91
						WBHa44	5:33:44.5	−06:35:24	W2-91
4-399	379						5:33:45.0	−05:42:19	P2-82
	378			V391		Ton10	5:33:45.3	−05:23:43	H2-54 H1-55 R1-56 P1-58 K1-59 P2-82
4-102	375			V824			5:33:45.4	−05:17:37	H1-53 K1-59 G1-76 P2-82
						Xray33b	5:33:46.3	−06:25:27	S3-90
4-396	373						5:33:46.5	−04:22:25	P2-82
4-397	374						5:33:46.5	−04:24:25	P2-82 G1-85
						Xray33a	5:33:46.6	−06:25:23	S3-90
						KiHa76-249	5:33:47.0	−05:17:23	W1-91
4-206	380					KiHa76-250	5:33:48.0	−06:15: 5	H1-53 A2-72 G1-76 P2-82 W1-91
4-212	383		P2369	BB			5:33:48.7	−06:19:26	P2-04 H1-23 S1-24 P1-52 H1-53 P1-54 K1-59 R1-62 M1-63 S3-71 B2-72 P2-82 M2-83 S3-90
4-208	382					KiHa76-251	5:33:49.0	−06:16:39	H1-53 K1-59 A2-72 G1-76 P2-82 W1-91
	381	162	P2368	AZ	982		5:33:49.3	−05:13:32	W1-01 W1-03 P2-04 H1-23 S1-24 B1-34 R1-46 H2-50 P1-52 B1-54 P1-54 R1-56 S1-58 K1-59 H2-62 R1-62 H3-69 W1-69 F1-70 B1-71 S3-71 H1-72 A1-74 B2-76 M1-76 B4-77 K1-78 C2-79 B2-81 M2-81 P2-82 M2-83 P1-85 C1-86 H2-86 H1-88 K3-88 M4-88 M3-89
						WBHa45	5:33:49.7	−07:29:24	W2-91
		160		PQ			5:33:49.8	−02:12:47	K1-59 H1-72 C1-74 C2-79 M4-80 H1-88
						IRAS05337−0639	5:33:49.8	−06:39:39	T1-86 S7-89
4-400	384						5:33:50.5	−06: 7:19	P2-82
						WBHa46	5:33:50.6	−07:26:34	W2-91
5-75		161		PU		KiHa4-46, IRAS05338−0044	5:33:51.4	−00:44: 0	M1-49 H2-53 F1-58 K1-59 F1-60 H2-62 G1-65 H1-72 C2-79 H1-88 W2-89 W2-90
4-401	385					KiHa76-252	5:33:52.0	−05:16:27	P2-82 G1-85 W1-91
4-213	388			V832		KiHa76-253	5:33:52.0	−06:22:27	H1-53 K1-59 M1-63 A2-72 B2-72? G1-76 P5-81 P2-82 W1-91
						WBHa47	5:33:52.3	−07:14:43	W2-91
						L1641-N, IRAS05338−0624	5:33:52.5	−06:23:53	T1-86 W5-86 W5-88 B4-89 S5-89 S6-89 S7-89 W1-89 W4-89 M4-90 W5-90 H1-91 M1-91 M2-91
4-402	387					KiHa76-254	5:33:53.0	−05:50:13	P2-82 W1-91
						Xray36b	5:33:53.6	−06:33: 7	S3-90
						WBHa48	5:33:53.9	−06:52:22	W2-91
4-75	386					KiHa76-255	5:33:54.0	−05: 7:40	H1-53 P2-82 W1-91
						St49	5:33:54.0	−06:46:40	S8-86 D1-88
			P2382				5:33:54.7	−06:32:58	P1-54 P5-81 S3-90
						KiHa4-47	5:33:55.1	+00:14:43	W2-89
	399			V839			5:33:55.1	−07: 7:16	P2-82 W2-91
		483				Cohen-Schwartz star, Nk40	5:33:55.6	−06:47:25	C3-79 H1-81 B7-82 E1-82 C1-83 C2-83 J2-83 M7-83 M8-83 C4-84 L1-85 P3-85 R5-85 S8-85 N1-86 H1-87 I1-87 H1-88 S11-89
						WBHa49	5:33:55.8	−06:43:21	W2-91
4-218	390			V582			5:33:56.1	−06:27:50	H1-53 K1-59 R1-62 M1-63 A2-72 G1-76 P1-79 P2-82
4-404	392		P2390		995		5:33:56.8	−05:48:26	B1-34 P1-54 A1-74 P2-82 M2-83
	391			V833		KiHa76-257	5:33:57.0	−05: 8:57	P2-82 W1-91
						WBHa50	5:33:57.0	−07:17:53	W2-91
						WBHa51	5:33:57.3	−06:55:47	W2-91
						WBHa52	5:33:57.9	−07:32:26	W2-91
						KiHa76-259	5:33:58.0	−04:52: 8	W1-91
						KiHa76-260	5:33:58.0	−06: 7: 1	W1-91
4-403	389					KiHa76-258	5:33:58.0	−06:25: 0	P2-82 W1-91
						WBHa53	5:33:58.4	−07:10:51	W2-91
			P2388	PR			5:33:58.5	−06:19:20	P1-54 K1-59 S3-71 B2-72? P5-81 S3-90
						WBHa54	5:33:58.7	−06:54:14	W2-91
4-203	393		P2391		993	KiHa76-261	5:33:59.0	−06: 9:52	B1-34 H1-53 P1-54 K1-59 W1-69 B1-72 B2-72 A1-74 B2-76 G1-76 B4-77 P2-82 M2-83 W1-83 M3-89 W1-91
4-235	395	164	P2393	V380		BD−6 1253, Nk51, KiHa76-263, IRAS05339−0644	5:33:59.5	−06:44:46	H1-46 M1-46 G1-48 J1-49 M2-49 H2-52 P1-52 H1-53 B1-54 P1-54 K1-59 B1-60 H2-60 H2-62 S2-62 J1-66 K1-66 M1-66 B1-68 K1-68 M1-68 M2-68 R1-68 D1-69 D2-69 G1-70 L1-70 M1-70 M3-70 W1-70 Z1-70 G1-71 S3-71 W1-71 B2-72 H1-72 S3-72 W2-72 A1-73 C2-73 C3-73 G3-73 L1-73 Z1-73 B2-74 B4-74 G3-74 I1-74 K1-74 L2-74 S4-74 D1-75 S1-75 A2-77 D1-77 G1-77 H1-77 G1-78 G2-78 S2-78 W2-78 C2-79 G2-79 P1-79 S2-79 V1-79 C2-80 C3-80 G1-80 H2-80 S1-80 W3-80 G1-81 L1-81 P5-81 T1-81 B10-82 C3-82 F1-82 K5-82 M3-82 P2-82 L2-83 W3-83 B1-84 C1-84 F1-84 F2-84 A1-85 C7-85 E2-85

TABLE 1. CONTINUED.

Haro (1)	PC (2)	HBC (3)	P (4)	Name (5)	Brun (6)	Other (7)	RA (1950) (8)	DEC (1950) (9)	References (10)
4-235									F1-85 G3-85 K2-85 L1-85 R5-85 E1-86 H1-86 N1-86 S1-86 S7-86 S9-86 T1-86 B2-87 B3-87 E2-87 H6-87 I1-87 M6-87 P2-87 H1-88 H2-88 K2-88 K3-88 L3-88 V2-88 Y1-88 A1-89 C2-89 C6-89 M3-89 S7-89 B1-90 C2-90 D1-90 J3-90 J4-90 M4-90 S3-90 W2-90 M1-91 M2-91 W1-91 W2-91
4-125	394	163		V951		KiHa76-264	5:34: 0.2	−05:32:44	H1-53 K1-59 B1-63? H1-72 C2-79 G1-76 A1-81 P2-82 H1-88 W1-91
						IRAS05339−0626	5:34: 0.4	−06:26:45	T1-86 S7-89 M1-91 M2-91
			P2385	V990			5:34: 0.4	−06:28:16	P1-54 P5-81 S3-90
						KiHa76-265	5:34: 1.0	−04:18: 0	W1-91
						KiHa76-266	5:34: 1.0	−04:55:39	W1-91
4-406	398					KiHa76-267	5:34: 1.0	−06:25: 0	P2-82 G1-85 W1-91
						WBHa55, Nk50?, IRAS05339−0646?	5:34: 2.0	−06:46:11	N1-86? S11-89? M1-91 M2-91 W2-91
4-405	397						5:34: 2.3	−06:17:26	P2-82
4-407	402		P2409				5:34: 2.4	−06:10: 8	P1-54 P2-82 G1-85
5-74						KiHa4-48	5:34: 2.6	−01: 4: 4	H2-53 F1-58 K1-59 F1-60 W2-89
						KiHa4-49	5:34: 2.9	−02:11:54	W2-89
4-105	396		P2395				5:34: 3.4	−05:21:50	H1-53 P1-54 K1-59 P2-82 M2-83 C1-86
						WBHa56	5:34: 3.5	−06:36:28	W2-91
						WBHa57	5:34: 3.7	−06:40: 0	W2-91
4-103	400		P2403	V367	1005	KiHa76-269	5:34: 4.0	−05:19: 1	P2-04 P4-04 H1-23 B1-34 R1-46 P1-52 H1-53 P1-54 R1-56 K1-59 A2-72 B2-72 G1-76 P2-82 M2-83 W1-91
4-214	401			V584		KiHa76-268	5:34: 4.0	−06:24:58	H1-53 R1-62 M1-63 A2-72 G1-76 P2-82 W1-91
						WBHa58	5:34: 5.4	−06:42:52	W2-91
4-408	404					KiHa76-270	5:34: 6.0	−06:14:25	P2-82 G1-85 W1-91
	405	165	P2412	BD			5:34: 6.1	−06:21: 8	P2-04 H1-23 S1-24 P1-52 P1-54 K1-59 H2-62 R1-62 M1-63 S3-71 B2-72 H1-72 D1-75 C2-79 M4-80 P2-82 M2-83 H2-86 H1-88
						WBHa59	5:34: 6.3	−06:42:21	W2-91
4-192	403					KiHa76-271	5:34: 7.0	−05:59:41	H1-53 K1-59 G1-76 P2-82 W1-91
						KiHa4-50	5:34: 8.0	−01: 9:40	W2-89
						WBHa60	5:34: 8.1	−06:45: 2	W2-91
4-187	409					KiHa76-272	5:34: 9.0	−05:57:16	H1-53 G1-76 P2-82 W1-91
4-409	406		P2415				5:34: 9.5	−05:13:21	P1-54 A1-74 P2-82 G1-85
4-70	407		P2459	V657	1043		5:34: 9.7	−05: 6:27	B1-34 H1-53 H2-54 P1-54 K1-59 B2-72 A1-74 G1-76 P2-82 M2-83 C1-86
4-119	408	166	P2421	BC	1014	KiHa76-273	5:34: 9.8	−05:28:13	P2-04 H1-23 B1-34 R1-46 H1-50 P1-52 H1-53 P1-54 H2-55 R1-56 K1-59 W1-66 B1-71 A2-72 H1-72 W1-72 A1-74 G1-76 C2-79 M4-80 P2-82 M2-83 H1-88 W1-91
4-227	410			V585		KiHa76-274	5:34:11.0	−06:35:11	H1-53 A2-72 P5-81 P2-82 W1-91
						KiHa76-275	5:34:12.0	−05:14:11	W1-91
						WBHa61	5:34:13.2	−07:22:11	W2-91
4-205	413					KiHa76-276	5:34:14.0	−06:15:20	H1-53 G1-76 P2-82 W1-91
4-413	416						5:34:14.4	−06:12: 9	P2-82
						WBHa62	5:34:14.6	−06:51:33	W2-91
				V845		WBHa63	5:34:14.9	−06:53:45	S3-90 W2-91
4-230	412			V846		KiHa76-277, IRAS05342−0635	5:34:15.2	−06:35:46	H1-53 A2-72 G1-76 P5-81 P2-82 S7-89 M4-90 S3-90 W2-90 W1-91 W2-91
4-410	411						5:34:15.3	−05:24: 3	P2-82 G1-85
4-412	415					KiHa76-278	5:34:17.0	−06: 0:19	P2-82 W1-91
						WBHa64	5:34:17.0	−06:58:58	W2-91
						KiHa76-279	5:34:18.0	−04: 0:59	W1-91
4-221	420					KiHa76-280	5:34:19.0	−06:29:57	H1-53 K1-59 A2-72 G1-76 P2-82 W1-91
						WBHa65	5:34:19.9	−06:37:13	W2-91
4-411	414					KiHa76-281	5:34:20.0	−05:38:18	P2-82 G1-85 W1-91
4-414	417						5:34:20.6	−06: 1:33	P2-82 G1-85
4-415	418						5:34:20.6	−06: 1:51	P2-82 G1-85
						KiHa76-282	5:34:22.0	−05: 5:56	W1-91
	419	167	P2441		1030	KiHa76-283, IRAS05343−0427?	5:34:22.7	−04:27:27	B1-34 P1-54 H2-62 M1-66 M1-68 W1-69 M3-70 B1-72 B2-72 H1-72 A1-74 B2-76 M2-76 B4-77 K1-78 C2-79 P2-82 M2-83 S9-83 R2-84 I1-87 H1-88 K3-88 Y1-88 M3-89 W2-90 W1-91
		484	P2441/c			IRAS05343−0427?	5:34:22.7	−04:27:27	C2-79 H1-88 W2-90
4-80	421		P2449	V852	1038	KiHa76-284	5:34:24.0	−05:10:22	B1-34 H1-53 P1-54 K1-59 B2-72 A1-74 G1-76 P2-82 M2-83 W1-91
4-416	422						5:34:24.1	−06:43:15	R1-62? P2-82 G1-85 S3-90 W2-91
						WBHa66	5:34:24.3	−07:13:13	W2-91
						WBHa67	5:34:24.4	−06:50:38	W2-91
						WBHa68	5:34:25.6	−06:37: 1	W2-91
4-418	424						5:34:26.2	−06:21:34	P2-82 G1-85
						KiHa76-285	5:34:27.0	−05:15:33	W1-91
4-417	423						5:34:28.5	−04:21: 4	P2-82
						KiHa4-51	5:34:28.7	+00:41:38	W2-89
						WBHa69	5:34:29.8	−07: 8:25	W2-91
4-113	425		P2470	PW	1047	KiHa76-286	5:34:32.0	−05:25:26	R1-90* P4-04 H1-23 B1-34 R1-46 P1-52 H1-53 P1-54 R1-56 K1-59 B2-72 A1-74 G1-76 P2-82 M2-83 P1-85 W1-91
						KiHa4-52	5:34:32.2	+00: 7: 8	W2-89
		485	P2473	V586	1051	HD37258, BD−6 1257, IRAS05345−0610	5:34:32.7	−06:11: 2	B1-34 P1-54 S1-62 B1-67 W1-69 S3-71 B1-72 S2-72 G3-74 B2-76 W2-77 B2-81 M1-82 M2-83 R3-83 K2-86 P3-86 H1-88 M3-89 W2-90
						KiHa4-53	5:34:33.7	+00:34: 3	W2-89

TABLE 1. CONTINUED.

Haro	PC	HBC	P	Name	Brun	Other	RA (1950)	DEC (1950)	References
(1)	(2)	(3)	(4)	(5)	(6)	(7)	(8)	(9)	(10)
4-226	427	168	P2479	BE		Nk59, KiHa76-287, IRAS05345−0635	5:34:33.7	−06:35:12	P2-04 H1-23 S1-24 P1-52 H1-53 P1-54 K1-59 H2-62 R1-62 M1-63 A2-72 B2-72 H1-72 D1-75 G1-76 C2-79 P2-82 M2-83 N1-86 H1-88 L3-88 S7-89 S11-89 M4-90 W2-90 W1-91
4-138	426	486	P2478	V381	1054	KiHa76-288	5:34:35.2	−05:38:16	B1-34 R1-46 P1-52 H1-53 P1-54 K1-57 K1-59 W1-69 F1-70 B1-71 B1-72 A1-74 B2-76 G1-76 B4-77 K1-78 P2-82 M2-83 W1-83 C1-86 H1-88 M3-89 W1-91
						WBHa70	5:34:35.2	−07:14:24	W2-91
						KiHa4-54	5:34:37.3	+01:16:32	W2-89
4-419	428						5:34:39.3	−05:25:11	P2-82
						WBHa71	5:34:40.0	−06:48:52	W2-91
						KiHa4-55	5:34:40.3	+00:50:13	W2-89
4-185	429		P2487		1061	KiHa76-289	5:34:41.0	−05:54:40	B1-34 H1-53 P1-54 K1-59 A1-74 G1-76 P2-82 M2-83 W1-91
						WBHa72	5:34:41.9	−06:54:37	W2-91
						KiHa4-56	5:34:42.2	+00:38:11	W2-89
		487	P2494		1069		5:34:42.9	−06: 8: 2	B1-34 P1-54 W1-69 B1-72 A1-74 B2-76 W2-77 M2-83 S7-83 S9-83 S10-83 W1-83 R2-84 M2-85 C1-86 H1-88 M3-89 S3-90
5-76						KiHa4-57	5:34:43.0	−01: 9:35	H2-53 K1-59 F1-60 G1-65 W2-89
						WBHa73	5:34:44.0	−06:41:47	W2-91
						WBHa74	5:34:44.7	−07:12: 1	W2-91
						WBHa75	5:34:44.9	−06:47:17	W2-91
5-79						KiHa4-58	5:34:45.4	−00:22:26	H2-53 K1-59 F1-60 G1-65 W2-89
4-420	430						5:34:48.4	−07: 5: 4	P2-82 G1-85 W2-91
4-229	432	169	P2510	BF		BD−6 1259, Nk62, IRAS05348−0636	5:34:48.5	−06:36:51	P3-04 P4-04 W1-06 H1-23 H1-50 H2-52 P1-52 H1-53 B1-54 P1-54 K1-59 H2-62 R1-62 S2-62 M1-63 K1-64 B1-67 M3-70 W1-70 S3-71 A2-72 B2-72 H1-72 C2-73 C3-73 G3-74 D1-75 G1-76 W2-77 C2-79 S3-80 P5-81 F1-82 P2-82 H4-83 M2-83 R3-83 F1-84 F2-84 F1-85 K2-85 S7-85 S7-86 N1-86 Z1-86 H6-87 I1-87 K1-87 M6-87 H1-88 H2-88 K1-88 M3-89 E1-89 G5-89 S7-89 S11-89 B1-90 D1-90 M4-90 W2-90 M1-91 M2-91 W2-91
4-421	431						5:34:48.6	−07: 5:22	P2-82 W2-91
						KiHa76-290	5:34:49.0	−05:34:48	W1-91
4-247	435			V587		KiHa76-291	5:34:49.9	−07: 0:43	H1-53 R1-62 M1-63 M2-63 A2-72 G1-76 P2-82 W1-91 W2-91
4-422	433		P2517		1086	KiHa76-294	5:34:51.0	−05:45:37	B1-34 P1-54 A1-74 P2-82 G1-85 W1-91
						KiHa76-292	5:34:51.0	−06: 0:11	W1-91
						KiHa76-293	5:34:51.0	−06:38: 3	W1-91
						WBHa76	5:34:51.2	−07:13:28	W2-91
4-423	434						5:34:51.4	−05:20: 0	P2-82
5-6							5:34:52.0	−03: 1:53	H2-53 F1-58 K1-59 F1-60 G1-65
						KiHa4-59	5:34:53.5	+00:41:20	W2-89
						WBHa77	5:34:53.7	−07:12:11	W2-91
			P2502	V865			5:34:54.5	−06:37:12	P1-54 P5-81 S3-90
						KiHa76-295	5:34:56.0	−06: 5: 7	W1-91
4-234	436						5:34:56.8	−06:46:23	H1-53 K1-59 A2-72 G1-76 P2-82 W2-91
						KiHa4-60	5:34:57.2	−00:50:36	W2-89
5-77							5:34:58.0	−01: 5:24	H2-53 F1-58 K1-59 F1-60 G1-65
						KiHa4-61	5:34:58.9	−01: 5:18	W2-89
5-5							5:34:59.0	−02:25:36	H2-53 K1-59 F1-60 G1-65
			P2542				5:34:59.1	−06:34:56	P1-54 S3-90
						KiHa4-62	5:35: 0.6	−01: 5:47	W2-89
						WBHa78	5:35: 0.7	−06:45:54	W2-91
						WBHa79	5:35: 1.5	−06:57:38	W2-91
4-425	438					KiHa76-296	5:35: 2.0	−06:48:23	P2-82 G1-85 W1-91 W2-91
						KiHa4-63	5:35: 2.3	+01:26: 5	W2-89
						KiHa76-298	5:35: 3.0	−05:32: 9	W1-91
						WBHa80	5:35: 3.0	−06:50:12	W2-91
						KiHa4-64	5:35: 3.1	+02: 0:41	W2-89
4-424	437					KiHa76-299	5:35: 5.0	−06:57:44	P2-82 G1-85 W1-91 W2-91
4-88	439		P2557	V368	1110	KiHa76-300	5:35: 6.0	−05:14:21	R1-90* P4-04 H1-31 B1-34 P1-52 H1-53 P1-54 K1-59 R1-62 S3-71 B2-72 A1-74 G1-76 P2-82 M2-83 W1-91
4-426	440					KiHa76-301	5:35: 6.0	−06:40:48	P2-82 G1-85 W1-91 W2-91
						WBHa81	5:35: 6.9	−07: 6:38	S3-90 W2-91
	441			V588		Ton11?	5:35: 8.7	−05:53:49	H1-54 K1-59 R1-62 R2-69 P2-82
4-427	443		P2572				5:35: 9.6	−05:10:19	P1-54 P2-82
	442			V874			5:35:11.2	−07: 4:45	P2-82 P1-85 W2-91
						WBHa82, KiHa76-302	5:35:13.0	−06:46:51	W1-91 W2-91
4-428	444						5:35:15.7	−05: 5:37	P2-82
4-429	445					KiHa76-303	5:35:16.0	−06:41:17	P2-82 W1-91 W2-91
						KiHa76-304	5:35:17.0	−04:39:29	W1-91
						WBHa83	5:35:17.9	−06:58:56	W2-91
						WBHa84	5:35:17.9	−07: 8:58	W2-91
4-432	449						5:35:18.3	−07:59: 2	P2-82
4-242	448					KiHa76-305	5:35:18.7	−06:52:13	H1-53 K1-59 R1-62 M1-63 A2-72 G1-76 P2-82 W1-91 W2-91
						KiHa76-306	5:35:20.0	−03:48: 1	W1-91
			P2599			HD37357, BD−6 1264, IRAS05353−0644	5:35:21.1	−06:44:13	S1-54 S1-62 L1-68 W2-77 W5-86 W5-88 S7-89 M4-90 W2-90 M1-91

TABLE 1. CONTINUED.

Haro	PC	HBC	P	Name	Brun	Other	RA (1950)	DEC (1950)	References
(1)	(2)	(3)	(4)	(5)	(6)	(7)	(8)	(9)	(10)
4-430	446					KiHa76-307	5:35:22.0	−04:27:40	P2-82 G1-85 W1-91
4-431	447					KiHa76-308	5:35:22.0	−04:27:59	P2-82 G1-85 W1-91
4-436	454						5:35:23.2	−06:46:49	P2-82 W2-91
4-433	450					KiHa76-309	5:35:23.9	−06:58: 5	P2-82 G1-85 W1-91 W2-91
						KiHa4-65	5:35:25.1	−00:49: 6	W2-89
4-246	451			V591		KiHa76-310	5:35:26.0	−06:58:33	H1-53 R1-62 M1-63 M2-63 A2-72 G1-76 P2-82 S3-90 W1-91 W2-91
4-434	452						5:35:27.9	−06:59:53	P2-82 G1-85 W2-91
4-438	456					IRAS05355−0658	5:35:28.8	−06:58:27	P2-82 W5-86 S7-89 M4-90 S3-90 M1-91 M2-91 W2-91
4-435	453			V592		KiHa76-311	5:35:28.8	−06:59:12	R1-62? M1-63? M2-63? P2-82 S3-90 W1-91 W2-9
4-436	455						5:35:29.0	−06:55:44	P2-82 W2-91
						WBHa85	5:35:29.6	−06:59:13	W2-91
						WBHa86	5:35:29.7	−07:18:28	W2-91
						KiHa76-312	5:35:31.0	−04:15:22	W1-91
						WBHa87	5:35:31.5	−07: 6:57	W2-91
5-7							5:35:32.0	−02:47:38	H2-53 F1-60 G1-65
5-80						KiHa4-66	5:35:32.5	−01:19: 0	H2-53 F1-60 G1-65 W2-89
4-439	457						5:35:32.8	−06:45: 8	P2-82 G1-85 W2-91
4-440	458					KiHa76-313	5:35:33.5	−07: 0:24	P2-82 G1-85 W1-91 W2-91
						Xray56	5:35:34.7	−07:35: 8	S3-90
		488		V1143		Sugano's star, Abastumani 24, KiHa76-314	5:35:35.1	−04:18:24	H3-83 I1-83 K1-83 K2-83 K3-83 L1-83 G3-84 N1-84 C3-85 V1-85 N2-86 G1-87 I2-87 P1-87 H1-88 M4-88 P2-88 G1-89 H2-89 G2-90 W1-91
						KiHa4-67	5:35:35.8	−02:32: 3	W2-89
4-251	459			V593		KiHa76-315	5:35:35.8	−07:17:36	H1-53 R1-62 M2-63 P2-82 P1-85 W1-91 W2-91
						KiHa76-316	5:35:37.0	−02:37:38	W1-91
4-65	460					KiHa76-318	5:35:39.0	−05: 2:59	H1-53 B2-72 G1-76 P2-82 W1-91
4-441	462					KiHa76-317	5:35:39.0	−07:23:45	P2-82 W1-91 W2-91
4-220	461						5:35:39.8	−06:31:23	H1-53 P2-82 W2-91
4-250	463			V878		KiHa76-319	5:35:40.0	−07:17:51	H1-53 K1-59 M2-63 P2-82 W1-91 W2-91
						Xray54	5:35:40.6	−06:54:55	S3-90
						KiHa76-321	5:35:41.0	−02:19:55	W1-91
						KiHa76-320	5:35:41.0	−02:19:58	W1-91
5-8							5:35:41.0	−02:47:45	H2-53 F1-58 K1-59 F1-60 G1-65
						KiHa76-322	5:35:42.0	−02:47:33	W1-91
						Nk81, IRAS05357−0650	5:35:43.5	−06:50:57	B2-86 N1-86 W5-86 W5-88 S7-89 S11-89 W4-89 M4-90 M1-91 W2-90
4-442	464						5:35:43.8	−06:26:56	P2-82 G1-85 W2-91
4-211	465					KiHa76-324	5:35:44.0	−06:23:49	H1-53 P2-82 W1-91 W2-91
4-248	466					KiHa76-323	5:35:44.0	−07: 7: 6	H1-53 K1-59 A2-72 G1-76 P2-82 W1-91 W2-91
			P2653			HD37411, BD−5 1346	5:35:47.1	−05:26:53	S1-54 S1-62 L1-68 S2-72 W2-77 M1-82 H4-89
						KiHa76-326	5:35:48.0	−02:53:20	W1-91
						KiHa76-327	5:35:52.0	−03:13:38	W1-91
						KiHa4-69	5:35:52.3	−02:38: 5	W2-89
		489		V883		*near Haro13a	5:35:54.0	−07: 3:51	M2-63 S3-74 A1-75 H1-88
5-10				V505			5:35:56.0	−02:47:34	H2-53 F1-58 K1-59 F1-60 G1-65
4-443	467						5:35:56.0	−06:59:46	P2-82 W2-91
						KiHa76-329	5:35:57.0	−02:36:45	W1-91
						KiHa76-328	5:35:57.0	−02:46:50	W1-91
			P2675				5:35:57.0	−06:39:22	P1-54 S3-90
5-9							5:35:58.0	−02:18:16	H2-53 F1-60 G1-65
						KiHa4-70, KiHa76-330	5:35:58.0	−02:17:54	W2-89 W1-91
4-107	468					KiHa76-331	5:35:58.0	−05:23:51	H1-53 G1-76 P2-82 W1-91
4-444	470					KiHa76-332	5:35:58.6	−07: 9:18	P2-82 W1-91 W2-91
4-445	471						5:35:58.8	−04: 4:34	P2-82
5-85							5:36: 0.0	−04: 4:22	H2-53 F1-58 K1-59 F1-60
4-240	473			V1002		KiHa76-333	5:36: 0.0	−06:49:37	H1-53 A2-72 G1-76 P2-82 W1-91 W2-91
						KiHa4-71, KiHa76-334	5:36: 0.6	−02:38:12	W2-89 W1-91
5-11							5:36: 1.0	−02:38:46	H2-53 F1-60
	469					KiHa76-335	5:36: 1.0	−04: 4:26	K1-59 P2-82 W1-91
4-446	472						5:36: 1.5	−07:39:44	P2-82 W2-91
4-447	474						5:36: 1.6	−06:40: 7	P2-82 G1-85 W2-91
4-245	475		P2682	V594		KiHa76-336	5:36: 2.0	−06:56:33	H1-53 P1-54 K1-59 R1-62 M2-63 S3-71 A2-72 G1-76 P2-82 M2-83 W1-91 W2-91
4-448	476						5:36: 2.2	−06: 5:41	P2-82 W2-91
						St50	5:36: 3.0	−02:30:19	M1-82 S8-86 D1-88
5-12		172		TX		IRAS05360−0245?	5:36: 3.2	−02:45:55	P3-04 P1-05 H1-31 P1-34 H2-53 F1-58 K1-59 F1-60 R1-60 G1-65 H1-72 C2-79 M4-80 S3-80 H2-86 H1-88 W2-90
						KiHa76-337	5:36: 4.0	−07:17:26	W1-91
4-449	478			V589		KiHa76-338	5:36: 4.1	−06:41:21	P2-82 G1-85 S3-90 W1-91 W2-91
		173		TY		IRAS05360−0245?	5:36: 5.3	−02:45:38	P3-04 P1-05 H1-31 P1-34 K1-59 R1-60 H1-72 C2-79 S3-80 H1-88 W2-90
4-451	480					KiHa76-339	5:36: 6.0	−06:54:18	P2-82 W1-91 W2-91
4-452	482						5:36: 6.5	−07:47:23	P2-82
4-450	479						5:36: 9.7	−05: 1:53	P2-82
5-13							5:36:10.0	−02:32:29	H2-53 F1-58 K1-59 F1-60 G1-65
	481	174				H7-1, IRAS05362−0751	5:36:10.6	−07:51:59	H1-72 C2-79 M4-80 P2-82 H1-88 S7-89 M4-90 W2-90
						KiHa4-72	5:36:12.5	+00: 1:56	W2-89
5-14							5:36:14.0	−02:44:11	H2-53 F1-58 K1-59 F1-60
4-453	483						5:36:14.6	−07: 0:51	P2-82 W2-91
4-249/c		490					5:36:16.5	−07:14:25	H1-53 S3-74 C2-79 G4-87 H1-88

TABLE 1. CONTINUED.

Haro	PC	HBC	P	Name	Brun	Other	RA (1950)	DEC (1950)	References
(1)	(2)	(3)	(4)	(5)	(6)	(7)	(8)	(9)	(10)
4-454	485						5:36:16.8	−06:54:49	P2-82 W2-91
4-249	484	491				Nk88, KiHa76-340, IRAS05363−0714	5:36:17.5	−07:14:22	H1-53 M2-63 C2-79 L2-79 C4-80 P2-82 B2-86 N1-86 S9-86 G4-87 S8-87 H1-88 L3-88 V4-88 S7-89 M4-90 W2-90 M1-91 M2-91 W1-91
4-455	487						5:36:18.5	−07:46:18	P2-82
						KiHa4-73	5:36:21.0	−00:50:58	W2-89
4-68	486						5:36:21.9	−04:53: 6	H1-53 G1-76 P2-82
4-253	488					KiHa76-341	5:36:24.8	−07:21:56	H1-53 K1-59 P2-82 S3-90 W1-91
4-254	489					Nk90, KiHa76-342, IRAS05364−0722	5:36:27.2	−07:22:46	H1-53 K1-59 P2-82 N1-86 W5-86 S7-89 M4-90 S3-90 W2-90 M1-91 M2-91 W1-91
5-15				RU			5:36:28.0	−02:49:18	H2-53 F1-58 F1-60 R1-60 G1-65
5-18						KiHa4-74	5:36:28.4	−02:35:27	H2-53 F1-60 W2-89
						KiHa76-343	5:36:30.0	−03:55:26	W1-91
5-16						KiHa4-75, KiHa76-344	5:36:30.2	−02:20: 4	H2-53 F1-58 K1-59 F1-60 G1-65 W2-89 W1-91
4-456	490						5:36:30.2	−08: 4:25	P2-82
						KiHa4-76	5:36:30.4	−01:22:10	W2-89
4-457	492						5:36:30.5	−07:46:19	P2-82
4-243	491					KiHa76-345	5:36:31.0	−06:54:36	H1-53 P2-82 W1-91
				V599		Nk92, IRAS05365−0718	5:36:33.3	−07:18:22	N1-86 W5-86 S7-89 S11-89 M4-90 W2-90 M1-91 M2-91
4-459	494						5:36:36.5	−07:47:19	P2-82
5-19				V507		KiHa4-77	5:36:36.8	−02:34:15	H2-53 F1-58 F1-60 G1-65 W2-89
4-458	493		P2778				5:36:39.1	−05:35:55	P1-54 A1-74 P2-82
						KiHa4-78, KiHa76-346	5:36:40.7	−02:32:42	W2-89 W1-91
5-17				V508		KiHa4-79	5:36:40.9	−01:28:58	H2-53 F1-58 K1-59 F1-60 G1-65 W2-89
5-20				V509			5:36:41.0	−02:33:19	H2-53 F1-58 F1-60 R1-60 G1-65
						KiHa4-80	5:36:45.8	−02:27:25	W2-89
		175				H7-5	5:36:46.7	−08:34:31	H1-72 M2-77 C2-79
5-21						KiHa4-81, KiHa76-347	5:36:48.0	−02:32:29	H2-53 F1-60 G1-65 W2-89 W1-91
4-252	496					KiHa76-348	5:36:49.0	−06:45:39	H1-53 G1-76 P2-82 W1-91
4-460	495						5:36:49.0	−07:23:20	P2-82
						KiHa4-82	5:36:49.3	+00:36:24	W2-89
						Xray61	5:36:53.0	−07: 1:44	S3-90
						Xray62	5:36:53.3	−06:56:51	S3-90
5-23				BG		KiHa4-83, KiHa76-349	5:36:54.5	−02:39:56	H2-53 F1-58 F1-60 G1-65 W2-89 W1-91
5-22						KiHa4-84	5:36:55.2	−02:16:38	H2-53 F1-58 K1-59 F1-60 G1-65 W2-89
5-87						KiHa4-85	5:36:55.4	+00: 2: 3	H2-53 F1-60 G1-65 W2-89
						KiHa4-86	5:36:55.9	+01:37:43	W2-89
4-255	497	176				Nk93, KiHa76-350, IRAS05369−0728	5:36:57.3	−07:28:20	H1-53 H1-72 C1-74 D1-75 C2-79 P1-79 P2-82 L1-85 E1-86 N1-86 W5-86 S8-87 H1-88 L3-88 W5-88 C2-89 F2-89 S5-89 S7-89 S11-89 W4-89 C2-90 M4-90 W2-90 H1-91 M1-91 M2-91 W1-91
						KiHa4-87	5:36:57.4	+00:11:16	W2-89
						KiHa76-351	5:36:59.0	−02:28:58	W1-91
						KiHa4-88	5:37: 0.0	+01:28:13	W2-89
						KiHa76-352	5:37: 0.0	−06:54:34	W1-91
5-24							5:37: 1.0	−02:13:39	H2-53 K1-59 F1-60 G1-65
						KiHa76-353	5:37: 4.0	−03:19:23	W1-91
5-86							5:37: 4.0	−04:14:39	H2-53 K1-59 F1-60
4-461	498						5:37: 4.6	−04:15: 9	P2-82
						KiHa76-354	5:37: 6.0	−02: 5:45	W1-91
4-463	500						5:37: 6.5	−07:45:58	P2-82
4-464	501						5:37: 6.8	−07:29:40	P2-82
4-462	499					KiHa76-355	5:37: 7.0	−04:37:49	P2-82 G1-85 W1-91
5-28						KiHa4-89	5:37: 7.5	−02:34:39	H2-53 K1-59 F1-60 G1-65 W2-89
5-25							5:37: 8.0	−02:19:21	H2-53 K1-59 F1-60 G1-65
						KiHa76-357	5:37: 9.0	−02:34:51	W1-91
5-26				RV		KiHa4-91	5:37: 9.1	−02:22:22	H2-53 F1-58 F1-60 G1-65 W2-89
5-27		177		V510		San4, KiHa4-90, KiHa76-356	5:37: 9.1	−02:32:57	H2-53 F1-58 K1-59 F1-60 G1-65 S1-71 H1-72 C2-79 C2-80 M4-80 J1-83 H1-88 W2-89 W1-91
5-29				RW			5:37:10.0	−02:44:21	H2-53 F1-60 R1-60 G1-65
						KiHa76-358	5:37:12.0	−03: 0:29	W1-91
4-465	502						5:37:12.5	−07:44:52	P2-82
5-33				V511			5:37:13.0	−03: 0:46	H2-53 F1-60 G1-65
						Xray63	5:37:17.4	−07: 6:33	S3-90
5-30							5:37:21.0	−02:24:58	H2-53 K1-59 F1-60 G1-65
5-32						KiHa4-92, KiHa76-359	5:37:22.8	−02:35:15	H2-53 F1-58 F1-60 G1-65 W2-89 W1-91
5-31						KiHa4-93, KiHa76-360	5:37:23.3	−02:26:12	H2-53 K1-59 F1-60 G1-65 W2-89 W1-91
5-34						KiHa76-361?	5:37:24.0	−02:48:22	H2-53 F1-58 K1-59 F1-60 G1-65 W1-91?
						KiHa4-94	5:37:27.1	−01:28:40	W2-89
5-89							5:37:30.0	−00:40:47	H2-53 K1-59 F1-60 G1-65
5-36						KiHa4-95, KiHa76-362	5:37:30.9	−02:23: 5	H2-53 F1-58 K1-59 F1-60 G1-65 W2-89 W1-91
						KiHa4-96	5:37:31.6	+01: 1:37	W2-89
						Xray64	5:37:32.4	−07:37: 0	S3-90
5-35						KiHa4-97	5:37:32.5	−02:18:19	H2-53 F1-60 G1-65 W2-89
						KiHa4-98	5:37:33.5	−01:28:17	W2-89
5-90						KiHa4-99	5:37:33.7	−00:40:11	H2-53 F1-60 G1-65 W2-89
4-466	503						5:37:34.2	−04:38:53	P2-82 G1-85

TABLE 1. CONTINUED.

Haro (1)	PC (2)	HBC (3)	P (4)	Name (5)	Brun (6)	Other (7)	RA (1950) (8)	DEC (1950) (9)	References (10)
						IRAS05375−0739	5:37:34.4	−07:39: 5	S7-89 W2-90
						KiHa76-363	5:37:37.0	−03:16:28	W1-91
5-39						KiHa4-100, KiHa76-364	5:37:38.0	−02:35: 5	H2-53 F1-58 F1-60 G1-65 W2-89 W1-91
4-468	505						5:37:38.0	−06:29:12	P2-82
4-469	506					KiHa76-366	5:37:39.0	−06:23:11	P2-82 G1-85 W1-91
4-467	504		P2888			KiHa76-365	5:37:39.0	−06:30:57	P1-54 P2-82 G1-85 W1-91
		178	P2893	BH			5:37:41.4	−06:17:29	P2-04 P1-52 P1-54 K1-59 R1-62 S3-71 H1-72 M2-83
						KiHa4-101	5:37:41.8	−02:23:34	W2-89
5-38							5:37:42.0	−02:23:48	H2-53 K1-59 F1-60 G1-65
4-471	508						5:37:42.4	−07:49:54	P2-82
4-473	510			V995			5:37:43.2	−07:11:36	P2-82
4-472	509						5:37:43.7	−06:45: 6	P2-82
						KiHa76-367	5:37:44.0	−02:23:59	W1-91
						KiHa4-102	5:37:45.5	+00:34:25	W2-89
4-470	507						5:37:45.5	−05:15:42	P2-82 G1-85
5-37						KiHa4-103	5:37:45.9	−02:19:43	H2-53 F1-60 G1-65 W2-89
4-474	511					KiHa76-368	5:37:46.0	−07:11:25	P2-82 W1-91
						Xray65a	5:37:48.6	−07:10: 5	S3-90
		493		V350		IRAS05378−0943	5:37:49.3	−09:43:42	H1-29 P1-46 S1-48 A1-51 T1-52 K1-54 W1-55 H2-58 B1-59 H3-60 S2-62 G3-74 H1-88 S7-89 M4-90 W2-90
5-88							5:37:51.0	−00: 5: 0	H2-53 F1-60 G1-65
5-91						KiHa4-104	5:37:51.0	−00:32:53	H2-53 F1-60 G1-65 W2-89
						KiHa4-105	5:37:51.7	−02:35:17	W2-89
4-475	512					KiHa76-369	5:37:52.0	−07:20:38	P2-82 W1-91
						KiHa4-106	5:37:52.9	−01:54: 2	W2-89
4-476	513					KiHa76-370	5:37:55.0	−07:27:26	P2-82 W1-91
						IRAS05379−0815	5:37:55.2	−08:15:48	B2-86 W5-86 S7-89 M4-90 M1-91 M2-91
						WBHa88	5:37:58.4	−09:11:13	W2-91
						KiHa4-107	5:38: 0.0	−02: 3:33	W2-89
4-478	515	179				H7-4, IRAS05380−0809	5:38: 0.7	−08: 9: 4	H1-72 D1-75 C2-79 M4-80 P2-82 H1-88 S7-89 W2-90 M1-91
4-477	514						5:38: 1.3	−07: 7:32	M2-63? P2-82
		494				Re50, IRAS05380−0728	5:38: 5.0	−07:30:26	B2-86 R3-85 R1-86 W5-86 C2-87 M14-87 Z3-87 H1-88 S3-88 W5-88 A6-89 C4-89 F2-89 S7-89 S11-89 W1-89 W4-89 H2-90 M4-90 W2-90 C1-91 M1-91 M2-91
						KiHa4-108	5:38: 5.2	+01:21:57	W2-89
5-92				V513			5:38: 6.0	−00:48:37	H2-53 F1-58 F1-60 G1-65
4-479	516						5:38: 7.3	−07: 8:44	P2-82
						KiHa76-371	5:38: 8.0	−04:33:33	W1-91
						KiHa4-109	5:38: 9.2	+01: 8: 3	W2-89
						KiHa76-372	5:38:10.0	−03:32:11	W1-91
						KiHa76-373	5:38:13.0	−06:36:42	W1-91
						IRAS05382−0805	5:38:13.0	−08: 5:32	S7-89 M4-90 M1-91 M2-91
5-41							5:38:14.0	−02:32:20	H2-53 F1-58 F1-60 G1-65
4-480	517					KiHa76-374	5:38:14.0	−06:33:20	P2-82 W1-91
5-40						KiHa4-110, KiHa76-375	5:38:15.5	−02:12:18	H2-53 F1-58 F1-60 G1-65 W2-89 W1-91
						IRAS05383−0731	5:38:19.7	−07:31:23	S7-89 W2-90
4-482	519					KiHa76-376	5:38:20.0	−07:23:55	P2-82 W1-91
						KiHa4-111	5:38:20.7	−02:37:31	W2-89
5-44						KiHa76-377?	5:38:21.0	−02:38: 9	H2-53 F1-58 K1-59 F1-60 R1-60 G1-65 W1-91?
						KiHa76-378	5:38:22.0	−03: 1:17	W1-91
		495				DL/G4	5:38:22.0	−08: 6:54	C2-79 H1-88
4-481	518	496				DL/G5	5:38:22.5	−08: 6:24	C2-79 P2-82 H1-88
		497				DL/G3	5:38:22.8	−08: 9: 1	C2-79 H1-88
5-43							5:38:23.0	−02:20:57	H2-53 K1-59 F1-60 G1-65
		498				DL/G1	5:38:23.8	−08: 7:28	C2-79 H1-88
						KiHa4-112	5:38:23.9	+02: 4:37	W2-89
5-42							5:38:24.0	−01:17:33	H2-53 F1-60
5-45							5:38:24.0	−03: 1:33	H2-53 F1-60 G1-65
4-483	520						5:38:24.4	−07:53:33	P2-82
						KiHa4-113	5:38:25.9	−01:18:34	W2-89
						HD37806, BD−2 1344	5:38:30.0	−02:44:15	M1-33 H1-64 W1-70 W2-77 P4-81 P2-85
						KiHa4-114	5:38:30.2	−01:19: 7	W2-89
						KiHa4-115	5:38:30.4	−02: 0:26	W2-89
						KiHa4-116	5:38:35.3	−00:22:42	W2-89
						KiHa76-379	5:38:38.0	−03:34:57	W1-91
4-484	521						5:38:42.5	−07:48:53	P2-82
						WBHa89	5:38:42.7	−09:20:13	W2-91
						KiHa76-380	5:38:46.0	−07:16:13	W1-91
						KiHa4-117	5:38:47.9	−02:39:58	W2-89
5-46						KiHa4-118	5:38:49.2	−02: 0:26	H2-53 K1-59 F1-60 H1-63 W2-89
5-48							5:38:51.0	−03: 7:41	H2-53 K1-59 F1-60 G1-65
		499		V615		IRAS05388−0224	5:38:53.4	−02:24:19	S2-86 M2-87 H1-88 W2-90
5-58							5:38:54.0	−02: 2: 5	H2-53 F1-60 R1-60
4-485	522					KiHa76-381	5:38:54.0	−07:27:49	P2-82 W1-91
						KiHa4-119	5:38:55.1	−01:44:15	W2-89
						KiHa4-120	5:38:56.3	−01:15:19	W2-89
						LkHa286	5:38:58.0	−01:39: 0	F1-60 H1-63
5-47						KiHa4-121	5:38:58.6	−01:39:29	H2-53 F1-60 R1-60 H1-63 G1-65 W2-89
						KiHa76-382	5:38:59.0	−03:45:36	W1-91
4-486	523	181		DL		San5, H7-3,	5:39: 1.1	−08: 7:21	W1-24 R1-30 B1-39 S1-71 C1-74 H1-72 D1-75

TABLE 1. CONTINUED.

Haro	PC	HBC	P	Name	Brun	Other	RA (1950)	DEC (1950)	References
(1)	(2)	(3)	(4)	(5)	(6)	(7)	(8)	(9)	(10)
4-486						IRAS05390−0807			B1-79 C2-79 P2-82 B10-82 C7-85 S10-85 I1-87 H1-88 S7-89 W2-90 M1-91 M2-91
5-62						KiHa4-122	5:39: 3.1	−01:40:21	H2-53 F1-60 G1-65 W2-89
5-49							5:39: 5.0	−02:19: 6	H2-53 F1-60
		500				NGC2023/C, 2023/108	5:39: 5.4	−02:18:13	S6-75 S6-83 W1-84 M2-87 H1-88 S2-89 D3-90
4-489	526						5:39: 6.3	−07:54:30	P2-82
4-488	525						5:39: 6.3	−07:57:30	P2-82
5-59						KiHa4-123	5:39: 7.5	−02: 1: 3	H2-53 F1-60 H1-63 G1-65 M3-75 W2-89
						WBHa90	5:39: 7.5	−09:13:52	W2-91
5-50							5:39: 9.0	−02:18:12	H2-53 F1-60
						LkHa287	5:39: 9.7	−02:16:39	H1-63 M3-75
						LkHa288	5:39: 9.8	−01:45:15	H1-63 M3-75
4-487	524					KiHa76-383	5:39:10.0	−06:22:10	P2-82 W1-91
						KiHa4-124	5:39:10.9	+00:29:45	W2-89
						KiHa4-125	5:39:14.0	−01:14:27	W2-89
						LkHa289	5:39:15.8	−01:51:15	H1-63 M3-75
						NGC2023/H, 2023/105	5:39:15.9	−02:17:48	S6-75 S6-83 D3-90
						IRAS05393−0838	5:39:18.7	−08:38:32	S7-89 M4-90 W2-90
5-51							5:39:20.0	−01:37:55	H2-53 F1-60 G1-65
5-60							5:39:23.0	−02: 2:37	H2-53 F1-58 K1-59 F1-60 G1-65
5-52						KiHa4-126	5:39:23.5	−01:42:22	H2-53 F1-60 H1-63 G1-65 M3-75 W2-89
	527	182				San6, H7-2, IRAS05394−0801	5:39:25.4	−08: 1:57	S1-71 H1-72 C1-74 D1-75 K1-78 B1-79 C2-79 P1-79 M4-80 P2-82 B10-82 S10-85 H1-88 S7-89 M4-90 W2-90 M1-91
						LkHa290	5:39:25.8	−01:16:27	H1-63 M3-75
						KiHa4-127	5:39:26.1	−01:35:40	W2-89
						KiHa76-384	5:39:29.0	−02:33:14	W1-91
						KiHa4-128	5:39:33.0	−01:13:26	W2-89
						KiHa4-129	5:39:33.5	−01:22:41	W2-89
						KiHa4-130	5:39:34.7	−02: 0:46	W2-89
						KiHa4-131	5:39:36.2	−01:17:23	W2-89
4-490	528						5:39:38.1	−06:25:14	P2-82
						KiHa4-132	5:39:38.7	−02:26:12	W2-89
						KiHa4-133	5:39:41.0	−02: 6:33	W2-89
5-54						KiHa4-134	5:39:44.5	−02: 8:10	H2-53 F1-60 G1-65 W2-89
5-53						KiHa4-135	5:39:44.7	−01:57:38	H2-53 F1-58 F1-60 G1-65 W2-89
						DL/G2	5:39:45.0	−08: 3:33	C2-79
5-55						KiHa4-136	5:39:48.3	−02:17: 4	H2-53 F1-58 F1-60 R1-60? G1-65 W2-89
5-61							5:39:51.0	−02: 1: 3	H2-53 F1-60 G1-65
						KiHa4-137	5:40: 0.0	−00:27:12	W2-89
5-56							5:40: 1.0	−01:39: 6	H2-53 F1-60 H1-63 G1-65
4-491	529					IRAS05400−0800	5:40: 2.0	−08: 0:14	P2-82 B2-86 W5-86 W5-88 S7-89 W4-89 M4-90 M1-91 M2-91
						KiHa4-138	5:40: 2.1	+01:53:10	W2-89
						KiHa4-139	5:40: 3.8	−02:30:33	W2-89
						KiHa76-385	5:40: 5.0	−05:11: 6	W1-91
						KiHa4-140	5:40: 5.6	−02: 3: 2	W2-89
						IRAS05401−0834	5:40: 6.8	−08:34:16	S7-89
						KiHa4-141	5:40: 8.9	−02:12:47	W2-89
						KiHa4-142	5:40:10.2	−00:36:38	W2-89
						KiHa4-143	5:40:14.6	−02:16:44	W2-89
						KiHa4-144	5:40:17.3	+01: 1: 0	W2-89
						B	5:40:18.0	−10: 1: 0	G1-73
						A	5:40:18.0	−10: 3: 0	G1-73
4-492	530						5:40:18.1	−08: 8:24	P2-82
						IRAS05404−0839	5:40:25.0	−08:39:50	B2-86 W5-86 S7-89 M4-90 W2-90
						LkHa291, KiHa4-145, KiHa76-386	5:40:27.7	−02:19:57	H1-63 W2-89 W1-91
						C	5:40:30.0	−09:51: 0	G1-73
4-493	532						5:40:30.2	−08: 2:18	P2-82
	531						5:40:31.0	−07:19:24	P2-82
						KiHa4-147	5:40:34.2	−00: 7:29	W2-89
5-93				V518		KiHa4-148	5:40:34.4	−00: 0:59	H2-53 F1-60 H1-63 G1-65 W2-89
4-494	533						5:40:36.1	−08: 6:55	P2-82
						KiHa4-149	5:40:40.8	−02:15: 2	W2-89
						KiHa76-387, IRAS05407−0501	5:40:44.0	−05: 1: 8	W1-91
						KiHa4-150	5:40:48.8	−01:41:35	W2-89
						St53	5:40:51.0	+01:22:43	S8-86 D1-88
						KiHa76-388	5:40:56.0	−02:34:41	W1-91
4-495	534						5:41: 0.0	−08:10:57	P2-82
						KiHa76-389	5:41: 5.0	−02:44:33	W1-91
						St54	5:41:11.0	−05: 5:15	S8-86
						KiHa4-151	5:41:19.2	−02:13:36	W2-89
						KiHa4-152	5:41:21.8	−00: 0:20	W2-89
						KiHa76-390	5:41:26.0	−05:55:11	W1-91
5-57				V522		KiHa4-153	5:41:32.5	−02:17:52	H2-53 F1-58 K1-59 F1-60 G1-65 W2-89
						KiHa76-391	5:41:41.0	−07: 1: 2	W1-91
						KiHa4-154	5:41:42.8	−00:27:41	W2-89
						KiHa76-392	5:41:47.0	−04: 8:20	W1-91
						HD38238, BD+00 1170	5:41:48.0	+00: 9: 0	S6-75
						KiHa4-155	5:41:49.4	−00: 6:39	W2-89
5-94				V523		KiHa4-156	5:41:57.0	−01:23:31	H2-53 F1-60 G1-65 R7-89 W2-89

TABLE 1. CONTINUED.

Haro (1)	PC (2)	HBC (3)	P (4)	Name (5)	Brun (6)	Other (7)	RA (1950) (8)	DEC (1950) (9)	References (10)
						KiHa76-393	5:41:57.0	−05:38:53	W1-91
						KiHa4-157	5:41:58.8	−01:46:24	W2-89
		501				CoKu N2068/1	5:42: 2.0	−01:23:15	C2-79 H1-88
						KiHa4-158	5:42: 2.2	−00:27:20	W2-89
						KiHa4-159	5:42: 2.7	−01:27:12	W2-89
						LkHa292	5:42: 6.0	−00:22:54	H1-63 J1-87
						KiHa76-394	5:42:11.0	−04:33: 0	W1-91
						KiHa4-160	5:42:12.1	−01:37:53	W2-89
						KiHa4-161	5:42:13.5	−02:15:30	W2-89
						KiHa4-162	5:42:20.4	+02:31: 2	W2-89
						KiHa4-163	5:42:25.6	+00:52:42	W2-89
5-96						KiHa4-164	5:42:30.9	−01:11:16	H2-53 F1-60 H1-63 G1-65 W2-89
5-95						LkHa293, KiHa4-165	5:42:39.9	−01:14:48	H2-53 F1-60 H1-63 G1-65 W2-89
5-98						KiHa4-166	5:42:44.8	−01: 1:15	H2-53 F1-60 H1-63 G1-65 W2-89
						KiHa76-395	5:42:48.0	−02:23:11	W1-91
						LkHa269, KiHa4-167	5:42:52.0	−00:38:18	H2-62 H1-63 W2-89
						LkHa268, KiHa4-167	5:42:52.1	−00:38:33	H2-62 H1-63 W2-89
						KiHa4-168	5:42:54.1	−00:41: 2	W2-89
						KiHa4-169	5:42:57.3	−00:45:38	W2-89
						LkHa294	5:42:58.0	−00:48:54	H1-63
						KiHa4-170	5:43:10.1	+00:21:49	W2-89
5-97						KiHa4-171	5:43:13.2	−00:45:49	H2-53 K1-59 F1-60 H1-63 G1-65 W2-89
						LkHa295, SSV66, KiHa4-172	5:43:15.2	−00:13:43	H1-63 M3-75 S6-75 S2-76 W2-89
						KiHa4-173	5:43:19.1	+00:32: 0	R7-89 W2-89
						KiHa4-174	5:43:19.5	−00:14:32	W2-89
						LkHa296, KiHa4-175	5:43:23.2	+00:19:13	H1-63 R7-89 W2-89
						LkHa297	5:43:26.0	+00: 2:18	H1-63 J1-87
						KiHa76-396	5:43:27.0	−05: 1:44	W1-91
						KiHa76-397	5:43:28.0	−03:11:15	W1-91
						KiHa76-398	5:43:29.0	−07:45:41	W1-91
						LkHa298, SSV51, KiHa4-176	5:43:30.7	+00: 3:50	H1-63 S6-75 S2-76 S6-83 J1-87 R7-89 W2-89
		502				SSV61, M78/140	5:43:34.4	−00:13: 4	H1-74 S6-75 S2-76 H1-88
						LkHa299, KiHa4-178	5:43:35.2	+00:12:25	H1-63 W2-89
						KiHa4-180	5:43:36.9	−00:32:28	W2-89
						LkHa300, SSV49	5:43:45.0	+00: 2:36	H1-63 S6-75 S2-76 S6-83 J1-87
		503				LkHa301, SSV64, KiHa4-181	5:43:45.8	−00: 6:26	H1-63 S6-75 S2-76 M4-80 C2-83 J1-87 H1-88 R7-89 W2-89
						RJ12	5:43:46.0	+01:19:28	R7-89
		504				LkHa302, SSV68, KiHa4-182	5:43:48.8	−00: 9:59	H1-63 S6-75 S2-76 J1-87 H1-88 R7-89 W2-89
						LkHa303, KiHa4-183	5:43:53.8	+00:23:36	H1-63 S6-75 W2-89
						KiHa4-184	5:43:56.7	+00:24:28	R7-89 W2-89
						KiHa76-399	5:44: 0.0	−02:24:52	W1-91
						KiHa76-400	5:44: 2.0	−03:54: 0	W1-91
						LkHa304, SSV11, M78/108, KiHa4-185	5:44: 3.2	+00: 0:16	H1-63 S6-75? S2-76? S6-83 J1-87 R7-89 W2-89
						LkHa305, SSV34, KiHa4-186	5:44:11.7	+00:15:58	H1-63 S2-76 R7-89 W2-89
						KiHa4-187, SSV14?	5:44:12.8	+00: 8: 2	S2-76? W2-89
						LkHa306, SSV3, M78-13, KiHa4-188	5:44:16.3	+00: 3:35	H1-63 S6-75 S2-76 S6-83 R7-89 W2-89
						KiHa76-401	5:44:24.0	−04:48:37	W1-91
		505				LkHa307, KiHa4-189, IRAS05445+0031	5:44:31.6	+00:31: 5	H1-63 H1-88 W2-89 R7-89 W2-90
						LkHa308, SSV21, KiHa4-190	5:44:33.0	+00:18:29	H1-63 S6-75 S2-76 R7-89 W2-89
		506				LkHa309, SSV46, KiHa4-191	5:44:33.1	−00: 0:14	H1-63 S2-76 H1-88 R7-89 W2-89
						KiHa4-192	5:44:33.4	+00:47:30	W2-89
						KiHa4-193	5:44:34.9	+02:25:46	W2-89
						LkHa310, SSV26	5:44:37.0	+00:18:24	H1-63 S6-75 S2-76 R7-89
						LkHa311	5:44:39.0	+00:44:18	H1-63
						KiHa4-194	5:44:39.5	−02:43: 7	W2-89
		187				LkHa314, SSV23, KiHa4-195, IRAS05446+0008	5:44:40.1	+00: 8: 5	H1-63 H1-72 D1-75 S2-76 M4-80 H1-88 R7-89 W2-89 W2-90
		507				LkHa313, SSV47, KiHa4-196	5:44:40.2	−00: 0:45	H1-63 S2-76 H1-88 R7-89 W2-89
		508				LkHa312, SSV47, KiHa4-196	5:44:40.3	−00: 0:46	H1-63 S2-76 H1-88 R7-89 W2-89
		509				LkHa315, KiHa4-197	5:44:42.8	+00:37:19	H1-63 H1-88 R7-89 W2-89
						KiHa4-198	5:44:43.0	+00:17:22	W2-89
						KiHa4-199	5:44:57.0	−01:10:24	W2-89
						KiHa76-402	5:44:59.0	−04:16:17	W1-91
						KiHa4-200	5:45: 0.8	−02: 0:10	W2-89

TABLE 1. CONTINUED.

Haro	PC	HBC	P	Name	Brun	Other	RA (1950)	DEC (1950)	References
(1)	(2)	(3)	(4)	(5)	(6)	(7)	(8)	(9)	(10)
		510				LkHa316, KiHa4-201	5:45: 1.2	+00:37:39	H1-63 H1-88 R7-89 W2-89
		511				LkHa316/c	5:45: 2.3	+00:38:13	H1-88
						LkHa317	5:45: 7.0	−00: 4:24	H1-63
						KiHa76-403	5:45: 8.0	−04:51:14	W1-91
						LkHa318	5:45:12.0	+00:58:42	H1-63
						KiHa4-202	5:45:13.6	−02:27: 8	W2-89
		512				LkHa319, KiHa4-203	5:45:13.8	+00:39:59	H1-63 H1-88 R7-89 W2-89
						KiHa4-204	5:45:17.1	−01: 7:43	W2-89
		513				LkHa320, KiHa4-205	5:45:26.6	+00:33:31	H1-63 H1-88 W2-89
						KiHa4-206	5:45:37.3	+02: 9:57	W2-89
						KiHa4-207	5:45:39.1	+02:34:48	W2-89
						KiHa4-208	5:46:13.6	−00:51:48	W2-89
						KiHa4-209	5:46:17.9	−00:45:47	W2-89
						KiHa4-210	5:46:24.4	−00:29:56	W2-89
						KiHa4-211	5:46:27.3	+01: 6:37	R7-89 W2-89
						KiHa76-404	5:46:30.0	−05: 7:47	W1-91
						KiHa4-212	5:46:43.1	−02:44:55	W2-89
						KiHa4-213	5:46:45.4	+01:51:59	W2-89
						KiHa76-405	5:46:58.0	−05:41:41	W1-91
						KiHa76-406	5:47:18.0	−04:28:53	W1-91
						KiHa4-214	5:47:30.8	−00:31:35	W2-89
						KiHa4-215	5:47:37.6	−02:41:55	W2-89
						KiHa4-216	5:47:51.0	+02:28:50	W2-89
						KiHa4-217	5:47:52.0	−01:29:25	W2-89
						KiHa76-407	5:47:52.0	−05:41: 5	W1-91
						KiHa4-218	5:48: 2.6	+00:46:27	W2-89
						KiHa76-408	5:48:11.0	−06:56:17	W1-91
						KiHa4-219	5:48:19.4	+01:56: 9	W2-89
						KiHa76-409	5:48:24.0	−03:49:23	W1-91
						KiHa4-220	5:48:31.7	+02:28:52	W2-89
						KiHa4-221	5:48:31.9	+00:17:35	W2-89
						KiHa4-222	5:48:43.9	+00: 3:47	W2-89
						KiHa76-410	5:48:45.0	−04:48:50	W1-91
						KiHa4-223	5:49: 9.1	+00:13: 1	W2-89
						KiHa4-224	5:49:19.0	+02: 2:52	W2-89
						KiHa76-411	5:49:21.0	−07:25:37	W1-91
						KiHa4-225	5:49:34.9	−02:32:28	W2-89
						RJ29	5:49:42.0	+01: 2:20	R7-89
						KiHa4-226	5:49:47.6	+01:53: 8	W2-89
						KiHa76-412	5:49:48.0	−06:55:50	W1-91
						RJ30	5:49:55.0	+01:40: 7	R7-89
						KiHa76-413	5:49:58.0	−06:58:51	W1-91
						KiHa4-227	5:50: 0.5	−02: 4: 6	W2-89
						KiHa4-228	5:50: 3.3	−02:49:53	W2-89
						KiHa76-414	5:50:11.0	−05:48:29	W1-91
						KiHa4-229	5:50:20.1	+01:25:37	W2-89
						L1622-1	5:50:22.9	+02: 0:44	O1-83
						KiHa76-415	5:50:32.0	−03:57:42	W1-91
						L1622-2	5:50:41.2	+01:26:11	O1-83
						KiHa4-230	5:50:48.1	+01: 7:35	W2-89
						L1622-3, KiHa4-231	5:50:56.6	+02:16:47	O1-83 W2-89
		188				LkHa334, L1622-4, KiHa4-232	5:51: 5.3	+01:37:41	H1-72 C1-74 C2-79 M4-80 O1-83 H1-88 R7-89 W2-89
						KiHa4-233	5:51:10.1	+01:54: 1	W2-89
						KiHa4-234	5:51:21.9	+02:34:37	W2-89
		189				LkHa335, L1622-5, KiHa4-235	5:51:22.9	+01:43:38	H1-72 C1-74 C2-79 M4-80 O1-83 H1-88 R7-89 W2-89
						L1622-6	5:51:26.2	+01:39:56	O1-83
						L1622-7	5:51:26.9	+02:35:49	O1-83
		515				HD288313, BD+1 1156, IRAS05513+0139	5:51:27.6	+01:39:43	R1-68 Z1-70 H1-77 P1-79 B10-82 H1-88 W2-90
						L1622-8	5:51:31.5	+01:38:30	O1-83
		190				LkHa336, L1622-9, KiHa4-236	5:51:44.4	+01:42:22	H1-72 D1-75 C2-79 M4-80 O1-83 H1-88 R7-89 W2-89
		516				LkHa336/c	5:51:44.8	+01:42:22	C2-79 H1-88
						L1622-S1	5:51:50.2	+01:39:46	O1-83
						L1622-10	5:51:51.0	+01:51:48	O1-83
						L1622-11	5:51:54.5	+01:50:30	O1-83
		191				LkHa337, L1622-12	5:52: 2.4	+01:29:22	H1-72 C1-74 C2-79 O1-83 H1-88 R7-89
						L1622-13	5:52:55.5	+01:23:49	O1-83
						L1622-14	5:53: 2.9	+02:25:32	O1-83
						L1622-S2	5:53:34.5	+02:12:54	O1-83
		517				L1622-15	5:54:39.5	+02:28:50	O1-83 H1-88 R7-89
						L1622-16	5:54:47.2	+02: 6:20	O1-83
						RJ36	5:55:22.0	+02:28: 8	R7-89

Notes to table 1: identifications in column (7)

1. 2023/: faint red stars in L1630, Strom *et al.* (S6-75).
2. /c denotes a companion star.
3. A, B, and C: H_α emission line stars in OH cloud G214.5-19.9, Grasdalen *et al.* (G1-73).
4. Chanal's object: a fuor-like star. First found by R. Chanal (apparently unpublished; reported by Hurst (H4-84)).
5. Cohen-Schwartz star: heavily obscured T Tauri star, long thought to be exciting star of HH1 and 2, Cohen and Schwartz (C3-79).
6. CoKu N2086: from Cohen and Kuhi (C2-79).
7. DL/G-: from Cohen and Kuhi (C2-79).
8. H7-: H_α emission line stars from Haro7-list, unpublished. See text section 1.
9. KiHa3-: Kiso H_α emission line star survey of area A-0903, Kogure *et al.* (K2-89).
10. KiHa75-: Kiso H_α emission line star survey of area A-0975, Wiramihardja *et al.* (W1-91).
11. KiHa4-: Kiso H_α emission line star survey of area A-0904, Wiramihardja *et al.* (W2-89).
12. KiHa76-: Kiso H_α emission line star survey of area A-0976, Wiramihardja *et al.* (W1-91).
13. L1622-: H_α emission line stars from Ogura and Hasegawa (O1-83).
14. L1641-N: optical counterpart of IRAS source, Strom *et al.* (S7-89).
15. LkHa: H_α emission line stars. Nrs. 286-320 from Herbig and Kuhi (H1-63); nrs. 321, 324-350 from Herbig and Rao (H1-72).
16. M78/: faint red stars in L1630, Strom *et al.* (S6-75).
17. M78-: NIR objects, Strom *et al.* (S6-75).
18. NGC2023/: NIR stars from Sellgren (S6-83).
19. Nk: optical counterparts of sources found in NIR survey of an area in L1641, Nakajima *et al.* (N1-86).
20. Re50: from catalogue of nebulous objects in Orion, Reipurth (R3-85).
21. RJ: faint Hα emission line stars, from survey by Robertson and Jordan (R7-89).
22. San: T Tau-type stars, Sanduleak (S1-71).
23. SS2-: H_α emission line stars, Stephenson and Sanduleak (S2-77).
24. SSV: from 2μm survey by Strom *et al.* (S2-76).
25. St: H_α emission line stars, Stephenson (S8-86).
26. Sugano's star: a fuor-like star. First found by Sugano (apparently unpublished; first reported by Kosai (K2-83)).
27. Ton: rapid variables found by Haro and Morgan (H3-53), Haro (H1-54), and Haro and Rivera Terrazas (H2-54).
28. WBHa: H_α emission line stars in L1641, Wouterloot and Brand (W2-91).
29. Xray: optical counterparts to *Einstein* X-ray sources, Strom *et al.* (S3-90).

TABLE 2. REFLECTION NEBULAE IN ORION, AND OTHER SMALL NEBULAE WHOSE NATURE IS UNCLEAR.

NAME	RA (1950)	DEC (1950)	OTHER NAMES/SOURCE	REFERENCES
vdB42	5:28:48.8	−05:42:23	BD−5 1281, HD36412	opt V1-66 R1-68
vdB44	5:29:34.8	−04:33:02	Bs113, DG56, IC420, BD−4 1162, HD36540	opt D1-95* D1-63 V1-66 R1-68 B1-77 mol K2-77 K2-80
RNO45	5:32:00.0	−03:01:00		opt C4-80
Haro6a	5:32:57.0	−05:05:54	Re19a, M42-5, IRAS05329−0505	opt H1-53 R3-85 O1-87 B2-88 nir W3-86
Haro5a	5:33:00.0	−05:05:48	Re19b, M42-6, IRAS05329−0505	opt H1-53 R3-85 O1-87 B2-88 nir W3-86
Re23	5:33:03.7	−06:29:54		opt R3-85
Re24	5:33:05.5	−06:28:34		opt R3-85
PP32	5:33:24.0	−05:29:28	T Ori, Haro4-123	opt S1-78* S1-82* S1-83* P1-93* P2-93* P1-95* opt W1-03 P2-04 B1-08 C1-12 C1-18 L1-19 H1-23 opt C1-24 C1-25 C1-26 C1-27 C2-27 C1-29 C2-30 opt J1-30 L1-30 C1-31 C1-32 Z1-32 C1-33 J1-33 opt B1-34 C1-34 C1-35 C1-36 C1-37 O1-40 S1-44 opt C1-46 G1-46 R1-46 H1-49 M2-49 P1-49 H1-50 opt L1-50 P1-50 L1-51 H2-52 H3-52 P1-52 H1-53 opt B1-54 P1-54 L1-56 S1-58 K1-59 H2-60 H2-62 opt K1-63 K1-64 J1-65 B1-68 W1-69 F1-70 M3-70 opt W1-70 S3-71 H1-72 P2-73 B2-74 B2-76 M1-76 opt C1-77 B3-77 B4-77 K1-77 W2-77 G2-78 C2-79 opt P1-79 V1-79 M4-80 F1-82 P2-82 M2-83 F1-84 opt F2-84 H3-84 F1-85 K2-85 S7-85 H1-86 S7-86 opt B3-87 H6-87 I1-87 M9-87 I1-87 H1-88 J1-88 opt K1-88 K3-88 V1-88 Y1-88 I1-89 M3-89 D1-90 opt J3-90 J4-90 nir G1-70 C2-73 C3-73 P2-73 G3-74 C2-79 B2-81 nir L2-83 K2-85 mol T1-81 T2-83 rad S2-90
Re29	5:33:32.1	−05:04:33	IRAS05334−0504	opt R3-85
Re30	5:33:34.7	−05:05:01		opt R3-85
Re33	5:33:36.2	−05:51:39		opt R3-85
Re34	5:33:40.6	−06:11:07		opt R3-85
RNO47	5:33:48.0	−06:27:00	Close to HH34	opt C4-80
RNO46	5:33:48.0	−06:30:00	Close to HH34, PP33, V582 Ori	opt H1-53 K1-59 R1-62 M1-63 A2-72 G1-76 P1-79 opt C4-80 P2-82 P2-86 mol T2-83
Re35	5:33:52.4	−06:23:03	IRAS05338−0624	opt R3-85 S7-89 nir S6-89 S7-89 fir B4-89 S6-89 mol W5-86 W5-88 H1-91
Re36	5:33:52.7	−06:21:24		opt R3-85 fir S6-89
Re37	5:33:57.0	−06:17:32		opt R3-85
Re38	5:33:57.6	−06:18:19		opt R3-85
Re39	5:33:59.0	−06:20:17		opt R3-85
Bs120	5:34:00.0	−06:29:00		opt B1-77
NGC1999	5:34:03.9	−06:43:45	vdB46, PP34, Bs122, BD−6 1253, V380Ori, IRAS05339−0644	opt R1-80* D1-88* G1-21 H1-46 M1-46 G1-48 J1-49 opt M2-49 H2-52 P1-52 H1-53 B1-54 P1-54 K1-59 opt B1-60 H2-60 H2-62 S2-62 J1-66 K1-66 V1-66 opt B1-68 K1-68 R1-68 D1-69 D2-69 L1-70 M3-70 opt W1-70 Z1-70 S3-71 B2-72 H1-72 S3-72 Z1-73 opt B2-74 B4-74 H1-74 I1-74 K1-74 S4-74 S1-75 opt A2-77 D1-77 G1-77 H1-77 G1-78 G2-78 W2-78 opt C2-79 G2-79 P1-79 S2-79 V1-79 S1-80 W3-80 opt G1-81 P5-81 B10-82 F1-82 M3-82 P2-82 W3-83 opt C1-84 C2-84 F1-84 F2-84 F1-85 G3-85 K2-85 opt H1-86 P2-86 S1-86 S7-86 S9-86 B2-87 H6-87 opt I1-87 M6-87 H1-88 H2-88 K2-88 K3-88 V2-88 opt Y1-88 A1-89 M3-89 S7-89 D1-90 J3-90 J4-90 opt S3-90 W2-90 W6-90 W1-91 W2-91 nir M1-66 M1-68 M2-68 G1-70 M1-70 G1-71 W1-71 nir A1-73 C2-73 C3-73 G3-73 G3-74 A2-77 S2-78 nir C2-79 C3-80 H2-80 L2-83 B1-84 A1-85 C7-85 nir K2-85 R5-85 N1-86 E2-87 B3-87 V2-88 S7-89 nir S11-89 fir E2-85 E1-86 C6-89 B1-90 mol W2-72 L1-73 L2-74 D1-75 G1-80 L1-81 T1-81 mol K5-82 W2-83 E1-84 L1-85 L2-85 T1-86 L3-88 mol S7-88 C2-89 C2-90 M1-91 M2-91 rad C2-80 C3-82 E2-87 M4-90
Re42	5:34:09.4	−06:17:14		opt R3-85
Re41	5:34:10.6	−06:16:42		opt R3-85
Re43	5:34:12.7	−06:23:04		opt R3-85
Re44	5:34:22.0	−06:22:25		opt R3-85
Re46	5:34:57.7	−05:45:21		opt R3-85
vdB48	5:35:40.7	−00:10:54	BD−0 1034, HD37370	opt V1-66 R1-68
GM63	5:36:54.0	−00:39:00		opt G3-77
RNO51	5:37:03.0	−03:38:00	IRAS05371−0338	opt C4-80
IC431	5:37:47.8	−01:28:59	Bs108, vdB50; WH446, HD37674, BD−1 1001	opt D1-95* H2-22 S1-36 V1-66 R1-68 D2-73 B1-77 opt W2-77 mol M3-75 K2-80
Re48	5:37:54.2	−07:15:29		opt R3-85 rad M4-90
Re49	5:37:59.4	−07:16:13		opt R3-85
Re50	5:38:05.0	−07:30:26	IRAS05380−0728	opt R3-85 R1-86 M14-87 S3-88 S7-89 H2-90 W2-90 nir C2-87 M14-87 S11-89 A6-89 C4-89 S7-89 H2-90 nir C1-91 fir B2-86 B4-89 mol W5-86 Z3-87 W5-88 W1-89 W4-89 M1-91 M2-91 rad W1-89 M4-90

TABLE 2. CONTINUED.

NAME	RA (1950)	DEC (1950)	OTHER NAMES/SOURCE	REFERENCES
B33	5:38:12.0	−02:28:00	Horsehead Neb, IC434	opt D1-95* R1-03 B1-13 B2-13 C2-18 B1-19 B1-27 opt H2-53 R1-68 L2-73 L3-73 D2-75 D1-83 R1-84 opt N1-85 W1-85 S2-86 M1-87 M2-87 Z1-87 B1-88 opt B2-88 mol C2-78 S7-82 S2-86 S9-87 nir R1-84 N1-85 fir S2-86
IC432	5:38:24.0	−01:31:55	vdB51, Bs109, WH465, HD37776, BD−1 1005	opt D1-95* H2-22 S1-36 V1-66 R1-68 D2-73 B1-77 opt W2-77 mol M3-75 K2-77 K2-80 S1-81
Bs130	5:38:24.0	−08:09:00	IRAS05384−0808	opt B1-77 G2-77 S7-89 nir S7-89 mol W5-86 W5-88
vdB53	5:38:57.1	−10:19:29	BD−10 1261	opt V1-66 R1-68 mol K2-80
NGC2023	5:39:09.3	−02:13:11	vdB52, Bs111, BD−2 1345, HD37903	opt D1-88* H1-22 H2-22 S1-36 C2-37 V1-66 R1-68 opt L1-68 D2-73 S6-75 B1-77 G3-78 D1-83 W1-84 opt W3-85 M1-87 M2-87 W4-88 R11-89 W3-89 W6-90 nir S6-75 S5-83 S6-83 S6-85 S2-89 R11-89 D3-90 nir L1-91 fir M2-74 E1-75 H1-80 M6-86 B4-89 mol M2-74 K1-75 M3-75 K2-76 P1-76 R1-77 W2-77 mol C2-78 P1-78 S1-81 W2-81 K2-82 W2-82 B1-83 mol W2-83 X1-84 L1-85 X1-85 X2-85 G2-87 G3-87 mol H4-87 T3-87 G1-88 H3-89 T1-89 S4-89 G3-90 mol W3-90 J1-90 J2-90 B4-90
Bs131	5:39:24.0	−08:03:00	PP42, Haro7-2, San6, IRAS05394-0801	opt S1-71 H1-72 B1-77 K1-78 B1-79 C2-79 P1-79 opt M4-80 B10-82 P2-82 S10-85 P2-86 H1-88 S7-89 opt W2-90 nir C1-74 C2-79 S7-89 mol D1-75 S1-81 T2-83 M1-91 rad M4-90
vdB54	5:39:26.4	−06:16:02	BD−6 1287 , Bs126, IRAS05394−0616	opt V1-66 R1-68 B1-77 mol K2-80 S1-81 W5-86
vdB55	5:40:06.0	−08:10:00	DG75/76, Bs132, RNO55	opt D1-63 V1-66 R1-68 B1-77 mol C4-80 K2-80 M1-84
IC435	5:40:30.9	−02:19:24	vdB57, Bs112, WH490, HD38087, BD−2 1350 IRAS05404−0220	opt D1-95* C1-37 C2-37 V1-66 R1-68 D2-73 B1-77 opt W6-90 W1-91 mol K2-80 S1-81 W5-86 W5-88 W4-89
RNO56	5:40:42.0	−03:40:00		opt C4-80
vdB58	5:42:03.9	−08:41:48	BD−8 1208	opt V1-66 R1-68
Bs106	5:43:30.0	−00:13:00	PP44, IRAS05435−0015?	opt B1-77 P1-79 P2-86 mol T2-83 W5-86 W5-88 W4-89 H1-91
NGC2068	5:44:13.0	+00:02:00	DG78,79,80, vdB59, NGC2064,2067, M78, Bs102, WH502, WH503, HD38563, BD+0 1177	opt D1-88* H1-22 H2-22 S1-36 C2-37 S2-52 S1-54 opt H1-63 D1-63 M1-65 V1-66 R1-68 L1-68 M3-70 opt S3-74 S6-75 D2-75 B1-77 W2-77 C2-83 M2-84 opt W3-85 W2-86 J1-87 W6-90 nir S3-74 S6-75 C2-83 S5-83 S6-83 L1-91 fir C5-84 B4-89 mol S1-70 J1-74 J2-74 L1-74 D1-74 B4-75 M3-75 mol K2-76 C2-78 P1-78 N1-79 K2-80 W1-81 L1-81 mol W2-81 W2-82 E1-84 J1-85 L1-85 W1-88 B10-89 mol K3-89 L3-89 rad A1-86
NGC2071	5:44:42.1	+00:16:28	Bs101, vdB60, DG81, BD+0 1181, HD290861, IRAS05445+0020, IRAS05445+0016	opt D1-88* H2-22 S1-36 C2-37 D1-63 V1-66 R1-68 opt B1-77 D1-83 W2-86 B2-87 B1-88 B2-88 W6-90 nir S2-76 M4-81 M5-83 S3-85 S4-87 L1-91 fir S2-81 M6-86 S4-87 B4-89 D1-89 S1-89 B5-90 mol J1-74 J2-74 S2-75 C1-78 P1-78 W1-81 M1-81 mol P2-81 P3-81 W2-81 B1-82 B2-82 B3-82 B4-82 mol C1-82 C2-82 L1-82 L2-82 L3-82 P1-82 P3-82 mol S1-82 S2-82 W2-82 B1-83 B3-83 S1-83 S8-83 mol T1-83 S1-84 T1-84 W2-84 F3-85 J1-85 L1-85 mol R4-85 S2-85 T1-85 T2-85 W4-85 B1-86 M4-86 mol R3-86 S4-86 S5-86 T2-86 W5-86 F2-87 I3-87 mol M7-87 M8-87 R4-87 S1-87 S5-87 T2-87 Z2-87 mol C4-88 I4-88 S1-88 T2-88 W1-88 W5-88 B3-89 mol B11-89 M4-89 T1-88 A5-89 K1-89 K3-89 M2-89 mol M5-89 M6-89 Y1-89 C5-90 G1-90 H1-90 K1-90 mol M5-90 Z1-90 rad B2-83 S1-85
PP45	5:45:00.0	+00:37:42	IRAS05451+0037	opt P1-79 P2-86 fir B2-86 mol W5-86 W5-88
RNO57	5:48:24.0	+03:06:00	IRAS05482+0306 Close to GGD8	opt G2-77 M1-84 G4-78 C4-80 M1-84 R1-91 nir C1-87 C1-88 fir B2-86 mol P3-80 G5-87
IRAS05487+0255	5:48:45.7	+02:55:02		nir R1-91 fir B2-86 mol R1-91
Bs99	5:51:24.0	+01:39:00	vdB62, PP46, HD288313	opt V1-66 R1-68 B1-77 P1-79 P2-86 mol K2-77 S1-81
GM18	5:53:00.0	+03:23:00	PP47	opt G3-77 P1-79 P2-86
vdB63	5:53:38.7	+01:49:00	BD+1 1163, HD288309	opt V1-66 R1-68 mol K2-80
Bs100	5:54:24.0	+00:38:00		opt B1-77 mol S1-81

Notes to table 2: identifications in columns (1) and (4)

1. B: Dark regions, Barnard (B1-27).
2. Bs: Bright nebulosities in opaque dust clouds, Bernes (B1-77).
3. DG: Reflection nebulae, Dorschner and Gürtler (D1-63).
4. GGD: Objects that look like HH objects, Gyulbudagian *et al.* (G4-78).
5. GM: Cometary nebulae, Gyulbudagyan and Magakyan (G3-77).
6. Haro4-: Emission-line star, Haro (H1-53).
7. Haro7-: Emission-line star, Haro (unpublished).
8. IC: Nebulae and Stars Clusters, Dreyer (D1-95*).
9. NGC: Nebulae and Star Clusters, Dreyer (D1-88*)
10. PP: Nebulous objects around cometary nebulae, Petrosyan and Petrosyan (P2- 86).
11. Re: Small nebulous objects, Reipurth (R3-85).
12. RNO: Red nebulous objects, Cohen (C4-80).
13. San: T Tau-type stars, Sanduleak (S1-71).
14. vdB: Reflection nebulae, van den Bergh (V1-66).
15. WH: Star, Warren and Hesser (W2-77).

TABLE 3. (CANDIDATE) HERBIG-HARO OBJECTS IN ORION.

NAME	RA (1950)	DEC (1950)	OTHER NAMES/SOURCE	REFERENCES
HH58	5:28:22.7	−04:11:44	IRAS05283−0412	opt R5-88 fir C4-90
HH59	5:29:52.0	−06:31:09		opt R5-88 fir C4-90
HH60	5:30:11.4	−06:28:50		opt R5-88 fir C4-90
HH83	5:31:05.3	−06:31:40	Re17, IRAS05311−0631	opt R3-85 R4-89 R6-89 R3-90 O1-91 mol W5-86 W5-88 W4-89
M42-2	5:31:34.0	−04:46:48		opt O1-87
HH84	5:31:45.3	−06:35:46	Re18, M42-1	opt R2-85 R3-85 O1-87 R4-89 R6-89
HH131	5:32:18.9	−08:30:03		opt O2-91
M42 HH2	5:32:44.0	−05:24:40		opt F1-76 C2-77 C1-80 W1-82 M3-86 V3-88 W2-88 mol H3-87 M1-90
M42 HH1	5:32:44.1	−05:23:44		opt G2-73 G5-74 M3-74 M3-77 C1-80 W1-82 A3-84 opt J2-85 T3-86 V3-88 mol H3-87 M8-89 M1-90 M6-90
M42 HH5	5:32:44.4	−05:22:18		opt A3-84 J2-85 V3-88 mol T2-84 H3-87 L2-89 M8-89 M1-90 M6-90
M42 HH6	5:32:45.0	−05:22:32		opt A3-84 V3-88 mol T2-84 H3-87 M8-89 M1-90 M6-90
M42-3	5:32:45.0	−06:31:36		opt O1-87
M42 HH7	5:32:45.2	−05:22:43		opt A3-84 V3-88 mol T2-84 H3-87 M8-89 M1-90 M6-90
M42 HH8	5:32:46.3	−05:24:15		opt A3-84 V3-88 mol H3-87 M8-89 M1-90 M6-90
M42 HH9	5:32:46.4	−05:23:40		opt A3-84 V3-88 mol H3-87 M8-89 M1-90 M6-90
HHL24	5:32:48.0	+03:55:00	G2-6	opt G2-84 mol G5-87
M42 HH10	5:32:48.0	−05:22:34		opt A3-84 J2-85 V3-88 mol T2-84 H3-87 M8-89 M1-90 M6-90
HH44	5:32:48.5	−05:12:19		opt S1-77 V3-88
HH33	5:32:51.4	−06:19:32	Bs118, Haro9a	opt H1-53 H1-74 B1-77 C2-83 M4-84 M3-85 S9-86 opt H1-87 H7-87 M13-87 S8-87 V3-88 R6-89 Z1-89 nir C2-83 fir C5-87 mol L2-79 H3-80 S1-81 E1-83 H2-83 E1-84 T1-86 mol S3-87 S8-87 L2-89 V1-89 Z1-89 rad B5-85 C8-89
HH40	5:32:54.4	−06:20:14	Bs118, Haro9a	opt H1-53 H1-74 B1-77 D2 -78 C2-83 M4-84 C1-85 opt M3-85 G2-86 S9-86 H1-87 H7-87 M13-87 S8-87 opt V3-88 R6-89 Z1-89 nir C2-83 C1-85 fir C5-87 mol L2-79 E1-80 H3-80 S1-81 B5-83 E1-83 H2-83 mol E1-84 C1-85 T1-86 M11-87 S3-87 S8-87 L2-89 mol V1-89 Z1-89 Z3-89 Z4-89 rad C1-85 B5-85 C8-89
M42 HH3	5:32:54.8	−05:26:51		opt T1-75 T1-78 C1-80 W1-82 V3-88 W2-88
M42-4	5:32:55.0	−04:42:06		opt O1-87
M42 HH4	5:32:55.2	−05:27:06		opt T1-75 C2-77 T1-78 C1-80 W1-82 V3-88 opt W2-88
HH85	5:32:57.3	−06:21:37	Re20	opt R3-85 R4-89 R6-89
HH126	5:33:00.4	−06:24:56	Re21	opt R3-85 O1-91
Re22	5:33:02.0	−06:28:54	M42-7, IRAS05329−0628	opt R3-85 O1-87 S7-89 nir S7-89 mol T1-86 W5-86 W5-88 W4-89 M1-91 M2-91
HH34	5:33:05.2	−06:30:33	incl HH34N (M42-8), HH34-*7/V571 Ori	opt H1-53 P1-54 K1-59 R1-62 M1-63 A2-72 B2-72 opt H1-74 G1-76 B1-77 P2-82 C2-83 M2-83 C4-84 opt P1-85 R1-85 R2-85 R2-86 S9-86 B5-87 B6-87 opt B7-87 C4-87 M12-87 M13-87 R3-87 S2-87 O1-87 opt B4-88 H1-88 M5-88 R1-88 S2-88 V3-88 M7-89 opt H1-89 R6-89 S3-90 nir C4-84 R1-85 R2-86 fir C2-83 C5-84 C5-87 B4-89 mol L1-75 L2-79 H3-80 S1-81 E1-83 H2-83 C4-84 mol R1-85 R2-86 T1-86 R3-87 S3-87 A2-89 C2-90 rad C2-83 B5-85 M11-87 Y2-89 Y1-90 Y2-90
HH45	5:33:06.3	−04:52:43		opt S1-77 V3-88 R4-89 mol H2-83
HH86	5:33:13.4	−06:37:45	Re25	opt R3-85 R4-89 R6-89
HH87	5:33:17.2	−06:39:21	Re26	opt R3-85 R4-89 R6-89
HH88	5:33:18.0	−06:39:46	Re27	opt R3-85 R4-89 R6-89
HH127	5:33:25.0	−07:01:47	Re28	opt R3-85 O1-91
HH41	5:33:34.0	−05:04:40	Haro3a, Bs115	opt H1-53 H1-74 B1-77 S1-77 V3-88 nir C5-80 R1-83 mol L2-79 H3-80 E1-83 H2-83 S3-87 rad C8-89
HH42	5:33:37.0	−05:06:30	Haro4a, Bs116	opt H1-53 H1-74 B1-77 S1-77 C2-83 C1-85 V3-88 nir C5-80 R1-83 C1-85 fir C2-83 C5-88

TABLE 3. CONTINUED.

NAME	RA (1950)	DEC (1950)	OTHER NAMES/SOURCE	REFERENCES
HH42				mol L2-79 H3-80 E1-83 H2-83 C1-85 S3-87
				rad C2-83 C1-85 C8-89
HH128	5:33:41.0	−05:06:30	Re31, M42-9	opt R3-85 O1-87 O1-91
HH129	5:33:43.0	−05:06:00	Re32, M42-10	opt R3-85 O1-87 O1-91
HH3	5:33:46.0	−06:44:55	Haro10a, Bs121	opt H1-53 M1-63 H1-74 B1-77 D2-78 S1-78 B4-81
				opt D1-82 B5-83 C2-83 J2-83 E1-84 R2-87 V3-88
				opt R4-89 R6-89 W1-91
				nir C5-80 R10-89
				fir C2-83 C5-84
				mol L2-79 E1-80 S1-81 E1-83 H2-83 S11-83
				rad C2-83 M6-83
HH61	5:33:47.4	−07:08:51		opt R5-88 O1-91
				fir C4-90
HH62	5:33:47.5	−07:12:51		opt R5-88 O1-91
				fir C4-90
HH1	5:33:55.0	−06:47:03	Haro11a, Bs123,	opt H1-51 H1-52 H1-53 A1-54 B1-55 B1-56 O1-58
			VLA1, CS*,	opt H1-60 M1-63 B1-73 H1-73 B1-74 G4-74 H1-74
			IRAS05338−0647	opt S1-74 S2-74 B2-75 G3-75 S1-75 S3-75 B1-76
				opt S1-76 B1-77 B1-78 B2-78 B3-78 D2-78 S1-78
				opt C3-79 M1-80 O1-80 B1-81 B3-81 B4-81 H1-81
				opt P5-81 S3-81 B7-82 B8-82 B9-82 D1-82 B5-83
				opt C2-83 J2-83 M7-83 M8-83 B4-84 C4-84 G1-84
				opt H1-84 B2-85 B3-85 B6-85 C1-85 C4-85 C5-85
				opt M3-85 S8-85 S3-86 S9-86 B4-87 E1-87 H1-87
				opt H2-87 I1-87 M11-87 M13-87 R1-87 S8-87 C2-88
				opt H1-88 L2-88 R2-88 R3-88 S5-88 V3-88 B5-89
				opt B6-89 B9-89 H1-89 N1-89 R1-89 R4-89 R6-89
				opt S7-89 Z1-89 N1-90 R1-90 W1-91
				nir S1-75 C3-79 C5-80 H1-82 C4-84 C1-85 R5-85
				nir S8-85 H3-86 N1-86 T4-87 R10-89 S7-89
				fir H1-82 C2-83 C5-84 R5-85 H3-86 P2-87 T4-87
				fir C5-88
				mol L1-74 L1-75 L2-79 E1-80 S1-81 B3-82 E1-82
				mol K5-82 S6-82 E1-83 H2-83 S11-83 C3-84 C4-84
				mol E1-84 C1-85 L1-85 T4-85 H3-86 H6-86 R3-86
				mol T1-86 W5-86 M3-87 M11-87 R4-87 S3-87 S8-87
				mol C4-88 M1-88 Z1-89 Z3-89 C5-90 D2-90 H1-90
				rad K1-79 C2-83 M6-83 C1-85 P3-85 M11-87 M4-90
				rad R2-90
Re40	5:33:57.0	−06:25:00	Nk43, M42-11	opt R3-85 O1-87 S7-89
			IRAS05338−0624	nir N1-86 S6-89 S7-89
				fir B4-89
				mol W5-86 W5-88 H1-91
V380 Ori-HH	5:33:59.5	−06:44:39	NGC1999, PP34,	opt R1-80* D1-88* G1-21 H1-46 M1-46 G1-48 J1-49
			Bs122, vdB46,	opt M2-49 H2-52 P1-52 H1-53 B1-54 P1-54 K1-59
			BD−6 1253,	opt B1-60 H2-60 H2-62 S2-62 J1-66 K1-66 V1-66
			IRAS05339−0644	opt B1-68 K1-68 R1-68 D1-69 D2-69 L1-70 M3-70
				opt W1-70 Z1-70 S3-71 B2-72 H1-72 S3-72 Z1-73
				opt B2-74 B4-74 H1-74 I1-74 K1-74 S4-74 S1-75
				opt A2-77 D1-77 G1-77 H1-77 G1-78 G2-78 W2-78
				opt C2-79 G2-79 P1-79 S2-79 V1-79 S1-80 W3-80
				opt G1-81 P5-81 B10-82 F1-82 M3-82 P2-82 W3-83
				opt C1-84 C2-84 F1-84 F2-84 F1-85 G3-85 K2-85
				opt H1-86 P2-86 S1-86 S7-86 S9-86 B2-87 H6-87
				opt I1-87 M6-87 H1-88 H2-88 K2-88 K3-88 V2-88
				opt Y1-88 A1-89 M3-89 S7-89 D1-90 J3-90 J4-90
				opt S3-90 W2-90 W6-90 W1-91 W2-91
				nir M1-66 M1-68 M2-68 G1-70 M1-70 G1-71 W1-71
				nir A1-73 C2-73 C3-73 G3-73 G3-74 A2-77 S2-78
				nir C2-79 C3-80 H2-80 L2-83 B1-84 A1-85 C7-85
				nir K2-85 R5-85 N1-86 E2-87 B3-87 V2-88 S7-89
				nir S11-89
				fir E2-85 E1-86 C6-89 P2-87 B1-90
				mol W2-72 L1-73 L2-74 D1-75 G1-80 L1-81 T1-81
				mol K5-82 E1-84 L1-85 L2-85 L3-88 S7-88 C2-89
				mol C2-90 M1-91 M2-91
				rad C2-80 C3-82 E2-87 M4-90
HH35	5:34:00.0	−06:45:00	vdB46, Bs122, PP34	opt R1-68 H1-74 B1-77 S1-78 V3-88 R6-89
				mol L1-75 E1-83 H2-83 S11-83 E1-84 L1-85
HH2	5:34:00.0	−06:49:00	Haro12a, Bs125,	opt H1-51 H1-52 H1-53 A1-54 H1-57 H1-60 M1-63
			VLA1, CS*	opt H4-69 B1-74 H1-74 S2-74 B2-75 G2-75 G3-75
				opt S1-75 S3-75 B1-76 B1-77 B1-78 B2-78 B3-78
				opt D2-78 S1-78 B2-79 C3-79 M1-80 B3-81 B4-81
				opt H1-81 S3-81 B7-82 B8-82 B9-82 D1-82 B5-83
				opt C2-83 J2-83 M7-83 M8-83 B5-84 C4-84 G1-84
				opt H1-84 B2-85 B3-85 C1-85 M3-85 S8-85 C2-86
				opt L1-86 S3-86 S9-86 B4-87 E1-87 H1-87 H2-87
				opt I1-87 M13-87 R1-87 S8-87 C2-88 H1-88 L2-88
				opt R2-88 R4-88 V3-88 B9-89 R4-89 R6-89 Z1-89
				opt R1-90 W1-91
				nir S1-75 C3-79 C5-80 R1-83 C4-84 C1-85 R5-85
				nir S8-85 H3-86 N1-86 T4-87 R10-89 S11-89
				fir C2-83 C5-84 R5-85 H3-86 P2-87 P4-87 T4-87
				fir C5-88
				mol L2-79 E1-80 F1-80 S1-81 E1-82 B3-82 S6-82
				mol E1-83 H2-83 C3-84 C4-84 E1-84 C1-85 L1-85
				mol T4-85 H3-86 H6-86 R3-86 M3-87 M11-87 R4-87

TABLE 3. CONTINUED.

NAME	RA (1950)	DEC (1950)	OTHER NAMES/SOURCE	REFERENCES
HH2				mol S3-87 S8-87 M1-88 Z1-89 Z3-89 D2-90
				rad C2-83 M6-83 C1-85 P3-85 M11-87 M4-90 R2-90
HH130	5:34:20.0	−06:51:42	Re45, M42-12	opt R3-85 O1-87 O1-91
HH63	5:34:21.0	−04:27:45	P2441, IRAS05343−0427	opt B1-34 P1-54 H2-62 W1-69 M3-70 B1-72 B2-72
				opt H1-72 A1-74 B2-76 M2-76 B4-77 K1-78 C2-79
				opt P2-82 M2-83 S9-83 I1-87 H1-88 K3-88 R5-88
				opt Y1-88 M3-89 W2-90 W1-91
				nir M1-66 M1-68 C2-79 R2-84
HH36	5:34:21.0	−06:46:02	Bs124	opt H1-74 B1-77 V3-88
				mol L1-75 L2-79 H3-80 S1-81 E1-83 H2-83 S11-83
				mol E1-84
				rad M6-83
HH64	5:35:22.3	−07:07:12		opt R5-88
				fir C4-90
HH89	5:35:22.8	−06:38:07	Re47	opt R3-85 R4-89
HH43	5:35:45.0	−07:11:06	Haro14a, Bs128,	opt H1-53 M2-63 H1-74 S3-74 B1-77 D2-78 M1-80
			IRAS05357−0710	opt C2-81 D1-82 S2-83 C4-84 S5-85 S3-86 S9-86
				opt I1-87 S8-87 L2-88 S4-88 V3-88 B6-89 B9-89
				opt S7-89 B2-90 W1-91
				nir S3-74 C5-80 B6-83 H2-83 S2-83 C4-84 S4-88
				nir S7-89
				fir C5-84 C6-85 B2-86 C5-87 D1-87 C5-88 B4-89
				mol D1-74 L2-79 H3-80 S1-81 B5-83 E1-83 S2-83
				mol C4-84 E1-84 W5-86 S3-87 S8-87 A2-89 Z3-89
				mol Z4-89 W4-90 M1-91 M2-91
				rad M11-87 C8-89
Haro13a	5:35:53.0	−07:03:59	DG69, Bs127,	opt D1-95* H1-53 D1-63 M2-63 D1-70 S3-74 B1-77
			IC429/430, PP37,	opt P1-79 M1-80 P2-86 S9-86 S8-87 H1-88 S7-89
			V883 Ori, Nk83	nir A1-75 N1-86 S7-89 S11-89
			IRAS05358−0704	mol K2-76 L2-79 T2-83 S8-87 L3-88 L4-88 M1-91
				mol M2-91
HH38	5:35:56.4	−07:13:17	Bs129	opt H1-74 B1-77 C2-83 C4-84 S9-86 V3-88
				nir C4-84
				fir C2-83 C5-87 C5-88
				mol L2-79 S1-81 E1-83 H2-83 C4-84 E1-84 S3-87
				mol A2-89
				rad C2-83 C8-89
Haro4-249	5:36:17.0	−07:14:14	Nk88,	opt H1-53 M2-63 S3-74 C2-79 C4-80 P2-82 S9-86
			IRAS05363−0714	opt G4-87 S8-87 H1-88 V4-88 S7-89 W2-90 W1-91
				nir C2-79 N1-86 S7-89
				fir B2-86
				mol L2-79 S8-87 L3-88 L4-88 M1-91 M2-91
				rad M4-90
Haro4-255	5:36:57.0	−07:28:18	PP39, M42-13,	opt H1-53 H1-72 C2-79 P1-79 P2-82 P2-86 O1-87
			IRAS05369-0728	opt S8-87 H1-88 S7-89 W2-90 W1-91
				nir C1-74 C2-79 N1-86 S5-89 S7-89 S11-89
				fir E1-86 S5-89 W2-90
				mol D1-75 L1-85 W5-86 S8-87 L3-88 W5-88 C2-89
				mol F2-89 M2-89 C2-90 W4-90 H1-91 M1-91 M2-91
				rad M4-90
HH65	5:37:53.8	−07:26:36		opt R5-88
				fir C4-90
HH66	5:37:55.0	−02:04:04		opt R5-88
GGD7	5:38:24.0	−08:09:00	HHL29, RNO55,	opt G4-78 S7-89
			IRAS05384−0808	nir C1-88 S7-89
				mol P2-79 P3-80 R1-80 M1-81 W5-86 G5-87 W5-88
				mol W4-89 H1-91
HH67	5:38:32.6	−01:48:06		opt R5-88
				fir C4-90
HHL30	5:38:42.0	−08:06:00	G1-16	opt G2-82
				mol G5-87
HH90	5:38:53.3	−01:11:39	Re51	opt R3-85 R4-89
N2023HH2	5:38:55.9	−02:24:32		opt M2-87 V3-88
N2023HH1	5:39:00.6	−02:18:52	IRAS05391−0217	opt M2-87 V3-88
				fir B4-89
				mol W5-86 W5-88 W4-89
N2023HH3	5:39:02.0	−02:25:07		opt M2-87 V3-88
N2023HH5	5:39:02.9	−02:18:44	IRAS05391−0217	opt M2-87 V3-88
				fir B4-89
				mol W5-86 W5-88 W4-89
N2023HH4	5:39:03.9	−02:18:24	IRAS05391−0217	opt M2-87 V3-88
				fir B4-89
				mol W5-86 W5-88 W4-89
HH68	5:39:08.7	−06:27:20		opt R5-88
				fir C4-90
HH69	5:39:15.6	−06:31:18		opt R5-88
				fir C4-90
HH91	5:39:24.8	−01:15:00	Re52/53	opt R3-85 R4-89
HH92	5:39:48.6	−01:19:52	Re54,	opt R3-85 R4-89
			IRAS05399−0121?	mol W5-86 W5-88 W4-89 H1-91
HH93	5:40:23.4	−01:27:03	Re55	opt R3-85 R4-89
HH94	5:40:56.3	−02:34:14	Re56	opt R3-85 R4-89
				rad C8-89
HH95	5:41:21.5	−02:38:58	Re57	opt R3-85 R4-89
				rad C8-89
HH19	5:43:16.0	−00:06:19	Bs104	opt H1-74 B1-77 M4-84 M3-85 S9-86 J1-87 M13-87
				opt V3-88 Z1-89

TABLE 3. CONTINUED.

NAME	RA (1950)	DEC (1950)	OTHER NAMES/SOURCE	REFERENCES
HH19				fir C5-87 B4-89
				mol L1-75 S1-81 E1-83 H2-83 B10-89 L2-89 Z1-89
				mol Z3-89 C5-90
				rad B5-85
HH20	5:43:21.5	−00:04:12	Bs103	opt H1-74 B1-77 S9-86 J1-87 V3-88
				mol L1-75 S1-81 E1-83 H2-83 S3-87
				rad B5-85
HH21	5:43:26.2	−00:06:07		opt H1-74 S9-86 J1-87 V3-88
				mol L1-75 L2-79 E1-83 H2-83
				rad B5-85
HH70	5:43:28.7	−00:06:43		opt R5-88
				fir C4-90
HH26	5:43:31.2	−00:15:42	Bs107, SSV59?,	opt H1-74 B1-77 C2-83 S9-86 J1-87 V3-88
			IRAS05435−0015	nir S2-76
				fir C2-83 M6-86 C5-88 B4-89
				mol L1-75 L2-79 S1-81 B3-82 S5-82 S6-82 B1-83
				mol E1-83 H2-83 M1-83 T1-83 E1-84 L1-85 L3-85
				mol W5-86 M5-87 S3-87 Z2-87 W5-88 T2-89 W4-89
				mol C2-90 H1-90 H1-91
				rad C2-83 B5-85 M11-87
HH25	5:43:33.2	−00:14:31	Bs107, PP44,	opt H1-74 B1-77 C2-83 C4-84 P2-86 S9-86 J1-87
			SSV59,	opt V3-88
			IRAS05435−0015;	nir S2-76 C5-80 H1-82 C2-83 C4-84
			near HH26IR	fir H1-82 B4-89
				mol H3-80 S1-81 B3-82 S6-82 B1-83 E1-83 H2-83
				mol M1-83 T2-83 C4-84 L3-85 T1-85 T2-85 M5-87
				mol M8-87 Z2-87 R4-87 T2-89 C2-90
				rad T3-85
HH24	5:43:34.5	−00:11:07	Bs105, M78A-E,	opt H1-74 S2-74 S3-74 B2-75 G3-75 S3-75 S6-75
			SSV63,	opt B1-77 D2-78 S1-79 B5-83 C2-83 B5-84 C4-84
			IRAS05435−0011	opt C3-86 C4-86 S9-86 H1-87 I1-87 J1-87 M12-87
				opt S2-87 S6-87 S7-87 L2-88 B9-89 M7-89 R2-89
				opt Z1-89
				nir S2-74 S3-74 S6-75 S2-76 C5-80 H1-82 C4-84
				fir H1-82 C2-83 C5-84 B2-86 C5-87 B4-89
				mol D1-74 L1-74 P2-79 E1-80 H3-80 P3-80 L1-81
				mol S1-81 W1-81 S6-82 B1-83 E1-83 H2-83 M1-83
				mol C4-84 E1-84 J1-85 L1-85 L3-85 W5-86 C4-87
				mol M5-87 M8-87 Z2-87 H1-90
				rad C2-83 B2-84 B5-85 M11-87
HH22	5:43:40.6	−00:06:37		opt H1-74 S9-86 J1-87 V3-88
				mol E1-83 H2-83
				rad B5-85
HH23	5:43:41.2	−00:04:37		opt H1-74 C1-85 S9-86 J1-87 V3-88
				nir C1-85
				mol E1-83 H2-83 C1-85
				rad C1-85
HH27	5:43:49.5	−00:14:46		opt H1-74 S9-86 J1-87 V3-88
				mol L1-75 L2-79 S6-82 E1-83 H2-83 M1-83 L3-85
				mol S3-87 B10-89 L2-89 C2-90 C5-90
HH71	5:44:46.1	+00:39:43		opt R5-88
				fir C4-90
				mol P2-79 P3-80 R1-80 G5-87
HH110	5:48:47.5	+02:54:07		opt R1-91
				mol R1-91
HH111	5:49:08.9	+02:47:50	IRAS05491+0247	opt R5-89 R6-89 R1-91
				nir R5-89 R1-91
				mol R1-91
HH112	5:49:14.4	+02:59:47		opt R1-91
				mol R1-91
HH113	5:50:57.2	+02:43:07		opt R1-91
				mol R1-91
GGD9	5:53:00.0	+03:23:00	HHL33	opt G4-78
				nir C1-88
				mol R1-80 G5-87

Notes to table 3: identifications in columns (1) and (4)

1. Bs: Bright nebulosities in opaque dust clouds, Bernes (B1-77).
2. CS*: Star found by Cohen and Schwarz (C3-79).
3. DG: Reflection nebulae, Dorschner and Gürtler (D1-63).
4. G1-: Candidate HH objects, Gyulbudagian (G2-82).
5. G2-: Objects looking like HH objects, Gyulbudagian (G2-84).
6. GGD: Objects that look like HH objects, Gyulbudagian *et al.* (G4-78).
7. Haro*a: Peculiar objects, Haro (H1-53).
8. HHL: Herbig-Haro-like nebulosities, Gyulbudagian *et al.* (G5-87).
9. M42-: Candidate HH objects, Ogura (O1-87).
10. M87A-E: Herbig-Haro objects, Strom *et al.* (S4-74).
11. N2023HH: Herbig-Haro objects in the vicinity of NGC2023, Malin *et al.* (M2-87).
12. Nk: Near IR sources in L1641, Nakajima *et al.* (N1-86).
13. PP: Nebulous objects around cometary nebulae, Petrosyan and Petrosyan (P2- 86).
14. Re: Small nebulous objects, Reipurth (R3-85).
15. RNO: Red nebulous objects, Cohen (C4-80).
16. SSV: from 2 micron survey by Strom *et al.* (S2-76).
17. vdB: Reflection nebulae, van den Bergh (V1-66).
18. VLA1: Radio source, Pravdo *et al.* (P3-85).

TABLE 4. MOLECULAR OUTFLOWS IN ORION.

NAME	RA (1950)	DEC (1950)	IRAS SOURCE	REFERENCES
OriA-w	5:30:14.5	−05:37:52	IRAS05302−0537	F2-86 F1-88 F1-89
OMC2	5:32:59.6	−05:11:32	IRAS05329−0512	F2-85 F1-89
L1641-n	5:33:52.7	−06:24:02	IRAS05338−0624	F2-86 F1-88 F2-88 F1-89 W5-90 M1-91 M2-91
			Nk43, Re35	
	5:33:57.8	−06:26:44	IRAS05339−0626	M1-91 M2-91
NGC1999	5:33:59.4	−06:44:45	IRAS05339−0644	S6-82 E1-83 S11-83 T2-83 E1-84 L1-85 L2-85
			V380 Ori	L3-88 L4-88 F1-89 M1-91 M2-91
OriA-e	5:34:11.0	−05:30:03	IRAS05341−0530	F2-86 F1-89
	5:34:15.4	−06:39:44	IRAS05342−0639	M1-91 M2-91
Ori-I-2	5:35:33.2	−01:46:50	IRAS05355−0146	F1-89 S9-89 S10-89
L1641-c	5:36:20.9	−07:02:43	IRAS05363−0702	F1-88 F2-89 M1-91 M2-91
Haro4-255	5:36:56.4	−07:28:14	IRAS05369−0728	L1-85 L2-85 F1-88 L3-88 L4-88 F1-89 F2-89
				M2-89 M1-91 M2-91
L1641-s3	5:37:31.1	−07:31:59	IRAS05375−0731	F1-89 F2-89 W5-90 M1-91 M2-91
Re50, L1641-s	5:38:02.7	−07:28:59	IRAS05380−0728	F2-86 R1-86 F1-88 F1-89 F2-89 M1-91 M2-91
	5:38:22.6	−08:07:13	IRAS05383−0807	M1-91 M2-91
L1641-s4	5:38:24.6	−08:08:20	IRAS05384−0808	F1-89 F2-89
			GGD7	
L1641-s2	5:40:23.2	−08:18:26	IRAS05403−0818	F1-88 F1-89 F2-89 W4-89
HH26IR	5:43:31.1	−00:15:28	IRAS05435−0015	S5-82 S6-82 B1-83 E1-83 E1-84 L1-85 F1-89
			Bs106	
HH24	5:43:34.2	−00:11:08	IRAS05435−0011	S6-82 B1-83 E1-83 E1-84 L1-85 F1-89
			SSV63	
NGC2068H_2O	5:43:58.0	−00:04:00	IRAS05437−0001	E1-84 L1-85 F1-89
			NGC2068	
NGC2071	5:44:30.3	+00:20:42	IRAS05445+0020	B1-82 B2-82 L3-82 B1-83 B3-83(HI) E1-84 S1-84
				W2-84(HCO+) F3-85 L1-85 R4-85 S4-86 S5-86
				M5-86(OH) F2-87 M7-87(OH) M8-87(OH) S5-87
				S1-88(CH) T1-88(NH3) F1-89 A1-89 M2-89 M6-89 K1-90
				M5-90
NGC2071-n	5:45:07.8	+00:37:41	IRAS05451+0037	F2-86 I3-87 I4-88 F1-89
			PP45	
IRAS05487+0255	5:48:45.7	+02:55:02		R1-91
HH111	5:49:09.1	+02:47:48	IRAS05491+0247	F1-89 R1-91

TABLE 5. H_2O MASERS IN ORION.

NAME	RA (1950)	DEC (1950)	REFERENCES
OMC2(2)	5:32:58.2	−05:07:36	C2-78 R2-83 C4-88 C5-90
OMC2(1)	5:32:59.5	−05:11:45	M2-76 R2-83 C4-88 B3-89 C5-90
HH1	5:33:53.2	−06:46:50	L2-75 H2-83 C4-88 C5-90
IRAS05375-0731	5:37:31.0	−07:31:51	W5-86 C4-88 C5-90
IRAS05413-0104	5:41:18.6	−01:04:17	W4-86 W5-86 C4-88 W4-89 C5-90
HH19-27	5:43:57.5	−00:03:40	H2-83 C4-88 C5-90
NGC2071	5:44:31.3	+00:20:48	S2-75 P1-77 C1-78 S1-81 L2-82 S2-85 W5-86
			B3-89 C5-90

References

S1-57* Struve,M.O.: MNRAS 17, 225
B1-67* Bond,G.P.: Harvard Ann 5
S1-78* Schmidt,J.F.J.: AN 93, 78
R1-80* Rosse, Lord: Sci Trans Royal Dublin Soc 2, Ser II
H1-82* Holden,E.S.: Astronomical and Meteorological Observations made during the Year 1878 at the US Naval Observatory, Appendix I
S1-82* Schmidt,J.F.J.: AN 101, 325
S1-83* Schmidt,J.F.J.: AN 104, 302
D1-88* Dreyer,J.L.E.: Mem RAS 49, 1
P1-89* Pickering,W.H.: Sidereal Mess 9, 1
R1-90* Roberts,I.: MNRAS 50, 316
P1-93* Parkhurst,H.M.: Harvard Ann 29, 99
P2-93* Parkhurst,H.M.: AJ 13, 167
B1-94* Barnard,E.E.: Popular Astron 2, 151
D1-95* Dreyer,J.L.E.: Mem RAS 51, 185
P1-95* Pickering,W.H.: Harvard Ann 32, 36
S1-98* Scheiner,J.: Potsdam Publ 11, 27
W1-01 Wolf,M: AN 157, 81
B1-03 Barnard,E.E.: ApJ 17, 77
R1-03 Roberts,I.: ApJ 17, 72
W1-03 Wolf,M.: AN 163, 161
H1-04 Hartwig,E.: AN 164, 415
P1-04 Parkhurst,J.A.: ApJ 20, 136
P2-04 Pickering,E.C.: Harvard Circ 78; AN 165, 215
P3-04 Pickering,E.C.: Harvard Circ 79; AN 166, 35
P4-04 Pickering,E.C.: Harvard Circ 86; AN 166, 313
P1-05 Pickering,E.C.: Harvard Circ 93; AN 168, 147
W1-06 Wolf,M., Wolf,G.: AN 171, 77
B1-08 Baranow,M.V.: Engelhardt Publ 2, 50
B1-10 Burns,K.: AJ 26, 138; AN 186, 175
C1-12 Campbell,L.: Harvard Ann 63, 32
M1-12 van Maanen,A.: AJ 27, 139
B1-13 Barnard,E.E.: Lick Obs Publ 11
B2-13 Barnard,E.E.: ApJ 38, 496
D1-14 Duner, Hartwig,E., Müller,G.: AN 199, 65
G1-14 Graff,K.: AN 197, 233
C1-18 Campbell,L.: Harvard Ann 79, 21
C2-18 Curtis,H.D.: PASP 30, 65
M1-18 Müller,G., Hartwig,E.: Geschichte und Literatur der veränderliche Sterne (1. Band)
B1-19 Barnard,E.E.: ApJ 49, 1 (correction ApJ 49, 390)
L1-19 Ludendorff,H.: AN 209, 275
M1-19 van Maanen,A.: Proc Nat Ac of Sciences 5, 225; Comm Mt Wilson 57
G1-20 Graff,K.: AN 212, 79
B1-21 Bailey,S.I.: Harvard Circ 225
G1-21 Gregory,C.C.L.: Helwan Obs Bul 1, 206
G1-22 Graff,K.: AN 217, 357
H1-22 Hubble,E.: ApJ 56, 162
H2-22 Hubble,E.: ApJ 56, 400
H1-23 Hoffmeister,C.: Mitt Sonneberg 3
H2-23 Hoffmeister,C.: AN 218, 313
C1-24 Campbell,L.: Harvard Circ 259
S1-24 Shapley,H.: Harvard Circ 254
S2-24 Shapley,H.: Harvard Bul 803
W1-24 Wolf,M.: AN 222, 335
B1-25 Becker,Fr: AN 225, 105
C1-25 Campbell,L.: Harvard Circ 279
C1-26 Campbell,L.: Harvard Circ 296
B1-27 Barnard,E.E.: Photographic atlas of selected regions of the Milky Way (Frost, Calvert eds)
C1-27 Campbell,L.: Harvard Circ 318
C2-27 Campbell,L.: Harvard Circ 319
C1-29 Campbell,L.: Harvard Circ 344
H1-29 Hoffmeister,C.: AN 236, 233
M1-29 Miller, Miss: Harvard Bul 868, 14
C1-30 Campbell,L.: Harvard Circ 353
C2-30 Campbell,L.: Harvard Circ 354
J1-30 Jacchia,L.: AN 240, 121
L1-30 Lause,F.: Perem Zv 2, 60
R1-30 Reinmuth,K.: AN 238, 333
C1-31 Campbell,L.: Harvard Circ 361
C2-31 Campbell,L.: Harvard Circ 367
H1-31 Hoffmeister,C., Morgenroth,O.: Sonneborg Mitt 20
T1-31 Trumpler,R.J.: PASP 43, 255
C1-32 Campbell,L.: Harvard Circ 376
Z1-32 Zinner,E.: Bamberg Veroeff 1, 229
C1-33 Campbell,L.: Harvard Circ 382
J1-33 Jacchia,L.: Bologna Publ 2, 173
M1-33 Merrill,P.W., Burwell,C.G.: ApJ 78, 87
B1-34 Brun,A.: Bul Ass Fr Observ Etoiles Variables 3, 149
C1-34 Campbell,L.: Harvard Circ 395
P1-34 Plaut,L.: BAN 7, 181
C1-35 Campbell,L.: Harvard Circ 407
C2-35 Campbell,L.: Harvard Circ 408
C1-36 Campbell,L.: Harvard Circ 415
C2-36 Campbell,L.: Harvard Circ 418
S1-36 Struve,O., Story,H.: ApJ 84, 203
B1-37 Baade,W., Minkowski,R.: ApJ 86, 119
B2-37 Böhme,S.: AN 264, 269
C1-37 Campbell,L.: Harvard Circ 427
C2-37 Collins,O.C.: ApJ 86, 529
C1-38 Campbell,L.: Harvard Ann 107, 280
B1-39 Böhme,S.: AN 268, 74
O1-40 Olivier,C.P., et al.: Flower Publ 5, part 3
S1-44 Stein,J.: Spec Vatican Ric 1, 301
C1-46 Campbell,L.: Popular Astr 45, 38; Harvard Repr 291, 14
G1-46 Greenstein,J.L., Struve,O.: PASP 58, 366
H1-46 Herbig,G.H.: PASP 58, 163
M1-46 Morgan,W.W., Sharpless,S.: ApJ 103, 249
P1-46 Parenago,P.P.: Perem Zv 6, 26
R1-46 Rosino,L.: Bologna Publ 5, 1
G1-48 Greenstein,J.L.: ApJ 107, 375
S1-48 Soloviev,A.W.: Astron Tsirk 79, 10
H1-49 Hoffmeister,C.: AN 278, 24
J1-49 Joy,A.H.: ApJ 110, 424
J2-49 Joy,A.H., Wilson,R.E.: ApJ 109, 231
M1-49 McKnelly,R.D.: AJ 55, 6
M2-49 Merrill,P.W., Burwell,C.G.: ApJ 110, 387
P1-49 Parenago,P.P.: Astron Tsirk 93, 6
H1-50 Haro,G.: AJ 55, 72
H2-50 Herbig,G.H.: ApJ 111, 15
K1-50 Kholopov,P.N.: Astron Zh 27, 233
L1-50 Lacchini,G.B.: Publ Trieste 240
P1-50 Parenago,P.P.: Perem Zv 7, 169
A1-51 Ashbrook,J.: AJ 56, 88
H1-51 Herbig,G.H.: ApJ 113, 697
L1-51 Lacchini,G.B.: Publ Trieste 244
H1-52 Haro,G.: ApJ 115, 572
H2-52 Herbig,G.H.: JRAS Canada 46, 222
H3-52 Herbig,G.H.: IAU Trans 8, 805
P1-52 Parenago,P.P.: Perem Zv 9, 89
P2-52 Payne-Gaposchkin,C.: Harvard Ann 118, 15
S1-52 Schneller,H.: Geschichte und Literatur des Lichtwechsels der veränderliche Sterne (2. Edition, 3. Band)
S2-52 Sharpless,S.: ApJ 116, 251
T1-52 Tsesevich,V.: Perem Zv 8, 412
H1-53 Haro,G.: ApJ 117, 73
H2-53 Haro,G., Moreno,H.: Bol Ton y Tac 1, nr7, 11
H3-53 Haro,G., Morgan,W.W.: ApJ 118, 16
K1-53 Kippenhahn,R.: ZfA 32, 185
P1-53 Parenago,P.P.: Astron Zh 30, 249
S1-53 Sacharov,G.P.: Perem Zv 9, 303

A1-54 Ambartsumian,V.: Soobshch Byurakan Obs. 13, 1
B1-54 Bidelman,W.P.: ApJ Suppl 1, 175
H1-54 Haro,G.: Bol Ton y Tac 2, nr11, 11
H2-54 Haro,G., Rivera Terrazas,L.: Bol Ton y Tac 1, nr10, 3
K1-54 Kippenhahn,R.: AN 282, 73
P1-54 Parenago,P.P.: Trudi Ast Sternberg Inst 25, 1
P2-54 Pismis,P.: Bol Ton y Tac 1, nr 10, 16
S1-54 Sharpless,S.: ApJ 119, 200
B1-55 Böhm,K.-H.: PASP 67, 338
H1-55 Haro,G., Chavira,E.: Bol Ton y Tac 2, nr12, 3
H2-55 Haro,G., Herbig,G.H.: Bol Ton y Tac 2, nr12, 33
K1-55 Kholopov,P.N.: Transactions of the 4th conf. on problems of cosmogony, Moscow
W1-55 Wassiljanovskaja,O.P.: Astron Tsirk 157, 19
B1-56 Böhm,K.-H.: ApJ 123, 379
L1-56 Lacchini,G.B.: Mem Soc Astron Ital 27, 383; Asiago Contr 70
R1-56 Rosino,L.: Mem Soc Astron Ital 27, 335; Asiago Contr 69
B1-57 Böhm,K.-H.: ZfA 43, 245
H1-57 Herbig,G.H.: Non-stable stars (IAU 3), 3 (Herbig ed)
J1-57 Johnson,H.L.: ApJ 126, 134
K1-57 Kukarkin,B.W., et al.: Astron Tsirk 177, 16
M1-57 Menon,T.K.: Radio astronomy (IAU 4), 56 (van de Hulst ed)
S1-57 Schneller,H.: Geschichte und Literatur des Lichtwechsels der veränderliche Sterne (2. Edition, 4. Band)
D1-58 Dall'Olmo,U.: Coelum 26, 50
F1-58 Fedorovich,V.P.: Astron Tsirk 189, 17
H1-58 Herbig,G.H.: Stellar Populations, 127 (O'Connell ed)
H2-58 Hoffmeister,C.: Veröff Sonneberg 3, 339
K1-58 Kholopov,P.N.: Astron Zh 35, 434; Sov Astron 2, 398
M1-58 Menon,T.K.: ApJ 127, 28
O1-58 Osterbrock,D.E.: PASP 70, 399
P1-58 Petit,M.: Contr Asiago 95, 29
S1-58 Strand,K.Aa.: ApJ 128, 14
B1-59 Brun,A., Petit,M.: Perem Zv 12, 18
K1-59 Kholopov,P.N.: Astron Zh 36, 295; Sov Astron 3,291
K2-59 Kopylov,I.M.: The Hertzsprung-Russell diagram (IAU 10), 41 (Greenstein, ed)
B1-60 Bonsack,W.K., Greenstein,J.L.: ApJ 131, 83
F1-60 Fedorovich,V.P.: Perem Zv 13, 166
H1-60 Haro,G., Minkowski,R.: AJ 65, 490
H2-60 Herbig,G.H.: ApJ Suppl 4, 337
H3-60 Herbig,G.H.: ApJ 131, 632
L1-60 Lallemand,A., et al.: PASP 72, 268
R1-60 Rosino,L.: Contr Asiago 109
M1-60 Mannino,G.: Mem Soc Astr Ital 30, 321
B1-61 Bonsack,W.K.: ApJ 133, 340
D1-61 Dall'Olmo,U.: Coelum 29, 41
S1-61 Schneller,H.: Geschichte und Literatur des Lichtwechsels der veränderliche Sterne (2. Edition, 5. Band)
W1-61 Walker,M.F.: C R Acad Sci Paris 253, 383
W2-61 Wenzel,W.: Veröff Sonneberg 5,1
H1-62 Herbig,G.H.: ApJ 135, 736
H2-62 Herbig,G.H.: Adv Astr Astrophys 1, 47
L1-62 Lynds,B.T.: ApJ Suppl 7, 1
R1-62 Rosino,L., Cian,A.: Mem Soc Astr Ital 32, 297; Asiago Contr 125
S1-62 Sharpless,S.: ApJ 136, 767
S2-62 Soloviev,A.W., Jerlexova,G.E.: Bul Inst Astrophys Duschanbe 34, 3
B1-63 Blanco,V.M.: ApJ 137, 513
D1-63 Dorschner,J., Gürtler,J.: AN 287, 257
G1-63 Garasdo-Lesnych,G.A., et al.: Perem Zv 14, 320
H1-63 Herbig,G.H., Kuhi,L.V.: ApJ 137, 398
K1-63 Kurotschkin,N.E.: Perem Zv 14, 284
M1-63 Maffei,P.: Mem Soc Astr Ital 34, 57
M2-63 Maffei,P.: Asiago Contr 140
W1-63 Walker,M.F.: AJ 68, 298
H1-64 Hardie,R.H., et al.: ApJ 140, 1472
H2-64 Haro,G.: The Galaxy and the Magellanic Clouds (IAU 20), 30 (Kerr, Rodgers eds)
K1-64 Kholopov,P.N.: Perem Zv 15, 3
K2-64 Kipper,T.A.: Tartu Astr Obs Publ 34, 396
S1-64 Shevchenko,W.S.: Perem Zv 15, 229
G1-65 Götz,G.: Veröff Sonneberg 7, 1
J1-65 Johnson,H.M.: ApJ 142, 964
M1-65 Magnan,C., Schatzman,E.: Cont R Acad Sci Paris 260, 6289
V1-65 van Schewick,H.: Die Eigenbewegung von Veränderlichen im Orion Nebel
H1-66 Haro,G., Chavira,E.: Vistas in Astron 8, 89
J1-66 Johnson,H.L., et al.: Comm Lunar and Plan Lab 4, 99
K1-66 Kuhi,L.V.: PASP 78, 430
M1-66 Mendoza V,E.E.: ApJ 143, 1010
V1-66 van den Bergh,S.: AJ 71, 990
W1-66 Walker,M.F.: Stellar evolution, 405 (Stein, Cameron eds)
B1-67 Bernacca,P.L.: Mem Soc Astr Ital 38, 169; Contr Asiago 195
B1-68 Bernacca,P.L.: Contr Asiago 202
H1-68 Haro,G.: Nebulae and interstellar matter, 141 (Middlehurst, Aller eds)
K1-68 Kuhi,L.V.: Interstellar ionized hydrogen, 13 (Terzian ed)
L1-68 Lee,T.A.: ApJ 152, 913
M1-68 Mendoza V,E.E.: ApJ 151, 977
M2-68 Mendoza V,E.E.: Publ Dep Astron Univ Chile, Obs Nac, Cerro Calan, Santiago 1, 106
R1-68 Racine,R.: AJ 73, 233
A1-69 Ambartsumian,V.: Stars, nebulae, galaxies, 283 (Boyarchuk et al. ed)
A2-69 Andrews,A.D.: Non-periodic phenomena in variable stars (IAU Coll 4), 137 (Detre ed)
A3-69 Andrews, A.D.: Bol Ton y Tac 5, 195
D1-69 Dibaj,E.A.: Astrofizika 5, 249; Astrophysics 5, 115
D2-69 Dibaj,E.A., Esipov,V.F.: Non-periodic phenomena in variable stars (IAU Coll 4), 107 (Detre ed)
H1-69 Haro,G., Parsamian,E.S.: Bol Ton y Tac 5, 45
H2-69 Haro,G., Chavira,E.: Bol Ton y Tac 5, 59
H3-69 Haro,G.: Bol Ton y Tac 5, 79
H4-69 Herbig,G.H.: Non-periodic phenomena in variable stars (IAU Coll 4), 75 (Detre ed)
M1-69 Mendoza V,E.E.: Asoc Arg Astron Bol, La Plata, 11, 39
R1-69 Rosino, L., Pigatto,L.: Mem Soc Astron Ital 40, 447
R2-69 Roslund,C.: Ark Astr 5, 381
R3-69 Rosino,L.: Low luminosity stars, 181 (Kumar ed)
R4-69 Rosino,L.: Non-periodic phenomena in variable stars (IAU Coll 4), 173 (Detre ed)
S1-69 Slee,O.B., et al.: Nature 224, 1087
S2-69 Shevchenko,V.S.: Perem Zv 16, 606
V1-69 Verschuur,G.L.: Nature 223, 140
W1-69 Walker,M.F.: ApJ 155, 447
W2-69 Walker,M.F.: Non-periodic phenomena in variable stars (IAU Coll 4), 103 (Detre ed)
D1-70 Dibaj,E.A.: Astron Zh 47, 977; Sov Astron 14, 785
F1-70 Ferrari d'Occhieppo,K., Göbel,E.: Astron Mitt Wien 6
G1-70 Geisel,S.L.: ApJ 161, L105
G2-70 Gordon,C.P.: AJ 75, 914
G3-70 Gurzadian,G.A.: Bol Ton y Tac 5, 263
L1-70 Lee,T.A.: PASP 82, 765
M1-70 Maihara,T.: Progr Theor Phys Japan 44, 99
M2-70 Mathewson,D.S., Ford,V.L.: MNRAS 175, 235
M3-70 Mendoza V,E.E.: Mem Soc Roy Sci Liege 19, 319
S1-70 Sancisi,R.: Mem Soc Roy Sci Liege 19, 313
W1-70 Wackerling,L.R.: Mem Roy Astron Soc 73, 153
Z1-70 Zellner,B.: AJ 75, 182
B1-71 Brück,M.T.: Publ Roy Obs Edinb 7, 63
G1-71 Gillett,F.C., Stein,W.A.: ApJ 164, 77
H1-71 Hoffman,W.F., et al.: ApJ 170, L89
S1-71 Sanduleak,N.: PASP 83, 95
S2-71 Sedyakina,A.N.: Perem Zv 18, 213
S3-71 Sinheskul,V.N.: Perem Zv 18, 201
S4-71 Slee,O.B., Higgins,C.S.: Austr J Phys 24, 247
W1-71 Wallerstein,G.: PASP 83, 77
A1-72 Ambartsumian,V.A., Mirzoyan, L.V.: New directions and new frontiers in variable star research (IAU Coll 15), 98 Publ Bamberg-Erlangen-Nürnberg 9, nr 100
A2-72 Andrews,A.D.: Bol Ton y Tac 6, 161
B1-72 Brück,M.T.: Publ Roy Obs Edinburgh 7, 85
B2-72 Brück,M.T.: Publ Roy Obs Edinburgh 7, 93
G1-72 Giacconi,R., et al.: ApJ 178, 281

H1-72 Herbig,G.H., Rao,N.K.: ApJ 174, 401
K1-72 Kiladze,R.I: Inf Bul V S 670
M1-72 MacConnell,D.J., Cowley,A.P.: Inf Bul V S 674
S1-72 Smith,M.A.: ApJ 176, 617
S2-72 Smith,M.A.: ApJ 175, 765
S3-72 Strom,S.E., et al.: ApJ 173, 353
W1-72 Walker,M.F.: ApJ 175, 89
W2-72 Wilson,W.J., Barrett,A.H.: AA 17, 385
A1-73 Allen,D.A: MNRAS 161, 145
B1-73 Böhm,K.-H., et al.: ApJ 179, 149
C1-73 Cohen,M.: MNRAS 161, 97
C2-73 Cohen,M.: MNRAS 161, 105
C3-73 Cohen,M.: MNRAS 164, 395
D1-73 Dieter,N.H.: ApJ 183, 449
D2-73 Dzhakusheva,K.G., Matyagin,V.S.: Trudy Astrofiz Inst Alma Ata 20, 69
E1-73 Eggen,O.J.: PASP 85, 42
G1-73 Grasdalen,G.L., et al.: PASP 85, 193
G2-73 Gull,T.R., et al.: PASP 85, 526
G3-73 Gurzadian,G.A.: AA 28, 147
H1-73 Herbig,G.H.: Inf Bul V S 832
I1-73 Isobe,S.: Interstellar dust and related topics (IAU 52), 433 (Greenberg, van de Hulst eds)
L1-73 Loren,R.B., et al.: ApJ 185, 67
L2-73 Louise,R., Sapin,C.: Ap Let 14, 119
L3-73 Louise,R., Sapin,C.: Interstellar dust and related topics (IAU 52), 465 (Greenberg, van de Hulst eds)
M1-73 Mann, M.F.St J.: unpublished MSc thesis, University of Sussex
P1-73 Penston,M.V.: Stellar Ages (IAU Coll 17), IX-1 (Cayrel de Strobel, Deplace eds)
P2-73 Penston,M.V.: ApJ 183, 505
T1-73 Tucker,K.D., et al.: ApJ 186, L13
Z1-73 Zajtseva,G.V., Kolotilov,E.A.: Astrofizika 9, 185; Astrophysics 9, 104
A1-74 Andrews,A.D.: Bol Tonantzintla 1, 101
A2-74 Appenzeller,I.: AA 36, 99
B1-74 Böhm,K.-H., et al.: ApJ 193, 353
B2-74 Breger,M.: ApJ 188, 53
B3-74 Breger,M.: Planets, Stars and Nebulae, 946 (Gehrels ed)
B4-74 Brück,M.T.: MNRAS 166, 123
C1-74 Cohen,M.: MNRAS 169, 257
D1-74 Dickinson,D.F., et al.: ApJ 194, L93
G1-74 Gatley,I., et al.: ApJ 191, L121
G2-74 Giacconi,R., et al.: ApJ Suppl 27, 37
G3-74 Glass,I.S., Penston,M.V.: MNRAS 167, 237
G4-74 Gurzadian,G.A.: AA 33, 307
G5-74 Gull,T.R.: HII regions and the Galactic Centre, 1 (Moorwood ed)
H1-74 Herbig,G.H.: Lick Obs Bul 658, 11
I1-74 Imhoff,C.L., Mendoza V,E.E.: Rev Mex A A 1, 25
J1-74 Johansson,L.E.B., et al.: Galactic radio astronomy (IAU 60), 301 (Kerr, Simonson III eds)
J2-74 Johansson,L.E.B., et al.: ApJ 189, 455
K1-74 Kuhi,L.V.: AA Suppl 15, 47
L1-74 Lada,C.J., et al.: ApJ 194, 609
L2-74 Lepine,J.R.D., Nguyen-Q-Rieu: AA 36, 469
M1-74 Morris,M., et al.: ApJ 192, L27
M2-74 Morris,M., et al.: ApJ 191, 349
M3-74 Münch,G., Taylor,K.: ApJ 192, L93
S1-74 Schwartz,R.D.: ApJ 191, 419
S2-74 Strom,K.M., et al.: ApJ 191, L93
S3-74 Strom,S.E., et al.: ApJ 191, 111
S4-74 Salmanov,I.R.: Astrofizika 10, 300; Astrophysics 10, 181
W1-74 Ward, M.J.: unpublished MSc thesis, university of Sussex
W2-74 Werner,M.W., et al.: ApJ 192, L31
A1-75 Allen,D.A., et al.: MNRAS 173, 47P
B1-75 Böhm,K.-H.: Problems in stellar atmospheres and envelopes (Baschek et al. eds), 205
B2-75 Böhm,K.-H.: Mitt Astr Ges 36, 31
B3-75 Breger,M., Rybski,P.M.: PASP 87, 607
B4-75 Brown,R.L., et al.: ApJ 195, L23
D1-75 Dieter,N.H.: ApJ 199, 289
D2-75 Dolidze,M.V.: Byull Abastumansk Astrofiz Obs 47, 145
E1-75 Emerson,J.P., et al.: MNRAS 172, 411
G1-75 Gasparian,K.G.: Astron Tsirk 867, 6
G2-75 Gurzadian,G.A.: Astrofizika 11, 531; Astrophysics 11, 354
G3-75 Gyulbudagian,A.L.: Astrofizika 11, 511; Astrophysics 11, 341
K1-75 Knapp,G.R., et al.: ApJ 196, 167
K2-75 Kuan,P.: ApJ 202, 425
L1-75 Lo,K.Y., et al.: ApJ 202, 81
M1-75 Martin,R.N., Barrett,A.H.: ApJ 202, L83
M2-75 Mendoza V,E.E.: PASP 87, 495
M3-75 Milman,A.S.: ApJ 202, 673
M4-75 Milman,A.S., et al.: AJ 80, 93
M5-75 Milman,A.S., et al.: AJ 80, 101
P1-75 Penston,M.V., et al.: MNRAS 171, 219
P2-75 Pugach,A.F.: Variable stars and stellar evolution (IAU 67), 143 (Sherwood, Plaut eds)
S1-75 Schmidt,G.D., Vrba,F.J.: ApJ 201, L33
S2-75 Schwartz,P.R., Buhl,D.: ApJ 201, L27
S3-75 Schwartz,R.D.: ApJ 195, 631
S4-75 Shevchenko,V.S.: Studies of extremely young stellar complexes, 3
S5-75 Sincheskul,V.N.: Astrometriya i Astrofizika Kiev 24, 75
S6-75 Strom,K.M., et al.: ApJ 196, 489
T1-75 Taylor,K., Münch,G.: PASP 87, 509
B1-76 Böhm,K.-H., et al.: ApJ 203, 399
B2-76 Breger,M.: ApJ 204, 789
F1-76 Feibelman,W.A.: PASP 88, 677
G1-76 Gasparian,K.G.: Soobshch Byurakan Obs 49, 23
G2-76 Gasparian,K.G.: Soobshch Byurakan Obs 49, 33
G3-76 Goss,W.M., et al.: AA 46, 1
H1-76 Haro,G.: Bol Tonantzintla 2, 3
H2-76 Hudson,H.S., Soifer,B.T.: ApJ 206, 100
K1-76 Kisyakov,A.G., Turner,B.E.: AJ 81, 302
K2-76 Knapp,G.R., Morris,M.: ApJ 206, 713
K3-76 Kutner,M.L., et al.: ApJ 209, 452
M1-76 McNamara,B.J.: AJ 81, 375
M2-76 McNamara,B.J.: AJ 81, 845
M3-76 Morris,M., Knapp,G.R.: ApJ 204, 415
M4-76 Murray,S.S., Ulmer,M.P.: ApJ 210, 230
P1-76 Pankonin,V., Walmsley,C.M.: AA 48, 341
P2-76 Parsamian,E.S.: Astrofizika 12, 235; Astrophysics 12, 145
P3-76 Penston, et al.: MNRAS 147, 449
S1-76 Schwartz,R.D.: PASP 88, 159
S2-76 Strom,K.M., et al.: AJ 81, 308
T1-76 Tomozov,V.M.: Astrofizika 12, 289; Astrophysics 12, 289
V1-76 Vrba,F.J., et al.: AJ 81, 958
W1-76 Westbrook,W.E., et al.: ApJ 209, 94
A1-77 Appenzeller,I.: The interaction of variable stars with their environment (IAU Coll 42), 80 (Kippenhahn et al. eds)
A2-77 Andrillat,Y., Swings,J.P.: The interaction of variable stars with their environment (IAU Coll 42), 100 (Kippenhahn et al. eds)
B1-77 Bernes,C.: AA Suppl 29, 65
B2-77 Bertout,C.: AA 58, 153
B3-77 Braune,W., et al.: AN 298, 121
B4-77 Breger,M.: ApJ 215, 119
C1-77 Connell,W.D., Ianna,P.A.: AJ 82, 360
C2-77 Cudworth,K.M., Stone,R.C.: PASP 89, 627
D1-77 de Boer,K.S.: AA 61, 605
G1-77 Garrison,L.M., Anderson,C.M.: ApJ 218, 438
G2-77 Gyulbudagian,A.L., Magakian,T.Yu.: Dokl AN Arm SSR 64, 104
G3-77 Gyulbudagian,A.L., Magakian,T.Yu.: Pisma Astron Zh 3, 113; Sov Astron Let 3, 58
H1-77 Herbig,G.H.: ApJ 214, 747
K1-77 Klyus,I.A.: Perem Zv 20,446
K2-77 Knapp,G.R., et al.: ApJ 214, 78
K3-77 Kutner,M.L., et al.: ApJ 215, 521
M1-77 Mezger,P.G., Smith,L.F.: Star formation (IAU 75), 133 (de Jong, Maeder eds)
M2-77 Mould,J.R., Wallis,R.E.: MNRAS 181, 625
M3-77 Münch,G.: ApJ 212, L77
M4-77 Mundt,R.: Sterne u Weltraum 16, 234

O1-77 Ohtani,H., Ichikawa,T.: Mem Fac Sci Kyoto Univ Sep Phys Astrophys Geophys Chem 35, 197
P1-77 Pankonin,V., et al.: AA 58, L25
R1-77 Righini-Cohen,G., Simon,M.: ApJ 213, 390
R2-77 Rössiger,S.: AN 298, 215
S1-77 Schwartz,R.D.: ApJ Suppl 35, 161
S2-77 Stephenson,C.B., Sanduleak,N.: ApJ Suppl 33, 459
T1-77 Thaddeus,P.: Star formation (IAU 75), 37 (de Jong, Maeder eds)
V1-77 Vrba,F.J.: AJ 82, 198
W1-77 Walker,M.F.: The interaction of variable stars with their environment (IAU Coll 42), 92 (Kippenhahn et al. eds)
W2-77 Warren Jr,W.H., Hesser,J.E.: ApJ Suppl 34, 115
W3-77 Warren Jr,W.H., Hesser,J.E.: ApJ Suppl 34, 207
W4-77 White,G.J., Ricketts,M.J.: Ap Let 18, 79
B1-78 Böhm,K.-H.: AA 64, 115
B2-78 Böhm,K.-H.: Problems of physics and evolution of the universe, 121 (ed Mirzoyan)
B3-78 Böhm,K.-H.: Protostars and planets, 632 (Gehrels ed)
C1-78 Campbell,P.D.: PASP 90, 262
C2-78 Cesarsky,C.J., et al.: AA 68, 33
C3-78 Chavushian,O.S., Melikian,N.D.: Flare stars, 74 (Mirzoyan ed)
C4-78 Cooke,B.A., et al.: MNRAS 182, 489
D1-78 den Boggende,A.J.F., et al.: AA 62, 1
D2-78 Dopita,M.A.: ApJ Suppl 37, 117
F1-78 Forman,W., et al.: ApJ Suppl 38, 357
G1-78 Garrison Jr,L.M.: ApJ 224, 535
G2-78 Garrison Jr,L.M., Anderson,C.M.: ApJ 221, 601
G3-78 Gorodetskij,D.I., Roshkovskij,D.A.: Trudy Ap Inst Alma Ata 31, 52
G4-78 Gyulbudagian,A.L., et al.: ApJ 224, L137
I1-78 Isobe,S.: PAS Japan 30, 499
K1-78 Kopatskaya,E.N., Shulov,O.S.: Trans Astr Obs Leningrad 34, Ser Mat nauk 56, 94
K2-78 Kuhi,L.V.: Protostars and planets, 708 (Gehrels ed)
P1-78 Pankonin,V., Walmsley,C.M.: AA 67, 129
R1-78 Reich,W.: AA 64, 407
S1-78 Schwartz,R.D.: ApJ 223, 884
S2-78 Shanin,G.I., Shevchenko,V.S.: Astrofizika 14, 191; Astrophysics 14, 108
T1-78 Taylor,K., Münch,G.: AA 70, 359
T2-78 Thronson Jr,H.A., et al.: AJ 83, 492
W1-78 Walker,M.F.: ApJ 224, 546
W2-78 Warner,J.W., et al.: AJ 83, 1614
B1-79 Bastien,U., Mundt,R.: AA Suppl 36, 57
B2-79 Böhm,K.-H., Brugel,E.W.: AA 74, 297
B3-79 Bradt,H.V., Kelley,R.L.: ApJ 228, L33
C1-79 Cohen,M., Kuhi,L.V.: ApJ 227, L105
C2-79 Cohen,M., Kuhi,L.V.: ApJ Suppl 41, 743
C3-79 Cohen,M., Schwartz,R.D.: ApJ 233, L77
F1-79 Few,R.W., Booth,R.S.: MNRAS 188, 181
G1-79 Genzel,R., Downes,D.: AA 72, 234
G2-79 Gondhalekar,P.M., et al.: The first year of IUE, 109
H1-79 Ho,P.T.P., et al.: ApJ 234, 912
K1-79 Kandalian,R.A., Sanamian,V.A.: Astrofizika 15, 705; Astrophysics 15, 462
K2-79 Ku,W.H.-M., Chanan,G.A.: ApJ 234, L59
L1-79 Laques,P., Vidal, J.L.: AA 73, 97
L2-79 Loren,R.B., et al.: ApJ 234, 932
N1-79 Nachman,P.: ApJ Suppl 39, 103
P1-79 Parsamian,E.S., Petrosian,V.M.: Soobshch Byurakan Obs 51, 3
P2-79 Pashchenko,M.I., Rudnitskij,G.M.: Astron Tsirk 1039, 3
Q1-79 Qian,B.-c., Xu,Z.-h.: Ann Shanghai Obs Acad Sinica 1, 66
Q2-79 Qian,B.-c., Xu,Z.-h.: Ann Shanghai Obs Acad Sinica 2, 107
S1-79 Schmidt,G.D., Miller,J.S.: ApJ 234, L191
S2-79 Schneeberger,T.J., et al.: ApJ Suppl 41, 369
S3-79 Shevchenko,V.S.: Astron Zh 56, 297; Sov Astron 23, 163
U1-79 Ulrich,R.K., Knapp,G.R.: ApJ 230, L99
V1-79 Vrba,F.J., et al.: ApJ 227, 185
B1-80 Baud,B., Wouterloot,J.G.A.: AA 90, 297
C1-80 Canto,J., et al.: AA 85, 128
C2-80 Cohen,M.: MNRAS 190, 865
C3-80 Cohen,M.: MNRAS 191, 499
C4-80 Cohen,M.: AJ 85, 29
C5-80 Cohen,M., Schwartz,R.D.: MNRAS 191, 165
E1-80 Elias,J.H.: ApJ 241, 728
F1-80 Fischer,J., et al.: ApJ 238, L155
G1-80 Gahm,G.F., et al.: AA 83, 263
G2-80 Gahm,G.F.: ApJ 242, L163
G3-80 Gurzadian,G.A.: Flare stars, Int Ser in Nat Phil 101 (Pergamon Press)
H1-80 Harvey,P.M., et al.: ApJ 235, 894
H2-80 Herbig,G.H., Soderblom,D.R.: ApJ 242, 628
H3-80 Ho,P.T.P, Barrett,A.H.: ApJ 237, 38
I1-80 Isobe,S.: PAS Japan 32, 423
K1-80 Kiladze,R.I., Natsvlishvili,R.Sh.: Inf Bul V S 1725
K2-80 Kutner,M.L., et al.: ApJ 237, 734
L1-80 Little,L.T., et al.: MNRAS 193, 115
M1-80 Melikian,N.D., Shevchenko,V.S.: Astrofizika 16, 789; not translated
M2-80 Mirzoyan,L.V., Brutian,G.W.: Astrofizika 16, 97; Astrophysics 16, 67
M3-80 Morris,M., et al.: Interstellar molecules (IAU 87), 197 (Andrew ed)
M4-80 Mundt,R., Bastian,U.: AA Suppl 39, 245
N1-80 Natsvlishvili,R.Sh., Melikian,N.D.: Inf Bul V S 1726
O1-80 Ortolani,S., D'Odorico,S.: AA 83, L8
P1-80 Parsamian.E.S.: Astrofizika 16, 87; Astrophysics 16, 60
P2-80 Parsamian,E.S.: Astrofizika 16, 677; Astrophysics 16, 391
P3-80 Pashchenko,M.I., Rudnitskij,G.M.: Astron Zh 57, 1204; Soviet Astron 24, 695
R1-80 Rodriguez,L.F. et al.: ApJ 235, 845
S1-80 Shanin,G.I.: Astrometr Astrofiz 40, 28
S2-80 Simard-Normandin,M., Kronberg,P.P.: ApJ 242, 74
S3-80 Sulakvadse,G.N.: Astrofizika 16, 505; Astrophysics 16, 297
T1-80 Tsvetkov,M.K., et al.: Inf Bul V S 1889
W1-80 Walker,M.F., Burstein,D.: PASP 92, 648
W2-80 Weaver,W.B., Frank,J.L.: MNRAS 191, 321
W3-80 Warren-Smith,R.F., et al.: MNRAS 192, 339
A1-81 Andrews,A.D.: A photometric atlas of the Orion Nebula, Armagh Observatory, Armagh.
B1-81 Böhm,K.-H., et al.: ApJ 245, L113
B2-81 Breger,M., et al.: ApJ 248, 963.
B3-81 Brugel,E.W., et al.: ApJ 243, 874
B4-81 Brugel,E.W., et al.: ApJ Suppl 47, 117
C1-81 Chanan,G.A.: X-ray symposium, 1 (Philip ed)
C2-81 Cohen,M., Schmidt,G.D.: AJ 86, 1228
G1-81 Gahm,G.F.: The universe at ultraviolet wavelengths, 105 (Chapman ed)
H1-81 Herbig,G.H., Jones,B.F.: AJ 86, 1232
H2-81 Huth,H., Wentzel,W.: Bibliographic catalogue of variable stars, Centre de donnees stellaires, Strasbourg
I1-81 Isobe,S., Sasaki,G.: Fundamental problems in the theory of stellar evolution (IAU 93), 99 (Sugimoto et al. eds)
L1-81 Loren,R.B.: AJ 86, 69
M1-81 Macdonald,G.H., et al.: MNRAS 195, 387
M2-81 Melikian,N.D.: Inf Bul V S 2018
M3-81 Mirzoyan,L.V., et al.: Astrofizika 17, 197; Astrophysics 17, 101
M4-81 Moorwood,A.F.M., Salinari,P.: AA 94, 299
N1-81 Natsvlishvili,R.Sh.: Inf Bul V S 1926
P1-81 Parsamian,E.S.: Astrofizika 17, 579; not translated
P2-81 Persson,S.E., et al.: ApJ 251, L85
P3-81 Phillips,T.C., et al.: ApJ 245, 512
P4-81 Pogodin,M.A.: Astron Zh 58, 796; Soviet Astron 25, 454
P5-81 Pravdo,S.H., Marshall,F.E.: ApJ 248, 591
S1-81 Sandell,G., Olofsson,H.: AA 99, 80
S2-81 Sargent,A.I., et al.: ApJ 249, 607
S3-81 Schwartz,R.D.: ApJ 243, 197
S4-81 Shevchenko,V.S.: Pisma Astron Zh 7, 37; Soviet Astron Let 7, 21
S5-81 Shulov,O.S., Kopatskaya,E.N.: Ser Mat Nauk 58, 49
T1-81 Thum,C., et al.: AA 94, 80
W1-81 White,G.J., Phillips,J.P.: MNRAS 194, 947

W2-81 White,G.J., et al.: MNRAS 197, 745
B1-82 Bally,J.: Regions of recent star formation, 287 (Roger, Dewdney eds)
B2-82 Bally,J.: ApJ 261, 558
B3-82 Bally,J.: Symposium on the Orion Nebula to honor Henry Draper, 191 (Glassgold et al. eds)
B4-82 Bally,J., Lane,A.P.: ApJ 257, 612
B5-82 Bertout,C., Thum,C.: AA 107, 368
B6-82 Bianchi,L.: Ap Sp Sci 82, 161
B7-82 Böhm,K.-H., Böhm-Vitense,E.: ApJ 263, L35
B8-82 Böhm,K.-H., et al.: Advances in ultraviolet astronomy, 223 (Kondo et al. eds)
B9-82 Böhm-Vitense,E., et al.: ApJ 262, 224
B10-82 Bastien,P.: AA Suppl 48, 153 (erratum AA Suppl 48, 513)
C1-82 Calamai,G., Felli,M.: Regions of recent star formation, 419 (Roger, Dewdney eds)
C2-82 Calamai,G., et al.: AA 109, 123
C3-82 Cohen,M., et al.: ApJ 253, 707
D1-82 Dopita,M.A., et al.: ApJ 261, 183
E1-82 Edwards,S., Snell,R.L.: ApJ 261, 151
F1-82 Finkenzeller,U.: Be stars (IAU 98), 501 (Jaschek, Groth eds)
G1-82 Goudis,C.: The Orion complex. ApSpSci library 90
G2-82 Gyulbudagian,A.L.: Pisma Astron Zh 8, 232; Soviet Astron Let 8, 123
H1-82 Harvey,P.M., et al.: Symposium on the Orion Nebula to honor Henry Draper, 199 (Glassgold et al. eds)
H2-82 Heiles,C., Troland,T.H.: ApJ 260, L23
H3-82 Heiles,C., Troland,T.H.: Symposium on the Orion Nebula to honor Henry Draper, 183 (Glassgold et al. eds)
H4-82 Herbig,G.H.: Symposium on the Orion Nebula to honor Henry Draper, 64 (Glassgold et al. eds)
I1-82 Isobe,S.: Symposium on the Orion Nebula to honor Henry Draper, 165 (Glassgold et al. eds)
I2-82 Isobe,S., Sasaki,G.: PAS Japan 34, 241
K1-82 Kiladze,R.I., Natsvlishvili,R.Sh.: Abastumanskaya Astrofiz Obs Bul 55, 123
K2-82 Koepf,G.A., et al.: ApJ 260, 584
K3-82 Ku.,W.H.-M., et al.: Science 215, 61
K4-82 Kuhi,L.V.: Second Cambridge workshop on cool stars, stellar systems, and the Sun II, 141 (Giampapa, Golub eds)
K5-82 Kutner,M.L., et al.: ApJ 259, L35
L1-82 Lane,A.P., Bally,J.: Regions of recent star formation, 301 (Roger, Dewdney eds)
L2-82 Lekht,E.E., et al.: Astron Zh 59, 276; Soviet Astron 26, 168
L3-82 Lichten,S.M.: ApJ 253, 593
L4-82 Lonsdale,C.J., et al.: AJ 87, 1819
M1-82 MacConnell,D.J.: AA Suppl 48, 355
M2-82 Matsakis,D.N., et al.: Symposium on the Orion Nebula to honor Henry Draper, 210 (Glassgold et al. eds)
M3-82 Melik-Alaverdian,Yu.K., Tovmasian,G.G.: Soobshch Byurakan Obs 53, 93
M4-82 Moran,J.M., et al.: Symposium on the Orion Nebula to honor Henry Draper, 204 (Glassgold et al. eds)
P1-82 Padman,R., et al.: MNRAS 200, 183
P2-82 Parsamian,E.S., Chavira,E.: Bol Tonantzintla 3, 69
P3-82 Persson,S.E., et al.: Regions of recent star formation, 155 (Roger, Dewdney eds)
S1-82 Sandqvist,Aa., et al.: Regions of recent star formation, 307 (Roger, Dewdney eds)
S2-82 Sandqvist,Aa., et al.: The scientific importance of submillimetre observations, 131 (de Graauw, Guyenne eds)
S3-82 Schloerb,F.P., Loren,R.B.: Symposium on the Orion Nebula to honor Henry Draper, 32 (Glassgold et al. eds)
S4-82 Shore,S.N.: Advances in ultraviolet astronomy: Four years of IUE research, 370 (Kondo et al. eds)
S5-82 Snell,R.L., Edwards,S.: Regions of recent star formation, 133 (Roger, Dewdney eds)
S6-82 Snell,R.L., Edwards,S.: ApJ 259, 668
S7-82 Stark,A.A., Bally,J.: Regions of recent star formation, 329 (Roger, Dewdney eds)
T1-82 Thaddeus,P.: Symposium on the Orion Nebula to honor Henry Draper, 9 (Glassgold et al. eds)
T2-82 Thronson,H.A., Thompson,R.I.: ApJ 254, 543
V1-82 Vidal,J.L.: Symposium on the Orion Nebula to honor Henry Draper, 176 (Glassgold et al. eds)
W1-82 Walsh,J.R.: MNRAS 201, 561
W2-82 White,G.J., et al.: Regions of recent star formation, 237 (Roger, Dewdney eds)
W3-82 Willner,S.P., et al.: ApJ 253, 174
B1-83 Bally,J., Lada,C.J.: ApJ 265, 824
B2-83 Bally,J., Predmore,R.: ApJ 265, 778
B3-83 Bally,J., Stark,A.A.: ApJ 266, L61
B4-83 Batrla,W., et al.: AA 128, 279
B5-83 Böhm,K.-H.: Rev Mex A A 7, 55
B6-83 Böhm,K.-H., et al.: AA 125, 23
C1-83 Cohen,M.: Rev Mex A A 7, 241
C2-83 Cohen,M., Schwartz,R.D.: ApJ 265, 877
C3-83 Cohen,R.J., et al.: MNRAS 203, 1123
C4-83 Crutcher,R.M., Kazes,I.: AA 125, L23
D1-83 de Boer,K.S.: AA 125, 258
D2-83 Durouchoux,P. et al.: 18th Cosmic Ray Conf 1, 74 (Durgaprasad et al. eds)
E1-83 Edwards,S., Snell,R.L.: ApJ 270, 605
H1-83 Harris,A., et al.: ApJ 265, L63
H2-83 Haschick,A.D., et al.: ApJ 265, 281
H3-83 Herbig,G.H.: IAU Circ 3778
H4-83 Herbst,W., et al.: AJ 88, 1648
I1-83 Iijima,T., Rosino,L.: IAU Circ 3771
J1-83 Jankovics,I., et al.: PASP 95, 883
J2-83 Jones,B.F.: Rev Mex A A 7, 71
K1-83 Klare,G., Appenzeller,I.: IAU Circ 3809
K2-83 Kosai,H.: IAU Circ 3763
K3-83 Kosai,H.: IAU Circ 3769
K4-83 Kuhi,L.V.: Observational basis for velocity fields in stellar atmospheres, 285 (Stalio ed)
L1-83 Locher,K.: IAU Circ 3778
L2-83 Lorenzetti,D, et al.: ApJ 264, 554
M1-83 Matthews,N., Little,L.T.: MNRAS 205, 123
M2-83 McNamara,B., Hüls,S.: AA Suppl 54, 221
M3-83 Meistas,E.: Vilniaus Astron Obs Biul 62, 3
M4-83 Mirzoyan,L.V., et al.: Astrofizika 19, 725; Astrophysics 19, 411
M5-83 Moorwood,A.F.M., Salinari,P.: AA 125, 342
M6-83 Moran,J.M.: Rev Mex A A 7, 95
M7-83 Mundt,R., Hartmann,L.: ApJ 268, 766
M8-83 Mundt,R., Witt,A.N.: ApJ 270, L59
O1-83 Ogura,K., Hasegawa,T.: PAS Japan 35, 299
R1-83 Reipurth,B., Wamsteker,W.: AA 119, 14
R2-83 Rodriguez,L.F., Canto,J.: Rev Mex A A 8, 163
R3-83 Rössiger,S.: Mitt Veränderliche Sterne 10, 23
S1-83 Schwartz,P.R., et al.: ApJ 267, L109
S2-83 Schwartz,R.D.: ApJ 268, L37
S3-83 Schwartz,R.D.: ARAA 21, 209
S4-83 Schwartz,R.D.: Rev Mex A A 7, 27
S5-83 Sellgren,K., et al.: ApJ 271, L13
S6-83 Sellgren,K.: AJ 88, 985
S7-83 Shulov,O.S., et al.: Trudi Ast Obs Leningrad 38, 76
S8-83 Simon,T., Joyce,R.R.: ApJ 265, 864
S9-83 Smith,M.A., et al.: ApJ 271, 237
S10-83 Smith,M.A., et al.: ApJ 272, 163
S11-83 Snell,R.L.: Rev Mex A A 7, 79
T1-83 Torrelles,J.M., et al.: ApJ 274, 214
T2-83 Torrelles,J.M., et al.: Rev Mex A A 8, 147
W1-83 Walker,M.F.: ApJ 271, 642
W2-83 Walmsley,C.M., Ungerechts,H.: AA 122, 164
W3-83 Warren-Smith,R.F.: MNRAS 205, 349
A1-84 Aiad,A., et al.: AA 130, 67
A2-84 Argyle,R.W.: IAU Circ 3924
A3-84 Axon,D.J., Taylor,R.: MNRAS 207, 241
B1-84 Beckwidth,S., et al.: ApJ 287, 793
B2-84 Bieging,J.H., et al.: ApJ 282, 699
B3-84 Bloemen,J.B.G.M., et al.: AA 139, 37
B4-84 Böhm,K.-H., et al.: Future of UV astron based on 6 yrs of IUE research, 167 (Mead et al. eds)
B5-84 Brugel,E.W., Shull,J.M.: Future of UV astron based on 6 yrs of IUE research, 171 (Mead et al. eds)

C1-84 Cardelli,J.A., Böhm,K.-H.: ApJ 285, 613
C2-84 Cardelli,J.A., Böhm,K.-H.: Future of UV astron based on 6 yrs of IUE research, 175 (Mead et al. eds)
C3-84 Choe,S.-U.: PhD Thesis, Univ Minnesota
C4-84 Cohen,M.: Effects of mass loss on the local stellar environment, 93 (Stalio, Thomas eds)
C5-84 Cohen,M., et al.: ApJ 278, 671
E1-84 Edwards,S.E., Snell,R.L.: ApJ 281, 237
F1-84 Finkenzeller,U., Jankovics,I.: AA Suppl 57, 285
F2-84 Finkenzeller,U., Mundt,R.: AA Suppl 55, 109
F3-84 Franco,J.: AA 137, 85
G1-84 Gyulbudagian,A.L.: Astrofizika 20, 115; Astrophysics 20, 75
G2-84 Gyulbudagian,A.L.: Astrofizika 20, 631; not translated
G3-84 Gasparian,K.G., et al.: Inf Bul V S 3024
H1-84 Hartmann,L., Raymond,J.C.: ApJ 276, 560
H2-84 Henning,Th., et al.: AN 305, 67
H3-84 Herbst,W., Stine,O.C.: AJ 89, 1716
H4-84 Hurst,G.M.: IAU Circ 3924
H5-84 Hyland,A.R., et al.: MNRAS 206, 465
M1-84 Magakian,T.Yu.: Pisma Astron Zh 10, 661; Sov Astron Let 10, 276
M2-84 Mannion,M.D., Scarrott,S.M.: MNRAS 208, 905
M3-84 Mundt,R.: ApJ 280, 749 (erratum ApJ 292, 763)
M4-84 Mundt,R., et al.: AA 140, 17
N1-84 Natsvlishvili,R.Sh.: Inf Bul V S 2565
R1-84 Reipurth,B., Bouchet,P.: AA 137, L1
R2-84 Rydgren,A.E., Vrba,F.J.: AJ 89, 399
S1-84 Snell,R.L., et al.: ApJ 284, 176
T1-84 Takano,T., et al.: ApJ 282, L69
T2-84 Taylor,K.N.R., et al.: Nature 311, 236
W1-84 Witt,A.N., et al.: ApJ 281, 708
W2-84 Wootten,A., et al.: ApJ 279, 633
X1-84 Xing,J., Winnewisser,G.: Publ Beijing Astr Obs, 6, 236 Sino-Japan workshop on stellar activity and obs techn (Hu, Dong eds)
A1-85 Andrillat,Y.: Birth and evolution of massive stars and stellar groups, 49 (Boland, van Woerden eds)
B1-85 Bally,J.: Birth and Infancy of stars, 585 (Lucas et al. eds)
B2-85 Böhm,K.-H., Solf,J.: ApJ 294, 533
B3-85 Bohigas,J., et al.: Rev Mex A A 11, 149
B4-85 Bouvier,J., Bertout,C.: Messenger 39, 33
B5-85 Brown,A., et al.: Radio stars, 105 (Hjellming, Gibson, eds)
B6-85 Brugel,E.W., et al.: ApJ 292, L75
C1-85 Canto,J.: Nearby Molecular Clouds, 181 (Serra ed)
C2-85 Canto,J.: Cosmical gas dynamics, 267 (Kalm ed)
C3-85 Chavira,E., et al.: Inf Bul V S 2746
C4-85 Choe,S.-U., et al: ApJ 288, 338
C5-85 Cohen,M., Fuller,G.A.: ApJ 296, 620
C6-85 Cohen,M., et al.: ApJ 296, 633
C7-85 Cohen,M., Witteborn,F.C.: ApJ 294, 345
E1-85 Erastova,L.K.: Astron Tsirk 1377, 7
E2-85 Evans II,N.J., et al.: Airborne astronomy symposium, 172 (Thronson, Erickson eds)
F1-85 Finkenzeller,U.: AA 151, 340
F2-85 Fischer,J., et al.: ApJ 293, 508
F3-85 Fukui,Y., Iwata,T.: Astron Her 78, 218
G1-85 Gasparian,K.G.: Astrofizika 22, 325; Astrophysics 22, 195
G2-85 Giampapa,M.S., Imhoff,C.L.: Protostars and Planets II, 386 (Black, Matthews eds)
G3-85 Gnedin,Yu.N., Pogodin,M.A.: Pisma Astron Zh 11, 37; Sov Astron Let 11, 15
H1-85 Henning,T.: Ap Sp Sci 114, 401
H2-85 Herbig,G.H.: Birth and evolution of massive stars and stellar groups, 41 (Boland, van Woerden eds)
H3-85 Houston,B.P., Wolfendale,A.W.: J Phys G 11, 407
J1-85 Jewell,P.R., et al.: ApJ 295, 183
J2-85 Jones,B.F., Walker,M.F.: AJ 90, 1320
K1-85 Kardopolov,V.I., Shutemova,N.A.: Perem Zv 22, 161
K2-85 Kilkenny,D., et al.: S Afr Astron Obs Circ 9, 55
L1-85 Lada,C.J.: Ann Rev A A 23, 267
L2-85 Levreault,R.M.: PhD Thesis, University of Texas Austin
L3-85 Little,L.T., et al.: AA 142, 378
M1-85 Mendoza V,E.E., et al.: Inf Bul V S 2817
M2-85 Mermilliod,J.-C., Mayor,M.: Stellar radial velocities (IAU Coll 88), 367 (Philip, Latham eds)
M3-85 Mundt,R.: Nearby Molecular Clouds, 160 (Serra ed)
M4-85 Mundt,R.: Protostars and Planets II, 414 (Black, Matthews eds)
N1-85 Neckel,T., Sarcander,M.: AA 147, L1
P1-85 Parsamian,E.S.: Astrofizika 22, 87; Astrophysics 22, 51
P2-85 Pogodin,M.A.: Astron Zh 62, 918; Sov Astron 29, 531
P3-85 Pravdo,S.H., et al.: ApJ 293, L35
R1-85 Reipurth,B., Sandell,G.: AA 150, 307
R2-85 Reipurth,B.: (Sub)millimeter astronomy, 459 (Shaver, Kjär, eds)
R3-85 Reipurth,B.: AA Suppl 61, 319
R4-85 Richardson,K.J., et al. ApJ 290, 637
R5-85 Rodriguez,L.F., et al.: MNRAS 214, 9P
R6-85 Rydgren,A.E., Cohen,M.: Protostars and Planets II, 371 (Black, Matthews eds)
S1-85 Sandell,G.: (Sub)millimeter astronomy, 433 (Shaver, Kjär, eds)
S2-85 Sandell,G., et al.: Nearby Molecular Clouds, 234 (Serra ed)
S3-85 Sato,S., et al: ApJ 291, 708
S4-85 Schwartz,R.D.: Protostars and Planets II, 405 (Black, Matthews eds)
S5-85 Schwartz,R.D., et al.: AJ 90, 1820
S6-85 Sellgren,K., et al.: ApJ 299, 416
S7-85 Shajmieva,A.F., Shutemova,N.A.: Perem Zv 22, 167
S8-85 Strom,S.E., et al.: AJ 90, 2281
S9-85 Strom,S.E., Strom,K.M.: Comments Astrophys 10, 179
S10-85 Sun,Y.L., et al.: AA Suppl 62, 309
T1-85 Takano,T.: (Sub)millimeter astronomy, 495 (Shaver, Kjär eds)
T2-85 Takano,T., et al.: AA 144, L20
T3-85 Torrelles,J.M., et al.: ApJ 288, 595 (erratum ApJ 295, 685)
T4-85 Torrelles,J.M., et al.: ApJ 294, L117
V1-85 Verdenet,M.: IAU Circ 4035
W1-85 Warren-Smith,R.F., et al.: MNRAS 215, 75P
W2-85 Wilson,T.L.: (Sub)millimeter astronomy, 401 (Shaver, Kjär eds)
W3-85 Witt,A.N., Schild,R.E.: ApJ 294, 225
W4-85 Wootten,A.: (Sub)millimeter astronomy, 443 (Shaver, Kjär eds)
X1-85 Xing,J., Winnewisser,G.: Chin Astr Ap 9, 328
X2-85 Xing,J., Xu,L.-p.: Chin Astron Ap 9, 283
Z1-85 Zhchenko,I.I., Kislyakov,A.G.: Nearby Molecular Clouds, 72 (Serra ed)
A1-86 Afanasev,G.M., et al.: Astrofiz Issled Izv Spets Astrofiz Obs 23, 3
B1-86 Bally,J.: Masers, molecules and mass ouflows in star forming regions, 179 (Haschick ed)
B2-86 Beichman,C.A.: Light on dark matter, 279 (Israel ed)
B3-86 Boulanger,F., et al.: Light on dark matter, 293 (Israel ed)
B4-86 Bouvier,J., et al.: AA 165, 110
C1-86 Caillaut,J.-P., Zoonematkermani.,S.: Adv Sp Res 6, 171
C2-86 Canto,J., Rodriguez,L.F.: Rev Mex A A 13, 57
C3-86 Cohen,M., et al.: ApJ 307, L21
E1-86 Evans II,N.J., et al.: ApJ 301, 894
F1-86 Fukui,Y., et al.: ApJ 311, L85
G1-86 Gahm,G.F.: Flares: solar and stellar, 124 (Gondhalekar ed)
G2-86 Goodrich,R.W.: AJ 92, 885
H1-86 Haro,G.: Flare stars and related objects, 223 (Mirzoyan ed)
H2-86 Hartmann,L., et al.: ApJ 309, 275
H3-86 Harvey,P.M., et al.: ApJ 301, 346
H4-86 Heiles,C., Stevens,M.: ApJ 301, 331
H5-86 Herbig,G.H., Terndrup,D.M.: ApJ 307, 609
H6-86 Heyer,M.H., et al.: ApJ 308, 134
J1-86 Jenniskens,P.M.M., et al.: Light on dark matter, 325 (Israel ed)
K1-86 Kolotilov,E.A.: Astron Zh 63, 298; Sov Astron 30, 181
K2-86 Kovalchuk,G.U.: Eruptive phenomena in stars, 443 (Szabados ed)
L1-86 Lightfoot,J.F., Glencross,W.M.: MNRAS 221, 47P
M1-86 Maddalena,R.J.: PhD Thesis, Columbia University New York
M2-86 Maddalena,R.J., et al.: ApJ 303, 375
M3-86 Meaburn,J.: AA 164, 358

M4-86 Mirabel,I.F.: Masers, molecules and mass ouflows in star forming regions, 189 (Haschick ed)
M5-86 Mirzoyan,L.V., Oganian,G.B.: Flare stars and related objects, 68 (Mirzoyan ed)
M6-86 Mozurkewich,D., et al.: ApJ 311, 371
N1-86 Nakajima,T., et al.: MNRAS 221, 483
N2-86 Natsvlishvili,R.Sh.: Flare stars and related objects, 116 (Mirzoyan ed)
O1-86 Oskanian,V.S.: Flare stars and related objects, 11 (Mirzoyan ed)
P1-86 Pendleton,Y., et al.: ApJ 311, 360
P2-86 Petrosian,V.M., Petrosian,A.R.: Soobshch Byurakan Obs 58, 36
P3-86 Pugach,A.F., Kovalchuk,G.U.: AN 307, 13
R1-86 Reipurth,B., Bally,J.: Nature 320, 336
R2-86 Reipurth,B., et al.: AA 164, 51
R3-86 Rodriguez,L.F.: Masers, molecules and mass ouflows in star forming regions, 155 (Haschick ed)
S1-86 Sa,C., et al.: MNRAS 222, 213
S2-86 Sandell,G., et al.: Light on dark matter, 295 (Israel ed)
S3-86 Schwartz,R.D.: Can J Phys 64, 414
S4-86 Scoville,N.Z., et al.: ApJ 303, 416
S5-86 Scoville,N.Z., et al.: Masers, molecules and mass ouflows in star forming regions, 201 (Haschick ed)
S6-86 Sellgren,K.: ApJ 305, 399
S7-86 Shevchenko,V.S.: Flare stars and related objects, 230 (Mirzoyan ed)
S8-86 Stephenson,C.B.: ApJ 300, 779
S9-86 Strom,K.M., et al.: ApJ Suppl 62, 39
T1-86 Takaba,H., et al.: AA 166, 276
T2-86 Takano,T., et al.: AA 167, 333
T3-86 Taylor,K., et al.: MNRAS 221, 155
T4-86 Troland,T.H. et al.: ApJ 304, L57
W1-86 Wiramihardja,S.D., et al.: Stellar activities and observational techniques, 137 (Sadakane, Yamasaki eds)
W2-86 Witt,A.N., Schild,R.E.: ApJ Suppl 62, 839
W3-86 Wolstencroft,R.D., et al.: MNRAS 218, 1P
W4-86 Wouterloot,J.G.A., Walmsley,C.M.: Light on dark matter, 313 (Israel ed)
W5-86 Wouterloot,J.G.A., Walmsley,C.M.: AA 168, 237
Z1-86 Zajtseva,G.V.: Astrofizika 25, 471; Astrophysics 25, 626
B1-87 Bally,J., et al.: ApJ 312, L45
B2-87 Bastien,P.: ApJ 317, 231
B3-87 Berrilli,F., et al.: MNRAS 228, 833
B4-87 Böhm,K.-H., et al.: ApJ 316, 349
B5-87 Bührke,T., Mundt,R.: Circumstellar matter (IAU 122), 175 (Appenzeller, Jordan eds)
B6-87 Bührke,T., Mundt,R.: Sterne u Weltraum 26, 616
B7-87 Bührke,T., Mundt,R.: Mit Astr Ges 70, 407
C1-87 Carballo,R., et al.: Circumstellar matter (IAU 122), 125 (Appenzeller, Jordan eds)
C2-87 Carrasco,L., et al.: Rev Mex A A 14, 518
C3-87 Churchwell,E., et al.: ApJ 321, 516
C4-87 Cohen,M., Jones,B.F.: ApJ 321, 846
C5-87 Cohen,M., Schwartz,R.D.: ApJ 316, 311
D1-87 Dopita,M.A., et al.: Star forming regions (IAU 115), 346 (Peimbert, Jugaku eds)
E1-87 Echevarria,J., et al.: Star forming regions (IAU 115), 340 (Peimbert, Jugaku eds)
E2-87 Evans II,N.J., et al.: ApJ 320, 364
F1-87 Feigelson,E.D.: Protostars and Molecular clouds, 123 (Montmerle, Bertout eds)
F2-87 Fukui,Y., et al.: Star forming regions (IAU 115), 328 (Peimbert, Jugaku eds)
G1-87 Gasparian,K.G., et al.: Inf Bul V S 3024
G2-87 Gatley,I., Kaifu,N.: Astrochemistry (IAU 120), 153 (Vardya, Tarafdar eds)
G3-87 Gatley,I., et al.: ApJ 318, L73
G4-87 Goodrich,R.W.: PASP 99, 116
G5-87 Gyulbudagian,A.L., et al.: Rev Mex A A 15, 53
H1-87 Hartigan,P.M.: PhD Thesis, Univ Arizona
H2-87 Hartigan,P., et al.: ApJ 316, 323
H3-87 Hasegawa,T.: Star forming regions (IAU 115), 123 (Peimbert, Jugaku eds)
H4-87 Hasegawa,T., et al.: ApJ 318, L77
H5-87 Heiles,C.: Physical processes in interstellar clouds, 429 (Morfill, Scholer, eds)
H6-87 Herbst,W., et al.: AJ 94, 137
H7-87 Heyer,M.H., et al.: AJ 94, 1653
I1-87 Imhoff,C.L., Appenzeller,I.: Exploring the universe with the IUE satellite, 295 (Kondo ed)
I2-87 Isobe,S.: Ap Sp Sci 135, 237
I3-87 Iwata,T., Fukui,Y.: Star forming regions (IAU 115), 357 (Peimbert, Jugaku eds)
J1-87 Jones,B.F., et al.: AJ 94, 1260
K1-87 Kardopolov,V.I., Rspaev,F.K.: Astron Tsirk 1499
M1-87 Malin,D.: Sky Telescope 74, 253
M2-87 Malin,D.F., et al.: MNRAS 227, 361
M3-87 Martin-Pintado,J., Cernicharo,J.: AA 176, L27
M4-87 Mendozo V,E.E., Rodriguez,L.F.: Inf Bul V S 2996
M5-87 Menten,K.M., et al.: Circumstellar matter (IAU 122), 179 (Appenzeller, Jordan eds)
M6-87 Mereghetti,S., Garilli,B.: AJ 94, 1616
M7-87 Mirabel,I.F.: Star forming regions (IAU 115), 315 (Peimbert, Jugaku eds)
M8-87 Mirabel,I.F., et al.: ApJ 318, 729
M9-87 Mirzoyan,L.V., Natsvlishvili,R.Sh.: Astrofizika 27, 605; not translated
M10-87 Missana,M.: Ap Sp Sci 136, 167
M11-87 Mundt,R.: Circumstellar matter (IAU 122), 147 (Appenzeller, Jordan eds)
M12-87 Mundt,R.: Mit Astr Ges 70, 100
M13-87 Mundt,R., et al.: ApJ 319, 275
M14-87 Myers,P.C., et al.: ApJ 319, 340
O1-87 Ogura,K.: Star forming regions (IAU 115), 341 (Peimbert, Jugaku eds)
P1-87 Parsamian,E.S., Gasparian,K.G.: Astrofizika 27, 447; Astrophysics 27, 598
P2-87 Pravdo,S.H., Chester,T.J.: ApJ 314, 308
R1-87 Raga,A.C., Böhm,K.-H.: ApJ 323, 193
R2-87 Ray,T.P.: AA 171, 145
R3-87 Reipurth,B., et al.: Star forming regions (IAU 115), 396 (Peimbert, Jugaku eds)
R4-87 Rodriguez,C.F.: Star forming regions (IAU 115), 239 (Peimbert, Jugaku eds)
S1-87 Sargent,A.I., et al.: Star forming regions (IAU 115), 329 (Peimbert, Jugaku eds)
S2-87 Scarrott,S.M., et al.: MNRAS 227, 1065
S3-87 Schwartz,R.D., et al.: ApJ 322, 403
S4-87 Smith,H.A., et al.: Star forming regions (IAU 115), 343 (Peimbert, Jugaku eds)
S5-87 Snell,R.L.: Star forming regions (IAU 115), 213 (Peimbert, Jugaku eds)
S6-87 Solf,J.: Circumstellar matter (IAU 122), 191 (Appenzeller, Jordan eds)
S7-87 Solf,J.: AA 184, 322
S8-87 Strom,S.E., Strom,K.M.: Star forming regions (IAU 115), 255 (Peimbert, Jugaku eds)
S9-87 Suzuki,H. et al.: Star forming regions (IAU 115), 90 (Peimbert, Jugaku eds)
T1-87 Takaba,H., Fukui,Y.: Star forming regions (IAU 115), 81 (Peimbert, Jugaku eds)
T2-87 Takano,T., et al.: Star forming regions (IAU 115), 361 (Peimbert, Jugaku eds)
T3-87 Takayanagi,K., et al.: ApJ 318, L81
T4-87 Tapia,M., et al.: MNRAS 224, 587
T5-87 Tomita,Y.: Star forming regions (IAU 115), 51 (Peimbert, Jugaku eds)
Z1-87 Zaritsky,D., et al.: AJ 93, 1514
Z2-87 Zinchenko,I.I., et al.: Pisma Astron Zh 13, 582; Sov Astron Let 13, 243
Z3-87 Zuckerman,B., Lo,K.Y.: AA 173, 263
A1-88 Ambarian,V.V.: Astrofizika 28, 149; Astrophysics 28, 86
A2-88 Aniol,R., et al.: Messenger 52, 39

B1-88 Bastien,P.: Galactic and extragalactic star formation, 303 (Pudritz, Fich eds)
B2-88 Bastien,P., Menard,F.: ApJ 326, 334
B3-88 Bouvier,J., et al.: AA Suppl 75, 1
B4-88 Bührke,T., et al.: AA 200, 99
C1-88 Carballo,R., et al.: MNRAS 232, 497
C2-88 Cardelli,J.A., Brugel,E.W.: AJ 96, 673
C3-88 Carter,B.D., et al.: MNRAS 231, 49
C4-88 Cesaroni,R., et al.: AA Suppl 76, 445
C5-88 Cohen,M., et al.: ApJ 329, 863
D1-88 Downes,R.A., Keyes,C.D.: AJ 96, 777
F1-88 Fukui,Y.: Vistas Astron 31, 217
F2-88 Fukui,Y., et al.: ApJ 325, L13
G1-88 Gatley,I.: Galactic and extragalactic star formation, 159 (Pudritz, Fich eds)
H1-88 Herbig,G.H., Bell,K.R.: Lick Obs Bul 1111
H2-88 Herbst,W., Koret,D.L.: AJ 96, 1949
I1-88 Ismailov,N.Z.: Astron Tsirk 1530, 9
I2-88 Ismailov,N.Z.: Astron Zh 65, 971; Sov Astron 32, 508
I3-88 Ismailov,N.Z.: Pisma Astron Zh 14, 327; Sov Astron Let 14, 138
I4-88 Iwata,T., et al.: ApJ 325, 372
J1-88 Jones,B.F., Walker,M.F.: AJ 95, 1755
K1-88 Kardopolov,V.I., et al.: Astron Zh 65, 951; Sov Astron 32, 498
K2-88 Kotyshev,V.V.: Tsirk Astron Inst Tashkent 127, 18
K3-88 Krivtsov,A.A., Yutanov,N.Yu.: Izv Glav Astron Obs Pulkovo 205, 74
L1-88 Lada,C.J.: Galactic and extragalactic star formation, 5 (Pudritz, Fich eds)
L2-88 Lee,M.G., et al.: AJ 96, 1690
L3-88 Levreault,R.M.: ApJ 330, 897
L4-88 Levreault,R.M.: ApJ Suppl 67, 283
M1-88 Marcaide,J.M., et al.: AA 197, 235
M2-88 Marshall,L.A., Mathieu,R.D.: AJ 96, 1956
M3-88 Mirzoyan,L.V., Ambarian,V.V.: Astrofizika 28, 375; Astrophysics 28, 220
M4-88 Mirzoyan,L.V., et al.: Astrofizika 28, 540; Astrophysics 28, 320
M5-88 Mundt,R.: Formation and evolution of low mass stars, 257 (Dupree, Lago eds)
P1-88 Parker,N.D.: MNRAS 235, 139
P2-88 Pavlenko,E.P., Prokofeva,V.V.: Astron Tsirk 1530, 7
R1-88 Raga,A.C., Mateo,M.: AJ 95, 543
R2-88 Raga,A.C., Mateo,M.: Rev Mex A A 16, 13
R3-88 Raga,A.C., et al.: AJ 95, 1783
R4-88 Raymond,J.C., et al.: ApJ 326, 323
R5-88 Reipurth,B., Graham,J.A.: AA 202, 219
S1-88 Sandell,G., et al.: ApJ 329, 920
S2-88 Scarrott,S.M.: MNRAS 231, 1055
S3-88 Scarrott,S.M., Wolstencroft,R.D.: MNRAS 231, 1019
S4-88 Schwartz,R.D., et al.: ApJ 334, L99
S5-88 Solf,J., et al.: ApJ 334, 229
S6-88 Sonneborn,G., et al.: A decade of UV astronomy with the IUE satellite 2, 231 (Longdon, Rolfe eds)
S7-88 Stacy,J.G., et al.: Interstellar matter, 179 (Moran, Ho eds)
S8-88 Strom,S.E., et al.: Galactic and extragalactic star formation, 53 (Pudritz, Fich eds)
T1-88 Takano,T., et al.: Interstellar matter, 213 (Moran, Ho eds)
T2-88 Tauber,J.A., et al.: ApJ 325, 846
V1-88 van Altena,W.F., et al.: AJ 95, 1744
V2-88 Vittone,A., et al.: The impact of very high S/N spectroscopy on stellar physics (IAU 132), 109 (Cayrel de Strobel, Spite eds)
V3-88 von Hippel,T., et al.: AA Suppl 74, 431
V4-88 Vrba,F.J., et al.: AJ 96, 680
W1-88 Walker,C.K., et al.: AA 205, 243
W2-88 Walker,M.F., Jones,B.F.: PASP 100, 1505
W3-88 Walmsley,C.M.: Galactic and extragalactic star formation, 181 (Pudritz, Fich eds)
W4-88 Witt,A.N., Schild,R.E.: ApJ 325, 837
W5-88 Wouterloot,J.G.A., et al.: AA 203, 367
Y1-88 Yudin,R.V.: Astron Zh 65, 1250; Sov Astron 32, 652
A1-89 Alonso-Costa,J.L., Kwan,J.: ApJ 338, 403
A2-89 Anglada,G., et al.: ApJ 341, 208
A3-89 Antokhina,Eh.A., et al.: Pisma Astron Zh 15, 837; Sov Astron Let 15, 362
A4-89 Appenzeller,I., Mundt,R.: AA Rev 1, 291
A5-89 Armstrong,J.T.: Physics and Chemistry of Interstellar Molecular Clouds, 143 (Winnewisser, Armstrong eds)
A6-89 Aspin,C., et al.: Low mass star formation and pre-main sequence objects, 349 (Reipurth ed)
B1-89 Bally,J.: Low mass star formation and pre-main sequence objects, 1 (Reipurth ed)
B2-89 Bally,J.: Structure and Dynamics of the Interstellar Medium (IAU Coll 120), 309 (Tenorio-Tagle et al. eds)
B3-89 Barvainis,R., Deguchi,S.: AJ 97, 1089
B4-89 Berrilli,F., et al.: MNRAS 237, 1 (erratum MNRAS 239, 255)
B5-89 Blondin,J.M., et al.: ApJ 337, L37
B6-89 Böhm,K.H.: Structure and Dynamics of the Interstellar Medium (IAU Coll.120), 282 (Tenorio-Tagle et al. eds)
B7-89 Bossi,M., et al.: AA 222, 117
B8-89 Braz,M.A., et al.: AA Suppl 77, 465
B9-89 Brugel,E.W.: Low mass star formation and pre-main sequence objects, 311 (Reipurth ed)
B10-89 Buj,J., et al.: Ap Sp Sci 156, 251
B11-89 Burton,M.G., et al.: MNRAS 238, 1513
C1-89 Caillault,J.-P., Zoonematkermani,S.: ApJ 338, L57
C2-89 Carr,J.S.: ApJ 345, 522
C3-89 Carter,B.D.: Proc Astr Soc Aust 8, 68
C4-89 Casali,M.M.: Infrared Spectroscopy in Astronomy, 287 (Kaldeich ed)
C5-89 Castets,A., et al.: Physics and Chemistry of Interstellar Molecular Clouds, 133 (Winnewisser, Armstrong eds)
C6-89 Ceccarelli,C., et al.: Infrared spectroscopy in astronomy, 343 (Kaldeich ed)
C7-89 Chromey,F.R., et al.: AJ 98, 2203
C8-89 Curiel,S., et al.: Rev Mex A A 17, 137
D1-89 Dent,W.R.F., et al.: MNRAS 238, 1497
E1-89 Evans,A., et al.: MNRAS 237, 695
F1-89 Fukui,Y.: Low mass star formation and pre-main sequence objects, 95 (Reipurth ed)
F2-89 Fukui,Y., et al.: Nature 342, 161
G1-89 Gasparian,K.G., Hakhverdian,L.G.: Inf Bul V S 3393
G2-89 Gasparian,K.G., Oganian,G.B.: Inf Bul V S 3327
G3-89 Gasparian,K.G., Oganian,G.B.: Astron Tsirk 1537, 22
G4-89 Genzel,R., Stutzki,J.: ARAA 27, 41
G5-89 Grinin,V.P., et al.: Pisma Astron Zh 15, 1028; Sov Astron Let 15, 448
H1-89 Hartigan,P.: ApJ 339, 987
H2-89 Herbig,G.H.: Low mass star formation and pre-main sequence objects, 233 (Reipurth ed)
H3-89 Hippelein,H.H., Münch,G.: AA 213, 323
H4-89 Hu,J.Y., et al.: AA 208, 213
I1-89 Ismailov,N.Z.: Astron Tsirk 1541, 9
K1-89 Kawabe,R., et al.: Structure and Dynamics of the Interstellar Medium (IAU Coll 120), 254 (Tenorio-Tagle et al. eds)
K2-89 Kogure,T., et al.: PAS Japan 41, 1195
K3-89 Krügel,E., et al.: AA 211, 419
L1-89 Lada,E.A.: BAAS 20, 1030
L2-89 Lane,A.P.: Low mass star formation and pre-main sequence objects, 331 (Reipurth ed)
L3-89 Lopez,R.: 4th IAP Astrophysics Meeting, 269 (Delache et al. eds)
M1-89 Maclaren,I., et al.: J Phys G 15, 1305
M2-89 Margulis,M., Snell,R.L.: ApJ 343, 779
M3-89 McNamara,B.J., et al.: AJ 97, 1427
M4-89 Mead,K.N., et al.: Molecular clouds in the Milky Way and external galaxies, 271 (Dickman et al. eds)
M5-89 Mirabel,I.F., et al.: ApJ 346, 180
M6-89 Moriarty-Schieven,G.H., et al.: ApJ 347, 358
M7-89 Mundt,R.: Physics and Chemistry of Interstellar Molecular Clouds, 152 (Winnewisser, Armstrong eds)
M8-89 Murata,Y., et al.: Structure and Dynamics of the Interstellar Medium (IAU Coll 120), 327 (Tenorio-Tagle et al. eds)
N1-89 Noriega-Crespo,N., et al.: AJ 98, 1388

R1-89 Raga,A.C.: Low mass star formation and pre-main sequence objects, 281 (Reipurth ed)
R2-89 Raga,A.C., Canto,J.: PASP 101, 1151
R3-89 Rayner,J., et al.: MNRAS 241, 469
R4-89 Reipurth,B.: AA 220, 249
R5-89 Reipurth,B.: Nature 340, 42
R6-89 Reipurth,B.: Low mass star formation and pre-main sequence objects, 247 (Reipurth ed)
R7-89 Robertson,T.H., Jordan,T.M.: AJ 98, 1354
R8-89 Rodriguez,L.F., et al.: Bul Am Phys Soc 34, 1290
R9-89 Rodriguez,L.F., et al.: Rev Mex 18, 45
R10-89 Roth,M., et al.: AA 222, 211 (erratum AA 229, 279 1990)
R11-89 Ryter,C., d'Hendecourt,L.: Interstellar dust (IAU135 contr papers), 111 (Tielens, Allamandola eds)
S1-89 Sandell,G., et al.: Molecular clouds in the Milky Way and external galaxies, 279 (Dickman et al. eds)
S2-89 Scarrott,S.M., et al.: MNRAS 237, 1027
S3-89 Shevchenko,V.S.: Ae/Be zvezdy Kherbiga, AN Uzbekskoj SSR, Tashkent. Astronomicheskij Inst., Fan.
S4-89 Sternberg,A.: ApJ 347, 863
S5-89 Strom,K.M., et al.: ApJ 345, L79
S6-89 Strom,K.M., et al.: ApJ 346, L33
S7-89 Strom,K.M., et al.: ApJ Suppl 71, 183
S8-89 Strom,K.M., et al.: Low mass star formation and pre-main sequence objects, 423 (Reipurth ed)
S9-89 Sugitani,K., et al.: ApJ 342, L87
S10-89 Sugitani,K.: Physics and Chemistry of Interstellar Molecular Clouds, 112 (Winnewisser, Armstrong eds)
S11-89 Suto,H., et al.: MNRAS 239, 139
T1-89 Tanaka,M., et al.: ApJ 336, 207
T2-89 Torrelles,J.M., et al.: ApJ 346, 756
T3-89 Troland,T.H., et al.: ApJ 337, 342
V1-89 Verdes-Montenegro,L., et al.: ApJ 346, 193
W1-89 Wilking,B.A., et al.: ApJ 345, 257
W2-89 Wiramihardja,S.D., et al.: PAS Japan 41, 155
W3-89 Witt,A.N., Malin,D.F.: ApJ 347, L25
W4-89 Wouterloot,J.G.A., et al.: AA 215, 131
Y1-89 Yamashita,T., et al.: ApJ 347, L85
Y2-89 Yusef-Zadeh,F., et al.: BAAS 21, 793
Z1-89 Zealey,W.J., et al.: Proc Astron Soc Aust 8, 62
Z2-89 Zinnecker,H.: Low mass star formation and pre-main sequence objects, 447 (Reipurth ed)
Z3-89 Zinnecker,H., et al.: ApJ 342, 337
Z4-89 Zinnecker,H., et al.: Physics and Chemistry of Interstellar Molecular Clouds, 174 (Winnewisser, Armstrong eds)
B1-90 Berrilli,F., et al.: Il Nuovo Cimento 13C, 293
B2-90 Böhm,K.H., Solf,J.: ApJ 348, 297
B3-90 Bouvier,J.: AJ 99, 946
B4-90 Burton,M.G., et al.: ApJ 352, 625
B5-90 Butner,H.M., et al.: ApJ 364, 164
C1-90 Caillault,J.P., Zoonematkermani,S.: Flare Stars in Star Clusters, Associations and the Solar Vicinity (IAU 137), 159 (Mirzoyan et al. eds)
C2-90 Carr,J.S.: AJ 100, 1244
C3-90 Castets,A., et al.: AA 234, 469
C4-90 Cohen,M.: ApJ 354, 701 (erratum ApJ 362, 758)
C5-90 Comoretto,G., et al.: AA Suppl 84, 179
D1-90 Davies,J.K., et al.: MNRAS 247, 517
D2-90 Davis,C.J., et al.: MNRAS 244, 173
D3-90 DePoy,D.L., et al.: ApJ 356, L55
F1-90 Feitzinger,J.V., Stüwe,J.A.: MNRAS 242, 395
G1-90 Garden,R.P., et al.: ApJ 354, 232
G2-90 Gasparian,L.G., et al.: Flare Stars in Star Clusters, Associations and the Solar Vicinity (IAU 137), 253 (Mirzoyan et al. eds)
G3-90 Graf,U.U., et al.: ApJ 358, L49
H1-90 Haschick,A.D., Ho,P.T.P.: ApJ 352, 630
H2-90 Heyer,M.H., et al.: AJ 99, 1585
I1-90 Ishida,K.: Flare Stars in Star Clusters, Associations and the Solar Vicinity (IAU 137), 225 (Mirzoyan et al. eds)
J1-90 Jaffe,D.T., et al.: ApJ 353, 193
J2-90 Jaffe,D.T., et al.: Submillimeter astronomy, 127 (Watt, Webster eds)
J3-90 Jain,S.K., et al.: AA Suppl 83, 237
J4-90 Jain,S.K., et al.: Galactic and Intergalactic Magnetic Fields (IAU 140), 323 (Beck et al. eds)
J5-90 Jenniskens,P., Wouterloot,J.G.A.: AA 227, 553
J6-90 Johnson,J.J., et al.: AJ 100, 518
K1-90 Kitamura,Y., et al.: ApJ 363, 180
L1-90 Lada,E.A.: PhD Thesis, University of Texas at Austin
L2-90 Lada,E.A.: Submillimeter astronomy, 267 (Watt, Webster eds)
M1-90 Martin-Pintado,J., et al.: ApJ 357, L49
M2-90 Mendoza V,E.E., et al.: AA Suppl 84, 29
M3-90 Mezger,P.G., et al.: AA 228, 95
M4-90 Morgan,J.A., et al.: ApJ 362, 274
M5-90 Moriarty-Schieven,G.H., et al.: Submillimeter astronomy, 37 (Watt, Webster eds)
M6-90 Murata,Y., et al.: ApJ 359, 125
N1-90 Noriega-Crespo,A., et al.: AJ 99, 1918
R1-90 Raga,A.C., et al.: AJ 99, 1912
R2-90 Rodriguez,L.F., et al.: ApJ 352, 645
R3-90 Rolph,C.D., et al.: MNRAS 242, 109
S1-90 Schmid-Burgk,J., et al.: ApJ 362, L25
S2-90 Skinner,S.L., et al.: ApJ 357, L39
S3-90 Strom,K.M., et al.: ApJ 362, 168
T1-90 Tsikoudi,V.: AJ 100, 1618
V1-90 Verdenet,M., et al.: IAU Circ 4966
W1-90 Walker,M.F.: PASP 102, 726
W2-90 Weintraub,D.A.: ApJ Suppl 74, 575
W3-90 White,G.J., et al.: AA 227, 200
W4-90 Wilking,B.A., et al.: AJ 99, 344
W5-90 Wilking,B.A., et al.: AJ 100, 758
W6-90 Witt,A.N., Boroson,T.A.: ApJ 355, 182
Y1-90 Yusef-Zadeh,F., et al.: ApJ 348, L61
Y2-90 Yusef-Zadeh,F., et al.: Galactic and Intergalactic Magnetic Fields (IAU 140), 329 (Beck et al. eds)
Z1-90 Zhou,S., et al.: ApJ 355, 159
C1-91 Casali,M.M.: MNRAS 248, 229
H1-91 Harju,J., et al.: AA, 245, 643
L1-91 Lada,E.A., et al.: ApJ 368, 432
L2-91 Lada,E.A., et al.: ApJ, in press
M1-91 Morgan,J.A., Bally,J.: ApJ 372, 505
M2-91 Morgan.J.A., et al.: ApJ 376, 618
O1-91 Ogura,K., Walsh,J.R.: AJ 101, 185
O2-91 Ogura,K.: AJ 101, 1803
R1-91 Reipurth,B., Olberg,M.: AA 246, 535
U1-91 Uchida,Y. et al.: Nature 349, 140
W1-91 Wiramihardja, S.D., et al.: PAS Japan 43, 27
W2-91 Wouterloot,J.G.A., Brand,J.: in preparation

This article was processed by the author using Springer-Verlag TEX AA macro package 1989.

The Canis Majoris OB1 Association

G.H. Herbig

Institute for Astronomy
University of Hawaii
Honolulu, Hawaii 96822, U.S.A.

In red light, the most conspicuous feature of CMa OB1 is the long arc of emission nebulosity S296, and the nearly circular nebulosity IC 2177 surrounding the Be star HD 53367: see the ESO Schmidt photograph, Fig. 1. The famous Herbig Ae/Be star Z CMa is embedded in a dark cloud at the outer edge of S296; identifications of many of the early-type and other interesting stars in the region are shown in Fig. 2. One unexpected object within the ring is the very bright carbon star W CMa, which itself is unusual among C stars in that it illuminates a faint reflection nebulosity of its own.

A color magnitude diagram based on the early-type stars in this region was published by Clariá (1974 a,b), from which a distance of 1.15 kpc was estimated, which locates the association on the Orion Arm. Recently, Ibragimov and Shevchenko (1990) obtained photometry and spectra of 154 early-type stars and derived a distance of 930 $\pm$ 120 pc. Since the association lies very nearly in the galactic plane, and because the background is not obscured significantly by dust associated with CMa OB1, there is some contamination of the field by distant stars in the next arm. Other photometric studies of association members were done by Feinstein (1967), Eggen (1981) and de Geus, Lub and van de Grift (1990). The most recent detailed mapping of the region in CO is by Machnik *et al.* (1980); their CO map of the area is shown as Fig. 3.

Herbst and Assousa (1977) noted that S296 and fainter nebulosity to the north and east define a ring about 3° in diameter. Since there was no luminous early-type star near the ring center (which is confirmed by the far ultraviolet image of the field by Henry *et al.* 1988), they proposed that the shell was in fact an old supernova remnant, and that star formation had been induced in CMa OB1 through compression of ambient material by the expanding shell. This idea was reinforced by the fact that one early-type star which lies within the ring, HD 54662 (O6.5 V), is not only well offcenter but has a radial velocity differing about 30 km s^{-1} from the mean association velocity. Although no reliable proper motion is available, the foregoing suggested to Herbst and Assousa that HD 54662 may be a runaway O star and thus additional evidence for a supernova event about 8 10^5 years ago. That age, derived from supernova shell theory, was regarded as acceptably near the age of 3 10^5 years obtained by Herbst, Racine and Warner (1978) from their color magnitude diagram of the OB stars (although Clariá earlier had estimated the age as 3 10^6 years). See also the review by Herbst (1980).

Reynolds and Ogden (1978) improved the information on the gas velocities in the region (the work of Herbst and Assousa was based on 21 cm data) by measuring the Hα, [N II] and [O III] lines with a Fabry-Perot spectrometer. They confirmed that the large shell was in expansion with a velocity of about 13 km s^{-1}, but considered that models involving strong stellar winds or an evolving H II region were equally plausible alternatives to the supernova hypothesis. They noted that the ultraviolet fluxes of the two hot stars within the ring, HD 54662 and 53975 (O7.5 V), were quite sufficient to account for the temperature and ionization of the shell. Weak diffuse interstellar bands were observed towards several early type stars by Whittet and Blades (1980).

The CMa OB1 region was examined for emission-Hα stars by Wiramihardja *et al.* (1974). Those that were found within the borders of Fig. 1 are indicated by double lines in Fig. 2. The two-color diagram for the emission-line stars, the brighter being OB stars, in the region is shown in Fig. 4. These data are from Clariá (1974a), but the diagram itself is from Wiramihardja *et al.* Recently, Schwartz, Persson and Hamann (1990) also found Hα emission stars in the region.

Among the stars in the region, Z CMa has attracted most attention (see Herbig 1960 for early references). The star is located in a complex region at the edge of the large molecular shell behind S296 (see Fig. 5). Low and high resolution optical spectra are presented by Covino *et al.* (1984), Finkenzeller and Jankovics (1984), Finkenzeller and Mundt (1984), and ultraviolet spectra by Kenyon *et al.* (1989). Significant spectral changes have been discussed by Covino *et al.* (1988) and Hessman *et al.* (1991). Photometric variability has been investigated by Kolotilov (1991). A major well-collimated Herbig-Haro jet emanating from Z CMa was discovered by Poetzel, Mundt and Ray (1989). Recently, Hartmann *et al.* (1989) suggested Z CMa is a FUor. Leinert and Haas (1987) and Koresko *et al.* (1989) have made near-infrared speckle observations which show Z CMa to be highly elongated with a size of about 0.1″ at 2.2μm, perhaps due to a disk or a close companion. Recently, more detailed near-infrared speckle interferometric observations confirmed the presence of a companion at a separation of 0.1″ at a PA = 122° (Christou *et al.* 1992, Koresko *et al.* 1992). Sub-millimeter observations reveal large amounts of cold dust around Z CMa (Weintraub, Sandell, and Duncan 1991). The star has also been detected at centimeter wavelengths by Cohen and Bieging (1986).

References

Christou, J., Zinnecker, H., Ridgway, S., Haas, M., Leinert, C.: 1992, in press

Clariá, J.J.: 1974a, Astr.Ap. **37**, 229

Clariá, J.J.: 1974b, *AJ* **79**, 1022

Cohen, M., Bieging, J.H.: 1986, *AJ* **92**, 1396

Covino, E., Terranegra, L., Vittone, A.A., Russo, G.: 1984, *AJ* **89**, 1868

Covino, E., Terranegra, L., Vittone, A.A., Giovanelli, F., Rossi, G.: 1988, in *Physics of Formation of Fe II lines Outside LTE*, eds. R. Viotti *et al.*, Reidel, p. 143

de Geus, E.J., Lub, J., van de Grift, E.: 1990, *A&AS* **85**, 915

Eggen, O.J.: 1981, *ApJ* **247**, 507

Feinstein, A.: 1967, *ApJ* **149**, 107

Finkenzeller, U., Jankovics, I.: 1984, *A&AS* **57**, 285

Finkenzeller, U., Mundt, R.: 1984, *A&AS* **55**, 109

Hartmann, L., Kenyon, S.J., Hewett, R., Edwards, S., Strom, K.M., Strom, S.E., Stauffer, J.R.: 1989, *ApJ* **338**, 1001

Henry, R.C. *et al.*: 1988, *Atlas of the Ultraviolet Sky* (Baltimore: Johns Hopkins Univ. Press)

Herbig, G.H.: 1960, *ApJS* **4**, 337

Herbst, W.: 1980, in IAU Symp. No. 85, *Star Clusters*, ed. J.E. Hesser, Reidel, p. 33

Herbst, W. and Assousa, G.E.: 1977, *ApJ* **217**, 473

Herbst, W., Racine, R. and Warner, J.W.: 1978, *ApJ* **223**, 471

Hessman, F.V., Eislöffel, J., Mundt, R., Hartmann, L.W., Herbst, W., Krautter, J.: 1991, *ApJ* **370**, 384

Ibragimov, M.A., Shevchenko, V.S.: 1990, in *Conference on Classical Be Stars and Ae/Be Herbig Stars*, ed. A. Kh. Mamatkazina, Alma Ata

Kenyon, S.J., Hartmann, L., Imhoff, C.L., Cassatella, A.: 1989, *ApJ* **344**, 925

Kolotilov, E.A.: 1991, *Sov. Astron. Lett.* **17**, 144

Koresko, C.D., Beckwith, S.V.W., Sargent, A.I.: 1989, *AJ* **98**, 1394

Koresko, C.D., Beckwith, S.V.W., Ghez, A.M., Matthews, K., Neugebauer, G.: 1992, in press

Leinert, Ch., Haas, M.: 1987, *A&A* **182**, L47

Machnik, D.E., Hettrick, M.C., Kutner, M.L., Dickman, R.L. and Tucker, K.D.: 1980, *ApJ* **242**, 121

Poetzel, R., Mundt, R., Ray, T.P.: 1989, *A&A* **224**, L13

Reynolds, R.J. and Ogden, P.M.: 1978, *ApJ* **224**, 94

Schwartz, R.D., Persson, S.E., Hamann, F.W.: 1990, *AJ* **100**, 793

Simonson, S.C.: 1976, Astr.Ap. **46**, 261

Weintraub, D.A., Sandell, G., Duncan, W.: 1991, *ApJ* **382**, 270

Whittet, D.C.B., Blades, J.C.: 1980, *MNRAS* **190**, 41P

Wiramihardja, S.D., Kogure, T., Nakano, M. and Yoshida, S.: 1986, *PASJ* **38**, 395

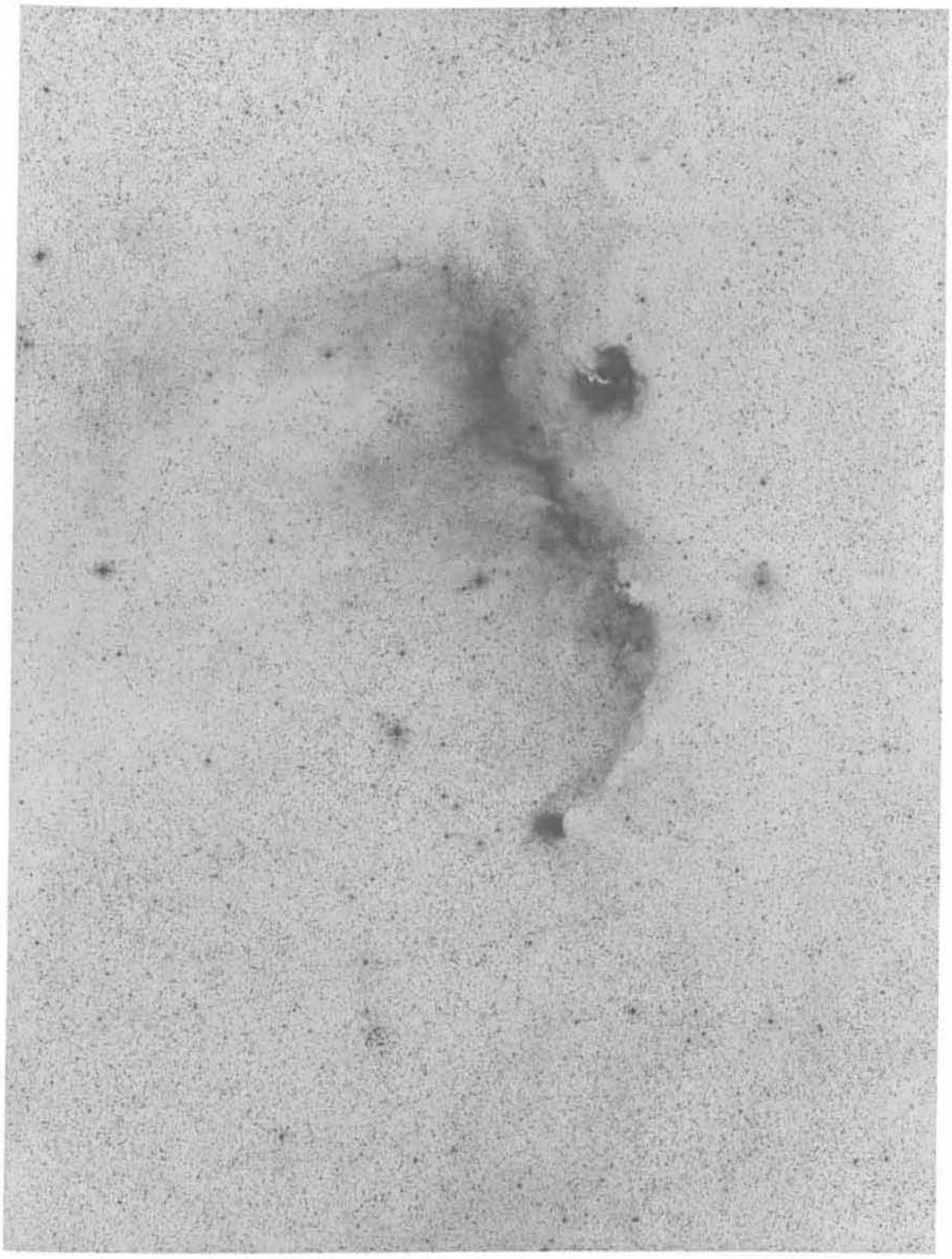

Figure 1. The CMa OB1 region as seen on a red ESO Schmidt plate. The arc of emission nebulosity is Sharpless 296.

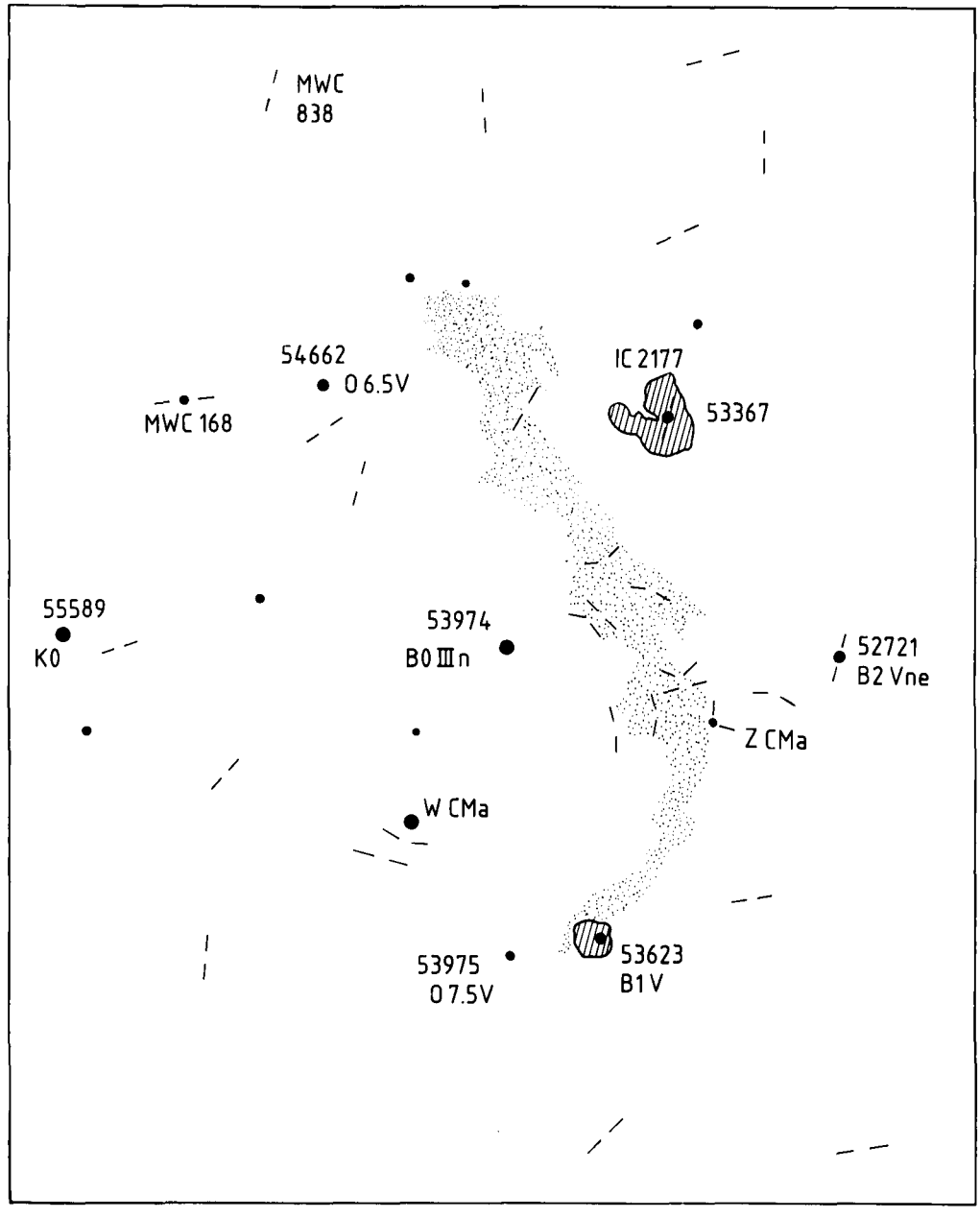

Figure 2. Identification of early-type stars (by their HD numbers) and reflection nebulae. The marks show the positions of emission-line stars found by Wiramihardja *et al.* (1986).

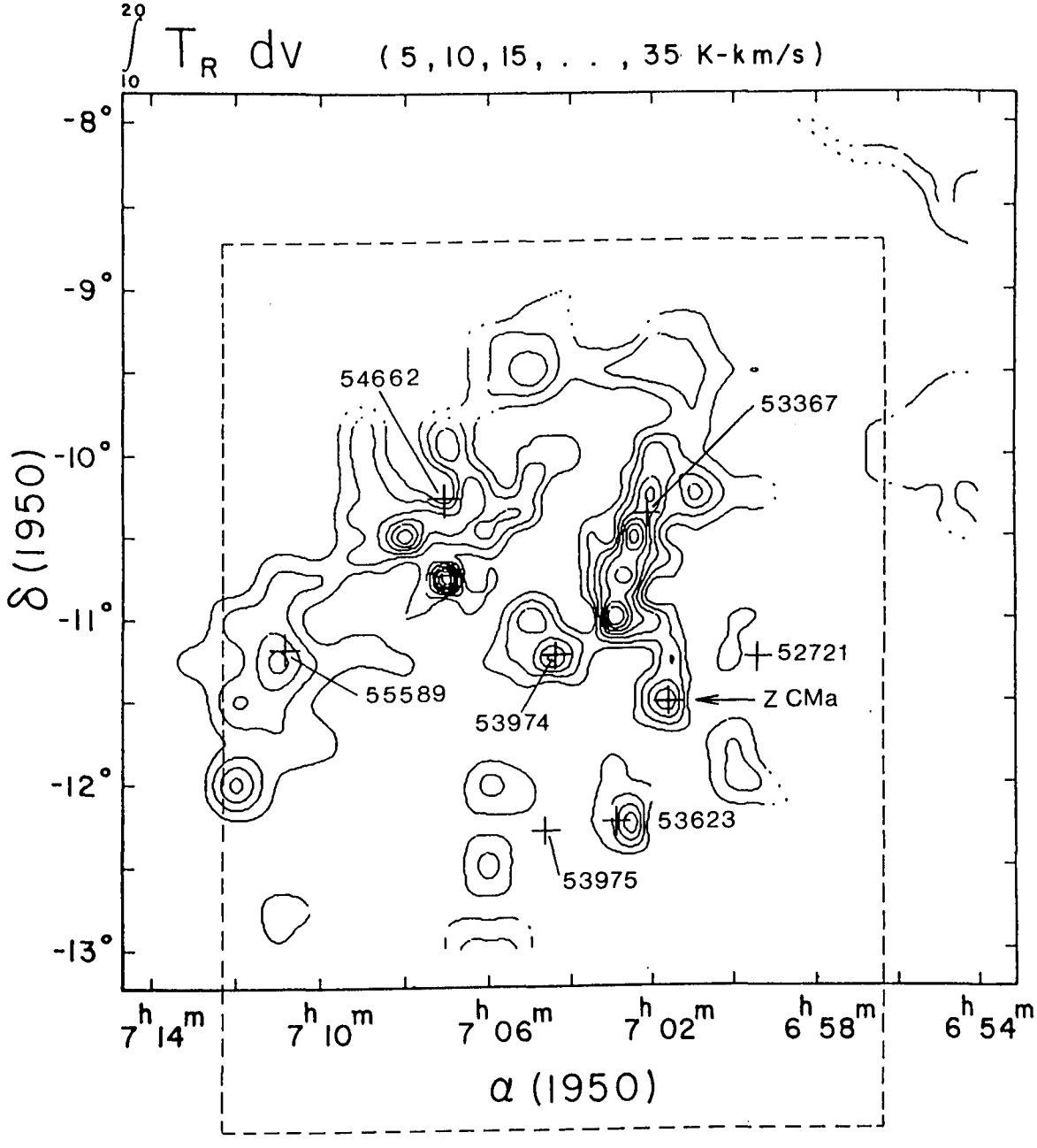

Figure 3. CO map of the central region of CMa OB1, from Machnik *et al.* (1980). The positions of early-type stars are indicated by their HD numbers. The box shows the area covered by the red Schmidt photograph.

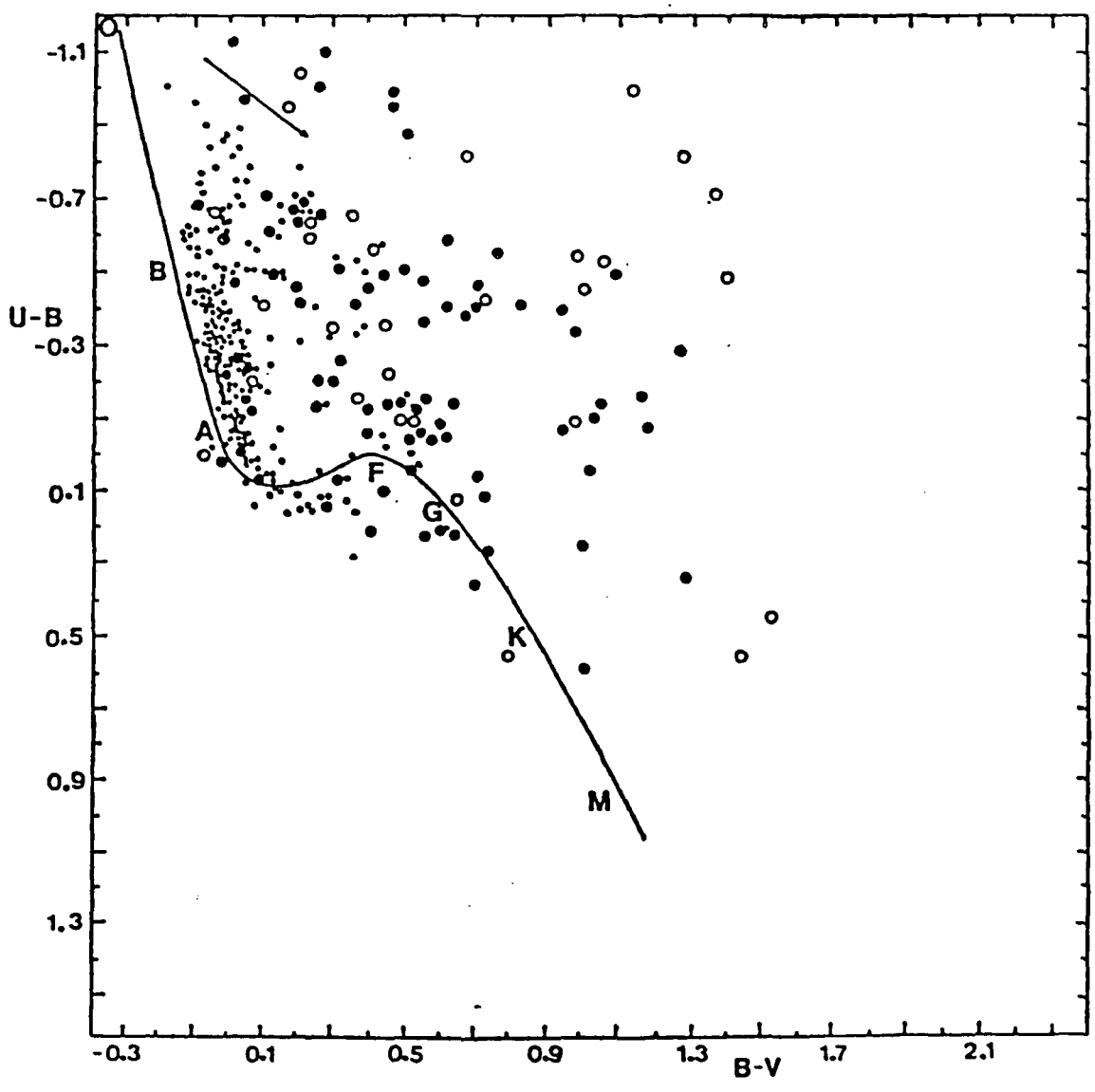

Figure 4. Two-color diagram for emission-line stars in the CMa OB1 region. The small dots are OB stars from Clariá (1974a). Large filled and open circles are emission-line stars from the central region of CMa OB1 and from a reference area, respectively. The unreddened main sequence is shown, and a normal reddening vector (from Wiramihardja *et al.* 1986).

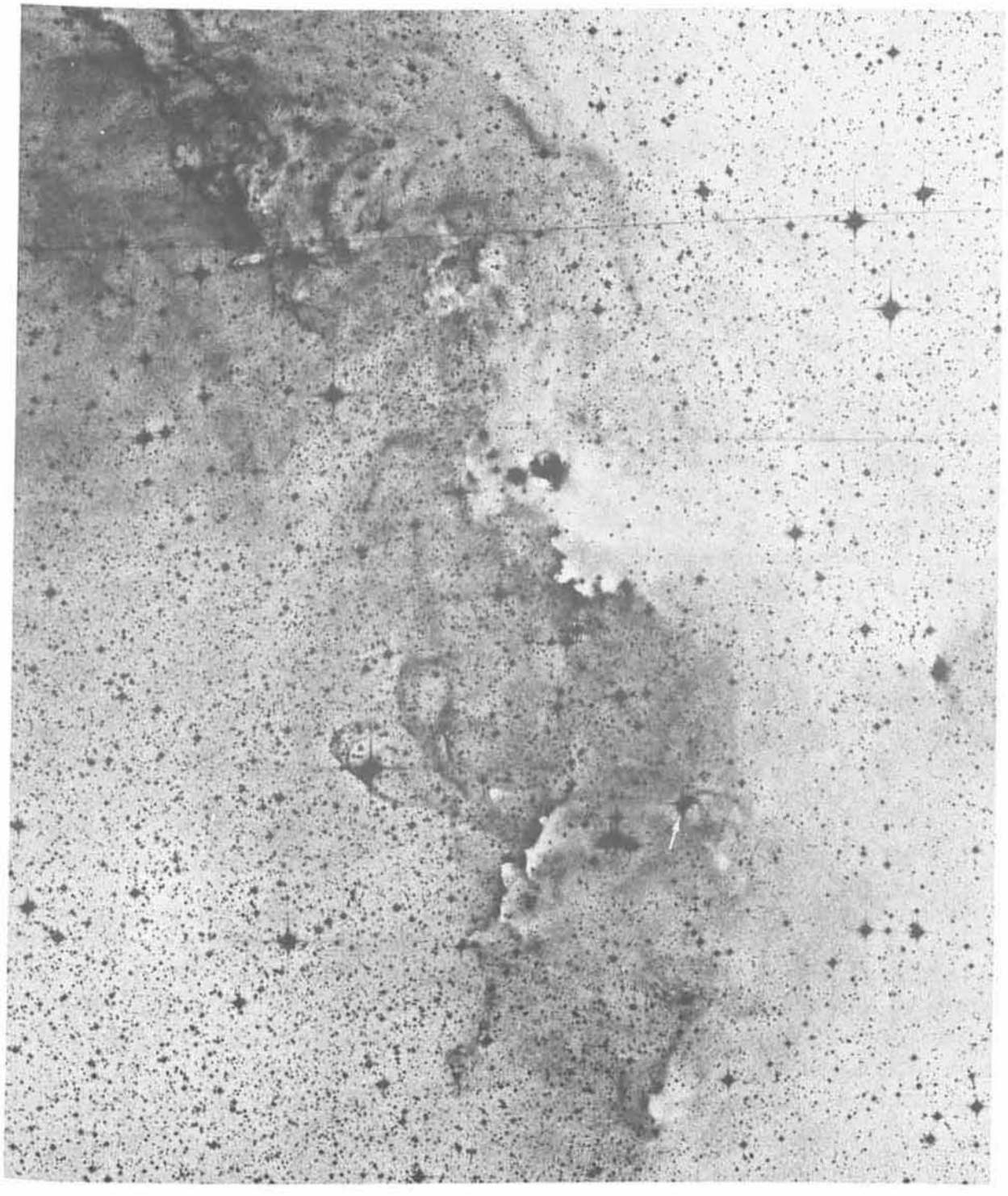

Figure 5. The location of Z CMa (at the arrow) near the interface between the H II region and the molecular shell is shown in this red ESO Schmidt plate. The print has been processed using unsharp masking by C. Madsen.

Low Mass Star Formation in Puppis and Vela

Bertil Pettersson

Astronomical Observatory
Box 515, S-751 20 Uppsala,
Sweden

1. Introduction

The region of Puppis and Vela encompasses roughly the galactic longitude interval $240° < l < 280°$. In this area of the southern Milky Way we find among other features the huge Gum Nebula with a diameter of 36° and centered at $l = 258°$ and $b = -2°$(Chanot and Sivan, 1983), and the Vela spiral arm feature at l ~265°, as delineated by different types of spiral arm tracers. In the longitude range 257°–274° we also find the Vela Molecular Ridge, VMR. This feature is described by May et al. (1988) as a ridge of intense compact molecular emission peaks, found during a low-resolution ^{12}CO survey of the third galactic quadrant. Murphy and May (1991) conclude that the VMR consists of a group of at least four $10^5 - 10^6 M_\odot$ giant molecular clouds between 1 and 2 kpc from the Sun. The VMR is certainly a feature well worth of future study with southern millimeter telescopes.

This chapter will predominantly deal with the regions of low-mass star formation found in Puppis and Vela, mainly related to the Gum Nebula. I will not make any attempt to include the prolific field of major surveys made at a variety of wavelengths unless they are more or less restricted to the galactic longitudes under consideration here.

2. The Gum Nebula

The Gum Nebula is a large ~36° diameter shell structure of ionized gas covering most of the Puppis-Vela region. It was originally described by Gum (1952, 1955) who found it during the course of an HII-survey of the southern Milky Way. Its distance has been estimated to about 450 pc, based on *uvby* photometry of a number of B stars seen towards its central parts (Brandt et al., 1971). The nature and origin of the nebula is not clear; several models exist to explain it as a fossil Strömgren sphere, a supernova remnant, an evolved HII-region or a stellar wind bubble.

Associated with the Gum Nebula is a system of dark opaque clouds with bright rims and faintly luminous tails pointing away from the centre of the nebula. These clouds were named cometary globules (CG:s) and they lie more or less on an annulus with a radius of roughly 10° and with a centre offset ~4° south from that of the large nebula. 36 cometary globules have so far been reported in the Gum Nebula (Hawarden and Brand, 1976; Sandqvist, 1976; Reipurth, 1983; Zealey et al., 1983) and a model for their formation as the left-over dense

cores of larger clouds has been proposed by Reipurth (1983), in which the UV radiation field from energetic field stars (notably ζ Pup and γ^2 Vel) has evaporated the outer part of the clouds leaving the cores behind as Bok globules. The tails are explained as left over material in the "shadow" of the core together with material ablated from the core. Another scenario, where the blast-wave from a supernova explosion is responsible for the forming of cometary globules, has been suggested by Brand et al. (1983). In this model the blast-wave sweeps past a cloud-clump, generates internal shocks that collide and compress cloud material and generate a rarefaction wave that causes material to stream out in a tail.

Although no massive star formation is seen today in the Gum Nebula we still find a number of, mostly isolated, low-mass star forming events, associated both with cometary globules and with other dark clouds seen in this direction. Those that are likely to be associated with the Gum Nebula will be treated in this section.

2.1 Star formation in cometary globules

Low-mass star formation has been detected in or near the cometary globules CG1, CG13, CG22 and CG30/31. Several other globules have been searched for Hα-emission stars by Reipurth and Pettersson (1992) but with negative result. They include CG2, CG5-6, CG8−10 and CG14−18. Below is a summary of the cases where star formation has been detected:

2.1.1 CG1 and NX Pup

CG1 = DC255.8−9.2 (Hartley et al. 1986) is a fairly large cometary globule with a 2' diameter opaque head, an unusually broad bright rim and with a 25' long tail stretching away from the centre of the Gum Nebula. If we adopt the distance of 450 pc, this corresponds to linear dimensions of 0.3 pc and 3.2 pc respectively. Harju et al. (1990) have made a detailed study in molecular lines of CG1 and arrive at a total mass of 20 - 45 $M_\odot$. At the front edge of CG1 there is a star, NX Pup = CoD−44°3318 = CPD−44°1442 = Hen3-32 (Henize, 1976) = Bernes 135 (Bernes, 1977). This star has been extensively observed by e.g. Brand et al. (1983), Reipurth (1983) and Tjin A Djie et al. (1984). It also appears in the catalogue of Herbig Ae/Be stars by Finkenzeller and Mundt (1984). Brand et al. and Reipurth present spectroscopic and photometric data (UBV, *uvby*, JHKL) and Tjin A Djie et al. present IUE spectroscopy and photometry in the Walraven, Johnson UBV and Cousins VRI systems. From these observations it is obvious that NX Pup is variable, that it has a substantial infrared excess, and that its spectral type is A0-1 III as derived from IUE spectra (Tjin A Djie) to F0-2(III) as derived from optical spectra (Irvine 1975, Brand et al. 1983, Reipurth 1983). The discrepancy between the UV and the optical spectral types is explained by Tjin A Djie et al. as due to the G-band being formed in a circumstellar shell and not in the photosphere of the star. The UV classification is also supported by Finkenzeller (1985) who assigns the star a spectral type of A1e. The conclusion is then that NX Pup is a pre-main-sequence star of the Herbig Ae type (Herbig, 1960), lying on the evolutionary track of a 2.5 - 3 $M_\odot$ star and with an age in the interval $8 \cdot 10^5$ - $1.2 \cdot 10^6$ years.

2.1.2 CG13

CG13 = DC259.4−16.4 = Sa102 (Sandqvist, 1977) is a large diffuse globule with a rather inconspicuous tail and with an opaque core surrounded by an extended bright rim. It is associated with a nebulous star, Bernes 136, which is an F-star merely passing through the globule (Reipurth, 1983). Reipurth and Pettersson (1992) report the presence of a 15:th magnitude Hα-emission line star at the projected distance of 2 pc in front of CG13. The star, designated CG-Hα8, is of spectral type M1-2 and its spectrum shows strong Balmer emission lines. Reipurth and Pettersson propose that this star was formed in the outer envelope of a larger cloud that was the progenitor of CG13.

2.1.3 CG22 and WRA220

CG22 = DC253.6+2.9 is the largest of the cometary globules in the Gum Nebula. It has a 1.'5 by 2.'5 bright-rimmed opaque head and a long luminous tail, exceeding a degree in length corresponding to 8 pc at the proposed distance of 450 pc. A detailed investigation of the far infrared properties of CG22 can be found in Sahu et al. (1988). They show that the globule, besides the dense head, also have two condensations in the tail. One Hα-emission star, Wray 220 = PHα92 (Pettersson, 1987b), is seen projected on the head of the globule. Reipurth and Pettersson (1992) have performed UBV and JHKLM photometry and low-resolution spectroscopy of the star. It is clear that the star is varying in the IR with an amplitude of 0.4 magnitudes in the K-band. It also exhibits an infrared excess. The spectrum shows a K2 continuum and emission lines of Hα - Hγ and of the forbidden [OI]-lines at 6300 Å and 6363 Å. It seems likely that this is a T Tauri star that was formed in or close to the head of CG22.

2.1.4 CG30/31 and HH120

CG30/31 = DC253.0−1.7C is a fairly large complex of globules and dark clouds, cf. Fig. 1. It is comprised of the cometary globules CG30, CG31ABCDE, CG38 (Reipurth, 1983) and the dark clouds DC252.9−1.6 and DC253.1−1.7 (Pettersson, 1987a). CG30 contains the Herbig-Haro object HH120 = Re2 (Reipurth, 1981) seen towards the centre of the globule. Pettersson (1984) has made a detailed study of CG30 in the optical and near infrared. He found that the spectrum of HH120 belongs to the class of very low excitation (VLE) Herbig-Haro objects and that the HH spectrum is restricted to a bright knot in the western part of the object. The rest of the nebula was proposed to be scattered light from the hidden energy source. Scans of the globule at 2.2μm revealed 5 IR sources, at least two of which were background stars. Of the remaining sources two, CG30-IRS3 and 4, were close to HH120. CG30-IRS4, slightly south-east of the nebula was proposed as the star exciting HH120 and responsible for the reflection nebula. A spectrum of the reflection part of the nebulosity shows a prominent and red continuum. This is also evident in an IRAS low resolution spectrum of the source published by Cohen (1990). A red continuum is seen but without any obvious spectral features. JHKLM photometry of the infrared sources is also reported. Far infrared observations were made by Cohen et al. (1984) between 53μm and

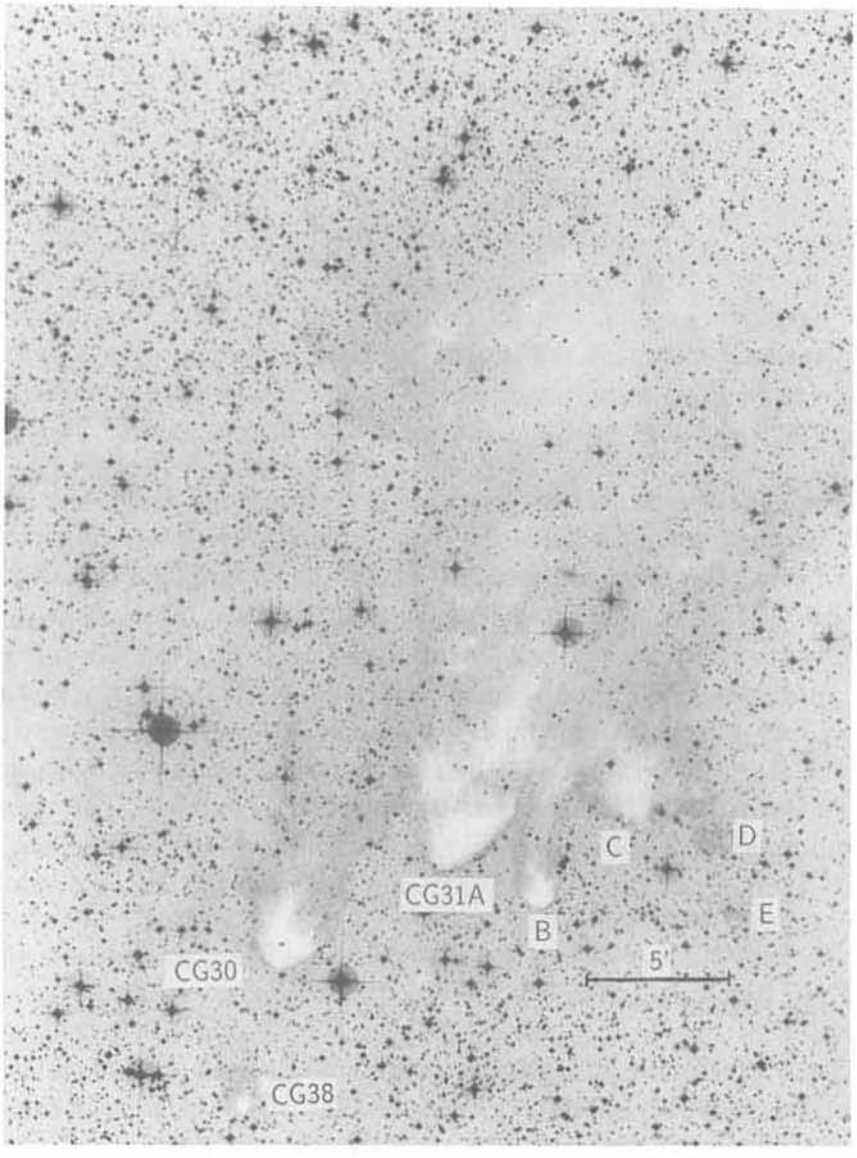

Figure 1. The Cometary Globules CG30, CG31A-E, and CG38 in the Gum Nebula. The Herbig-Haro object HH120 is seen towards the centre of the head of CG30 (lower left). This globule also contains a young star, CG30 IRS4, that excites HH120. North is up and east is to the left in the picture. Photograph reproduced from the SRC(J)-survey.

130μm. Graham and Heyer (1989) present JHKL photometry and use IR imaging to identify CG30-IRS4 in an image taken at 2.2μm with an IR array detector. The position agrees within the observational errors with the source found by Pettersson. The source is also listed in the IRAS Point Source Catalogue as IRAS 08076−3556 and these fluxes have been used to derive a bolometric luminosity of 17.8–18.6 $L_{\odot}$ for CG30-IRS4 (Berrilli et al., 1989; Cohen and Schwartz, 1987). Indications of mass outflow was found by de Vries et al. (1984) from observations in the ^{12}CO line. They also state a V_{LSR} of +5.2 km s^{-1} for the globule. Olberg

et al. (1991) have mapped the complex in ^{13}CO, and the region around CG30 IRS4 in ^{12}CO. Schwartz et al. (1987) and Wilking et al. (1990) report detection of H_2 1→0 S(1) emission from HH120, consistent with the view that H_2-emission is mainly found in low excitation HH objects. The reflection nebulosity has been further studied by Cohen et al. (1986) who obtained an optical spectrum of the "halo" surrounding the HH120 knot. They confirm the presence of a red continuum but not the stellar features reported by Pettersson. Scarrott et al. (1990) have studied the CG30 nebulosity with an imaging polarimeter. They confirm Pettersson's conclusion that the shocked emission is concentrated to the bright western knot and that the rest of the nebulosity is scattered light. Polarization maps are published that allow determination of the position of the illuminating source which is found to coincide with that of CG30-IRS4 and IRAS 08076−3556. It is suggested that the reflection nebula represents the walls of a cavity excavated by outflow activity from the embedded source.

Pettersson (1987a) has also reported the presence of 3 T Tauri stars in front of the CG30/31 complex, PHα12, 14 and 15. They are on the side facing the interior of the Gum Nebula at a projected mean distance of 0.6 pc in front of CG31C (PHα12) and CG31B (PHα14 and 15). It seems likely that these stars were formed during an earlier phase from material from the precursor cloud to CG30/31. An additional Hα-emitting star, SPH 37, has been found by Schwartz et al. (1990) about 5' NE of PHα15.

2.2 Star formation in other dark clouds

2.2.1 Sa101

Sa101 = DC259.2−13.2 is a rather large, diffuse cloud with a dense L-shaped core region. It is obviously associated with the nearby cometary globules CG4 and CG6. Reipurth and Pettersson (1992) have identified 7 Hα-emission line stars towards Sa101, CG-Hα1 - 7. CG-Hα2 - 6 are seen towards the opaque centre of the cloud, CG-Hα1 is about 30' to the south-west and CG-Hα7 is between Sa101 and the cometary globule CG4. Low-resolution spectra in the spectral range 4200 Å to 7100 Å are presented. All stars are found to be of late type (K2 - M4) and they all have prominent Hα-emission and, in some cases, also lines from [OI] at 6300 Å and 6363 Å. They are proposed to be likely candidates for T Tauri stars, due to their spectral appearance and their association with the dark material.

2.2.2 Sa109 with Re4 and Re5

In the dark cloud Sa109 = DC265.8−7.4 Reipurth found two nebulous objects, Re4 and Re5, that were included in his list of small nebulae and Herbig-Haro objects (Reipurth, 1981). Both objects are lying in dust concentrations in the large Sa109. Graham (1986) has presented extensive observations of Re4 and 5, both spectroscopy, infrared photometry and deep imagery, that are summarized below. A deep CCD image revealed that Re4 is made up of two parts, a bright Re4 *head* close to a 15:th magnitude K5V (foreground-) star and a fainter extended *tail* extending about 1' towards the south. Re5 is described as a faint cometlike structure approximately 6' to the south of Re4 *head*. On a deep CCD-image

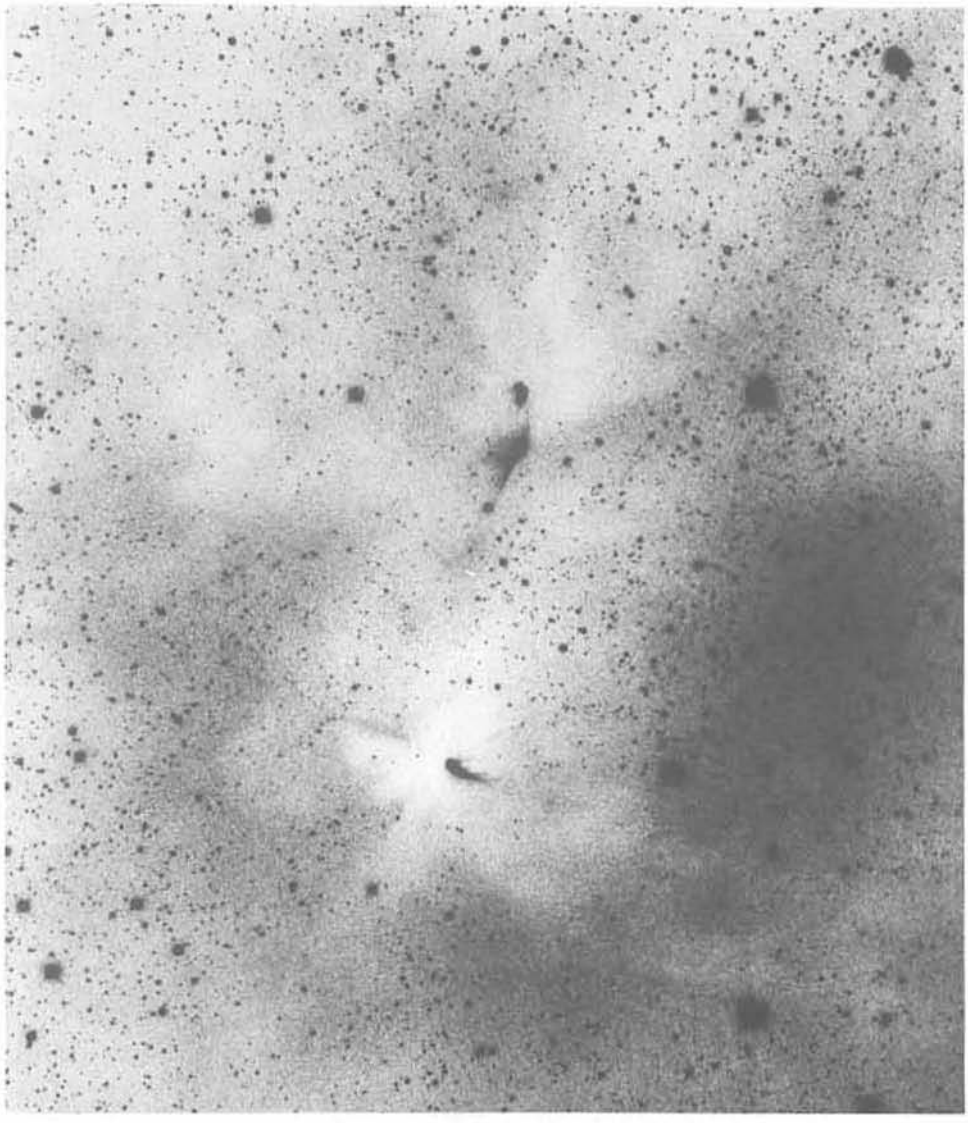

Figure 2. The field of Sa 109. The Re4 nebula with the comma-shaped *head* and the *tail* is just north of center and the Re5 nebula to the south. The photograph was taken with the CTIO 4m telescope prime focus camera, on IIIa-F emulsion through an OG570 filter. Reproduced from Graham (1986).

a second, fainter, comet-shaped nebula is seen opposite to Re5. Spectroscopy showed that Re4 *head* has a Herbig-Haro type spectrum belonging to the VLE-class of spectra, superposed on a very red continuum showing the NaI D-lines in absorption. Close to Re4 *head*, two small clumps are seen, probably also Herbig-Haro objects. The spectrum of Re5 shows no emission lines and was proposed to be a scattered continuum from a hidden G-type star that might be the source of the object. JHKL photometry around Re4 *head* and the K5 star revealed an infrared source ~5" west of the star. This source, Re4 star, is within 2" of the IRAS point source 08194−4925 and it appears as Re4 FIR in the tables of Cohen and

Schwartz (1987). Also Re5 is associated with an IRAS source (IRAS 08196−4931). The IRAS sources are probably corresponding to the hidden energy sources.

Cohen and Schwartz (1987) and Berrilli et al. (1989) have used flux values from IRAS to estimate the bolometric luminosity of Re4 star to 28.6 and 26.7 $L_\odot$, respectively. In a recent paper by Graham and Heyer (1989) 2.2μm images and near infrared photometry of the exciting sources in both Re4 and Re5 are presented.

Obviously star formation is taking place at two nearby sites in Sa109. There is also some indication of previous star formation from the presence of an 18:th magnitude star with a small gaseous appendage (jet?) found to the NE of Re5 (Graham, 1986). The star is classified as an M3.5e dwarf (Graham and Heyer, 1989), lying close to the main sequence. Wilking et al. (1990) report detection of the 1→0 S(1) transition of H_2 towards this object.

2.2.3 Sa 111 and HH46/47

Sa111 = DC267.4−7.5 = ESO 210-6A is a dense, 3' diameter, globule near two other small dark clouds, Sa110 and Sa112. Morphologically it is related to the CG:s with a sharp and bright rim directed towards the centre of the Gum Nebula, but although the cloud is elongated and ill defined towards the other end, there is no evidence for a luminous tail (Reipurth, 1983). It is probably located in the Gum Nebula as it is seen in projection against the nebulosity. Bok (1978) first estimated its mass to 25 $M_\odot$ from its visual absorption, A_V=20. Later Emerson et al. (1984) gave a mass of 7−15 $M_\odot$ based on H_2CO observations by Goss et al. (1980), and Sahu et al. (1989) proposed a mass of at least 8 $M_\odot$ from observations in the far infrared.

Schwartz found two Herbig-Haro objects, HH46 and HH47 (later renamed to HH47A), near the northern edge of the cloud, connected by a filamentary and knotty bridge, HH47B (Dopita et al., 1982b). Two faint arclike structures appear on both sides of HH47A and HH46, namely HH47C to the south-west of HH46 and HH47D to the north-east of HH47A (Dopita et al., 1982b), cf. Fig. 3. HH46/47 is a beautiful example of a tightly collimated Herbig-Haro jet, and they and the globule have been the subject of a large number of studies covering a variety of subjects. The observations support a scenario in which HH46 and HH47A, B and D constitute the approaching part of a bipolar flow, driven by a hidden source in the globule, and where HH47C is part of a receding, partly obscured, counterflow. Recently the discovery of a faint "counter jet" between HH46 and HH47C, about 15" to the SW of HH46, has been reported by Reipurth (1989) and Reipurth and Heathcote (1991).

Radial velocity measurements (Dopita et al., 1982b, Graham and Elias, 1983, Meaburn and Dyson, 1987, Graham and Heyer, 1989, Hartigan et al., 1990, Reipurth and Heathcote, 1991) show that the brighter parts, HH46, HH47A and B are approaching with heliocentric velocities, V_{HEL}, in the range −100 to −190 km s^{-1} and that the "counter jet" and the knots in HH47C move away from us with $V_{HEL} \simeq +100$ km s^{-1}. A model for explaining the observed velocity structure as interaction between a stellar jet and its surrounding is presented by Meaburn and Dyson (1987). Schwartz et al. (1984) have obtained proper

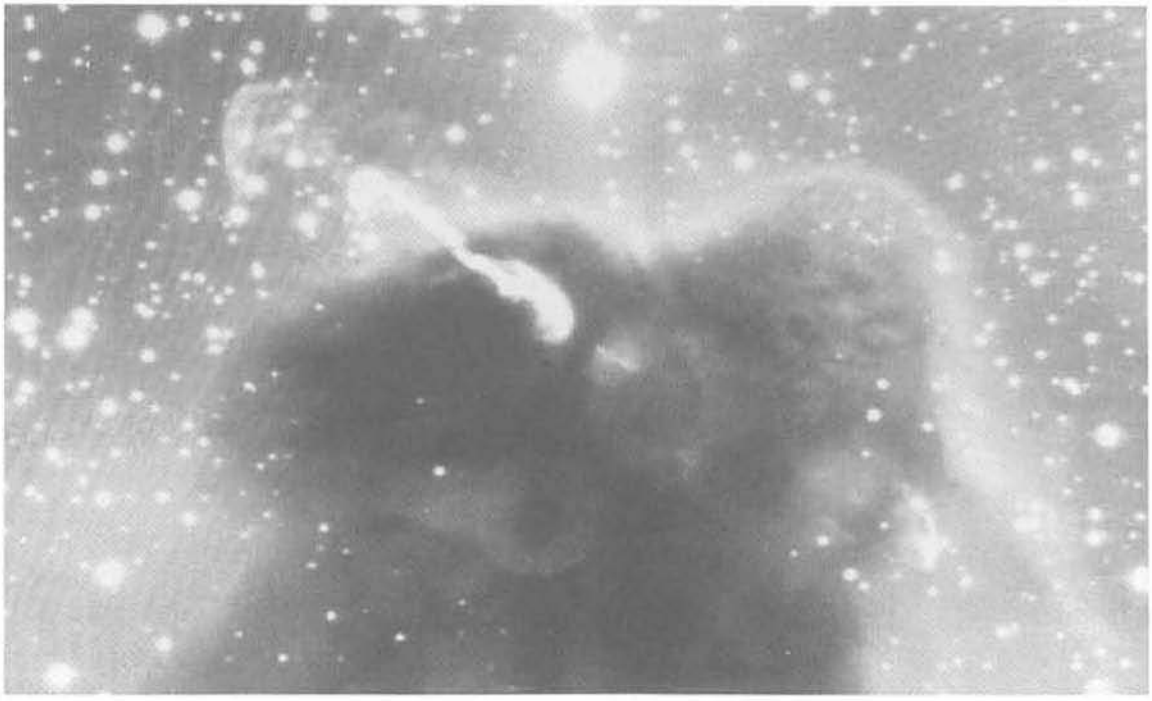

Figure 3. A wide-field Hα + [SII] CCD image of the HH46/47 jet-complex in the Bok globule ESO 210−6A. The infrared source is located behind the dark ridge at the base of the jet. Reproduced from Reipurth and Heathcote (1991).

motion data for a number of condensations in HH46/47. They conclude the existence of a collimated flow that is inclined about 27° to the plane of the sky, and derive an age of 2000 years for the condensations in HH47A and C.

Spectrophotometry by Dopita (1978) showed that HH47A has a spectrum of the low-excitation type, while the central part of HH46 exhibits a red continuum with a strong Hα-emission line. He suggested that the continuum is the reflected spectrum of the embedded stellar energy source, possibly of T Tau type. Cohen et al. (1986) confirm the presence of a scattered T Tauri like continuum from an optical spectrum of HH46A. They also report a diminishing in brightness from the 1977 observation of Dopita by a factor of 16. On the other hand Graham (1987) reports an increase in the surface brightness of the HH46 reflection nebula by a factor 7–10 over the period Jan 1984 to May 1986 and it seems obvious that the exciting source is highly variable. Raga and Mateo (1987) have observed HH47A/B and HH46 using narrow-band imaging in [SII] 6717+6731 Å and Hα. They conclude that HH47A has the highest electron density as determined from the [SII] 6731/6717 line ratio and at the same time have the lowest excitation, whereas HH47B, in the filamentary and knotty bridge, and HH46 have lower density but a higher degree of excitation. Very high resolution CCD images obtained at the ESO New Technology Telescope show a wealth of structural details in the jet-system and a complex distribution of excitation conditions (Reipurth and Heathcote, 1991).

Both HH46 (Elias 1980) and HH47A (Wilking et al. 1990) have been detected in the emission lines of shocked H_2, especially in the 1→0 S(1) transition at 2.1μm.

Schwartz (1983) obtained an ultraviolet spectrum of HH47, where he found emission lines attributed to H_2 produced by fluorescence from the Lyα line, and a continuum, peaking around 1500 Å. This peak could be caused by the presence of two-photon emission as already suggested by Dopita et al. (1982a) from optical spectrophotometry. Krautter et al. (1984) have observed the UV spectrum of HH46 and report a faint, featureless continuum increasing towards shorter wavelengths, and the possible presence of OI emission at 1305 Å.

The role played by magnetic fields in Sa111 have been discussed by Hodapp (1987) and Glencross et al. (1989).

The embedded exciting source has been located by Cohen et al. (1984) who observed HH46/47 at 10μm from the ground and at 40–160μm with the Kuiper Airborne Observatory. They found a faint 10μm source, HH46IRS, ~0.'2 south-west of HH46 and proposed that it is the exciting source. Emerson et al. (1984) also independently located the source by identifying it with the IRAS source IRAS 08242−5050. Graham and Heyer (1989) have detected HH46IRS at 2.2μm using an infrared imaging array. They were able to obtain two optical spectra of the scattered light from the hidden star and find a late G – early K continuum with numerous emission lines, typical of a T Tauri star spectrum. They also report JHKL photometry of the star. Reipurth and Heathcote (1991) have confirmed the T Tauri character of the central object. They have observed the HH46 reflection nebula spectroscopically at both low and high resolution and report a rich T Tauri emission line spectrum. Optical linear polarization maps of the region around HH46 have been presented by Scarrott and Warren-Smith (1988). From these they find a position for the illuminating source that coincides with HH46IRS. Kuiper et al. (1987) have detected ammonia emission that they attributed to a circumstellar toroid or disc with a size of 6000–7500 AU and a mass of 0.09–0.14 $M_\odot$. The bolometric luminosity for the object is given as 23.6 $L_\odot$ (Berrilli et al., 1989) to 24.2 $L_\odot$ (Cohen and Schwartz, 1987).

Olberg et al. (1992) present a complete ^{13}CO map of the globule and have found a bipolar molecular outflow around the infrared source.

Three stars near Sa111, illuminating reflection nebulosity, have been discussed by Herbst (1977). They are vBH12a (B7V), 12b and 16 (van den Bergh and Herbst, 1975). From UBV-photometry Herbst arrives at a mean distance of 400 pc for these stars and conclude that they belong to the same part of the Gum Nebula as Sa111 and, probably, Sa109. He also presents UBVRI photometry of vBH16 and of two anonymous Hα-emission stars, (1977) close to Sa111. vBH16 is particularly interesting in that it illuminates the cloud Sa112 next to Sa111. Reipurth and Zinnecker (1992) report it to be a T Tauri binary, and they find yet another T Tauri binary a few arcminutes north of vBH16, also in Sa112.

2.2.4 DC253.6−1.3 and DC253.9−0.6

Pettersson (1987a) reports the finding of 9 T Tauri stars from an Hα objective prism survey in Puppis (Pettersson, 1987b). Three of the stars, in front of the CG30/31 complex, are discussed in Sect. 2.1.4. Of the remaining six, PHα21 and 34 are seen projected towards DC253.6−1.3 and PHα40, 41, 44 and 51 towards DC253.9−0.6, a chain of small patchy clouds seen towards the background HII-region RCW19 (Rodgers et al., 1960). Low-resolution spectroscopy, UBVRI and JHK photometry is presented. Also seen towards DC253.6−1.3 is PHα27A, found in the objective prism survey but not yet observed with a slit spectrograph. The distance of this group of T Tauri stars is given to 450 pc, i.e. the associated clouds are inside the Gum Nebula.

2.2.5 WRA218

This star was originally noted by Wray (1966) who gave it number 218 in his catalogue and it reappeared in the Hα survey of Pettersson (1987b) as PHα91. It is situated about 1° south of the cometary globule CG22. A low resolution slit spectrum of WRA218, kindly obtained for the author by Dr. Thé, shows a late type continuum of approximately spectral type K2 superposed by strong Balmer line emission (Hα– Hδ), CaII H and K and numerous fainter lines from FeII and HeI. Near infrared JHK photometry indicates the presence of an infrared excess. Despite the fact that no dark matter is visible in the immediate neighbourhood it is proposed that WRA218 is a T Tauri star and that it is likely to be a part of the isolated star forming events taking place in the Gum Nebula.

3. Other Star Forming Events

3.1 RCW27, 32 and 33

The three HII-regions RCW27, 32 and 33 constitute a striking configuration in the longitude interval 259° – 264° along the galactic plane. RCW27 is the largest of the three with an apparent diameter of ∼2°, RCW32 the smallest with a diameter of 25' and RCW33 has a diameter of ∼1°.5. Across all of the bright surfaces an irregular pattern of dark, obscuring matter can be traced out, most obviously across the SE part of RCW27. This instigated the undertaking of an Hα objective prism survey to look for likely candidates for any recent star formation that might have taken place in the dark clouds (Pettersson and Reipurth, 1992). In all, 278 Hα-emission-line stars were found in a 5° by 5° field centered ∼1° south of field 313 of the ESO/SRC survey. Of these, almost half are seen projected against RCW27, 21 against RCW32 and 69 are seen against the background of RCW33. The survey reaches a V-magnitude of ∼20.

3.1.1 RCW27 and Vela T1

Pettersson and Reipurth (1992) have surveyed the region around the large HII-region RCW27 and the dark cloud complexes seen projected against it for Hα-emission line stars. About

120 Hα-emitting stars have so far been found, many seemingly related to the region of the dark clouds. Of the 22 brightest stars that have since been observed with a slit spectrograph, 15 were found to be of late type with prominent Balmer line emission and, in many cases, with other lines typical for T Tauri stars, they are presented in Table 1. It seems likely that we are observing a new T association towards RCW27 which the authors name Vela T1. The distance to the dark clouds and Vela T1 remains an open question. Looking at the deep red image of RCW27 reproduced in Fig. 4, one gets the impression that we see two different sets of clouds, one in the foreground comprised of the very dark and irregular DC260.2+0.7, DC260.4+0.4C = SL1 (Sandqvist and Lindroos, 1976), DC260.6+0.8 and DC260.8+0.2, and one set of more diffuse clouds that may be connected with RCW27. This impression is enhanced by the lower star density seen towards the DC-clouds as compared to the star density towards other clouds and towards RCW27 itself. If this is really the case, we may also see two layers of emission-line stars and, possibly, two associations.

In the field are also stars belonging to the Pup R2 association (Herbst, 1975a), vBH17a and b, vBH18 and vBH20. Herbst has estimated the distance to Pup R2 to 950 pc and, if Vela T1 and Pup R2 are associated, then Vela T1 is on the far side of the Gum Nebula. Georgelin and Georgelin (1970) have given a distance of 1100 pc to HD 73882, an O8 star exciting the HII-region, which could mean that RCW27 and Pup R2 are associated.

Recently, Ogura (1990) reported a new Herbig-Haro object close to vBH17a, HH132, detected on narrow-band CCD-frames. HH132 is in a region with both emission nebulosity (NGC2626, illuminated by vBH17a) and a small compact dark cloud. Pettersson and Reipurth also report a number of faint Hα-emission-line stars in this region.

It is interesting to note that the first strong emission peak in the Vela Molecular Ridge (region D in Murphy and May, 1991), at l=260° and b=0°, coincides with RCW27. This could mean that we see low mass star formation in a cloud in the near end of a "molecular arm" in Vela.

3.1.2 RCW32 and RCW33

RCW32 and 33 are also sites of Hα-emission line stars found during the same survey by Pettersson and Reipurth that was described in Sect. 3.1.1. Towards the bright RCW32 21 Hα-stars were found and in the region of RCW33 another 69. Only two slit spectra are available from these regions (cf. Table 1) but it is very likely that there are more young stellar objects towards these HII-regions. The southern half of RCW33 is partly obscured by a lane of dark matter, the dark cloud SL4. In this cloud Pettersson and Reipurth (1992) discuss a small reflection nebulosity at $\alpha_{1950.0}$: $8^h51^m19\overset{s}{.}1$ and $\delta_{1950.0}$: $-42°01'36''$. The nebulosity is associated with the strong IRAS source 08513-4201 that is likely to be an embedded young star. Its positions in the IRAS colour-colour diagrams indicate that it is an object of the "core"-type, i.e. a deeply embedded young source.

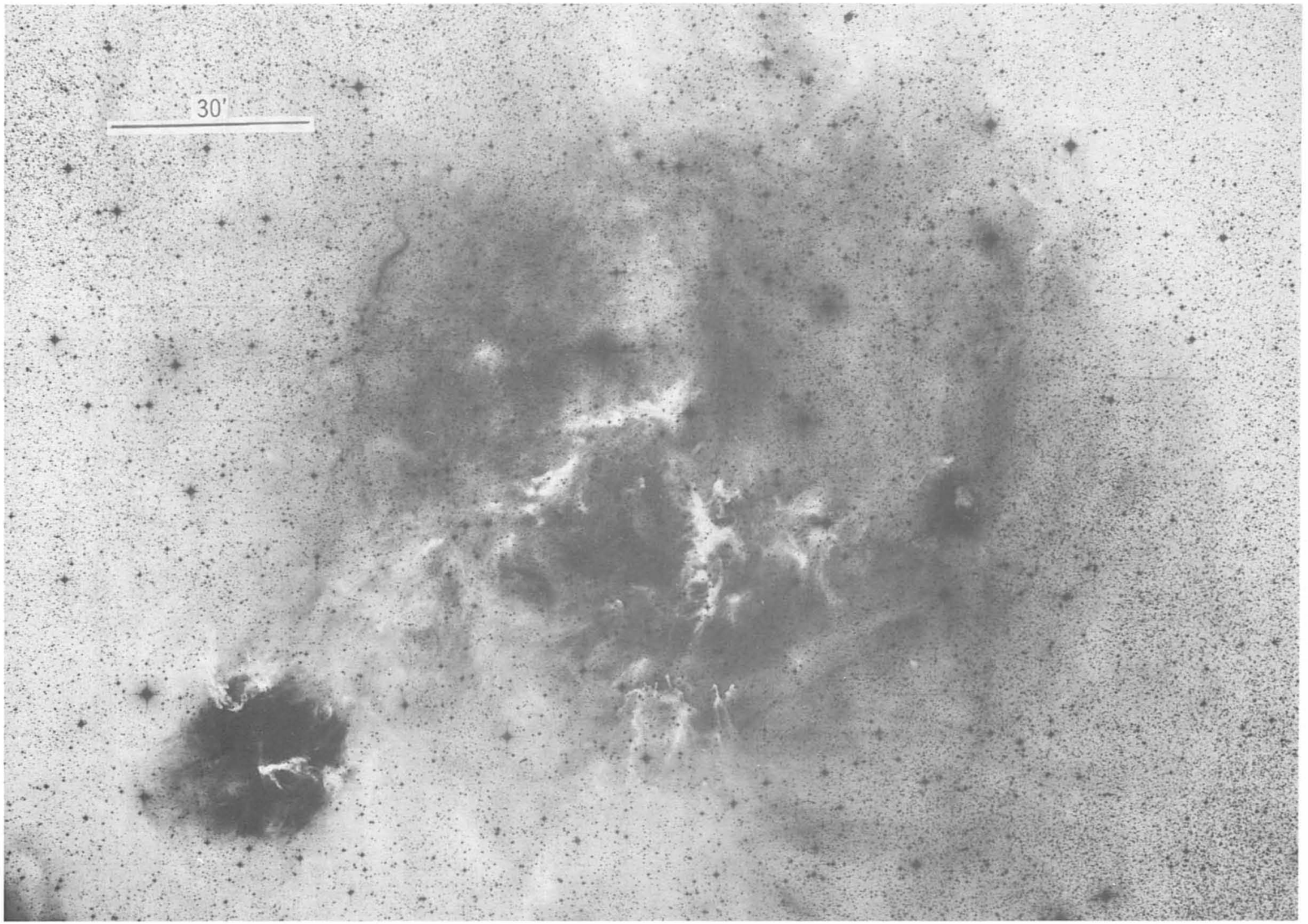

Figure 4. The region of the HII-regions RCW27 (centre) and RCW32 (lower left). Towards RCW27 is the new T Tauri association Vela T1 and the dark clouds DC260.2+0.7, DC260.4+0.4C (SL1), DC260.6+0.8 and DC260.8+0.2. The cloud seen towards the centre of RCW32 is DC263.2+1.6 (SL2). North is up and east is to the left. A photograph from the ESO Schmidt telescope, obtained in red light.

3.2 IC2391

IC2391 is a fairly loose and large young open cluster in Vela at l = 270° and b = −7°. Its brightest member is the 4^m star *o* Vel and its age is estimated to $3 \cdot 10^7$ years, based on its upper main-sequence turn-off (Mermilliod, 1981). The distance to IC2391 is of the order of 150 pc. From spectroscopic and photometric observations of 40 stars, Stauffer et al. (1989) have identified 8 new late-type (K) pre-main-sequence stars that they suggest to be members of the cluster. When plotted in a colour-magnitude diagram the stars fall above the cluster ZAMS, approximately along an isochrone for $3 \cdot 10^7$ years. Five of the stars show Hα in emission and six have strong LiI 6707 Å absorption. Both stars without visible Li absorption are rapid rotators, something that could explain why the line is not detected.

3.3 HH73/74

Reipurth and Graham (1988) report the discovery, from narrow-band imaging (Hα, [SII] 6717+6731 Å and continuum at 6650 Å), of two Herbig-Haro objects, HH73 and 74, close to the arc-shaped nebula Re6 (Reipurth, 1981) in the dark cloud DC266.1+1.1. Re6 is a reflection nebula surrounding a faint red binary star. HH73 is a highly collimated chain of faint HH knots with a total extent of 29" and situated about 1' south of Re6. No energy source is seen but should be found somewhere along the axis of the chain.

About 20" north of Re6 is HH74, seen as an isolated almost stellar-like object. Also here no energy source was found by Reipurth and Graham, but it could be the same source that is responsible for the nearby Re6 reflection nebula. Cohen (1990) reports the discovery from coadded IRAS images of a point-like red source situated about 1.'0 west of HH74. It was detected at 25, 60 and 100μm and a bolometric luminosity of 5.57 $L_\odot$ is given, assuming a distance of 450pc. Nothing was found near Re6 or at HH73.

3.4 The Herbig-Haro objects in Sa114

The dark cloud Sa114 is a small, irregular cloud seen in the direction of the Gum Nebula. It is associated with three nebulous stars, vBH29a, b and c (van den Bergh and Herbst, 1975) belonging to the Vela R2 association (Herbst, 1975b). A distance of 870 ±80 pc is given by Herbst for these stars. Reipurth and Graham (1988) report a chain of patchy Herbig-Haro objects, HH75, near the south-east edge of Sa114. They present narrow-band images and a low-resolution spectrum. No obvious energy source was found although there are some nearby IRAS sources (IRAS 09099−4526 and IRAS 09098−4535). The region of HH75 has been searched for possible energy sources by Cohen (1990), using coadded IRAS images. No obvious source was detected, the one most plausible according to Cohen was IRAS 09094−4522 situated 8.'2 from the center of the HH complex. This IRAS source is coincident with vBH29b and it is fairly well aligned with the HH chain. The bolometric luminosity is given as 130 $L_\odot$ for a distance of 450 pc. Cohen also gives a plot the spectrum of IRAS 09094-4522 from the IRAS low resolution spectrograph.

About 14'northwest of HH75 Ogura (1990) has found another Herbig-Haro object, HH133, using the same narrow-band technique as Reipurth and Graham. HH133 is composed of 3 or 4 small knots connected by faint wisps of nebulosity and is located near the western border of Sa114.

3.5 BBW76 – a southern FUOR

BBW76 (Brand et al. 1986) is a small arc-shaped nebula situated in the constellation of Puppis at $\alpha_{1950.0}$: $7^h48^m40\overset{s}{.}4$ and $\delta_{1950.0}$: $-32°58'43''$. Associated with the nebula is a 12:th magnitude star that has been identified by Reipurth (1985, 1990) and by Eislöffel et al. (1990) as a FU Orionis object. For convenience, the star is also referred to as BBW76. The arguments for identifying BBW76 as a FUOR are mostly based on spectral information. The spectral appearance of BBW76 both at low and at high resolution strongly suggest that the object is a FUOR. A low resolution spectrum shows a strong LiI 6707 Å absorption line and an over-all appearance very similar to that of FU Ori itself. High resolution spectra of the sodium D-lines at 5889/5996 Å and the Balmer Hα and Hβ lines show very broad absorption troughs, up to 200 km s^{-1} wide, with structures indicating temporal changes in the winds causing them. A slow decrease of the brightness both at visual and at near infrared wavelengths is also reported by Reipurth (1990); the V-magnitude is decreasing at a yearly rate of $0\overset{m}{.}025$.

The object has been associated with the IRAS source 07426−3258 by Eislöffel et al. and they estimate a total flux for BBW76 of 550 $L_\odot$, assuming a distance of 1700pc as deduced from the associated CO line emission (Brand et al. 1987). This luminosity is typical for FUOR:s, that of FU Ori being 340 $L_\odot$.

3.6 IRAS 08211−4158

The area around the IRAS point source 08211−4158 was searched for near infrared sources by Persson and Campbell (1988). They found two point sources close to the IRAS source and present JHK photometry of them and a red CCD image of the region surrounding the sources. They also give the spectral energy distribution of the objects.

Graham (1991) reports the finding of a Herbig-Haro object close to the IRAS source. It consists of a bright and a faint part at a distance of 1' southeast of the near IR sources of Persson and Campbell. Spectroscopy of low and intermediate resolution is presented both of the HH object and of a diffuse nebula close to the IR sources. The HH object belongs to the class of low-excitation objects and show strong [SII] lines at 6717+6731 Å. A mean heliocentric radial velocity of −21 km s^{-1} is given, based on several lines.

The energy source is identified with the IRAS point source and with source 1 of the Persson and Campbell near IR sources. The spectrum of the diffuse nebula near the sources shows a red featureless continuum with a strong Hα-emission line and fainter lines from the IR CaII triplet and OI at 8447Å. From the near IR and the IRAS fluxes Graham estimates

the luminosity of the source to be 160 $L_{\odot}$, assuming that the object is associated with the Gum Nebula. This is, however, not conclusively shown to be the case.

3.7 The R Associations

Within the area covered by this chapter are 6 of the southern R associations, i.e. associations of stars embedded in reflection nebulosity, as defined by Herbst (1975a) — Puppis R1, R2 and R3 and Vela R1, R2 and R3. Two of the associations have already been the subject of some discussion, Puppis R2 (Sect. 3.1.1) possibly associated with Vela T1, and Vela R2 (Sect. 3.4). As for the others they appear, at least from what we currently know, to be mostly associated with the high mass end of star formation inasmuch as they mostly seem to be made up from B and A stars. However this may partly be a selection effect, deep Hα-objective prism surveys have shown that when the low end of the luminosity function can be reached, the low mass stars may indeed be there. One example is the case of Vela R2, where Pettersson and Reipurth (1992) have found 16 faint Hα-emission line stars in the region of vBH25b, 27a, 27b and 28. It seems very likely that they constitute the low mass component of the same generation of stars making up (the NW parts of) Vela R2. One of the stars in Vela R2, vBH25a, has been the subject of some controversy over the years as it was lying well below the ZAMS in the association HR-diagram (Herbst, 1977) but according to Heydari-Malayeri (1988) this discrepancy is resolved since vbH25a, and the small HII region RCW34 which it excites, is not a member of the R association but is a distant background object seen through Vela R2.

One other object that also is likely to be associated with high mass star formation is ESO 313−N*10 (Lauberts, 1982). It is associated with an IRAS point source, IRAS 08404−4033. This compact cluster of two fairly bright and a number of fainter objects, associated with a nebulosity, was described by West (1980) as either a distant Trapezium system or a system of Herbig Ae/Be stars. Pettersson and Reipurth (1992) detected the two brightest stars in their Hα-survey. They have been observed by them both spectroscopically and photometrically in the UBV system. They find that the stars, ESO-Hα161 and 162, are of spectral type intermediate B and early A respectively, with prominent Balmer emission. Both stars are heavily reddened according to the observed continuum slope and to the UBV-photometry. This seems to favour the interpretation that they may be Herbig Ae/Be stars, however more observations are needed, particularly in the infrared.

4. Discussion and Summary

This chapter has dealt with the low-mass star formation in Puppis and Vela as it was known to the author up to October 1991. Tab. 1 summarizes the known and suspected low mass pre-main sequence objects in the region, Tab. 2 lists the Herbig-Haro objects, and, finally, in Tab. 3 the known deeply embedded young stars are given. Fig. 5 shows the contours of the Gum Nebula taken from the RCW-atlas together with a plot of the young stellar objects

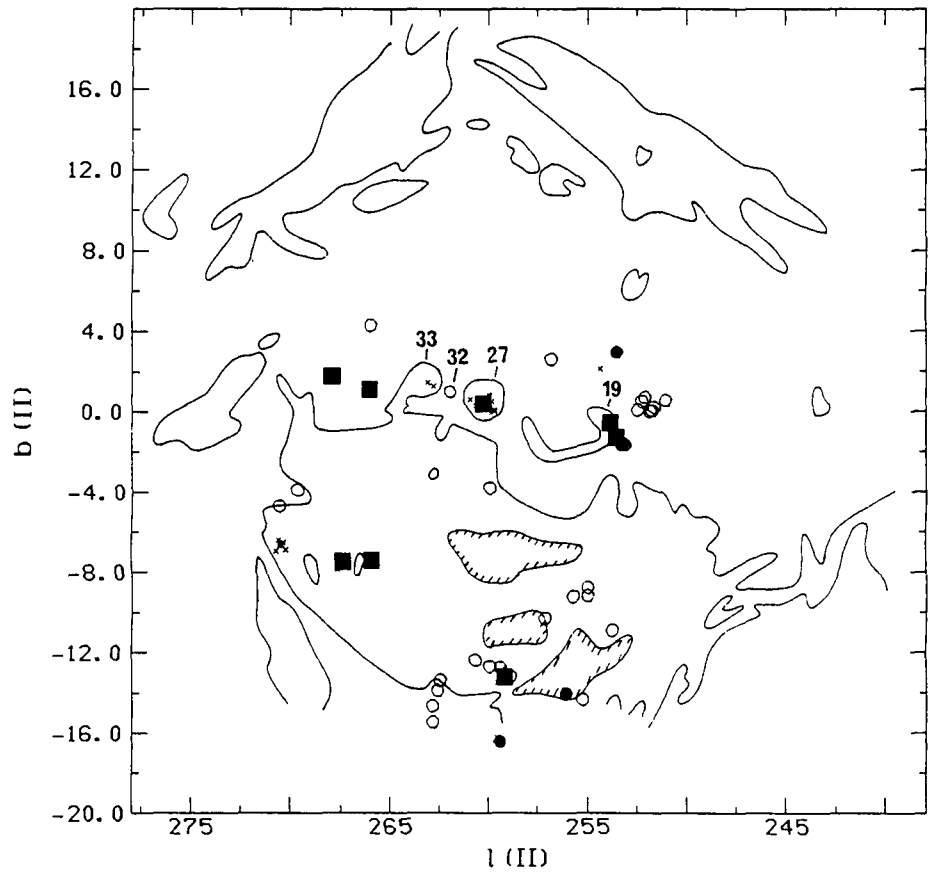

Figure 5. The full lines are contours of the Gum Nebula adapted from *An Atlas of H-alpha Emission in the Southern Milky Way* (Rodgers et al., 1960) and "×" signify young stellar objects (YSO:s) from Table 1. All of the cometary globules are plotted and indicated by circles and other dark clouds by squares. Filled symbols indicate clouds associated with low-mass star formation. The HII-regions mentioned in the text are shown by their RCW-numbers.

(YSO:s) from Tables 1 and 2, and their associated clouds. Fig. 6 shows the same YSO:s and clouds as in Fig. 5, but on a larger scale. The clouds discussed in the text in connection with star formation are identified.

It is obvious that formation of low-mass stars is going on within the Gum Nebula, particularly along the same annulus as that defined by the system of cometary globules, and also in more distant regions along the Milky Way band, as e.g. the Vela T1 association seen towards RCW27. The presence of the giant molecular clouds represented by the Vela Molecular Ridge is of particular interest here. It seems obvious that there is a connection between the western part of the VMR (region D) and the large complex of Hα-emission line stars in Vela T1. A more extended search for YSO candidates along the VMR will probably be rewarding.

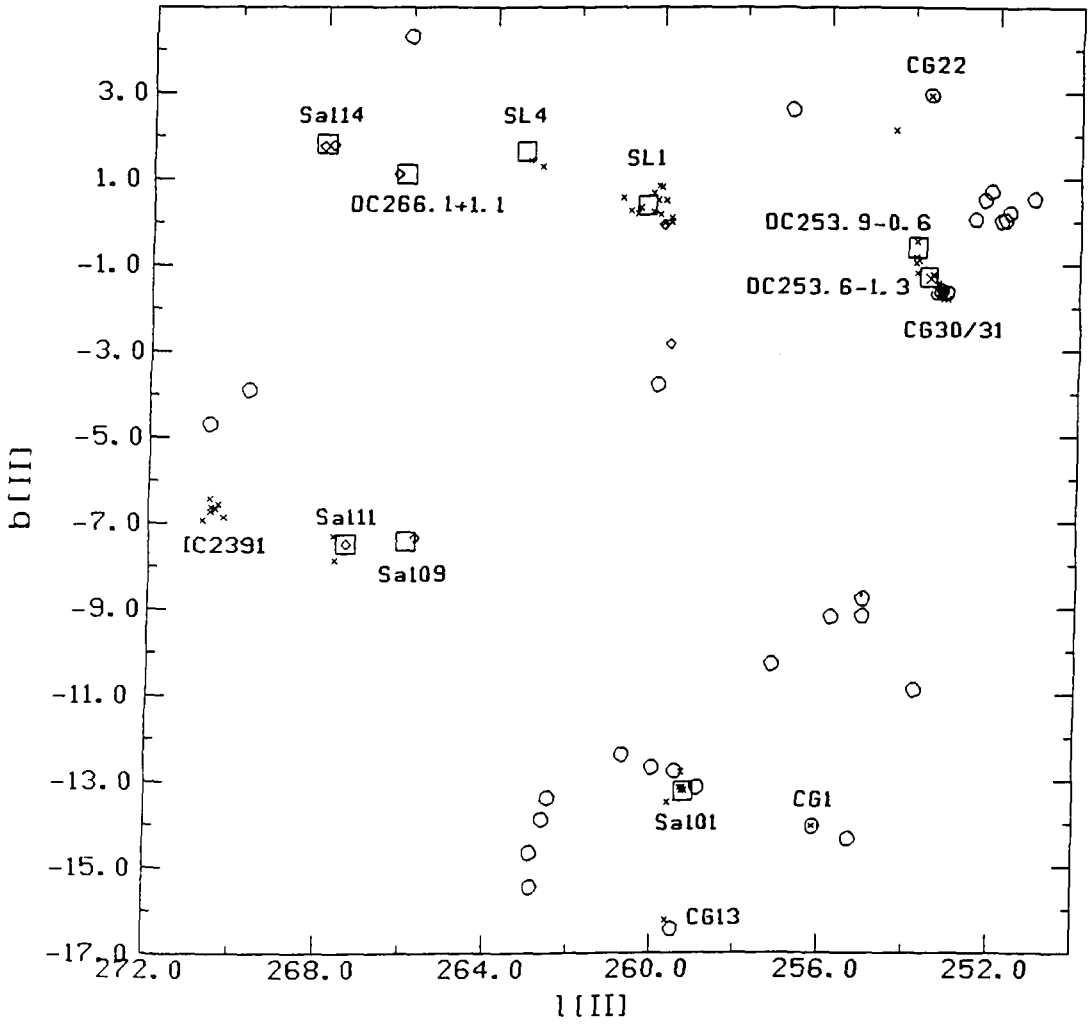

Figure 6. The same YSO:s and clouds as in Fig. 5, but on a larger scale and with the Herbig-Haro-objects from Table 2 added (diamonds). Symbols are the same as in Fig. 5, except that clouds associated with star formation are identified instead of shown with filled symbols. The position of WRA218 is indicated by a "×" at l = 254° and b = +2°. The two "×":s at l = 263° and b = +1° are two T Tauri stars seen towards RCW33.

In several cases we see what apparently is the formation of isolated low-mass stars both in the CG:s themselves, e.g. in CG1, CG30 and in other clouds such as Sa109 and Sa111. One case of an isolated T Tauri star with no obvious associated dark cloud, WRA218, has also been found, its position is indicated in Fig. 6 by a "×" at l = 254° and b = +2°.

From Fig. 5 it can be seen that all the known star forming regions in the Gum Nebula are located in its south-western parts, approximately following the outline of a large, bright HII-emission complex, while nothing has been found towards the northern parts with the

large arc structures. This may be a selection effect since not much observational work is available towards these regions. A systematic search for YSO:s at positive galactic latitudes larger than b = +4° could help in clarifying the situation.

One class of observations that is badly needed for the understanding of what is going on in the dark clouds is detailed radio observations in the mm wavelength range. No doubt the Swedish ESO Submillimeter Telescope, SEST, is going to make many important contributions in the near future.

References

van den Bergh, S. and Herbst, W.: 1975, *AJ* **80**, 208

Bernes, C.: 1977, *A&AS* **29**, 65

Berrilli, F., Ceccarelli, C., Liseau, R.,Lorenzetti, D., Saraceno, P. and Spinoglio, L.: 1989, *MNRAS* **237**, 1

Bok, B.J.: 1978, *PASP* **90**, 489

Brand, J., Blitz, L. and Wouterloot, J.G.A.: 1986, *A&AS* **65**, 537

Brand, J., Blitz, L., Wouterloot, J.G.A., and Kerr, F.J.: 1987, *A&AS* **68**, 1

Brand, P.W.J.L, Hawarden, T.G., Longmore, A.J., Williams, P.M., Caldwell, J.A.R.: 1983, *MNRAS* **203**, 215

Brandt, J.C., Stecher, T.P., Crawford, D.L., Maran, S.P.: 1971 *ApJ* **163**, L99

Chanot, A. and Sivan, J.P.: 1983, *A&A* **121**, 19

Cohen, M.: 1990, *ApJ* **354**, 701

Cohen, M. and Schwartz, R.D.: 1987, *ApJ* **316**, 311

Cohen, M., Dopita, M.A. and Schwartz, R.D.: 1986, *ApJ* **307**, L21

Cohen, M., Schwartz, R.D., Harvey, P.M. and Wilking, B.A.: 1984, *ApJ* **281**, 250

Dopita, M.A., Binette, L. and Schwartz, R.D.: 1982a, *ApJ* **261**, 183

Dopita, M.A., Schwartz, R.D. and Evans, I.: 1982b, *ApJ* **263**, L73

Dopita, M.A.: 1978, *A&A* **63**, 237

Eislöffel, J., Hessman, F.V. and Mundt, R.: 1990, *A&A* **232**, 70

Elias, J.H.: 1980, *ApJ* **241**, 728

Emerson, J.P., Harris, S., Jennings, R.E., Beichman, C.A., Baud, B., Beintema, B.A.,

Marsden, P.L and Wesselius, P.R.: 1984 *ApJ* **278**, L49

Finkenzeller, U. and Mundt, R.: 1984, *A&AS* **55**, 109

Finkenzeller, U.: 1985, *A&A* **151**, 340

Georgelin, Y.P. and Georgelin, Y.M.: 1970 *A&A* **6**, 349

Glencross, W.M., Cameron, D.H.M., Lightfoot, J.F. and Whitmore, B.: 1989, *MNRAS* **238**, 639

Goss, W.M., Manchester, R.N., Brooks, J.W., Sinclair, M.W. and Manefield, G.A.: 1980, *MNRAS* **191**, 533

Graham, J.A.: 1986, *ApJ* **302**, 352

Graham, J.A.: 1987, *PASP* **99**, 1174

Graham, J.A.: 1991, *PASP* **103**, 79

Graham, J.A. and Elias, J.H.: 1983, *ApJ* **272**, 615

Graham, J.A. and Heyer, M.H.: 1989, *PASP* **101**, 573

Gum, C.S.: 1952, *Observatory* **72**, 151

Gum, C.S.: 1955, *Mem. R. Astron. Soc. Can.* **67**, 155

Harju, T., Sahu, M., Henkel, C., Wilson, T.J., Sahu, K.C. and Pottasch, S.R.: 1990, *A&A* **233**, 197

Hartigan, P., Raymond, J. and Meaburn, J.: 1989, *ApJ* **362**, 624

Hartley, M., Manchester, R.N., Smith, R.M., Tritton, S.B. and Goss, W.M.: 1986, *A&AS* **63**, 27

Hawarden, T.G., Brand, P.W.J.L: 1976, *MNRAS* **175**, 19P

Henize, K.G.: 1976, *ApJS* **30** ,431

Herbig, G.H.: 1960, *ApJS* **4**, 337

Herbig, G.H. and Bell, K.R.: 1988, *Lick Obs. Bull.* No. 111

Herbst, W.: 1975a, *AJ* **80**, 212

Herbst, W.: 1975b, *AJ* **80**, 683

Herbst, W.: 1977, *PASP* **89**, 795

Heydari-Malayeri, M.: 1988 *A&A* **202**, 240

Hodapp, K.-W.: 1987, *ApJ* **319**, 842

Irvine, N.J.: 1975, *PASP* **87**, 87

Krautter, J., Reipurth, B. and Eichendorf, W.: 1984, *A&A* **133**, 169

Kuiper, T.B.H, Peters III, W.L., Forster, J.R., Gardner, F.F. and Whiteoak, J.B.: 1987, *PASP* **99**, 107

Lauberts, A.: 1982, *The ESO/Uppsala Survey of the ESO(B) Atlas*, European Southern Observatory

May, J., Murphy, D.C. and Thaddeus, P.: 1988, *A&AS* **73**, 51

Meaburn, J. and Dyson, J.E.: 1987, *MNRAS* **225**, 863

Mermilliod, J.: 1981, *A&A* **97**, 235

Murphy, D.C.: 1985, Ph.D. Thesis, Massachusetts Institute of Technology

Murphy, D.C. and May, J.: 1991, *A&A* **247**, 202

Ogura, K.: 1990, *PASP* **102**, 1366

Olberg, M., Reipurth, B. and Booth, R.: 1992, *A&A*, in press

Persi, P., Ferrari-Tonioli,M., Busso, M., Origlia, M., Robberto, M., Scaltriti, F. and Silvestro, G.: 1990, *AJ* **99**, 303

Persson, S.E. and Campbell ,B.: 1988, *AJ* **96**, 1019

Pettersson, B.: 1984, *A&A* **139**, 135

Pettersson, B.: 1987a, *A&A* **171**, 101

Pettersson, B.: 1987b, *A&AS* **70**, 69

Pettersson, B. and Reipurth, B.: 1992, in preparation

Raga, A.C. and Mateo, M.: 1987, *AJ* **94**, 684

Reipurth, B.: 1981, *A&AS* **44**, 379

Reipurth, B.: 1983, *A&A* **117**, 183

Reipurth, B.: 1985, *Proc. ESO-IRAM-Onsala Workshop on "(Sub) Millimeter Astronomy"*, eds. P.A. Shaver and K. Kjär, p. 458.

Reipurth, B.: 1989, in *ESO Workshop on Low Mass Star Formation and Pre-Main Sequence Objects*, ed. Bo Reipurth, p. 247

Reipurth, B.: 1990, *IAU Symposium No. 137 on "Flare Stars in Star Clusters, Associations and the Solar Vicinity"*, eds. L.V. Mirzoyan, B.R. Pettersen and M.K. Tsvetkov, p. 229

Reipurth, B. and Graham, J.A.: 1988, *A&A* **202**, 219

Reipurth, B. and Heathcote, S.: 1991, *A&A* **246**, 511

Reipurth, B. and Pettersson, B.: 1992, in preparation

Reipurth, B. and Zinnecker, H.: 1992, in preparation

Rodgers, A.W., Campbell, C.T.,Whiteoak, J.B., Bailey, H.H. and Hunt, V.O.: 1960, An Atlas of H-alpha Emission in the Southern Milky Way, Mount Stromlo Observatory, Australian National University, Canberra

Sahu, M., Pottasch, S.R., Sahu, K.C., Wesselius, P.R., Desai, J.N.: 1988, *A&A* **195**, 269

Sahu, M., Sahu, K.C. and Pottasch, S.R.: 1989, *A&A* **218**, 221

Sandqvist, Aa.: 1976, *MNRAS* **177**, 69p

Sandqvist, Aa.: 1977, *A&A* **57**, 467

Sandqvist, Aa. and Lindroos, K.P.: 1976, *A&A* **53**, 179

Scarrott, S.M. and Warren-Smith, R.F.: 1988, *MNRAS* **232**, 725

Scarrott, S.M., Gledhill, T.M., Rolph, C.D. and Wolstencroft, R.D.: 1990, *MNRAS* **242**, 419

Schwartz, R.D.: 1977, *ApJ* **212**, L25

Schwartz, R.D.: 1983, *ApJ* **268**, L37

Schwartz, R.D., Cohen, M. and Williams, P.M.: 1987, *ApJ* **322**, 403

Schwartz, R.D., Jones, B.F. and Sirk, M.: 1984, *AJ* **89**, 1735

Schwartz, R.D., Persson, S.E. and Hamann, F.E.: 1990, *AJ* **100**, 793

Stauffer, J., Hartmann, L.W., Jones, B.F. and McNamara, B.R.: 1989, *ApJ* **342**, 285

Tjin A Djie, H.R.E., Remijn, L., Thé, P.S.: 1984 *A&A* **134**, 273

de Vries, C.P., Brand, J., Israel, F.P., de Graauw, Th., Wouterloot, J.G.A., van de Stadt, H. and Habing, H.J.: 1984, *A&AS* **56**, 333

West, R.M.: 1980, *A&A* **90**, 366

Wilking, B.A., Schwartz, R.D., Mundy, L.D. and Schultz, A.S.B.: 1990, *AJ* **99**, 344

Wray, J.D.: 1966, Thesis, Northwestern University

Zealey, W.J., Ninkov, Z., Rice, E., Hartley, M., Tritton, S.B.: 1983, *Astrophys. Letters* **23**, 119

Table 1. Optical properties of the pre-main sequence objects and candidates

Object[1]	α_{1950}	δ_{1950}	V[2]	ref	K[2]	ref	Sp.type[1]	ref	Associated cloud	Comments[3]
CG-Hα8	7 14 18.6	−48 26 05	15.3	1			M1-2	1	DC259.5−16.4	CG13, Sa102
NX Pup	7 17 56.0	−44 29 36	9.8	†	5.9	8,9	A0-1 III	‡	DC256.2−14.1	CG1, CoD−44°3318, Bernes 135, HBC552, var.
CG-Hα1	7 29 11.1	−47 18 44	>17				M3-4	1	DC259.2−13.2	Sa101
CG-Hα2	7 29 29.8	−46 49 48	>17				M2:	1	DC259.2−13.2	Sa101
CG-Hα3	7 29 43.2	−46 54 08	15.0	1			K7	1	DC259.2−13.2	Sa101
CG-Hα4	7 29 54.1	−46 51 19	14.6	1			K7-M0	1	DC259.2−13.2	Sa101
CG-Hα5	7 30 08.9	−46 53 47	15.2	1			K2-5	1	DC259.2−13.2	Sa101
CG-Hα6	7 30 09.7	−46 53 55	14.2	1			K7	1	DC259.2−13.2	Sa101
CG-Hα7	7 31 58.5	−46 42 09	14.0	1			K5	1	DC259.2−13.2	Sa101
BBW76	7 48 40.4	−32 58 43	12.3	5			G	5		FU Ori-object
PHα12	8 06 29.7	−35 54 59	15.2	2	10.4	2	M1.5	2	(DC253.0−1.7C)	near CG30/31, HBC553
PHα14	8 06 41.4	−35 59 21	15.8	2	10.3	2	M2:	2	(DC253.0−1.7C)	near CG30/31, HBC554, var.
PHα15	8 06 54.3	−35 59 03	14.8	2	10.8	2	M3	2	(DC253.0−1.7C)	near CG30/31, HBC555, var.
PHα21	8 08 38.0	−35 52 51	16.3	2	10.8	2	M4	2	DC253.6−1.3	HBC556
PHα27A	8 09 53.1	−35 54 00	17.5	3					DC253.6−1.3	
PHα34	8 10 54.2	−36 10 14	14.9	2	11.3	2	K3:	2	DC253.6−0.6	HBC557, var.
PHα40	8 11 58.7	−36 04 54	16.5	2	11.2	2	M0.5	2	DC253.9−0.6	HBC558
PHα41	8 12 02.9	−35 58 54	13.0	2	8.8	2	Cont.	2	DC253.9−0.6	HBC559, var., IRAS 08120−3559
PHα44	8 12 28.7	−36 00 54	16.0	2	11.4	2	K7-M0	2	DC253.9−0.6	HBC560
PHα51	8 14 01.7	−35 48 43	15.8	2	11.1	2	K7-M0	2	DC253.9−0.6	HBC561
WRA218	8 26 00.0	−34 44 54	13.9	10			K2:	10	Isolated	PHα91, CaII H and K in em.
vBH16	8 26 12.0	−50 59	15.3	6					DC267.4−7.5	Sa111, T Tau binary
WRA220	8 26 42.6	−33 36 21	13.4	1	9.0	1	K2	1	DC253.6+2.9	PHα92, seen towards CG22
ESO-Hα22	8 33 23.5	−40 17 50	16.2	4			K:	4	(DC259.9−0.0)	
ESO-Hα30	8 33 35.3	−40 27 25	17.7	4			Cont.	4	DC259.9−0.0	
ESO-Hα34	8 33 41.5	−40 14 48	15.8	4			K2-5	4	(DC259.9−0.0)	
ESO-Hα49	8 34 52.7	−40 24 52	16.2	4			K:	4	DC260.4+0.4C	SL1
ESO-Hα58	8 35 36.2	−40 30 54	14.9	4			K2-5	4	DC260.4+0.4C	SL1
ESO-Hα66	8 35 51.2	−40 05 49	14.8	4			K0-2	4		
ESO-Hα77	8 36 32.5	−40 15 50	15.6	4			Cont.	4	(DC260.4+0.4C)	SL1
ESO-Hα88	8 36 48.7	−40 49 17	15.0	4			K0-2	4	DC260.4+0.4C	SL1
ESO-Hα94	8 36 59.6	−40 40 41	14.2	4			K5-7	4	DC260.4+0.4C	SL1, IRAS 08369-4040
ESO-Hα105	8 37 23.8	−39 59 18	16.1	4			Cont.	4	DC260.2+0.7	
ESO-Hα112	8 37 33.4	−40 14 35	16.0	4			K:	4	DC260.2+0.7	
ESO-Hα113	8 37 34.4	−40 53 31	16.9	4			K7-M0	4	DC260.8+0.2	
ESO-Hα116	8 37 40.6	−40 02 24	14.0	4			G8:	4		
SHJM 6	8 38 27.2	−52 47 17	11.9	7			K	7		IC2391
ESO-Hα153	8 39 30.9	−40 52 35	15.3	4			M2	4		
SHJM 3	8 40 00.5	−53 11 58	12.6	7			K	7		IC2391
SHJM 8	8 40 13.5	−52 48 49	13.4	7			K	7		IC2391
SHJM 7	8 40 26.0	−52 55 59	12.5	7			K	7		IC2391
SHJM 9	8 40 31.3	−52 41 28	13.5	7			K	7		IC2391
SHJM 1	8 40 52.1	−52 51 08	14.0	7			K	7		IC2391
SHJM 4	8 42 00.9	−52 46 51	14.2	7			K	7		IC2391
SHJM 5	8 42 00.9	−52 46 48	14.2	7			K	7		IC2391
ESO-Hα225	8 48 55.6	−41 55 19	17.6	4			M0	4	DC263.2+1.6C	Seen towards RCW33, SL4
ESO-Hα249	8 50 29.3	−42 03 54	13.6	4			K5-7	4	DC263.2+1.6C	Seen towards RCW33, SL4

[1] Spectral types for the ESO-Hα stars (Pettersson and Reipurth, 1992) are preliminary! [2] Maximum light for variable stars. [3] HBC = Third Catalog of Emission-Line Stars of the Orion Population, Herbig and Bell, 1988.

Ref: 1. Reipurth and Pettersson, 1992
2. Pettersson, 1987a
3. Pettersson, 1987b
4. Pettersson and Reipurth, 1992
5. Reipurth, 1990
6. Herbst, 1977
7. Stauffer et al., 1989
10. This work

†: 8. Reipurth, 1983
9. Brand et al., 1983
Tjin A Djie, 1984

‡: 8. Reipurth, 1983
9. Brand et al., 1983
Finkenzeller and Mundt, 1984
Finkenzeller, 1983
Irvine, 1977

Table 2. Herbig-Haro objects.

Object	α_{1950}	δ_{1950}	ref	V_{HEL} (km s^{-1})	ref	Observed flux (Hβ=100)[1] [OIII] 5007	[OI] 6300	[SII] 6717	[SII] 6731	ref	Location	Comments
HH120	8 07 40.0	−35 56 02	9	−42±12	1	<2	680	803	988	1	DC253.3−1.6	CG30
Re4 head	8 19 28.9	−49 25 12	2	−30±11	2		48α	17α	24α	2	DC266.0−7.4	Sa109
Anon.				−21	10		44α	74α	81α	10		1' SE IRAS 08211−4158
HH47C	8 24 05.6	−50 51 48	8	+91±15	3		240	350	270	5	DC267.4−7.5	Sa111=ESO 210-6A
HH46	8 24 16.8	−50 50 41	8	−182±7	2	10	399	229	274	7	DC267.4−7.5	Sa111=ESO 210-6A
HH47B	8 24 19.3	−50 50 23	8	−144±15	3,6						DC267.4−7.5	Sa111=ESO 210-6A
HH47A	8 24 22.9	−50 50 03	8	−111±15	3,6		342	486	511	5	DC267.4−7.5	Sa111=ESO 210-6A
HH47D							344	990	420	5	DC267.4−7.5	Sa111=ESO 210-6A
HH132	8 33 35.2	−40 28 52	11								DC259.9−0.0	Near vBH17a, NGC2626
HH73	9 00 26.6	−44 39 25	4		4						DC266.1+1.1	Chain of HH:s near Re6
HH74	9 00 28.6	−44 37 59	4		4						DC266.1+1.1	Near Re6
HH133	9 09 06.5	−45 18 30	11								DC268.8+1.8	Sa114
HH75	9 09 50.7	−45 30 07	4	−100±25	4		31α	44α	37 α	4	DC268.0+1.8	Sa114

Ref : 1. Pettersson, 1984
2. Graham, 1986
3. Graham and Elias, 1983
4. Reipurth and Graham, 1988
5. Dopita et al., 1982b
6. Meaburn and Dyson, 1987
7. Dopita, 1978
8. Schwartz et al., 1984
9. Reipurth, 1981
10. Graham, 1991
11. Ogura, 1990

[1] An α after the flux indicates flux rel. to Hα=100

Table 3. Embedded young stellar objects

Object	α_{1950}	δ_{1950}	ref	K	J–H	H–K	ref	[12]	[25]	[60]	[100]	$L_{bol}/L_{\odot}$	ref	IRAS
								IRAS fluxes (Jy)						
CG30IRS4	8 07 41.0	−35 56 08	1	11.9	1.6	1.9	1,2	0.6	3.7	18.2	47.5	18	3,4	08076−3556
Re4 star	8 19 28.8	−49 25 10	1	11.7	1.3	1.3	1	<0.1[a]	2.3	29.8	80[a]	28	3,4	08194−4925
Re5 star	8 19 36.9	−49 31 13	1	11.6	2.3	1.6	1	<0.3	7.1	53.3	<74.6			08196−4931
08211-4158/1	8 21 07.4	−41 58 12	8	7.6	3.4	2.9	8	11.0	32.0	209.	622.	160	8,9	08211−4158
HH46IRS	8 24 16.5	−50 50 43	1	12.9	1.7	1.8	1,5,6	0.8	6.3	26.1	58.3	24	3,4	08242−5050
Anon	8 51 19.1	−42 01 36	7	00.0	0.0	0.0	7	12.4	136.	455.	618.			08513−4201

Ref: 1. Graham and Heyer, 1989
2. Pettersson, 1984
3. Cohen and Schwartz, 1987
4. Berrilli et al., 1989
5. Elias, 1980
6. Graham and Elias, 1983
7. Pettersson and Reipurth, 1992
8. Persson and Campbell, 1988
9. Graham, 1991

[a] Cohen and Schwartz, 1987

The Chamaeleon Dark Clouds and T–Associations

Richard D. Schwartz

Department of Physics
University of Missouri – St. Louis
8001 Natural Bridge Road
St. Louis, Missouri 63121, USA

I. Introduction

Early investigations of the Chamaeleon dark cloud regions established the presence of Hα emission line stars (Henize 1954) and a number of variables, some with Hα emission, which Hoffmeister (1962) described as RW-Aur-like variables. Among the three dark cloud complexes in Chamaeleon, Cha I appears to possess the largest populations of young stellar objects (YSOs) as evidenced by the first extensive search for Hα emission stars by Henize and Mendoza (1973). Cha II (labeled Cha III by Hoffmeister) also contains a significant number of YSOs, whereas Cha III (Cha II in Hoffmeister) appears to be devoid of current star formation activity.

Lying at high galactic latitude ($-15°$), the clouds are relatively uncluttered with background sources, especially at infrared wavelengths. Moreover, unlike the Taurus-Auriga star forming region which is scattered widely on the sky in a loose quilt-work of dark cloud extinction, the Chamaeleon dark clouds are well-defined, coherent structures with dimensions of order 4 sq. degrees each. Thus the Chamaeleon star-forming clouds present an attractive arena for the study of evolving YSOs.

Owing in part to their extreme southerly declination ($-77°$), the Chamaeleon clouds have yet to receive the detailed scrutiny experienced by other star-forming regions. Nevertheless, within the past 15 years a number of important strides have been made, especially in the study of Cha I. The purpose of this review is to summarize the current observational states of Cha I and Cha II, especially regarding the populations of YSOs obtained from both optical and infrared studies. To this end, candidate members for each association are tabulated along with updated finder charts. The results of spectroscopic and photometric studies (optical and infrared) are briefly summarized with a focus upon particularly interesting objects within each association. The distance(s) to the Chamaeleon associations remains an outstanding unresolved issue which will be discussed in some detail.

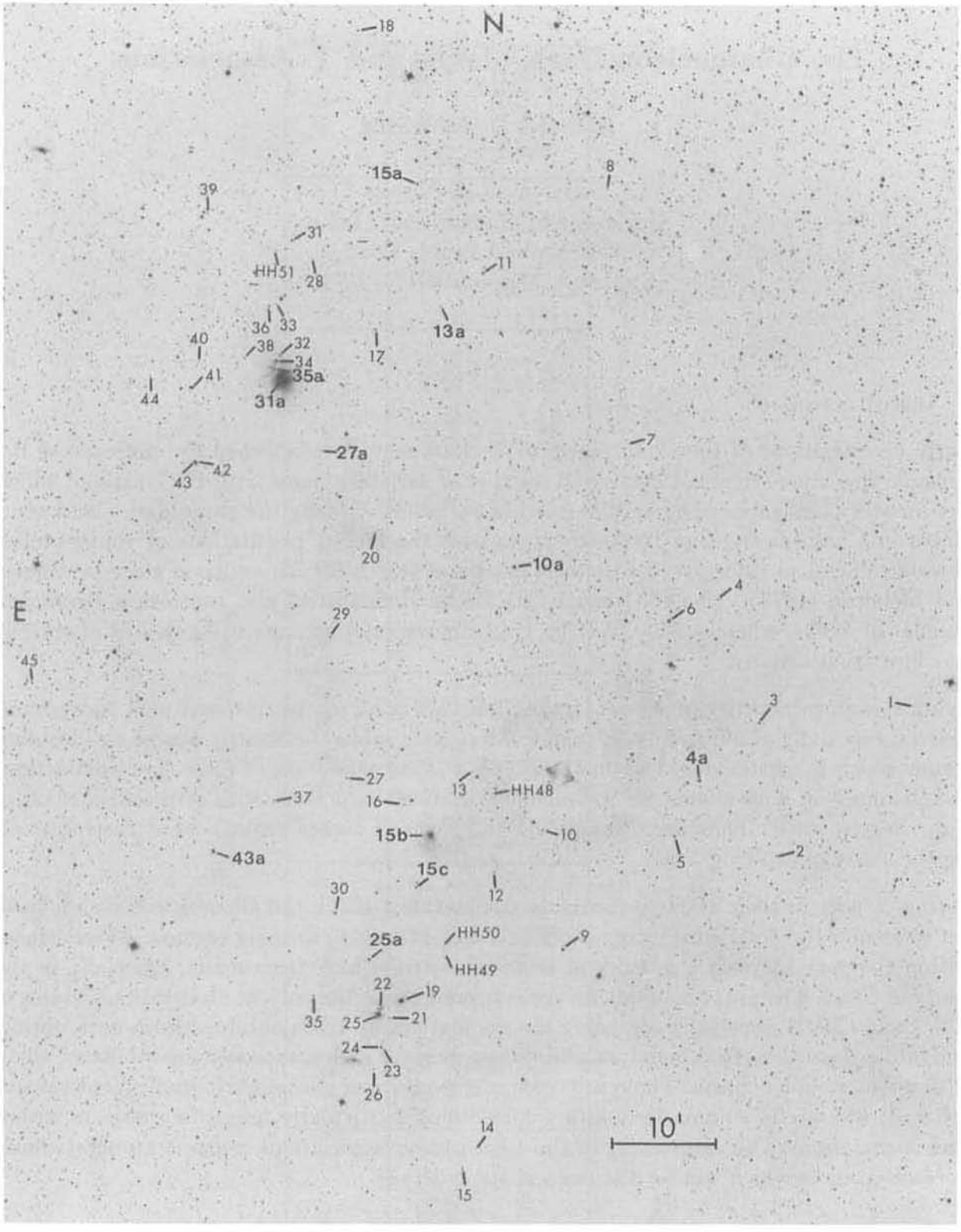

Figure 1. The Cha I Association adapted from the Schwartz (1977) survey. The star identification numbers are contained in Table 1. The peculiar, extended feature near HH 48 is a ghost image from a bright star elsewhere in the plate field.

II. Chamaeleon I

A. Visible Members

Combined with Hoffmeister's (1962) work, the Hα survey of Henize and Mendoza (HM) (1973) provided a basic catalogue of YSO candidates in Cha I. Schwartz's (1977) survey confirmed most of the HM sources, and added a number of fainter Hα sources scattered in and about the cloud. More recently, Whittet *et al.* (1987) have compiled a list of visible association members. Table 1 contains a list of these members. The numbering scheme of Whittet *et al.* has been used in Column 1, with the addition of two sources (T14a, T45a) not contained in the Whittet *et al.* list. Column 2 gives other designations as footnoted. Column 3 gives the finder chart (Figure 1) number for each star, where a colon designates uncertainty in identification for several of the Hoffmeister variables for which finder charts were not readily available to the author. Columns 4 and 5 give the 1950 epoch right ascension and declination for each object. Columns 6 and 7 list the visual magnitudes and spectral types where available, information gleaned primarily from the Herbig-Bell Catalog (HBC) (Herbig and Bell 1988) which contains additional information, including U, B, V, R, I magnitudes for many of the objects. Photometry for T21, T29, and T54 is from Schwartz and Henize (1983), and magnitudes for T8, T24, T39, and T51 are from Schwartz and Noah (1978). Column 8 gives cross identifications of optical sources to far-infrared sources, mainly as defined by IRAS point source identifications, by the IRAS pointed observation coadds of Baud *et al.* (1984) and Wesselius *et al.* (1984), and the Kuiper Airborne Observatory work of Jones *et al.* (1985). Finally, column 8 gives references as footnoted to near-infrared photometry on association members.

Two features of Table 1 should be noted. First, although most of the candidate members have been identified upon the basis of Hα emission surveys, several sources are included upon the basis of their variability and RW-Aur-like spectra as indicated by Hoffmeister (T2, T6, T13, T17, T20, T22, and T36). In addition, several non-Hα sources are included where reflection nebulae indicate an association with the dark cloud (T21, T41, and T54), or where infrared excesses indicate possible YSO activity (T33, T45a). The Herbig-Haro object HH48 (T14a) is included in view of the spectra of Cohen *et al.* (1986) which shows that a very faint T Tauri star (Hα, FeII, and CaII emission) sits at the core of the semi-stellar HH nebula. The positions of the remaining HH objects in Cha I along with more detailed finder charts are contained in Schwartz (1977). A second feature to note is that several candidate members are yet to be confirmed as Hα emitters since they were identified only in the Schwartz (1977) survey as marginal identifications (Hα emission intensity =1; T1, T18, T19, T30, T39, T43, and T51). However, possible far-IR identifications of T30, T43, and T51 and X-ray detections (Feigelson and Kriss 1989) of T30, T39, T43, and T51 suggest membership for these stars. Finally, several objects (T10, T25, T56) lie outside of regions of significant obscuration, and could be field objects. These caveats regarding membership are important to population studies of this association, and point to the need for additional spectroscopic work.

The principle spectroscopic classification work on Cha I stars has been carried out by Ap-

penzeller (1977, 1979) and Appenzeller *et al.* (1983). At least 8 of the stars studied appear to exhibit YY Ori-type spectra, possibly indicative of a youthful accretion stage. Finkenzeller and Basri (1987) have examined T8 and T26 in some detail, deriving estimates for bolometric luminosity, visual absorption, radial velocity, $v \sin i$, rotational period, radius and mass for each star. Franchini *et al.* (1988a,b) have reported $v \sin i$ data from high resolution spectra of 15 T Tau stars in Cha I and Cha II, deriving estimates of masses and evolutionary phases for the stars. In agreement with findings in other associations, these authors report that faster rotators are found preferentially among the higher mass stars, a feature which may be due to the shorter "convective braking lifetime" of the higher mass stars. Bouvier *et al.* (1986) had earlier carried out rotation studies of SYCha (T4) and TWCha (T7). More recently, Bouvier and Bertout (1989) have observed rotational modulation due to spots on SYCha, deriving a period of 6.1 days and a fractional spot coverage of 8–10%.

Photoelectric UBVRI photometry has been reported for most of the prominent members of Cha I by various authors (Glass and Penston 1974, Grasdalen *et al.* 1975, Schwartz and Noah 1978, Mundt and Bastian 1980, Appenzeller *et al.* 1983, Kilkenny *et al.* 1985, and Whittet *et al.* 1987). Characteristic of T Tauri stars in other associations, the more "advanced" T Tau stars (those probably still on convective tracks) tend to show the greatest light variations with strong ultraviolet excesses (T7, T27, T31, T40, T48, T47, T49, and T53). It must be borne in mind that the visual magnitudes listed in Table 1 for many of the stars are subject to considerable variability.

In addition to optical photometry, satellite UV measurements have been reported on T4 by Schaefer (1983), on T52 by Penston and Lago (1983), and on T8, T11, T14, T26, T31, T32, T40, and T51 by Imhoff and Appenzeller (1987). Finally, Feigelson and Kriss (1989) have recently reported X-ray detections and optical spectrophotometry of a number of Cha I members which are cross-referenced in Table 1 in column 2 with CHX designations. Although some of the candidate objects are classical T Tauri stars, many of the stars are identified by Feigelson and Kriss as "naked T Tauri stars" (NTTS) from their optical spectrophotometric data. Four of the X-ray sources (CHX6, 10, 13, 21) are associated with NTTS which are not incorporated in Table 1. The presence of both "advanced" classical T Tauri stars and NTTS suggest a typically wide time span for a star formation in Cha I.

Recently, Gauvin and Strom (1991) have derived spectral energy distributions for a large sample of stars in Cha I and II, and place the stars in the HR diagram. They also compare age and mass distributions and the luminosity function for the Chamaeleon stars to those in the Taurus-Auriga dark clouds, and find that they are similar.

B. Infrared Members

Near-IR photometry is an important tool in characterizing the IR excess radiation in T Tauri stars, and references to J, H, K, L photometric studies of visible Cha I members are incorporated in Table 1. In addition, a number of the visible members have been identified with IRAS sources (Whittet *et al.* 1987, Gregorio Hetem *et al.* 1988, this study using the IRAS

Point Source Catalog) as cross-referenced in column 8 of Table 1. Also, the deep IRAS survey of Baud *et al.* (1984) which covered a portion of the southern block of Cha I suggests additional identifications with the visible members (T22=B33?, T23=B34, T29=B37?, T30,31=B41?, T35=B42).

Of great interest is the identification of IR sources which have no optical counterparts, indicating that they may be deeply embedded in dark cloud and/or circumstellar dust. Hyland *et al.* (1982) carried out a 2μm survey complete to K = 10.5 in a central strip between $11^h\ 07^m$ and $11^h\ 10^m$, and $-77°\ 45'$ and $-76°\ 15'$ and to K = 11.5 in an eastern strip between $\sim 11^h\ 10^m$ and $\sim 11^h\ 12^m$, and $-76°\ 50'$ and $-76°\ 15'$. On the basis of subsequent J, H, K photometry, the majority of the sources turned out to be associated with background stars. However, 10 of the 84 sources are identified with visible members (Table 1), and 8 additional sources without optical counterparts have colors suggestive of association membership. A deeper 2μm survey with J, H, K photometry was carried out by Jones *et al.* (1985) in a $9' \times 9'$ block centered near HD 97300 (=T41) in the northern block of Cha I. Twelve new sources were reported in this block, including 5 probable background stars, 3 associated with visible association members (C1–16 = T46, C1–17 = T43, and C1–23 = T48), and 3 new embedded association members. In combination with the sources discovered in the earlier survey of Hyland *et al.*, it was concluded that the star formation efficiency is at least 25% in this portion of the cloud. It was also suggested that HD 97300, a ZAMS B9 star used for distance determinations to Cha I (discussed below), has been responsible for producing an increased density gradient about 2′ north of the star where star formation has been triggered as evidenced by the presence of several near-IR sources.

In a most recent study, Assendorp et al. (1990) carried out high resolution IRAS mapping and ground-based infrared photometry for the regions around HD 97048 and HD 97300. Fifteen IR sources were detected, including three which are not listed in the IRAS PSC. The results confirm that each region is a center of low mass star formation with IR luminosities in the range $0.2 < L < 16 L_\odot$. Although most of the sources are identified with visible T Tauri stars, two appear to be in an earlier accretion phase. Also, Whittet et al.(1990) have reported JHKL photometry for 28 IRAS-selected sources in Cha I unassociated with previously known members of the pre-main sequence population. Four of these sources are identified as PMS objects, with 11057–7606 (=B35, see below) possessing properties of a deeply embedded star, possibly in an accretion phase. With serendipitous survey data included, it is found that IRAS identifications exist for only 57% of the visible T Tauri stars, indicating that IRAS survey data do not provide a complete census of YSOs in nearby dark clouds. Owing to the fact that the tables for this review were prepared prior to the author's receipt of the Assendorp et al. (1990) and Whittet et al. (1990) papers, information from these recent works is not incorporated in Table 2. It can be noted, however, that B35, B38, and C7–11 in Table 2 correspond to three of the four sources reported by Whittet et al. (1990).

The deep pointed IRAS observations of Baud *et al.* (1984) covered a strip about 30′ wide through the southern block of Cha I. Reaching a limit about 10 times fainter than the

IRAS Point Source Catalog (PSC), 70 sources are identified, including a number of sources which clearly lie outside the dark cloud boundary. At first glance, the source plot gives the impression that the surface density of sources outside the cloud is comparable to that within the cloud boundaries. This is probably a consequence of the detection of much fainter background sources which do not appear in the PSC.

To complement this review article, I have carried out an IRAS PSC survey of all sources within the Cha I region bounded by $10^h\ 50^m$ and 11^h12^m, and $-77°\ 45'$ and $-76°\ 00'$. This region contains 36 sources, 28 of which can be associated with cloud members. The remaining objects, detected only at 12μm and 25μm with F(12)>F(25), are almost certainly field stars. As a control experiment, a sky area of identical size, centered at the same galactic latitude ($-15.7°$) as Cha I but at a greater galactic longitude (300.2°), was scanned in the PSC. This area, completely clear of dark cloud obscuration, revealed only 11 IRAS sources, most of which have F(12)>F(25) and which are evidently associated with field stars. Two sources are detected at 100μm only and one source has F(100)>F(60). The statistics of field objects in the Cha I region and the control region appear to be similar.

In the Baud *et al.* study, it is pointed out that there is a distinct excess of "warm" sources with F(60)>F(25), indicative of embedded objects within the confines of the dark cloud. Using Fig. 1 of Baud *et al.*, and the finder chart (Fig. 1) in this review, approximate positions for the Baud *et al.* sources have been computed. Some of the sources are tentatively identified with visible association members listed in Table 1 (see column 8). Several of the "warm" sources, however, have no visible counterparts.

The infrared sources within the dark cloud boundaries but without visible counterparts, as discovered in the studies of Hyland *et al.* 1982, Jones *et al.* 1985, and Baud *et al.* 1984, are listed in Table 2. Column 1 gives the identification number, columns 2 and 3 the 1950 coordinates, column 4 the J, H, K, L magnitudes, and column 5 the IRAS fluxes in Janskys. In particular, the Baud *et al.* sources are limited to the "warm" [F(60)>F(25)] objects which are almost certainly association members. Wesselius *et al.* (1991) have recently compiled a list of 73 association members, and have derived source luminosities from existing optical and infrared data. It is found that the luminosity function for Cha I is very similar to that of ρ Oph.

Attention is directed to the two most luminous sources in Table 2. First, the Infrared Nebula (IRN, Schwartz and Henize 1983, Cohen and Schwartz 1984) is associated with IRAS 11072-7727. Source 41 of Baud *et al.* (1984) almost certainly represents this source, although it is misplaced northward in their Fig. 1. The survey of Hyland *et al.* (1982) listed two sources near the position with nearly identical magnitudes (K = 7.85, J–H=2.02, H–K=1.20). The photometry of Cohen and Schwartz (1985), however, shows that there is a single source located near the "gap" in the bipolar reflection nebula. Figure 2 is a deep red CTIO 4-meter photograph of the IRN with nearby Hα stars identified (cf. Fig. 1). Cohen and Schwartz interpret this object as a star obscured by a circumstellar disk viewed nearly edge-on, with light scattered into two lobes, the eastern lobe being the dominant, least obscured one. It is interesting that the spectrum of IRN obtained with the Anglo-Australian Telescope (Dopita,

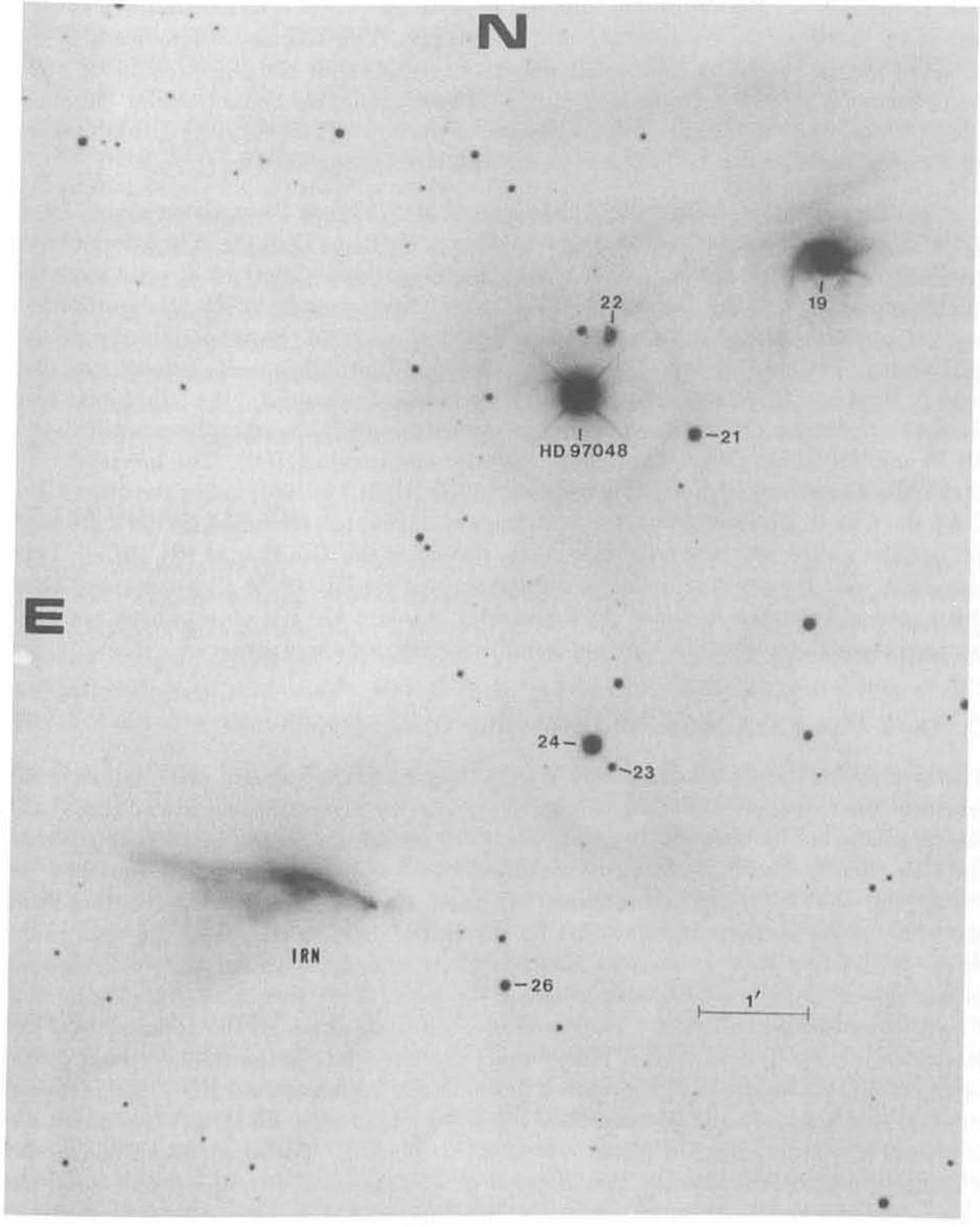

Figure 2. A CTIO 4-meter red photograph showing detail of the Infrared Nebula and nearby Hα-stars in the southern portion of Cha I.

Schwartz, and Cohen, unpublished) exhibits a nearly featureless, extremely red continuum (with a possible weak Hα absorption feature). In particular, there is no indication of emission lines which would signal the presence of mass outflow. The bolometric luminosity ($18L_{\odot}$) estimated for the source by Cohen and Schwartz suggests that the object could be a mid-to-late A-type ZAMS star. Scarrott *et al.* (1987) have conducted linear polarization studies of IRN, confirming the bipolar reflection nature of the object, and suggesting that magnetic alignment of particles can be traced from the disk into the bipolar lobes.

A second source, B35, is suggested by Schwartz *et al.* (1984) as the exciting source for HH 49/50. The infrared source is located about 2.5′ east of T21 (=Ced110). The group of knots in HH 49-50, located about 10.5′ SSW of B35, have high proper motions directly away from B35 (Schwartz *et al.* 1984). The source B35 is extremely cool, and a substantial portion of its luminosity may be radiated beyond 100μm. Prusti *et al.* (1991) have conducted a study of IRAS sources around Ced 110. In particular, they find that B35 is really two sources, called Ced 110 IRS4 and IRS6, and suggest that IRS4 is the driving source of the HH objects. They also find a molecular outflow apparently emanating from IRS4. Spectrophotometric data for HH 49 and HH 50 have been reported by Schwartz and Dopita (1980). The spectrum of HH 49 exhibits a relatively high-excitation spectrum ([O III]/H$\beta \cong$ .66), unlike the other HHs in Cha I and Cha II. The recent study of Mattila *et al.* (1989) has identified B35 as a prominent CO outflow source with the redshifted lobe oriented in the direction of HH 49/50. This is consistent with the positive radial velocities reported for HH 49/50 (Schwartz and Dopita 1980), and indicates an irregular cloud geometry in which the HH objects have apparently emerged through an optically-thin portion of the extended cloud structure.

C. Dark Cloud Extinction and Molecular Observations

The location of the Chamaeleon dark clouds away from the galactic plane is nicely illustrated in the catalogue of dark nebulae and globules by Feitzinger and Stüwe (1984). Star counts conducted by Gregorio Hetem *et al.* (1988) reveal the general extinction patterns in the Cha clouds. The highest density region of Cha I appears to be in the southern block ($\sim 11^h\ 03^m$, $-77°$) where visual extinctions reach $A_v > 6$. The visual extinction around HD 97300 in the northern block reaches $A_v \sim 4.0$, although it is clear from the work of Jones *et al.* (1985) that local extinctions associated with embedded IR sources reach somewhat higher values. Rydgren (1980) and Vrba and Rydgren (1984) have studied the extinction in Cha I using background stars. These authors find that, although the ratio of total to selective extinction $R = A_v/E(B-V)$ has normal values (~ 3.1) in the thinner, outer portions of the cloud, the values of R approach 5 in the denser region around HD 97300. Grasdalen *et al.* (1975) reached a similar conclusion regarding a high value for R, an observation which is pivotal for determining the distance to Cha I (see below). The recent IRAS images of the Chamaeleon Clouds studied by Boulanger *et al.* (1990) reveal a complexity of cloud structure with color variations on all size scales. It is suggested that the mid-IR (12μm) emission is dominated by transiently-heated small grains, whereas the far-IR (100μm) emission arises from larger grains. The color variations (seen in the attractive color plate in Boulanger *et*

al.) therefore trace variations in the abundances of transiently-heated particles.

Only a limited amount of molecular line observations have been reported for the Cha clouds. Toriseva *et al.* (1985) reported on H_2CO and OH line intensities, and this data was used by Toriseva and Mattila (1985) to examine the correlation of gas and dust. Significant correlations are found between the H_2CO distribution and the locations of Hα stars, 2μm sources, warm IRAS sources, and X-ray objects. It is interesting that the H_2CO line area contour map (their Fig. 4) shows a maximum near the position of B35, the embedded IRAS source suggested as the exciting star for HH 49/50. A ^{12}CO (J = 2–1) survey at the position of HH 49/50 by de Vries *et al.* (1984) detected emission with V_{LSR} = +4.5 kms^{-1}, and H_2CO emission at +4.7 kms^{-1} was reported at the position of HH 48. The work of Mattila *et al.* (1989) using the Swedish-ESO Submillimeter Telescope (SEST) to map regions of Cha I in the lines of ^{12}CO, ^{13}CO, and $C^{18}O$ represents an important step in characterizing the dynamics of star formation in the region. In addition to the B35 outflow source noted above, an outflow source was discovered in the Cha I northern block centered about 2′ north of HD 97300. It suggested that T42 (=HM23) is the source of this outflow.

D. The Distance to Cha I

Distance estimates to the Cha I cloud have been derived principally from analyses of HD 97300. Grasdalen *et al.* (1975) assumed a ratio of total to selective extinction of 5.5, and for an A0V spectrum derived a distance of 115pc. The work of Rydgren (1980) and Vrba and Rydgren (1984) gave observational support to the idea that HD 97300 may suffer abnormal extinction, and using a value of R∼5 for a carefully derived spectral type of B9V, a distance of 145pc was proposed.

On the other hand, Thé *et al.* (1986) carried out an analysis of the spectral energy distributions of both HD 97300 and HD 97048 with the assumption of normal extinction (R = 3.1) for a three-component model (foreground interstellar extinction, cloud extinction, and circumstellar shell extinction). Using the results of model atmospheres of Kurucz (1979) to obtain intrinsic energy distributions, it was found that the observed energy distribution (0.12–100μm) of HD 97300 could be generated by a star with $T_{eff} \cong 10500$K, $L \cong 50L_\odot$, $R \cong 2.2R_\odot$, at a distance of 220pc, assuming A_v values of 0.36, 0.71, and 0.36 respectively, for the three extinction components. Likewise, HD 97048 gave self-consistent results for a star with $T_{eff} \cong 10000$ K, $L \cong 40L_\odot$, $R \cong 2.1R_\odot$, at a distance of 170pc, with component A_v values of 0.28, 0.62, 0.34. To account for the apparent near-IR excess in these stars which results from the assumption that $R \cong 3.1$, at least three Planck curves (dust shells at different temperatures) are required. For HD 97300, a dust shell 0.1 A.U. from the star and with a temperature of 2740K is required to produce the excess in the J, H, K bands. Cooler and more distant dust shells (280K and 50K) suffice to reproduce the IRAS fluxes which are almost certainly due to reprocessed stellar radiation. The study of Jones *et al.* (1985) concurs with a distance estimate of ∼215pc to HD 97300 based upon a recovered luminosity of $\sim 40L_\odot$ over all wavelengths, and the claim that this is appropriate for an A0V star at this distance.

Problems arise when one examines the details of these studies. For example, the conclusion of Jones *et al.* rests upon the assumption that all the stellar radiation effected by absorption and scattering is recovered, mainly in the far-IR. This is a very dubious assumption if there is a significant component of extinction due to cold, dark cloud material which would have an effect similar to interstellar extinction (i.e., luminosity is not totally "recovered"). Moreover, a value of 40 $L_\odot$ is more appropriate for an evolved A0V star, not a ZAMS A0 star for which $L \sim 30 L_\odot$ and which would probably be a more accurate representation of HD 97300.

The study of Thé *et al.* presents several difficulties. First, it should be noted that the Thé *et al.* study did not prove the existence of normal (R = 3.1) extinction toward HD 97300 and HD 97048 as indicated in subsequent comments by various authors. Rather, the study simply showed that normal extinction was consistent with the data if the multi-component extinction models and multi-dust shell models are appropriate along with a higher stellar luminosity. But significant problems are present with these models which may owe their success to the multiplicity of free parameters. First, a 2740K dust shell 0.1 A.U. from HD 97300 seems rather implausible. Even if carbon could survive in such a circumstance, it is difficult to understand how a static shell of this nature could exist. The complete absence of emission lines or other indicators of mass infall or mass outflow in HD 97300 suggests that this star has settled onto the ZAMS (possibly accompanied by a thin disk), a feature inconsistent with a close-lying dust shell. Second, the parameters derived for HD 97300 are not consistent with a ZAMS B9–A0 star which should exhibit $L \sim 30\text{–}35 L_\odot$ (Allen 1973). Although the effective temperature is appropriate, the radius computed by Thé *et al.* is probably too large by a factor of ~1.2. Third, the discrepancy in distances for HD 97300 (220pc) and HD 97048 (170pc) implies a very improbable cloud geometry and viewing angle. In this respect the sketch in Fig. 6 of Thé *et al.* is somewhat misleading. The angular separation of the two stars (i.e., representing the northern and southern blocks of Cha I) is about 1°, corresponding to a separation of ~3pc for a distance of 170pc. Since HD 97300 is computed to be 50pc more distant than HD 97048, the cloud would have to be very narrow (~3pc) and elongated (>50pc), viewed nearly along its elongated axis. The discrepancy in distances to the two stars may stem from a more fundamental difficulty, namely, the assumption that the intrinsic energy distribution of HD 97048 is amendable to the Kurucz (1979) models. This star is typed $A0_{pe}$, exhibiting emission lines indicative of pre-main sequence activity. It is thus risky to assume an intrinsic energy distribution which is more appropriate for a standard main sequence star.

The fundamental problem for distance estimates to Cha I using HD 97300 depends not only on the assumed value for R, but also on the bolometric luminosity of the star. It is possible to show that a distance of ~140pc is fully consistent with a 10500K ZAMS B9 star with $L \sim 35_\odot$, suffering an integrated extinction component (presumably mainly dark cloud extinction) with R~4. Using the observed energy distribution (0.12μm – 100μm) for HD 97300 in Thé *et al.* (after correcting the fluxes in their Fig. 3 for the foreground extinction component of $A_v = 0.36$), it is possible to derive the reddening curve required to achieve the observed flux distribution assuming that the intrinsic energy distribution is that of the Kurucz 10500K, log g = 4 model. The result is shown in Fig. 3, along with the

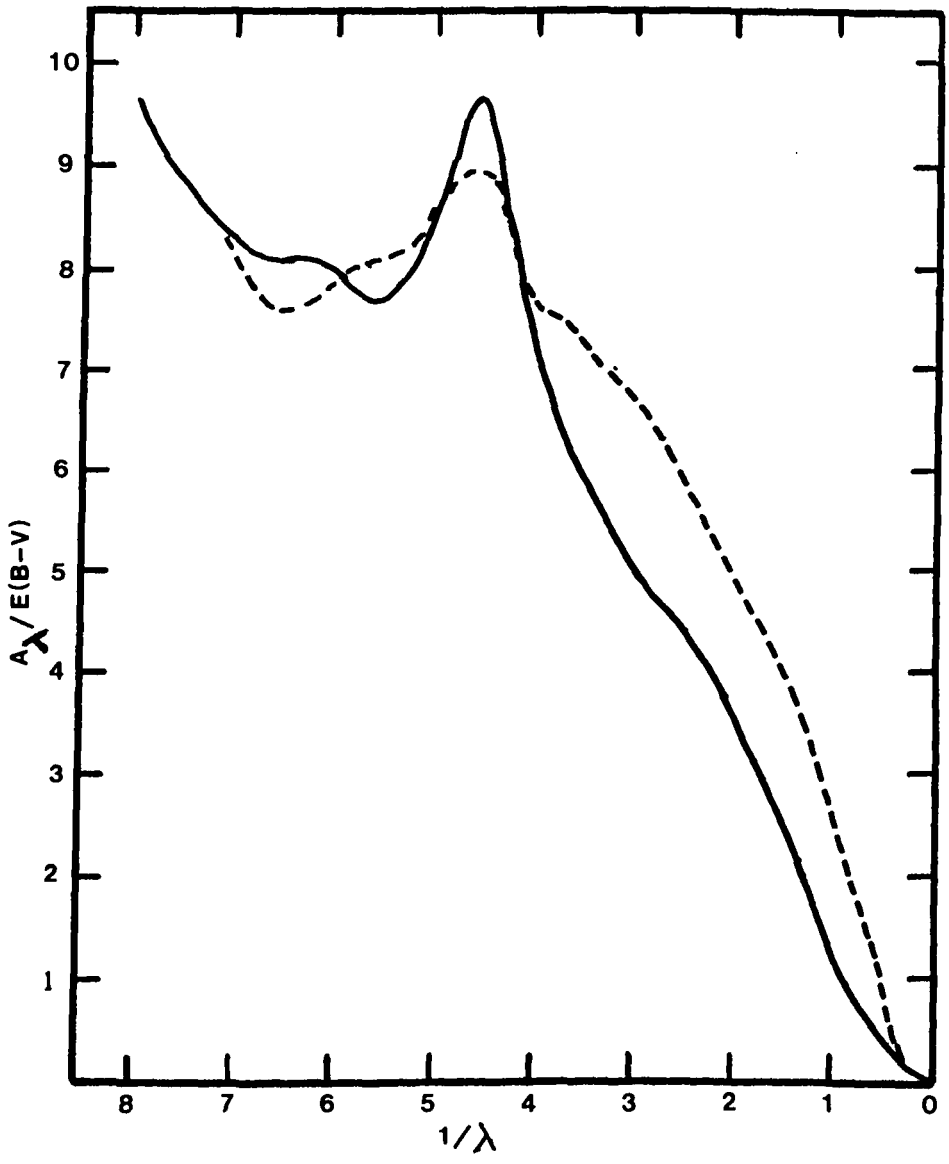

Figure 3. The normalized extinction curve (dashed-line) required to produce the observed flux distributions of HD 97300 [E(B–V) = 0.46] if it has the intrinsic energy distribution of a B9 ZAMS star with T_{eff} = 10500 K and L = $30L_{\odot}$ observed at a distance of 140 pc. The solid curve is the standard interstellar extinction curve of Savage and Mathis (1979). The dashed-line yields R ≅ 4.5.

standard interstellar extinction curve of Savage and Mathis (1979). The fit requires a higher ratio of total to selective extinction in the range 0.25μm – 3.5μm than that indicated by the standard curve. In particular, for the fit $A_v \cong 4.3$, and the "excess" flux in the J, H, K, and L bands is seen to result from the non-standard extinction of a ZAMS star. The upturn in fluxes at and beyond 5μm (see Fig. 3 of Thé *et al.*) is almost certainly due to dust heated by HD 97300, but at temperatures <300K.

For a distance of 140pc, the integrated 0.12μm – 135μm flux is $\sim 14 L_\odot$. The contribution at wavelengths greater than 135μm is estimated at $\sim 5 L_\odot$ using the extrapolation method of Cohen (1973) with Chavarría's (1981) amended constant. This suggests a "recoverable" luminosity of $\sim 19 L_\odot$. If HD 97300 is a B9 ZAMS star with $R \sim 1.8 R_\odot$ and T~10500K, its luminosity of $\sim 35 L_\odot$ implies that about 46% of its light is scattered and not recovered in the observations. This interpretation has the benefit of accounting for the observations without recourse to an excessively hot dust shell to generate near-IR radiation. Also, it is in agreement with the more recent work of Whittet *et al.* (1987) and Franco (1989, 1991) where detailed extinction studies toward the Cha clouds give persuasive evidence for significant extinction commencing at a distance of about 140pc. Of course the interpretation does require a rather non-standard extinction curve (although it is in general agreement with the value of R found by Vrba and Rydgren, 1984). It remains to be determined if there is any realistic size distribution and composition of grains which could produce the non-standard extinction. Concurrent with the analysis above which was drafted for the 1989 ESO Workshop on Low Mass Star Formation and Pre-Main Sequence Objects, Steenman and Thé (1989) re-evaluated the data on HD 97300 and HD 97048, concluding that abnormal extinction (R~5) is present, that a hot dust shell is not required for HD 97300, and that the data are consistent with a distance of 150±15pc. Thus there now appears to be a general agreement upon the distance to Cha I.

III. Chamaeleon II

A. Visible Members

The Cha II dark cloud has received only limited attention since Hoffmeister's (1962) work which identified three RW-Aur-like stars (BC, BK, and BMCha), and one BO Cep star (BFCha). Schwartz (1977) included this cloud in an objective prism Schmidt survey for Hα stars and HH objects. Nineteen Hα stars were identified, including the four stars found earlier by Hoffmeister. These objects are listed in Table 3 where column 1 contains a running T-number in the fashion of Table 1, column 2 lists various designations (see Table 1 references), column 3 lists the finder chart numbers (Fig. 4), columns 4 and 5 give the 1950 coordinates, column 6 the visual magnitude, and column 8 cross-identifications from the IRAS PSC (this study, Gregorio Hetem *et al.* 1988). The Schwartz (1977) survey also identified and listed coordinates for the objects HH 52–54 which are located in Fig. 4. It should be noted that approximate red mags and Hα emission-line strengths for the Hα stars are also contained in the 1977 survey article.

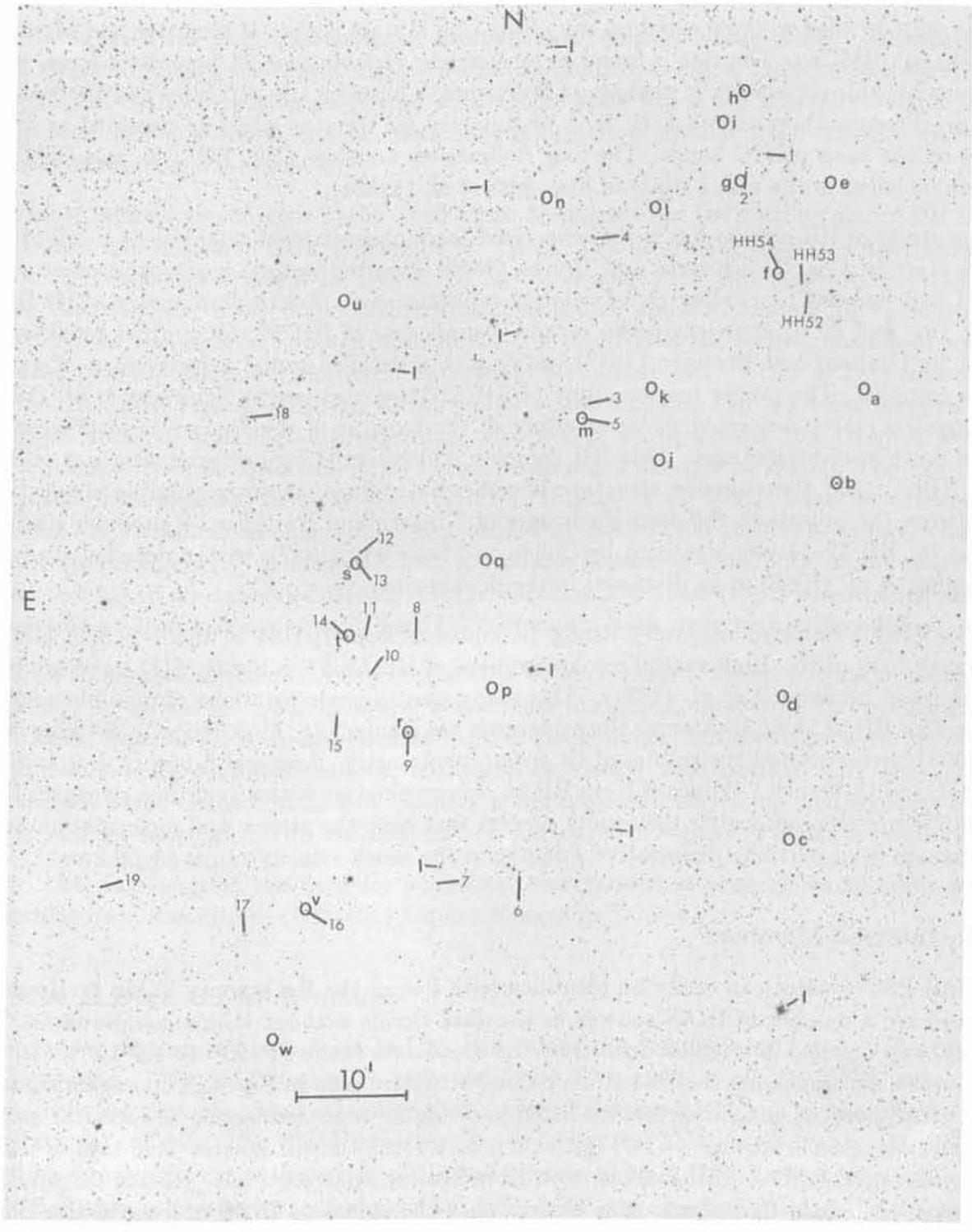

Figure 4. The Cha II Association adapted from Schwartz (1977). Stellar identifications are summarized in Table 3. IRAS source positions from the PSC are indicated with circles, and letter identifications are summarized in Table 4. Stars labeled with an "I" are IRAS sources but are probably not members of the association.

The only detailed work reported on any of the Cha II stars is that of Krautter and Mouchet (1983) on BMCha. The star is found to be strongly variable on a 24 hour time scale, with a possible anti-correlation in changes of line strength between the FeII lines and the Balmer lines. These authors report J, H, K, L photometry for the star which is classified as M0 – M1 on the basis of TiO bands. The four Hoffmeister variables (BC, BF, BK, and BMCha) were included in the $v \sin i$ study of Franchini *et al.* (1988a).

The group of HH objects has perhaps received more observational attention than all of the Hα stars in Cha II. Schwartz and Dopita (1980) reported optical spectrophotometry for HH 54B and 54C, including radial velocity computations. Spectrophotometry of [O I], [N II], Hα, and [S II] emission in the various components of HH 52, 53, and 54 was carried out by Graham and Hartigan (1988), along with a detailed radial velocity map of gas in the complex. The proper motion study of HH 52-54 carried out by Schwartz *et al.* (1984) suggested rather disjointed motions, although the baseline of the study was insufficient to pin down specific motions. This HH complex is dominated by low-excitation gas (I[S II] > I(Hα)), and the emission structure is somewhat diffuse, showing possible connections between the objects in the deep Hα images of Graham and Hartigan. A probable exciting star for HH 52–54 was identified by Cohen and Schwartz (1987), with a detailed study by Hughes *et al.* (1989) to be discussed in the next section.

Elias (1980) reported relatively strong IR emission from HH 54 in the 1–0 S(1) and Q-branch lines of H_2. High spatial resolution maps of HH 52–54 in the H_2 S(1) line have been published by Sandell *et al.* (1987). This study also suggests locations of possible exciting stars for HH 52 and 53, although the evidence is not compelling. Most recently, Wilking *et al.* (1990) have reported the results of IR spectrophotometry of several S-branch 1–0 and 2–1 lines, and Q–branch 1–0 lines of H_2 in HH 54. In combination with atomic line strengths from optical spectrophotometry, the results suggest that both the atomic and molecular emission emanate from partially dissociative J-shocks in the shock velocity range 40–50 kms^{-1}.

B. Infrared Members

IRAS PSC sources can easily be identified with five of the Hα stars in Table 1. However, there are a number of IRAS sources in the dark clouds without visible counterparts. The PSC was scanned in a region defined by the coordinate range $12^h\ 40^m$ to $13^h\ 10^m$, $-76°\ 20'$ to $-78°$, encompassing the Cha II dark cloud structure seen in Fig. 4. This region contains 34 IRAS sources, including the five listed in Table 3. A control region of identical area at the same galactic latitude ($-14°$) but at a galactic longitude 3° greater than that of Cha II reveals only 17 IRAS PSC sources, with 12 indicating relatively "hot" IR flux distributions typical of certain field stars. It is evident that the excess of IRAS sources in the Cha II block signals the presence of a number of cloud-associated sources. Measurement of IRAS source positions on the optical photograph of Cha II (Fig. 4) yields a list, given in Table 4, of far-infrared candidate members. Column 1 gives the IRAS identification, column 2 the identification letter for the position plotted on the finder chart (Fig. 4), columns 3 and 4 the 1950 coordinates, and column 5 the IRAS fluxes in Janskys. The list includes the sources

associated with Hα stars (Table 3), in addition to all sources whose colors and positions with respect to the dark clouds suggest cloud membership. Fig. 4 includes identification (letter I) of 8 IRAS sources associated with visible stars which are generally outside the cloud boundary and which exhibit colors more indicative of normal stars. These 8 sources are *not* incorporated in Table 4.

The most interesting source is 12496–7650 which is suggested as the exciting star of HH 52–54 (Cohen and Schwartz 1987, Hughes *et al.* 1989). The source (a) is located nearly dead center in a dense cloud about 14′ SW of HH 52–54. Hughes *et al.* have provided a detailed study (including J, H, K, L photometry) of this source and surrounding IRAS sources. Extended far-IR emission is noted both to the SW and NE of the source, consistent with the idea of a bipolar flow. Moreover, de Vries *et al.* (1984) find ^{12}CO(J = 2–1) emission in the HH 52–54 region, although the structure of the emission has not been mapped in sufficient detail to determine if it represents a portion of a true bipolar flow. Hughes *et al.* find a luminosity of 50L$_\odot$ for the IRAS source (assuming a distance of 200pc). The near-IR magnitudes are reported to be strongly variable. Hughes *et al.* (1991) have very recently reported the identification of an optical counterpart to IRAS 12496-7650. The object, a faint star of approximately 17th mag and with a probable history of variability, shows spectral characteristics of an embedded Herbig Ae star. Graham and Chen (1991) detected ice band absorption at 3μm in the star, and Knee (1992) found a weak molecular outflow there.

Figure 4 shows several other IRAS sources located within regions of high obscuration, notably sources j, k, q, and u. Sources k and u are most intriguing, indicating the presence of substantial, cool far-IR emission. Sources j and q, like a number of other sources in Table 4, exhibit only weak 100μm detections, and must be viewed with caution since they may represent infrared cirrus fluctuations. Sources b and h exhibit interesting far-IR colors, and are apparently associated with visible stars near the edges of regions of high obscuration.

The IRAS data suggest the need for additional observations at near-IR wavelengths and molecular line observations (CO, etc.) for key sources in Table 4.

C. Cha II Dark Cloud Structure

The general pattern of obscuration in Cha II contains the "thumbprint nebula" identified by Fitzgerald (1974) and studied in more detail by Fitzgerald *et al.* (1976) in which it was concluded that the cloud structure meets several criteria for clouds in the process of gravitational collapse. The Cha II structure is somewhat less homogeneous than the Cha I cloud structure. The extinction study of Gregorio Hetem *et al.* (1988) shows A$_v$ obscurations up to 5.5 mags in the darkest cloud near $12^h\ 50^m$, $-77°$, the cloud containing IRAS source 12496–7650. One should note apparent errors in Fig. 6 of Gregorio Hetem *et al.* which shows significant obscuration (A$_v \sim 5$) in a region near $12^h\ 43^m$, $-76.3°$. This structure does not appear in their Fig. 7, nor does it appear on direct plates.

The distance to the Cha II complex is an open question which will require additional obser-

vations. Its proximity to Cha I and its general cross-sectional area which is also comparable to Cha I lead to an impression that they could share the same distance. Indeed, King *et al.* (1979) suggest that the "thumbprint nebula" might be part of a much more extensive layer of material underlying the local galactic plane at an altitude of 40–80pc. If indeed both Cha I and Cha II are associated with such material as close as 40 pc to the plane, the galactic latitudes of the complex suggest distances of $\sim$ 150pc for Cha I and $\sim$ 165pc for Cha II. At 80pc altitude the distances would be doubled. The "broken layer" may well be scattered between 40 and 80pc, allowing a distance of $\sim$150pc for Cha I and a distance of $\sim$330pc for Cha II. However, this is entirely conjectural since the detailed distribution of material in this region is unknown. It should be noted, however, that Fitzgerald *et al.* (1976) arrived at a distance of 400pc for the "thumbprint nebula" on the basis of star counts. Also, favoring the idea of a greater distance is the fact that Hα stars in general give the appearance of being 1–2 mag fainter than their counterparts in Cha I, although this could be caused by a higher average obscuration for the Cha II stars in comparison with the Cha I stars.

IV. The Chamaeleon III Dark Cloud

The rather irregular distribution of obscuration in Cha III centered near $b^{II} = -17.5°$, $\ell^{II} = 302.5°$ is evident in the sketches of Feitzinger and Stüwe (1984) and Franco (1989, 1991). An objective prism survey of the cloud by Schwartz (1977) revealed no Hα emission stars. The exposure, however, was only half that used on the Cha II cloud, so very faint Hα stars could have been missed. At the same time, the extinction study of Gregorio Hetem *et al.* (1988) show most regions of the cloud with $A_v < 3$, with only one small patch near $12^h\ 50^m$, $-79.3°$ reaching $A_v \sim 5$. Evidently conditions in this cloud have not been appropriate for gravitational collapse. A scan of the IRAS PSC in the range $11^h\ 59^m$ to $13^h\ 15^m$, $-78°$ to $-81.5°$ reveals 63 sources, most of which are indicative of galactic background sources. A control region of the same area at the same galactic latitude but at $\ell^{II} = 306.6°$ reveals 55 IRAS sources. The difference of 8 sources probably has no statistical significance. In Cha III 22 of the sources are weak 100μm only detections, possibly reflecting infrared cirrus structure in the clouds. The control region shows 10 sources with 100μm only detections.

V. Summary

This review has presented lists of prospective association members in Cha I and Cha II, including the results of X-ray, visible (Hα), and infrared surveys. Updated finder charts have been presented, and short discussions of some of the more intriguing objects in these clouds are given. The distances to Cha I and Cha II are discussed in some detail. Although firm conclusions are not possible, existing data appear to be most consistent with the smaller ($\sim$ 140pc) distance to Cha I.

Acknowledgements

I would like to thank B. Reipurth for bringing to my attention several recent papers which I have used to update the original June, 1989 version of this review article. I am especially thankful to T. Prusti for providing preprints of the recent Assendorp *et al.* (1990), Whittet *et al.* (1990), and Wesselius *et al.* (1991) papers, and for providing some additional information for Tables 1 and 2. P.S Thé kindly provided a preprint of the Steenman and Thé (1990) work, and J. Graham communicated to me the results of the study of Hughes *et al.* (1991). Any glaring omissions involving other studies of the Chamaeleon clouds is solely the author's responsibility. The author acknowledges the assistance of NSF grant AST 8813917 in the preparation of this chapter.

References

Allen, C.W.: 1973, *Astrophysical Quantities*, 3rd ed., (Athlone Press: London), p. 200

Appenzeller, I.: 1977, *A&A* **61**, 21

Appenzeller, I.: 1979, *A&A* **71**, 305

Appenzeller, I., Jankovics, I., Krautter, J.: 1983, *A&AS* **53**, 291

Assendorp, R., Wesselius, P.R., Whittet, D.C.B., Prusti, T.: 1990, *MNRAS* **247**, 624

Baud, B., Young, E., Beichmann, C.A., Beintema, D.A., Emerson, J.P., Habing, H.J., Harris, S., Jennings, R.E., Marsden, P.L., Wesselius, P.R.: 1984, *ApJ* **278**, L53

Boulanger, J.D., Falgarone, E., Puget, J.L., Helou, G.: 1990, *ApJ* **364**, 136

Bouvier, J., Bertout, C.: 1989, *A&A* **211**, 99

Bouvier, J., Bertout, C., Benz, W., Mayor, M.: 1986, *A&A* **165**, 110

Cederblad, S.: 1946, *Medd. Lunds Astron. Obs.*, Series II, No. 119

Chavarría, K.-C.: 1981, *A&A* **101**, 105

Cohen, M.: 1973, *MNRAS* **164**, 395

Cohen, M., Schwartz, R.D.: 1984, *AJ* **89**, 277

Cohen, M., Schwartz, R.D.: 1987, *AJ* **316**, 311

Cohen, M., Dopita, M.A., Schwartz, R.D.: 1986, *ApJ* **307**, L21

De Vries, C.P., Brand, J., Israel, F.P., de Graauw, Th., Wouterloot, J.G.A., van de Stadt, H., Habing, H.J.: 1984, *A&AS* **56**, 333

Elias, J.H.: 1980, *ApJ* **241**, 728

Feigelson, E.D., Kriss, G.A.: 1989, *ApJ* **338**, 262

Feitzinger, J.V., Stüwe, J.A.: 1984, *A&AS* **58**, 365

Finkenzeller, U., Basri, G.: 1987, *ApJ* **318**, 823

Fitzgerald, M.P.: 1974, *A&A* **32**, 465

Fitzgerald, M.P., Stephens, T.C., Witt, A.N.: 1976, *ApJ* **208**, 709

Franchini, M., Magazzu, A., Stalio, R.: 1988a, *A&A* **189**, 132

Franchini, M., Magazzu, A., Stalio. R.: 1986b, erratum *A&A* **197**, 354

Franco, G.A.P.: 1989, IAU Coll. No. 120, *Structure and Dynamics of the Interstellar Medium*, eds. G. Tenorio-Tagle, M. Moles, J. Melnick, Springer-Verlag, p. 133

Franco, G.A.P.: 1991, *A&A*, in press

Gauvin, L.S., Strom, K.M.: 1991, preprint

Glass, I.S.: 1979, *MNRAS* **187**, 305

Glass, I.S., Penston, M.V.: 1975, *MNRAS* **172**, 227

Graham, J.A., Hartigan, P.: 1988, *AJ* **95**, 1197

Graham, J.A., Chen, W.P.: 1991, *AJ* **102**, 1405

Grasdalen, G., Joyce, R., Knacke, R.F., Strom, S.E., Strom, K.M.: 1975, *AJ* **80**, 117

Gregorio Hetem, G.C., Sanzovo, G.C., Lépine, J.R.D.: 1988, *A&AS* **76**, 347

Henize, K.G.: 1954, *ApJ* **119**, 459

Henize, K.G., Mendoza, E.E.: 1973, *ApJ* **180**, 115

Herbig, G.H., Bell, K.R.: 1988, *Lick Obs. Bull* No. 1111

Hoffmeister, C.: 1962, *Zs. f. Ap.* **55**, 290

Hughes, J.D., Emerson, J.P., Zinnecker, H., Whitelock, P.A.: 1989, *MNRAS* **236**, 117

Hughes, J.D., Hartigan, P., Graham, J.P., Emerson, J.P., and Marang, F.: 1991, *AJ* **101**, 1013

Hyland, A.R., Jones, T.J., Mitchell, R.M.: 1982, *MNRAS* **201**, 1095

Imhoff, C.L., Appenzeller, I.: 1987, *Scientific Accomplishments of the IUE* (ed. Y. Kondo), p. 295

Jones, T.J., Hyland, A.R., Harvey, P.M., Wilking, B.A., Joy, M.: 1985, *AJ* **90**, 1191

Kilkenny, D., et al.: 1985, *Circ. So. African Astr. Obs.* **9**, 55

King, D.J., Taylor, K.N.R., Tritton, K.P.: 1979, *MNRAS* **188**, 719

Knee, L.B.G.: 1992, in preparation

Krautter, J., Mouchet, M.: 1983, *A&A* **125**, 378

Kurucz, R.L.: 1979, *ApJS* **40**, 1

Mattila, K., Liljeström, T., Toriseva, M.: 1989, in ESO Workshop on *Low Mass Star Formation and Pre-Main Sequence Objects*, Proceedings No. 33, ed. B. Reipurth (ESO: Garching bei München), p. 153

Mundt, R., Bastian, U.: 1980, *A&AS* **39**, 245

Penston, M.V., Lago, M.T.V.T.: 1983, *MNRAS* **202**, 77

Prusti, T., Clark, F.O., Whittet, D.C.B., Laureijs, R.J., Zhang, C.Y.: 1991, *MNRAS* **251**, 303

Rydgren, A.E.: 1980, *AJ* **85**, 444

Sandell, G., Zealey, W.J., Williams, P.M., Taylor, K.N.R., Storey, J.M.V.: 1987, *A&A* **182**, 237

Savage, B.D., Mathis, J.S.: 1979, *ARA&A* **17**, 73

Scarrott, S.M., Warren-Smith, R.F., Wolstencroft, R.D., Zinnecker, H.: 1987, *MNRAS* **228**, 827

Schaefer, B.E.: 1983, *ApJ* **266**, L45

Schwartz, R.D.: 1977, *ApJS* **35**, 161

Schwartz, R.D., Dopita, M.A.: 1980, *ApJ* **236**, 543

Schwartz, R.D., Henize, K.G.: 1983, *AJ* **88**, 1665

Schwartz, R.D., Noah, P.: 1978, *AJ* **83**, 785

Schwartz, R.D., Jones, B.F., Sirk, M.: 1984, *AJ* **89**, 1735

Steenman, H., Thé, P.S.: 1989, *Ap&SS* **161**, 99

Thé, P.S., Wesselius, P.R., Tjin-A-Djie, H.R.E., Steenman, H.: 1986, *A&A* **155**, 347

Toriseva, M., Mattila, K.: 1985, *A&A* **153**, 207

Toriseva, M., Höglund, B., Mattila, K.: 1985, *Rev. Mex. Astron. Astrofis.* **10**, 135

Vrba, F., Rydgren, A.E.: 1984, *ApJ* **283**, 123

Wesselius, P.R., Beintema, D.A., Olnon, F.M.: 1984, *ApJ* **278**, L37

Wesselius, P.R., Prusti, T., Whittet, D.C.B., Assendorp, R.: 1991, in Proceedings of the 7th Manchester Astronomical Conference on *Molecular Clouds*, p. 149

Whittet, D.C.B., Kirrane, T.M., Kilkenny, D., Oates, A.P., Watson, F.G., King, D.J.: 1987, *MNRAS* **224**, 497

Whittet, D.C.B., Prusti, T., Wesselius, P.R.: 1991, *MNRAS* **249**, 319

Wilking, B.A., Schwartz, R.D., Mundy, L.G., Schultz, A.S.B.: 1990, *AJ* **99**, 344

Table 1

Chamaeleon I Association – Optical Candidate Members

ID ChaI	Other[1] Designations	Finder Chart	R.A. (1950)	Dec. (1950)	V	Spectral Type	IRAS[2] Far-IR	Near-IR[3] refs
T1	Sz1	1	$10^h\ 50^m\ 54.7^s$	−76° 53′ 52″				
T2	SWCha, S6319		10 53 24	−77 39 18		M0:		
T3	SXCha, S6320	2	10 54 49.7	−77 08 36	14.65	M0.5	10548-7708	1
	HM1, Sz2, HBC564							
T4	SYCha, S6321, HM2	3	10 55 18.5	−76 55 35	13.03	M0:	10552-7655	1
	Sz3, HBC565, CHX1							
T5	Sz4	4	10 56 27.5	−76 43 30				
T6	SZCha, S6323, Glass V	4a	10 57 05.7	−77 01 17:	11.99	K0	10570-7701	1,2
	HBC566, CHX2							
T7	TWCha, S6326	5	10 57 47.2	−77 06 34	13.08		10577-7706	1, 2, 3
	HM3, Sz5, HBC567							
T8	LHα332-20, HM4	6	10 57 50.8	−76 45 33	11.22	K2(Li)	10578-7645	1, 3
	Sz6, HBC244, CHX3							
T9	HM5, Sz7	7	10 58 54.9	−76 28 07			10589-7628	1
T10	HM6, Sz8	8	10 59 18.2	−76 03 18				1
T11	CSCha, HM7	9	11 01 07.8	−77 17 25	11.63	K5:	11011-7717	1, 3
	Sz9, HBC569, CHX4						B24	
T12	HM8, Sz10	10	11 01 36.2	−77 05 39				1
T13	TZCha, S6334	10a	11 02 28	−76 39 36				
T14	CTCha	11	11 02 43.6	−76 11 06	12.36	K7:	11027-7611	1, 3
	HM9, Sz11, HBC570							
T14a	HH48	HH48	11 03 01.9	−77 01 55			11030-7702	
T15	HM10, Sz12	12	11 03 03.8	−77 09 36				1
T16	Sz13	13	11 03 35.0	−76 59 44				
T17	UUCha, S6335	13a	11 03 57	−76 14 24				
T18	Sz14	14	11 03 56.5	−77 36 40				
T19	Sz15	15	11 04 22.4	−77 38 30				
T20	UVCha, S6336	15a:	11 04 25.2	−76 02 00:	13.79			
	HBC571							
T21	Glass F, Ced 110	15b	11 04 52.4	−77 05 41	11.28	G:	11048-7706	1
	CHX7						B32	
T22	UXCha, S6337, CHX8	15c:	11 05 15	−77 10 30			B33?	
T23	UYCha, S6340	16	11 05 34.8	−77 02 38			B34	
	HM11, Sz16							
T24	UZCha, S6341, Sz17	17	11 05 43.6	−76 16 06	14.90			
T25	HM12, Sz18, HBC572	18	11 05 48.1	−75 46 47	15.35	M2,3	11057-7546	1
T26	CoD-76° 486, HM13	19	11 05 57.5	−77 21 50	10.68	G2V(Li)	11059-7721	1,3,4
	Sz19, HBC245, CHX9						B37?	
T27	VVCha, S6342	20	11 06 01.1	−76 35 55	14.80	M1.5		1
	HM14, Sz20, HBC573							
T28	HM15, Sz21, HBC574	21	11 06 20.4	−77 23 25	15.34	M0.5		1
T29	HM16, Sz22	22	11 06 34.3	−77 22 28	14.2		B37?	1,6
T30	Sz23, CHX11:	23	11 06 34.8	−77 26 24			B41?	
T31	VWCha, S6343, HM17	24	11 06 38.1	−77 26 12	12.51	K2	B41?	1,2
	Sz24, HBC575, CHX11:							
T32	HD97048, HM18	25	11 06 39.6	−77 23 01	8.45	A0pe	11066-7722	1,3,4
	Sz25, HBC246n, Ced 111						B37, WBO	
T33	Glass I, CHX12	25a	11 06 50.2	−77 17 31			11068-7717	1
							B40?	

Table 1 (continued)

Chamaeleon I Association – Optical Candidate Members

ID ChaI	Other[1] Designations	Finder Chart	R.A. (1950)	Dec. (1950)	V	Spectral Type	IRAS[2] Far-IR	Near-IR[3] refs
T34	HM19, Sz26	26	$11^h\ 06^m\ 52.9^s$	−77° 28′ 20″				1
T35	HM20, Sz27, HBC576	27	11 07 12.5	−76 59 47	16.28		B42	5, 6
T36	VXCha, S6345	27a	11 07 19	−76 28 12				
T37	Sz28	28	11 07 20.0	−76 08 55				
T38	VYCha, S6346 HM21, Sz29, HBC577	29	11 07 26.6	−76 45 55	17.5:	M0.5		1, 5
T39	Sz30, CHX14	30	11 07 45.9	−77 12 55	13.17			
T40	VZCha, S6347 HM22, Sz31, HBC578	31	11 07 51.9	−76 07 02	12.75	K6	11078–7607	1, 3
T41	HD 97300, Ced 112	31a	11 08 17.9	−76 20 30		B9V	11082–7620 WBO, J	5, 8
T42	HM23, Sz32, HBC579	32	11 08 21.9	−76 18 06			11083–7618	5, 6
T43	Sz33, CHX15:	33	11 08 22.1	−76 13 06			J(C1–17)	7
T44	WWCha, S6348, HM24 Sz34, HBC580, CHX16	34	11 08 28.5	−76 18 38	13.27	K5:		1, 3, 5
T45	WXCha, S6349, HM25 Sz35, HBC581, CHX17	35	11 08 32.2	−77 20 50	14.86	K7, M0	11085–7720 B44	5, 6
T45a	GK-1, HBC582	35a	11 08 33.2	−76 19 25	14.34	M0		6
T46	WYCha, S6351, HM26 Sz36, HBC583, CHX15:	36	11 08 34.8	−76 13 18	13.98	K7,M0	11085–7613	1, 7
T47	HM27, Sz37, HBC584	37	11 09 20.4	−77 01 32	15.54	K7:	11093–7701 B46	6
T48	WZCha, S6352 HM28, Sz38, HBC585	38	11 09 20.6	−76 18 12	15.26	M1		1, 7
T49	XXCha, HM29, Sz39 HBC586, CHX18	39	11 10 05.0	−76 03 53	15.28	M2	11101–7603	1
T50	Sz40, HBC587	40	11 10 35.6	−76 18 14		K0		5
T51	Sz41, HBC588, CHX20:	41	11 10 50.2	−76 20 45	11.60	K0	11108–7620	5
T52	CVCha, LHα 332-21, HM30, Sz42, HBC247, CHX19:	42	11 10 53.8	−76 28 01	10.96	G8V(Li)	11108–7627	
T53	CWCha, HM31, Sz43, HBC589, CHX19:	43	11 10 57.1	−76 28 02	14.45	G:		1, 3, 5
T54	HMAnon, CHX22	43a	11 11 09.6	−77 05 48	11.16		11111–7705 B50	
T55	Sz44	44	11 11 57.8	−76 19 15				5
T56	HM32, Sz45, HBC590	45	11 15 58.4	−76 48 12	13.50	M0.5	11159–7648	1

[1]Other Designations

Sz: Schwartz (1977)
S: Hoffmeister (1962)
HM: Henize and Mendoza (1973)
HBC: Herbig and Bell (1988)
Glass: Glass (1979)
LHα: Henize (1954)
Ced: Cederblad (1946)
CHX: Feigelson and Kriss
GK: Appenzeller *et al.* (1983)

[2]IRAS, Far-IR references:

IRAS Point Source Catalog
B: Baud *et al.* (1984)
WBO: Wesselius *et al.* (1984)
J: Jones *et al.* (1985)

[3]Near-IR references:

1. Glass (1979)
2. Glass and Penston (1974)
3. Grasdalen *et al.* (1975)
4. Kilkenny *et al.* (1985)
5. Hyland *et al.* (1982)
6. Appenzeller *et al.* (1983)
7. Jones *et al.* (1985)
8. Thé *et al.* (1986)

Table 2

Chamaeleon I Association
Candidate IR Members Not Associated with Visible Stars

ID[1]	R.A. (1950)	Dec. (1950)	J, H, K, L (mags)				IRAS Fluxes (Jy) [12]	[25]	[60]	[100]	Notes[2]
B23	$11^h\ 00^m\ 30^s$	−77° 27.7′						0.15	0.22	2.34	
B29	11 03 41	−77 25.3						0.08	0.30		
B31	11 05 03	−77 18.1						0.04	0.37	12.1	
B35	11 05 55	−77 06.3					0.47	1.97	8.62	82.5	1
B38	11 06 32	−77 01.1					0.23	0.28	0.34		
B40	11 06 52	−77 16.1					9	20	>30	C	3
IRN	11 07 15.1	−77 27 35			8.10	6.12	11.6	83.1	233.3	250.1	2
C9–1	11 07 25.6	−77 27 23	13.84	11.98	10.66						
C1–15	11 07 43.1	−76 12 30	12.02	11.26	10.95						
C1–18	11 07 44.6	−76 14 15	12.00	10.26	9.20						
C1–6	11 07 49.5	−76 18 19	13.26	10.76	9.22						
C1–25	11 08 10.8	−76 18 45	13.97	11.53	10.12						
C2–3	11 08 12.7	−76 27 38	12.00	10.81	10.20						
C1–24	11 08 14.8	−76 18 37	12.19	10.79	10.08						
C7–1	11 08 15.5	−77 09 43	12.43	11.19	10.61						
C1–2	11 08 20.7	−76 16 24	13.24	10.73	9.25						
B43	11 08 24	−77 10.0					0.07	0.14	0.28	C	3
C7–11	11 09 08.2	−77 16 34	9.83	8.78	8.29		0.27	0.41	0.28		4
C2–5	11 09 21.5	−76 29 16	11.39	10.47	9.97						
B47	11 09 39	−77 10.0					0.07	0.10	0.23	C	3

[1]Designations
B: Baud *et al.* (1984)
C: Hyland *et al.* (1982), Jones *et al.* (1985)

[2]Notes

1. Probable exciting star for HH 49/50.
2. Source associated with the "Infrared Nebula", Schwartz and Henize (1983). Position and photometry from Cohen and Schwartz (1984). (=C9–2,3 in Hyland *et al.* 1982; = IRAS 11072-7727=B41?)
3. Confusion at 100μm.
4. IRAS fluxes from PSC, source 11091-7716. Although Hyland *et al.* (1982) do not list an optical association, the position is coincident with a prominent star 5.7′ SE of T39 (Sz30, See Fig. 1). See also Hetem *et al.* (1988).

Table 3

Chamaeleon II Association - Optical Candidate Members

ID Cha II	Other Designations	Finder Chart	R.A. (1950)	Dec. (1950)	V[1]	IRAS	Notes[2]
T1	Sz46	1	$12^h\ 52^m\ 52.9^s$	−76° 29′ 33″	14.32		
T2	Sz47	2	12 53 17.2	−76 30 54			
T3	Sz48	3	12 57 05.7	−76 53 00			
T4	Sz49	4	12 57 06.9	−76 38 06			
T5	Sz50	5	12 57 07.4	−76 54 13		12571−7654	
T6	BCCha, S6428 Sz51, HBC593	6	12 58 05.7	−77 35 13	14.49v		1
T7	Sz52	7	13 00 28.5	−77 36 25			
T8	Sz53	8	13 01 17.6	−77 14 48			
T9	BFCha, S6437, Sz54	9	13 01 24.6	−77 22 57	12.43v	13014−7723	2
T10	Sz10	10	13 02 33.6	−77 17 58			
T11	Sz56	11	13 02 42.1	−77 14 33			
T12	Sz57	12	13 03 00.3	−77 07 08			
T13	Sz58	13	13 03 01.0	−77 07 39		13030−7707	
T14	BKCha, S6443,Sz59	14	13 03 11.8	−77 14 29	14.97v	13031−7714	1
T15	Sz60	15	13 03 24.9	−77 21 21			
T16	BMCha, S6445 Sz61, HBC594	16	13 04 04.9	−77 39 04	14.96v	13040−7738	1,3
T17	Sz62	17	13 05 46.6	−77 41 25	15.35v		
T18	Sz63	18	13 06 05.5	−76 54 47			
T19	Sz64	19	13 09 55.2	−77 37 14			

[1]Visual magnitudes from Schwartz and Noah (1978) which contains full U, B, V, R mags. A "v" indicates strong variability.

[2]Notes:

1. Hoffmeister (1962) classifies as RW Aur-like star.
2. Hoffmeister (1962) classifies as BO Cep-like star.
3. Listed as M0-M1 by Krautter and Mouchet (1983).

Table 4

Chamaeleon II Association – Far Infrared Candidate Members

IRAS	Finder Chart	R.A. (1950)	Dec. (1950)	IRAS Fluxes (Jy) [12]	[25]	[60]	[100]	Notes
12496-7650	a	$12^h\ 49^m\ 38.0^s$	$-76°\ 50'\ 45''$	39.3	85.6	104.9	87.4	1
12500-7658	b:	12 50 03.0	-76 58 49		1.01	2.72		2
12506-7730	c:	12 50 39.3	-77 30 52				4.36	3
12510-7718	d:	12 51 04.2	-77 18 34				3.12	3
12510-7631	e	12 51 05.7	-76 31 36				3.44	3
12522-7640	f	12 52 12.4	-76 40 01			.59		4
12533-7632	g	12 53 19.3	-76 32 12			.83		
12535-7623	h	12 53 30.6	-76 23 57	.47	.55	.26	3.57	2
12539-7627	i	12 53 57.6	-76 27 02				7.60	3
12551-7657	j	12 55 07.1	-76 57 20				4.19	3
12553-7651	k	12 55 20.3	-76 51 22	.62	3.82	9.68		
12554-7635	l	12 55 29.5	-76 35 00				3.16	3
12571-7654	m	12 57 07.6	-76 54 31		.52	.86	5.82	=T5
12583-7634	n:	12 58 19.9	-76 34 59				2.26	3
12591-7719	p	12 59 10.5	-77 19 09				3.28	3
12594-7707	q	12 59 24.6	-77 07 32				3.93	3
13014-7723	r	13 01 27.9	-77 23 16	.36	.35		3.65	=T9
13030-7707	s	13 03 03.3	-77 07 52	.40	.47	.74	3.00	=T13
13031-7714	t	13 03 09.4	-77 14 08	.33	.30	.39		=T14
13036-7644	u	13 03 41.4	-76 44 03		1.05	6.38	22.57	
13040-7738	v	13 04 02.7	-77 38 44	.68	.77	.78		=T16
13047-7750	w	13 04 43.5	-77 50 11				4.27	3

Notes:

1. Exciting star for HH52-54 (Cohen and Schwartz 1987, Hughes *et al.* 1989).
2. Associated with prominent star at edge of dark cloud.
3. Weak, 100μm sources only may be due to IR cirrus.
4. Possibly due to dust and/or [OI] 63μm emissions in HH 54 (see Hughes *et al.* 1989).

The Southern Coalsack: Where are all the Young Stars?

L.-Å. Nyman

SEST Project
European Southern Observatory
Casilla 19001, Santiago 19
Chile

Summary

The Southern Coalsack is the most prominent, isolated dark cloud in the southern Milky Way. It is situated on the Galactic equator at $l = 303°$ and has a diameter of about 6°. The visual extinction over the cloud varies between 1 and 3 magnitudes but can be much higher in small condensations and globules. From photometric studies the distance to the Coalsack has been estimated to $\sim$ 180 pc. A CO (1–0) survey of the whole cloud shows that it is very fragmented, consisting of clumps and filaments, and the total mass is estimated to $\sim 3500 M_{\odot}$. A cloud of this size and mass would be expected to contain young stars, but so far none has been found (except maybe one object), although searches have been made for T Tauri stars, flare stars, and HH objects. There are also several IRAS point sources with the color-color characteristics of embedded young stellar objects in the direction of the Coalsack. Some of them, however, are associated with a massive background molecular cloud, and there is no evidence that the others are located within the Coalsack.

1. Extinction and globules

The Coalsack is an irregular, inhomogeneous cloud (see Fig. 1) with an average visual extinction between 1 and 3 magnitudes although it can be much higher in some regions (Unsöld, 1929; Müller, 1934; Rodgers, 1960; Mattila, 1970; Tapia, 1973). The existence of globules in the Coalsack was first noted by Westerlund (1960) who found regions of high extinction in the northern part of the nebula. Tapia (1973) found six globules in four selected areas, of which his globule no 2 is the densest globule in the cloud. It has been studied extensively by several groups and will be described in detail below. Positions of globules in the Coalsack have been published by Bowers et al. (1980) and as part of catalogs of globules in the southern sky by Hartley et al. (1986), Sandqvist and Lindroos (1976), and Sandqvist (1977). The 23 globules listed in Bowers et al. (1980) are part of a list of 27 globules mentioned in Bok et al. (1977).

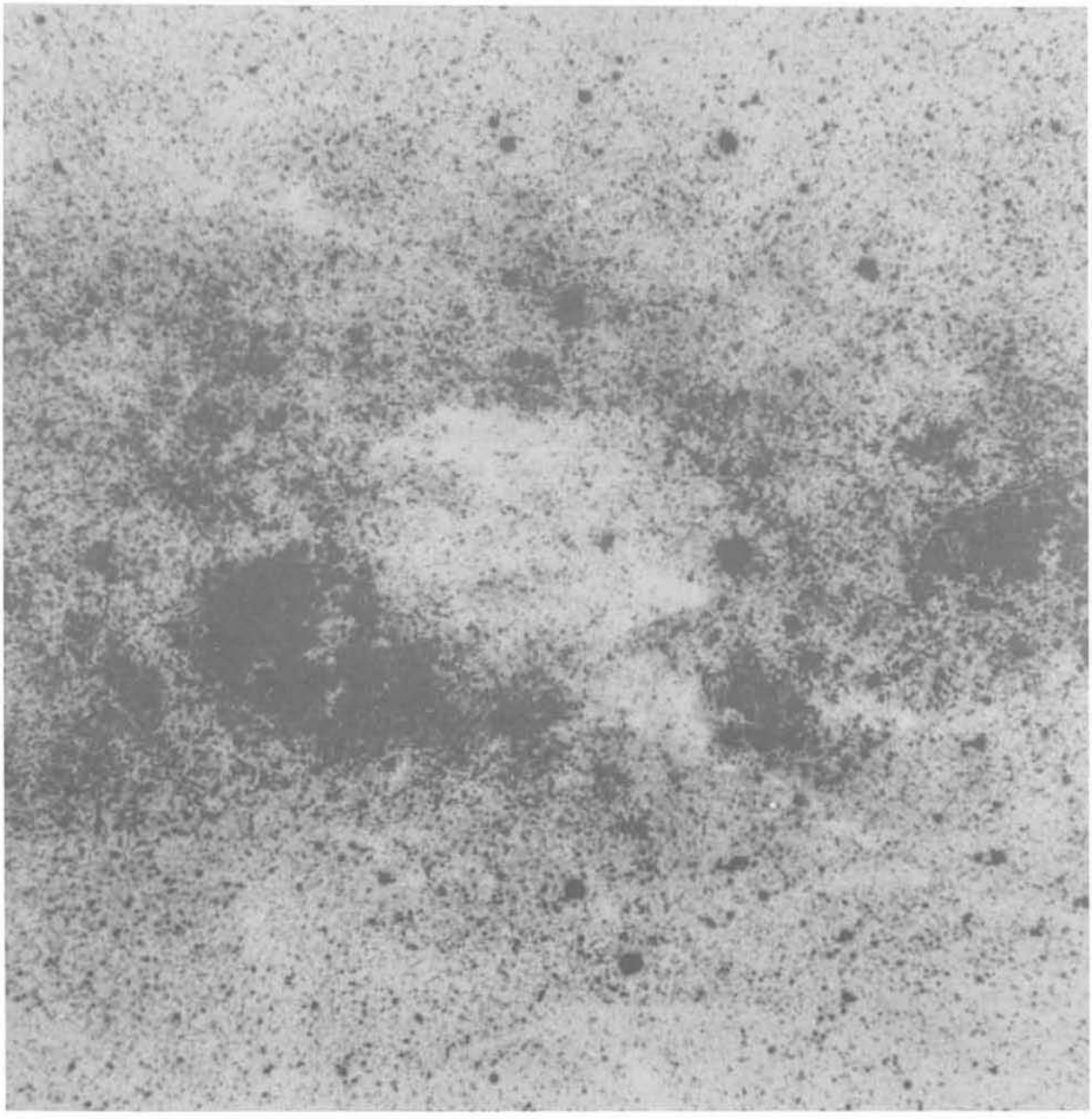

Figure 1: A photograph of the Coalsack kindly supplied by C. Madsen. It is part of a panorama of the Milky Way published in "Exploring the Southern Sky" (Laustsen, Madsen, West; Springer–Verlag.

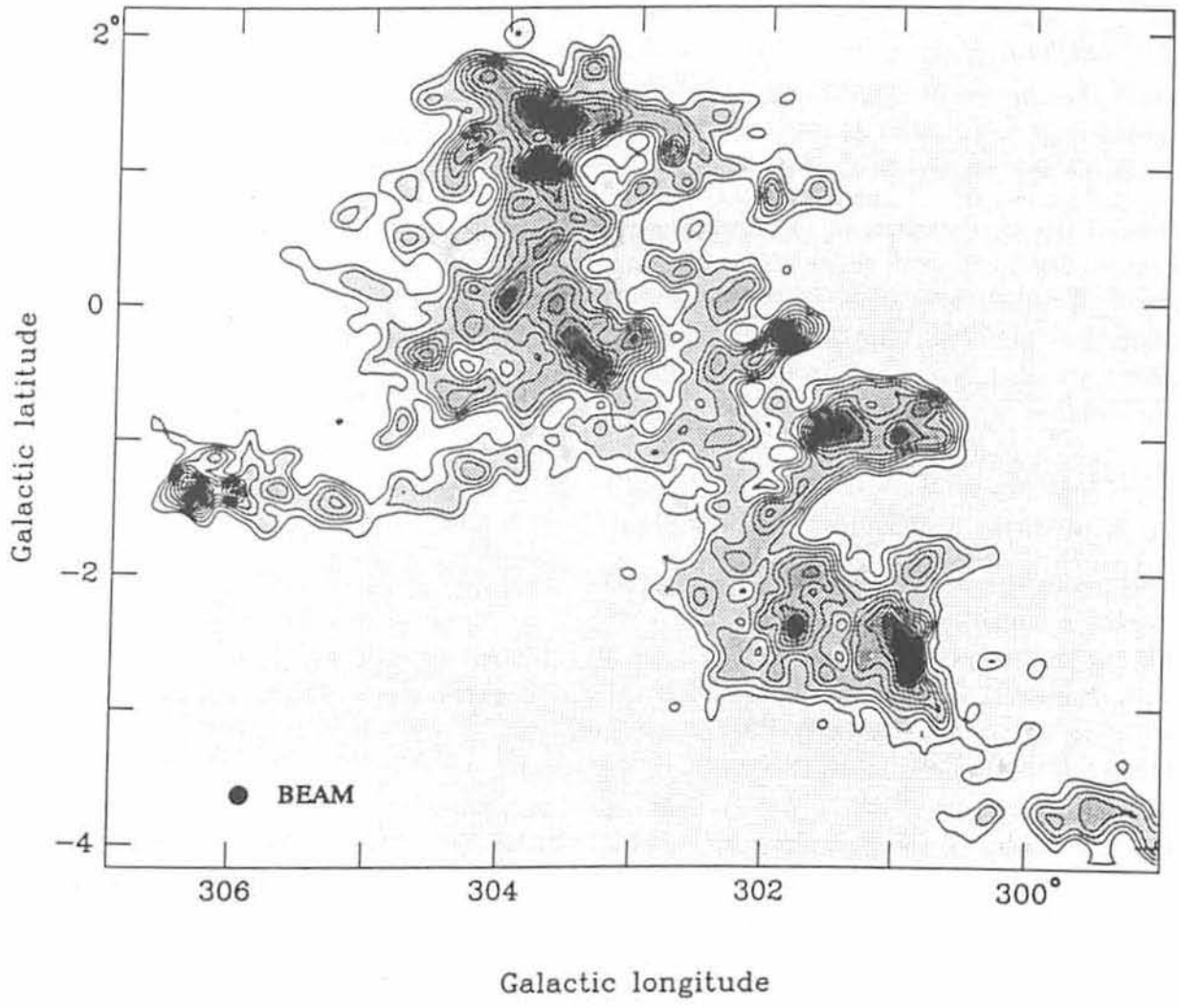

Figure 2: Map of the velocity integrated CO (1-0) emission from the Coalsack (Nyman et al., 1989). The integration interval is from -10 to 8 kms^{-1}, contours are from 2 K kms^{-1} in steps of 1 K kms^{-1}.

2. Distance

The distance to the Coalsack has been determined from photometric studies described in several papers:

1) Rodgers (1960) estimates the distance to 174 ± 18 pc.

2) Seidensticker and Schmidt–Kaler (1989) concludes that the Coalsack is mainly composed of two clouds, one at a distance of 188 pc, the other at 243 pc.

3) Franco (1989) gives an upper distance estimate of 180 ± 26 pc to the main parts of the cloud, although he finds some evidence suggesting the presence of absorbing material as near as 120 pc.

In conclusion, the distance to the Coalsack seems to be $\sim$ 180 pc although some parts of the nebula may be situated as near as 120 pc and others as far as 240 pc. Assuming a distance of 180 pc the linear extent of the cloud is $\sim$ 20 pc.

Behind the Coalsack is an interarm region extending out to $\sim$ 1000 pc (Rodgers, 1960; Franco, 1989) beyond which the reddening suggests the presence of a massive molecular cloud. This background cloud is seen in a CO survey of molecular clouds in the Carina arm (Cohen et al., 1985; Grabelsky et al., 1987), and is situated in the near side of the arm. There are also two clouds in the far side of the arm, at a distance of about 14 kpc, which are situated in the direction of the Coalsack.

3. Molecular and atomic gas

A complete survey of the CO (1–0) emission from the Coalsack with a resolution of 8.8′ has been made by Nyman et al. (1989). A map of the integrated CO intensity is shown in Figure 2. The CO distribution clearly reveals the very complex appearance of the Coalsack with many clumps and filaments. Several parts of the cloud have multiple line profiles with up to 3 or 4 lines at velocities between -8 and $+2$ kms^{-1}. The upper part has a more positive velocity than the lower part, suggesting that they may be situated at slightly different distances. There is a very good agreement between the optical extinction and the CO intensity, and the globules are generally situated on or near the peaks of CO emission. The total mass of the Coalsack was found to be $\sim 3500 M_{\odot}$, derived from the relation between CO intensity versus molecular hydrogen column density (Bloemen et al., 1986). The CO excitation temperature was found not to exceed 11 K and the lines are narrow, typically 1.0–1.3 kms^{-1}. The CO (1-0) emission in a 27′ by 21′ region around $l = 303.7, b = 0.9$ has been mapped by Wang and Otrupcek (1989) with a resolution of 2.7′, including the dark cloud DC303.6+0.9 in the list of Hartley et al. (1986). The CO line profiles typically consist of two components in agreement with the data of Nyman et al. (1989). Bowers et al. (1980) have searched for neutral hydrogen self absorption features toward 23 globules. HI features were found only in the western part of the nebula, which is the region of the highest extinction and where the densest globule is situated (see below). This is also the place of

the strongest CO emission.

4. The densest region

The densest region in the Coalsack is situated in its western part, centered around $l = 301°$, $b = -1°$ (see Fig. 2). The region seems to consist of a lower density medium with an average visual extinction of 3–5 mag (Rodgers, 1960; Tapia, 1973; Jones et al., 1984) in which globules no 1, 2, and 3 in Tapia's list are embedded. An extinction map over 1 square degree of this region has been made by Gregorio Hetem et al. (1988). They found four high extinction cores with $A_V > 3$ mag, the three largest corresponding to the three globules. This part of the Coalsack has been mapped with 8.8′ resolution in CO (1-0) and ^{13}CO (1-0) by Nyman et al. (1989), and in CO (1-0) with a resolution of 2.7′ by Otrupcek and Wang (1987). Previous CO observations have been made by de Vries et al. (1984) who made a CO (2-1) strip map across the globules and by Huggins et al. (1977) who observed the 1-0 line at six positions close to the globules. Bowers et al. (1980) found an HI self absorption feature extended over the region. The CO and HI observations give similar results:

i) there is no enhancement of the CO emission or the HI absorption toward the globules, implying that the surrounding gas and not the globules themselves are probed by these lines,

ii) the spatial distribution of the line intensities has a sharp edge in the west and a gradual decline toward east in good agreement with the distribution of the extinction,

iii) the lines have an almost constant velocity of about -6 kms^{-1} toward the globules and a well defined velocity gradient of 0.5 kms^{-1}pc^{-1} eastward.

The globules do not appear in the ^{13}CO observations which could be due to the low resolution of those observations. The ^{13}CO optical depths, however, are fairly high, between 0.3 and 0.9, and have a smooth distribution over the globules, suggesting that also here we mainly see the surrounding gas. Observations of H_2CO and OH (Sinclair and Brooks, 1972; Brooks et al., 1976), however, show that the H_2CO distribution agrees quite well with that of the globules, while the OH emission is more widespread but has a peak close to globule 2, indicating that these molecules probe the inner part of the globules.

5. Globule no 2

The densest globule in the Coalsack is globule no 2 in Tapia's list. It has been investigated by means of star counts and is found to have a diameter of about 6′ (Bok et al., 1977) and a central visual extinction of about 20 mag (Bok, 1977). Bok et al. (1977) derive a mass of the globule that can be as high as $25M_\odot$. Using near infrared photometry, spectroscopy, and polarimetry Jones et al. (1984) find no sign of a central density enhancement in the globule down to a level of 15″, a gas and dust temperature ≤ 10 K, and weak evidence of a mildly compressed magnetic field. They derive a mass of the globule of $\sim 12M_\odot$, which is about

half the value estimated by Bok et al., mainly because a "background" visual extinction of 5 mag was removed before calculating the mass. There is no evidence that the globule is collapsing neither from its density structure nor from the shapes of the observed radio lines. It is possible that the globule is supported by turbulence or a magnetic field. There is no evidence for a protostellar object or a young cluster associated with it (Jones et al., 1980). Nyman et al. (1991) mapped the globule in the CO (1–0), ^{13}CO (1–0), C^{18}O (1–0), and CS (2–1) lines with the Swedish-ESO Submillimetre Telescope (SEST, described in Booth et al., 1989). They found a CO excitation temperature of 12 K, that the C^{18}O and CS line intensities are peaked toward the center of the globule, and they derived a mass of $\sim$10 M$_\odot$ for the globule.

6. Star formation

In a cloud as massive as the Coalsack one would expect to find some evidence of recent star formation. However, no young stellar objects were found in searches for Hα emission objects such as T Tauri stars, flare stars, and HH objects (Andrews, 1972; Weaver, 1973, 1974a, 1974b; Schwartz, 1977; Gahm and Malmort, 1980; Reipurth, 1981), although it is not clear whether some of the flare stars are young or not. Recently Eaton et al. (1990) discovered that the object Re 10 (Reipurth, 1981) in the direction of the Coalsack is a bipolar reflection nebula, with a central object that is obscured by a circumstellar disc. It is not clear, however, if this object is associated with the Coalsack.

It is difficult to investigate the presence of IRAS point sources in the Coalsack because it is situated in the Galactic plane, which gives a high confusion particularly at 100μm. However, Nyman et al. (1989) found about 200 point sources with the color-color characteristics of young stellar objects toward the Coalsack. Most of these sources outline the massive background molecular cloud in the Carina arm behind the upper part of the Coalsack. Toward the lower part they found 6 point sources within the 2 K kms^{-1} CO contour, but none of them are situated near a CO peak or a dark globule. Gregorio Hetem et al. (1988) list 10 IRAS sources in the western part of the cloud that could be young stellar objects, however none of them have any known optical counterpart. To find out if there are any molecular outflows or dense cores associated with the IRAS sources, Nyman et al. (1991) have observed the CO (1-0), C^{18}O (1-0), and CS (2-1) lines with the SEST in the direction of 25 IRAS point sources toward the Coalsack, three of which are the first three sources listed in Gregorio Hetem et al. (1988). There is no evidence for an outflow or a dense core toward any of the objects. Some of them turn out to be associated with HII regions in the background molecular cloud.

The reason for the absence of star formation in the Coalsack is not clear. It maybe one of the few larger clouds where star formation has not yet started, perhaps because of lack of some external triggering mechanism or because the globules are stable against collapse due to turbulence and/or magnetic fields. Note that there is no evidence for collapse or the presence of any young stellar objects in the densest globule.

Further sensitive searches for and studies of Hα emission objects should be done to truly investigate if there is no star formation taking place in the cloud.

References

Andrews, A.D.: 1972, *Bol. Obs. Tonantzintla and Tacubaya No 38* **6**, 179

Bloemen, J.B.G.M., Strong, A.W., Blitz, L., Cohen, R.S., Dame, T.M., Grabelsky, D.A., Hermsen, W., Lebrun, F., Mayer-Hasselwander, H.A., Thaddeus, P.: 1986, *Astron. Astrophys.* **154**, 25

Bok, B.J.: 1977, *Publ. Astron. Soc. Pac.* **89**, 597

Bok, B.J., Sim, M.E., Hawarden, T.G.: 1977, *Nature* **266**, 145

Booth, R.S., Delgado, G., Hagström, M., Johansson, L.E.B., Murphy, D.C., Olberg, M., Whyborn, N.D., Greve, A., Hansson, B., Lindström, C.O., Rydberg, A.: 1989, *Astron. Astrophys.* **216**, 315

Bowers, P.F., Kerr, F.J., Hawarden, T.G.: 1980, *Astrophys. J.* **241**, 183

Brooks, J.W., Sinclair, M.W., Manefield, G.A.: 1976, *Monthly Notices Roy. Astron. Soc.* **175**, 117

Cohen, R.S., Grabelsky, D.A., May, J., Bronfman, L., Alvarez, H., Thaddeus, P.: 1985, *Astrophys. J.* **290**, L15

Eaton, N., Rolph, C.D., Scarrott, S.M., Wolstencroft, R.D.: 1990, *Monthly Notices Roy. Astron. Soc.* **244**, 527

de Vries, C.P., Brand, J., Israel, F.P., de Graauw, Th., Wouterloot, J.G.A., van de Stadt, H., Habing, H.J.: 1984, *Astron. Astrophys. Suppl. Ser.* **56**, 333

Franco, G.A.P.: 1989, *Astron. Astrophys.* **215**, 119

Gahm, G.F., Malmort, A.M.: 1980, *Astron. Astrophys.* **82**, 295

Grabelsky, D.A., Cohen, R.S., Bronfman, L., Thaddeus, P.: 1987, *Astrophys. J.* **315**, 122

Gregorio Hetem, J.C., Sanzovo, G.C., Lépine, J.R.D.: 1988, *Astron. Astrophys. Suppl. Ser.* **76**, 347

Hartley, M., Manchester, R.N., Smith, R.M., Tritton, S.B., Goss, W.M.: 1986, *Astron. Astrophys. Suppl. Ser.* **63**, 27

Huggins, P.J., Gillespie, A.R., Sollner, T.C.L.G., Phillips, T.G.: 1977, *Astron. Astrophys.* **54**, 955

Jones, T.J., Hyland, A.R., Robinson, G., Smith, R., Thomas, J.: 1980, *Astrophys. J.* **242**, 132

Jones, T.J., Hyland, A.R., Bailey, J.: 1984, *Astrophys. J.* **282**, 675

Mattila, K.: 1970, *Astron. Astrophys.* **8**, 273

Müller, R.: 1934, *Z. Astrophys* **8**, 66

Nyman, L.-Å., Bronfman, L., Thaddeus, P.: 1989, *Astron. Astrophys.* **216**, 185

Nyman, L.-Å., Bronfman, L., Thaddeus, P.: 1991, in "Molecular Clouds", eds. R.A. James and T. Millar, Cambridge University Press, p. 23

Otrupcek, R.E., Wang, J.-S.: 1987, *Proc. Astron. Soc. Australia* **7**, 194

Reipurth, B.: 1981, *Astron. Astrophys. Suppl. Ser.* **44**, 379

Rodgers, A.W.: 1960, *Monthly Notices Roy. Astron. Soc.* **120**, 163

Sandqvist, Aa.: 1977, *Astron. Astrophys.* **57**, 467

Sandqvist, Aa., Lindroos, K.P.: 1976, *Astron. Astrophys.* **53**, 179

Schwartz, R.D.: 1977, *Astrophys. J. Suppl. Ser.* **35**, 161

Seidensticker, K.J., Schmidt–Kaler, Th.: 1989, *Astron. Astrophys.* **225**, 192

Sinclair, M.W., Brooks, J.W.: 1972, *Astrophys. Lett.* **11**, 207

Tapia, S.: 1973, in *Interstellar Dust and Related Topics, IAU Symp.* **52**, Greenberg, Van de Hulst, Reidel, Dordrecht, p. 43

Unsöld, A.: 1929, *Harvard Bull.* **13**, 870

Wang, J.-S., Otrupcek, R.E.: 1989, in *Structure and Dynamics of the Interstellar Medium, Lecture Notes in Physics*, eds. G. Tenorio–Tagle, M. Moles, and J. Melnick, Springer Verlag, p.13

Weaver, W.B.: 1973, *Astrophys. J.* **184**, 881

Weaver, W.B.: 1974a, *Astrophys. J.* **189**, 81

Weaver, W.B.: 1974b, *Astrophys. J.* **189**, 263

Westerlund, B.: 1960, *Ark. Astron.* **2**, 451

The Star Forming Region in Lupus

Joachim Krautter

Landessternwarte, Königstuhl
D–6900 Heidelberg, Germany

I. Introduction

First evidence for ongoing star formation in Lupus was given by Joy's (1945) discovery of a T Tauri star in Lupus (RU Lup). However, due to its southern location, for the next thirty years the Lupus star forming region received only little attention. This is best demonstrated by the fact that the '*Second Catalog of Emission-Line Stars of the Orion Population*' by Herbig and Rao (1972) contains only 6 stars in the Lupus area. However, mainly due to strongly improved observing facilities in the southern hemisphere, the situation has considerably changed by now. Since the T association in Lupus represents one of the most nearby regions of star formation, it is especially well suited for more detailed observations.

Observations within the last fifteen years have shown that the star forming region in Lupus contains one of the largest T associations of the southern sky. However, no massive OB stars are found in Lupus. The T Tauri stars, which are believed to be low-mass ($M \leq 3M_{\odot}$) pre-main-sequence (PMS) stars, are concentrated in four subgroups designated Lupus 1 to Lupus 4. The Lupus 1 and Lupus 2-4 subgroups are associated with small dark clouds which are embedded in a larger complex of CO emission (Murphy 1986). The four subgroups, which are located between the galactic coordinates $335° \leq l^{II} \leq 341°$ and $7° \leq b^{II} \leq 17°$, are shown in Figures 1a and 1b, respectively. Galactic and equatorial coordinates of the centers of the individual subgroups are given in Table 1. Apart from T Tauri stars other objects related to star formation have been found in Lupus: One Herbig Ae/Be star, and Herbig-Haro object/jet sources.

In this review on the Lupus star forming region the collective properties of the T Tauri star population will be described and results obtained on individual PMS objects will be presented. CO observations, magnetic field structure, and distance estimates will be summarized and discussed. It is not intended to give a complete list of all the many papers published about Lupus, rather a selection of the relevant literature (which must be necessarily subjective) will be given.

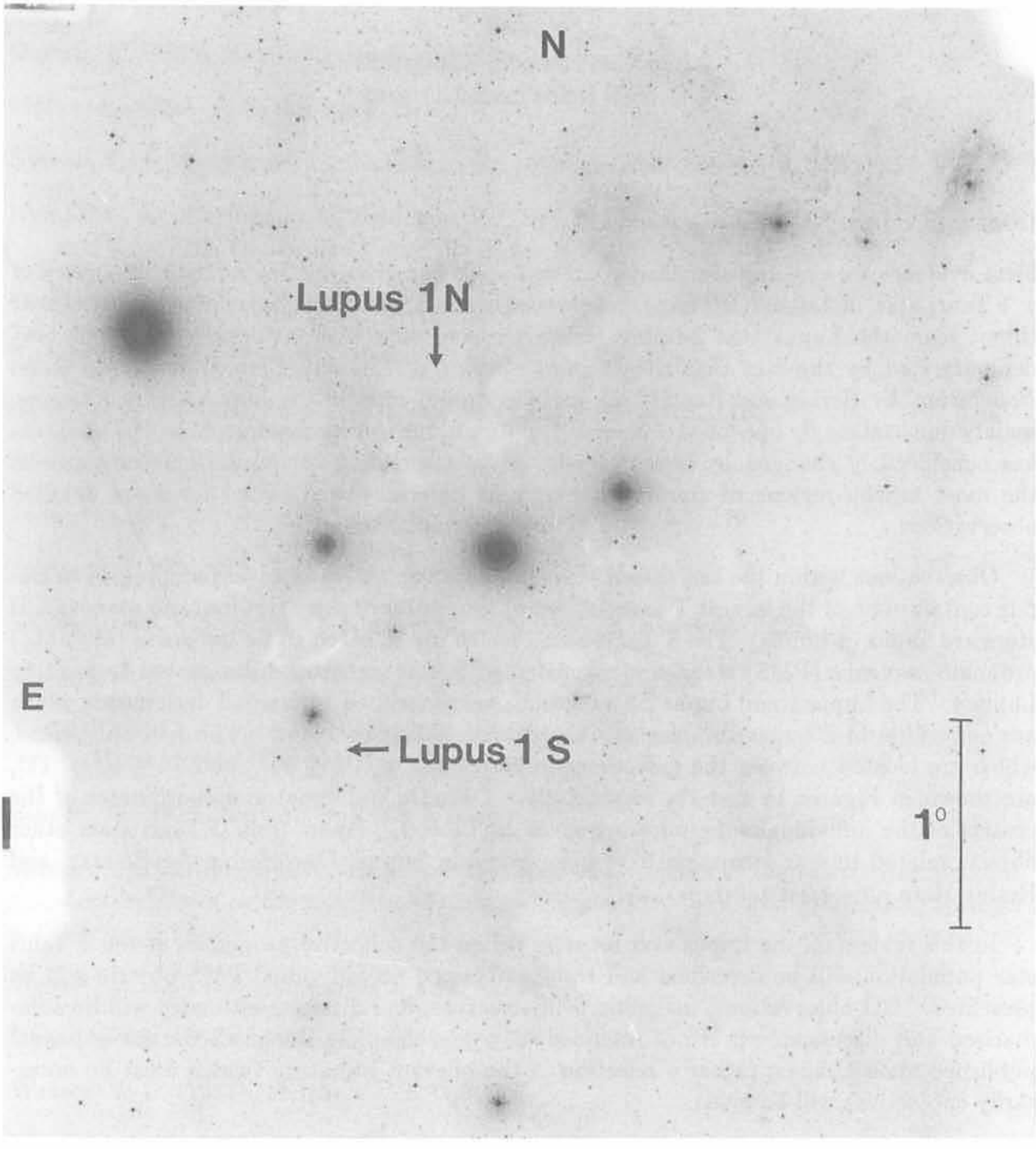

Figure 1a: Reproduction of a blue SERC-J sky survey plate showing the Lupus 1 dark cloud region. The southern and the northern part of the Lupus 1 dark cloud are indicated according to Schwartz's (1977) distinction.

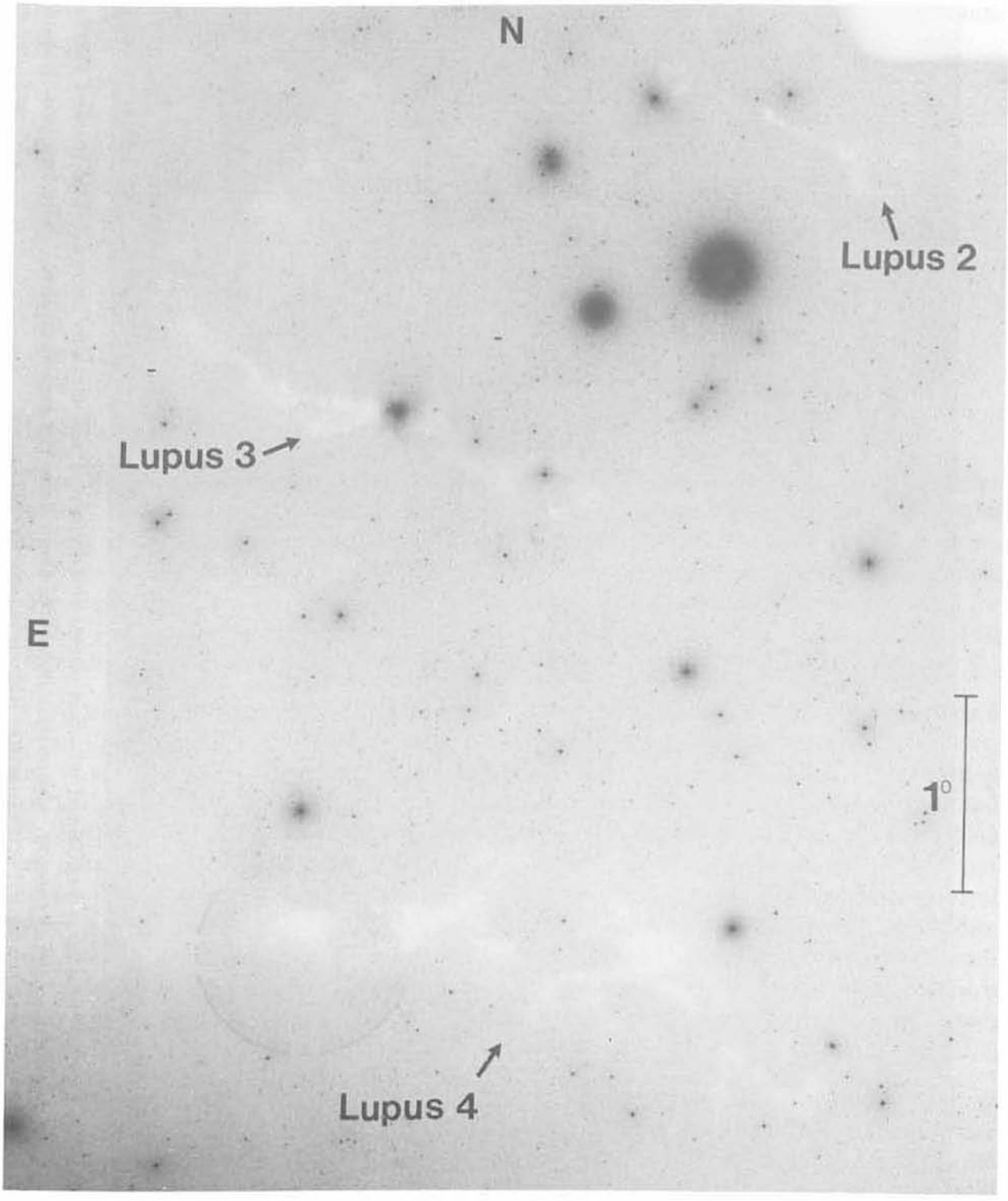

Figure 1b: Reproduction of a blue SERC-J sky survey plate showing the Lupus 2-4 dark cloud regions. The southern and the northern part are indicated according to Schwartz's (1977) distinction. The individual dark cloud areas are marked.

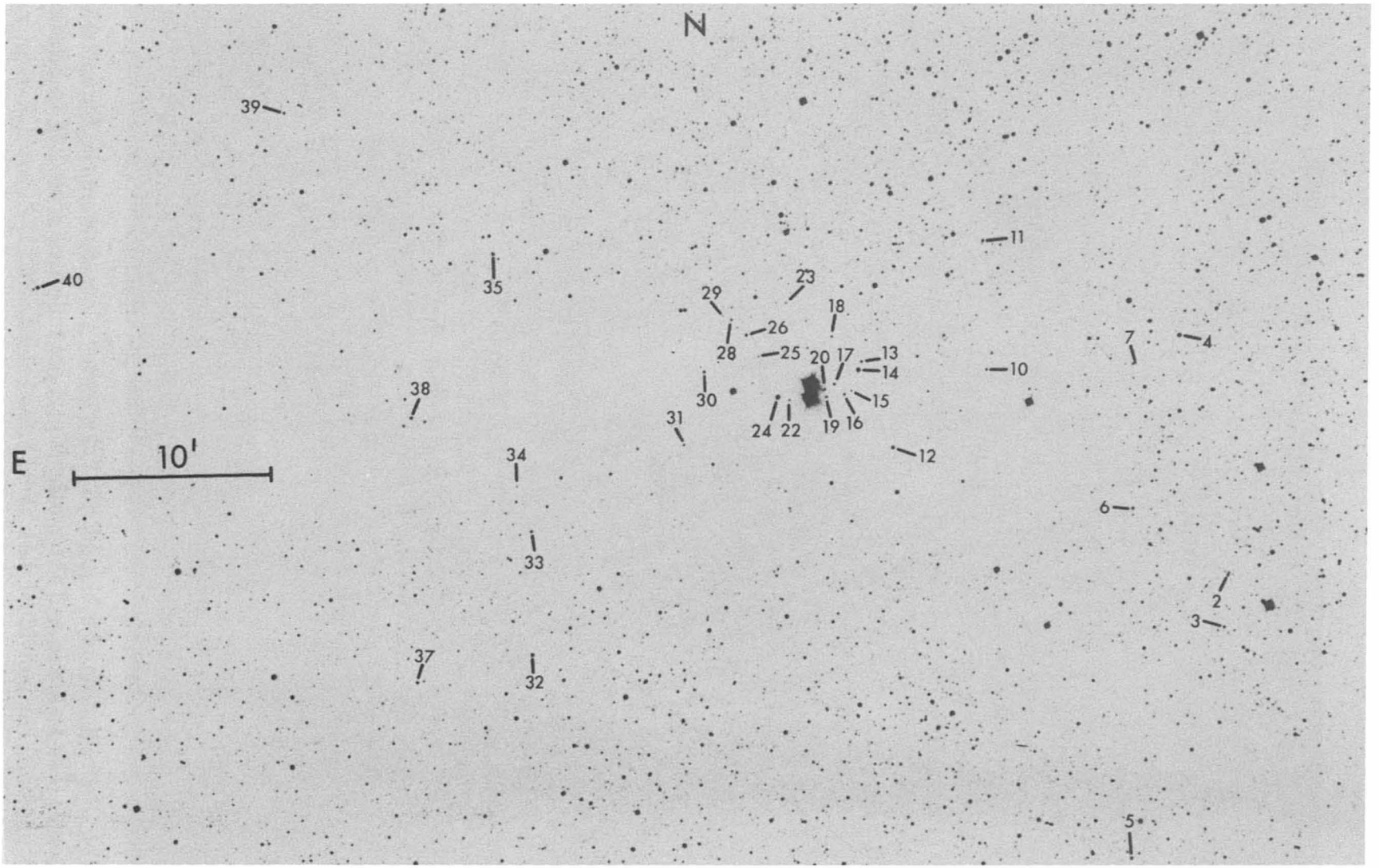

Fig. 2: Central part of the Lupus 3 subcloud which is one of the densest T associations known. The marked stars are the objects from Schwartz's (1977) catalog. Note that not all of them have Hα emission lines. The two bright stars in the center are HR 5999 (south) and HR 6000 (north). (From Schwartz, 1977).

Table 1: Approximate equatorial and galactic coordinates of the centers of the four subgroups in Lupus.

Name	*R.A. (1950)*	*Dec. (1950)*	l^{II}	b^{II}
Lupus 1	$15^h\,34^m$	-35°	339°	+15°
Lupus 2	$15^h\,52^m$	-38°	338°	+12°
Lupus 3	$16^h\,05^m$	-39°	340°	+ 9°
Lupus 4	$15^h\,57^m$	-41°	337°	+ 8°

II. Collective properties of the T Tauri stars

Three Hα objective prism surveys provided the basis for more detailed studies of the stellar content in the Lupus dark cloud. Eight years after a first survey by Henize (1954), who found 6 Hα emission line stars, the discovery of 39 Hα emission line stars in the Lupus 1 - 3 clouds was reported by Thé (1962), who introduced the subdivision in three subgroups. 15 years later, Schwartz (1977) carried out an objective prism survey in order to search for Herbig-Haro objects and Hα emission line stars. He found one HH object and a total of 60 Hα emission line stars which include in part the objects already found by Thé.

As already mentioned above, Herbig and Rao's (1972) catalog of PMS stars contains 6 T Tauri stars in Lupus. The first major study was undertaken by Appenzeller, Jankovics, and Krautter (1983) who studied in detail 34 stars of Schwartz's (1977) list. They carried out low-resolution spectrophotometry with a spectral resolution (FWHM) of about 7 Å and IR photometry of all 34 objects. In addition, medium resolution spectroscopy ($\Delta\lambda \simeq 1.4$ Å) was obtained for 19 T Tauri stars. The catalog published by Appenzeller et al. has a format similar to Cohen and Kuhi's (1979) catalog of northern PMS stars. They present spectral types, equivalent widths W_λ of Balmer and several other emission lines, visual magnitudes, and luminosities. Since no extinction values were derived, the luminosities, which were calculated for a distance of 125 pc, represent lower limits only. However, Appenzeller et al.'s catalog is biased by selection effects, since mainly bright and/or strong emission line stars of Schwartz's list were observed.

Spectroscopic and infrared observations of the remaining 35 stars of Schwartz's Hα survey were carried out by Krautter and Kelemen (1987). For the determination of luminosities Krautter and Kelemen (1992) used a distance of 150 pc (for a discussion of the distance see below) and included IRAS data for 9 stars. In their final catalog, which contains a total of 60 T Tauri stars, also the stars of Appenzeller et al.'s catalog are included with updated luminosities. Two Hα objects of Schwartz's list turned out to be an active galaxy (Sz 80) and a planetary nebula (Sz 132). Two isolated T Tauri stars (EX Lup and RY Lup) which don't belong to any of the four subgroups are included too in the catalog.

In Table 2 a list of the identified T Tauri stars in Lupus is compiled. The data are taken from Appenzeller et al. (1983) and Krautter and Kelemen (1992). Column 1 gives the names used in the above mentioned catalogs, column 2 gives other designations, and column 3 lists the number in the Herbig and Bell (1988) catalog which contains additional information. In column 4 the approximate visual magnitude of the star at the epoch of the low resolution spectrogram is given; note, that all stars are variable. If no number is given, no calibrated spectrum was available. Column 5 shows the approximate photospheric spectral type as derived from low resolution spectra. The luminosity of the star in solar units is presented in column 6. Only lower limits are given, since no interstellar extinction correction was applied. All luminosities were calculated for a distance of 150 pc. The equivalent width of Hα is given in column 7. Column 8 gives the identification of the IRAS point source catalog. If AJK is given in the last column, data are taken from Appenzeller et al., otherwise from Krautter and Kelemen. We would like to note, that additional data (infrared photometry, equivalent widths and fluxes of emission lines) can be found in these two catalogs. Coordinates are given by Schwartz (1977).

Heyer and Graham (1989) carried out imaging, near infrared photometry, and spectroscopic observations of 8 T Tauri stars in the Barnard 228 molecular cloud in which the Lupus 1 subgroup is located. The spectral types determined by Heyer and Graham differ in part significantly from those of Krautter and Kelemen. In addition, they found three previously unknown Hα emission line stars. UBVR photometric observations of 26 of Schwartz's Hα emission line objects were carried out by Schwarz and Noah (1978). Bastien (1985) obtained linear polarimetric data of 11 T Tauri stars in Lupus.

More than half of the T Tauri stars (33) are found in the Lupus 3 subgroup which forms at its central part one of the densest T associations known. The central part of the Lupus 3 subgroup is shown in Figure 2 (from Schwartz 1977). The marked stars are the Hα emission line stars found by Schwartz. The two bright stars in the central part are the Herbig Ae/Be star HR 5999 (south) and HR 6000 (north). Pictures of the other subgroups are presented in Schwartz (1977).

Figure 3 shows a histogram with the distribution of T Tauri stars by spectral type (Krautter and Kelemen, 1987). A comparison with corresponding histograms of the Chamaeleon I and II clouds (Krautter and Kelemen) and with the histograms published by Cohen and Kuhi (1979) shows that the relative amount of late type T Tauri stars with spectral types M1 to M5.5 is much higher in Lupus than in any other known major T association. This also implies that the relative amount of stars with masses below 0.5 $M_\odot$ is much higher in Lupus than in any other T association. A comparison with convective-radiative evolutionary tracks (taken from Cohen and Kuhi) in the HR-diagram of the T Tauri stars in Lupus presented in Figure 4 (Krautter and Kelemen, 1992) shows that for stars with masses $\leq$ 0.5 $M_\odot$ close to the Hayashi-track, the stellar mass and the temperature behave roughly in the same way, i.e., if the temperature decreases the mass decreases too.

The unusual mass spectrum of the Lupus T Tauri stars suggests that the initial mass function (IMF) in Lupus differs from those in other star forming regions. A possible expla-

Table 2: The T Tauri stars in Lupus. The data with AJK in the last column are taken from Appenzeller et al. (1977), the other data from Krautter and Kelemen (1992). For further explanation see text. The following designations are used – He: Henize (1976), Sz: Schwartz (1977), Th: Thé (1962).

Star	Other Designation	HBC	m_V [mag]	Sp. T.	Lum. [$L_\odot$]	W_λ (Hα)	IRAS source	Ref.
Sz 65		597	12.7	K7-M0	0.98	19.4	15362-3436 ?	AJK
Sz 66			15.5	M2.5	0.29	63.7	15362-3436 ?	
Sz 67			14.3	M2	0.32	5.9		
CoD -33° 10685	Sz 68	248	10.8	K2	5.50	2.8	15420-3408	AJK
Hα 450-5	Th 2, Sz 69	598	17.2	M1	0.20	306.5		AJK
Sz 70			16.4	M4	0.51	19.4	15435-3421	
GW Lup	LHα450-6, Sz 71	249	13.9	M1.5	0.35	90.3		AJK
HM Lup	LHα450-8, Th 4, Sz 72	599	15.3	M4	0.25	115.3	15446-3519	AJK
Th 5	Sz 73	600	16.2	K7-M0	0.55	97.2		AJK
HN Lup	LHα450-7, Th 6, Sz 74	601	14.6	M1.5	1.91	49.6	15448-3506	AJK
GQ Lup	CoD -35° 10525, Sz 75	250	12.7	K7	2.02	38.6	15459-3529	AJK
Sz 76			15.1	M1	0.30	10.3		
Sz 77		603	12.5	M0	1.05	12.4	15485-3547	AJK
Th 10	Sz 81	604	14.5	M5.5	0.35	35.8		AJK
Th 12	Sz 82	605	12.2	M0	1.62	8.1	15528-3747	AJK
RU Lup	Th 13, Sz 83	251	11.8	K7	3.72	216.4	15534-3740	AJK
Sz 84			16.0	M5.5	0.12	43.7		AJK
HO Lup	Th 18, Sz 88, He 1140	612	13.6	M1	0.52	219.8		AJK
Th 21	Sz 90	613	15.4	K7	0.40	28.5		AJK
Th 20	Sz 91	614	15.7	M0	0.12	95.9		AJK
Sz 94			15.9	M4	0.08	7.3		
Sz 95			15.8	M0.5	0.13	10.2		
Sz 96		615	13.7	M1.5	0.33	11.0		AJK
Th 24	Sz 97		15.7	M3	0.13	58.2		
HK Lup	Sz 98	616	12.4	K7-M0	0.98	29.1		AJK
Th 25	Sz 99		17.1	M1.5	0.06	49.8		
Th 26	Sz 100		17.0	M1.5	0.14	21.4		
Th 27	Sz 101		15.5	M4	0.22	26.0		
Th 28	Sz 102	617	16.3	K?	0.01	377.4		AJK
Th 29	Sz 103	618	16.1	M4	0.08	33.1		AJK
Th 30	Sz 104			M5.5	0.07	13.3		
Th 31	Sz 105		15.0	M1	0.83	63.9		
Sz 106			18.1	K7-M0	0.05	81.7		
Sz 107				M5.5	0.09	16.1		
Sz 108		620	13.2	M0.5	0.55	0.5		AJK
Sz 109				M5.5	0.08	21.7		
Th 32	Sz 110	621	15.4	M1	0.18	60.1		AJK
Th 33	Sz 111, He 1145	622	14.5	M0.5	0.14	145.2		AJK
Sz 112			17.0	M3	0.14	46.7		
Th 34	Sz 113		18.7	M1.5	0.03	160.1		
Th 35	Sz 114	623	15.5	M4	0.27	33.0		
Sz 115			16.2	M3	0.09	7.1		
Th 36	Sz 116	625	14.8	M1	0.25	3.9		AJK
Th 37	Sz 117	626	14.3	M2	0.17	20.5		AJK
Sz 118			18.3	K6	0.24	28.3		
Th 38	Sz 119	627	15.4	M5	0.28	4.5		AJK
Th 40	Sz 121		14.9	M2	0.22	6.5		
Th 41	Sz 122	628	14.5	M3	0.13	4.8		AJK
Th 42	Sz 123	629	15.4	M2	0.14	250.6		AJK
Th 43	Sz 124	631	13.1	M0	0.32	1.6		AJK
Sz 126		606		K-M	0.34			AJK
Sz 127				M4	0.37	75.6		
Sz 128		607	14.5	M1	0.19	9.9		AJK
He 1125	Sz 129	609	13.6	K7-M0	0.55	22.3		AJK
Sz 130		610	14.7	M1.5	0.21	52.9		AJK
Sz 131				M1.5	0.11	31.9		
Sz 133				K2	0.21	20.0		
He 1146	Sz 134	624	14.6	M4	0.17	90.5		AJK
RY Lup		252	11.1	K4			15561-4013	AJK
EX Lup		253	13.7	M0.5		43.3	15597-4010	AJK

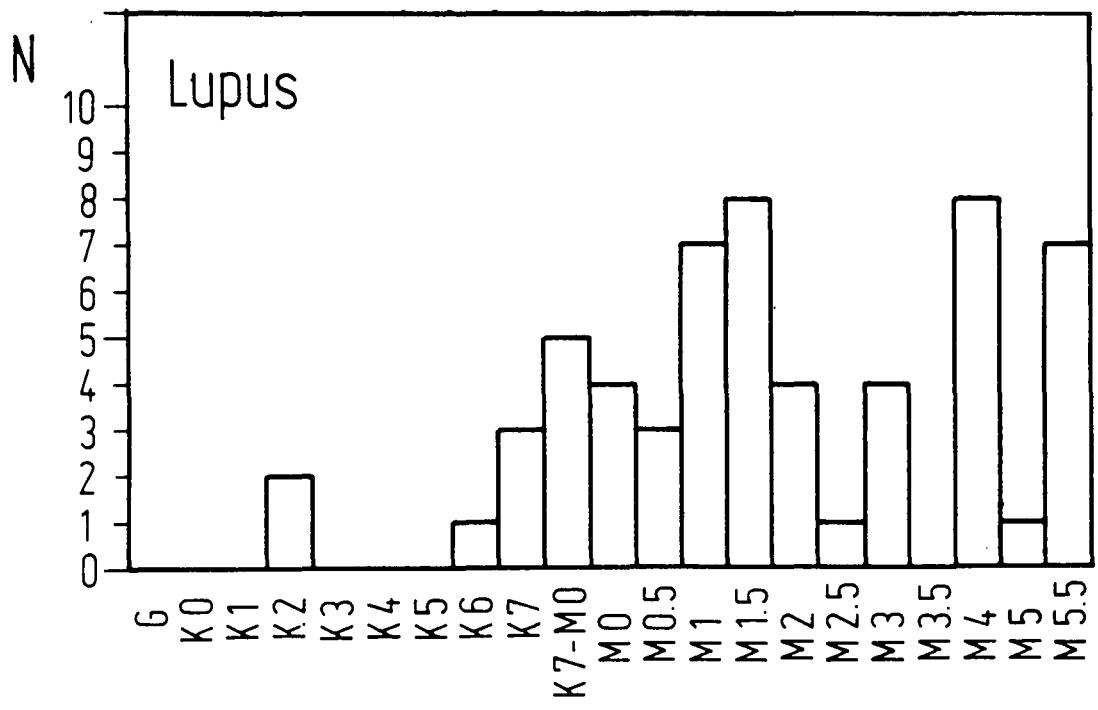

Figure 3: Histogram of the distribution of the T Tauri stars in Lupus by spectral type. (From Krautter and Kelemen, 1987).

nation might be that the star formation process in Lupus is controlled by magnetic forces. According to Shu, Adams, and Lizano (1987), the IMF depends on the relative magnitude of gravitational and magnetic forces in a molecular cloud. In the subcritical regime, if the magnetic forces exceed the gravitational forces, preferentially low mass stars should be formed, as found in Lupus.

Additional strong evidence that the star formation in Lupus is controlled by magnetic forces is provided by polarization measurements in the Lupus 1 region (Strom et al., 1988). Figure 5 shows the observed polarization vectors for stars in the Lupus 1 cloud superposed on an R-band photograph of this region (from Strom et al., 1988). The e-vectors (which define the magnetic field direction) lie perpendicular to the long axis of the cloud and show relatively small dispersion in position angle. Strom et al. conclude that the Lupus 1 cloud has probably been constrained to collapse along the magnetic field lines, and that the magnetic field has played a major role in controlling the properties of the protostellar cores.

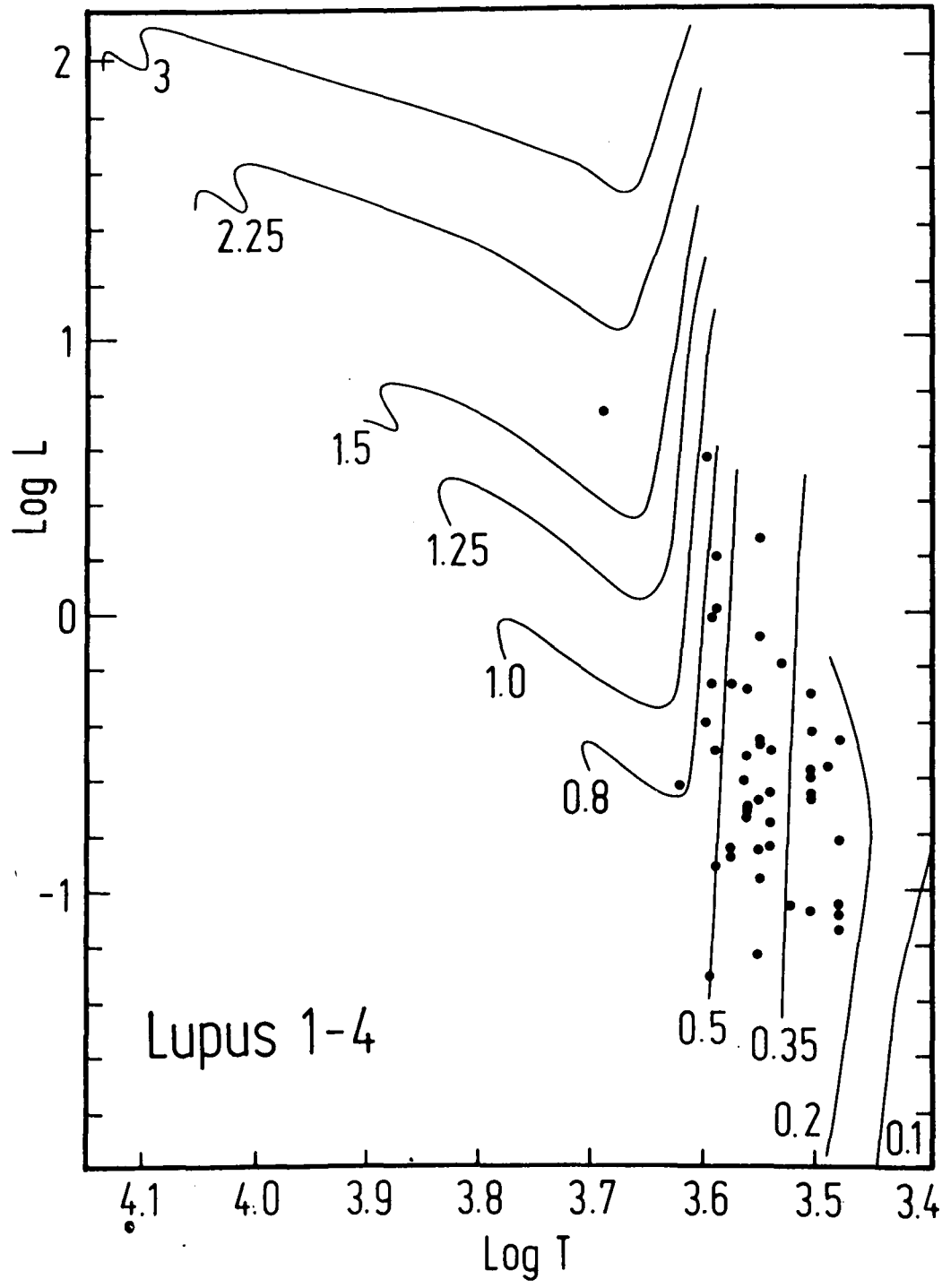

Figure 4: HR diagram of the T Tauri stars in Lupus. (From Krautter and Kelemen, 1992). The convective-radiative evolutionary tracks are taken from Cohen and Kuhi (1979).

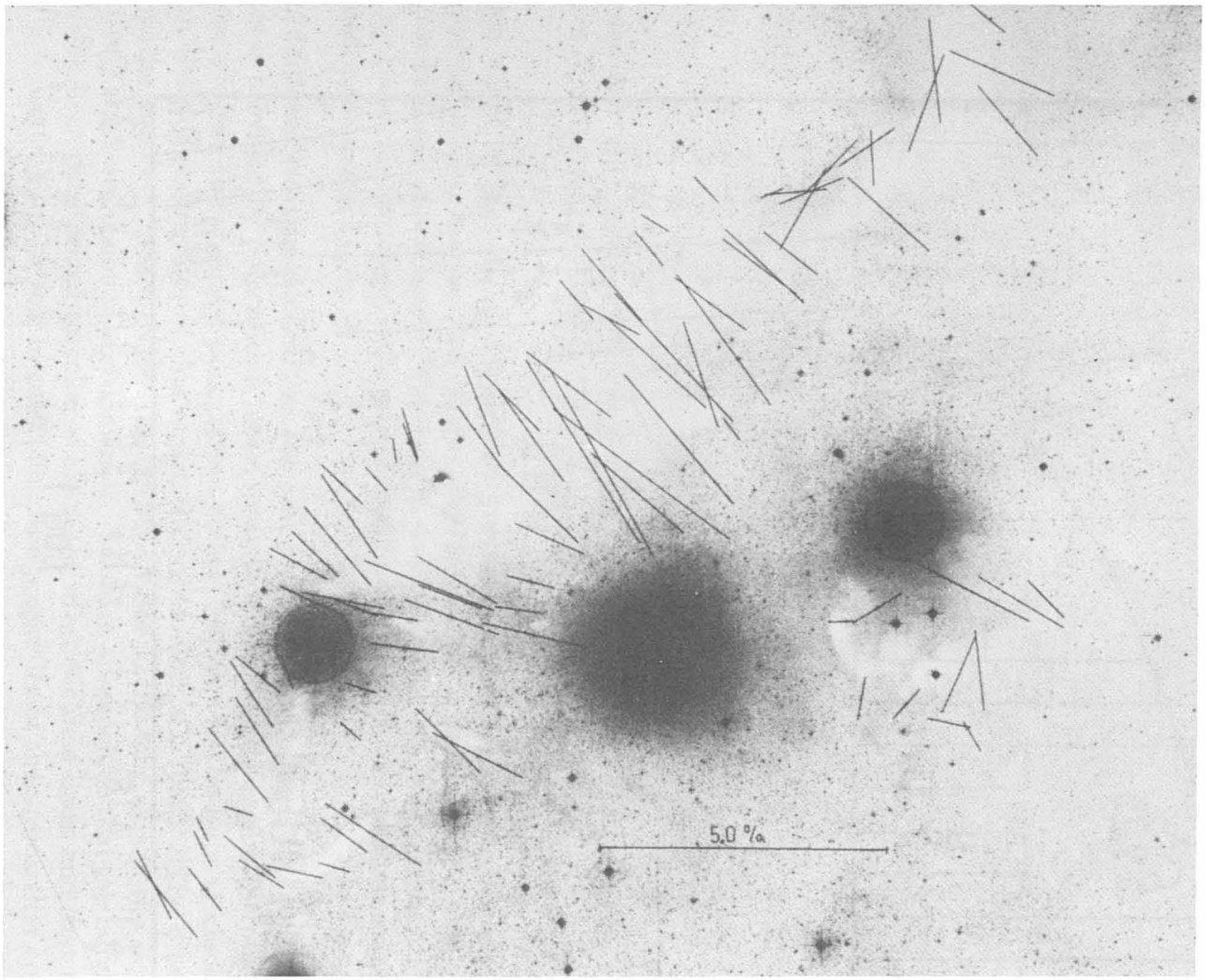

Fig. 5: The observed polarization vectors for the Lupus 1 cloud superposed on an R-band photograph of the region; North is to the top and East to the left. The vertical dimension of the image is $\sim$ 50′. The e-vectors (which define the magnetic field direction) lie perpendicular to the long axis of the cloud and show relatively small dispersion in position angle. (From Strom et al., 1988)

III. Individual objects

RU Lup and HH 55

RU Lup is one of the brightest T Tauri stars known ($V_{mean} \simeq 11.0$ mag). It was included in Joy's (1945) pioneering paper which defined the characteristics of T Tauri stars. RU Lup belongs to the extreme members of the T Tauri class; it exhibits in the visual spectral range strong emission lines superimposed on a nearly featureless continuum. Due to the strong veiling of the photospheric absorption spectrum it has been difficult to classify the photospheric spectral type of RU Lup. In an attempt to model the continuous energy distribution of RU Lup, Gahm et al. (1974) derived $T_{eff} = 4400$ K implying a mid-K classification. This is consistent with Schwarz and Heuermann's (1981) classification of K0-K5 on the basis of high resolution spectra and with the K7 classification by Appenzeller et al. (1983). Indications for a pseudoperiod of about 3.7 days have been found by Plagemann (1969), Drissen et al. (1989), and Hutchinson et al. (1989), who find that the variability of RU Lup may be described by a simple spot model.

Analysis of high dispersion spectra (Schwartz and Heuermann, 1981; Lago 1982) showed that the Balmer lines sometimes exhibit P Cygni profiles indicating a stellar wind with $v \sim 200\,\mathrm{km\,s^{-1}}$. Lago (1984) developed a magnetically driven wind model which satisfactorily explains the optical observations. Jankovics et al. (1983) found that the forbidden lines of [SII] and [OI] are blueshifted. This can be interpreted according to Appenzeller (1983) in terms of the presence of flattened or disk-like opaque structures around RU Lup. Evidence for circumstellar matter is also given by the strong IR excess of RU Lup (e.g. Gahm et al., 1975; Appenzeller et al. 1983).

UV observations (Gahm et al. 1979) have shown that the chromospheric and transition region around RU Lup at $T \sim 10^5$ K is about 10^4 times stronger than the corresponding solar region. However, as the absence of coronal lines demonstrates (Gahm et al., 1981, Gahm and Krautter, 1982) there is virtually no corona of corresponding strength around RU Lup. From simultaneous multiwavelength observations from X-ray to UV, Giovanelli et al. (1988) conclude that the strong variability in the UV and optical spectral range is due to a strong activity in the chromosphere and due to large scale flare-phenomena.

RU Lup is located in the Lupus 2 dark cloud close ($d \sim 3'$) to HH 55. The region around RU Lup and HH 55 is shown in Figure 6 (from Krautter et al., 1984). Krautter et al. found indication of a faint continuum in the spectrum of HH 55. They considered RU Lup very likely to be the energy source of the HH object, particularly since the IR survey by Reipurth and Wamsteker (1983) did not uncover any other plausible candidate. On the other hand, Cohen et al. (1986) report on photospheric absorption features of spectral type M3.5 which excludes RU Lup, that has no recognizable photospheric features, as the exciting star of HH 55. Heyer and Graham (1990) made a detailed study of HH 55, and conclusively showed that the HH object coincides with a relatively unobscured M-dwarf star, also detected in IRAS coadded images. A careful search for other nebular emission by Krautter et al. (1984)

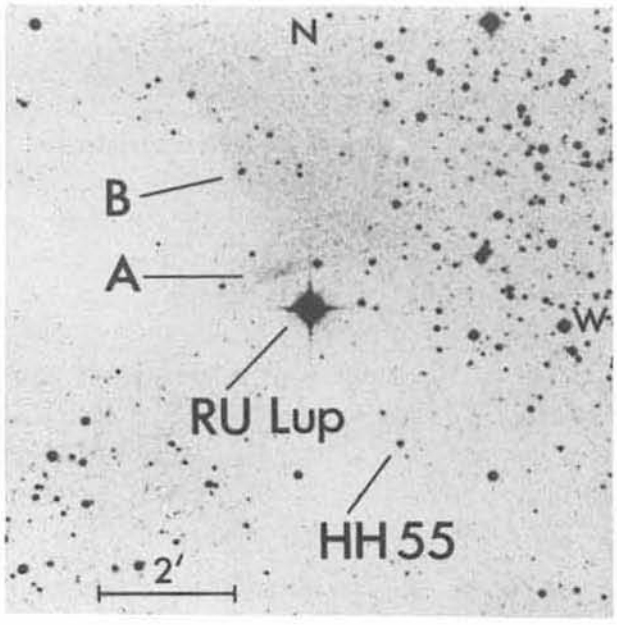

Figure 6: Region around RU Lup and HH 55 in the Lupus 2 cloud. On the north side of RU Lup is a faint luminous ridge (**A**), probably a reflection nebula. (From Krautter et al., 1984). B is an unrelated object.

revealed a faint luminous ridge north of RU Lup, probably a reflection nebula (feature 'A' in Figure 6).

GQ Lup

Appenzeller et al. (1978) recognized that GQ Lup (≡ CoD −35°10525) is one of the brightest members of the YY Ori subclass of the T Tauri stars, showing inverse P Cygni profiles of certain emission lines. Like other stars of this group, GQ Lup exhibits a strong UV excess. GQ Lup combines a moderate-emission line spectrum with a conspicuous photospheric absorption spectrum of spectral type K7 which is only weakly veiled. On the basis of high-resolution spectroscopy, Bertout et al. (1982) found variations of the emission line profiles from one night to the next, which are correlated with strong photometric changes in the UV part of the spectrum. Appenzeller and Wagner (1989) report that the line profiles in GQ Lup differ in part significantly from those found in the spectra of strong-emission line T Tauri stars. According to Appenzeller and Wagner, the observed differences are due to a lower optical thickness of the less massive gaseous envelopes of the lower-emission T Tauri stars. GQ Lup is one of the two YY Ori stars (the second example is EX Lup, Mundt 1984) which do not show blueshifted absorption components too (Appenzeller and Wagner, 1989). Like in RU Lup, Jankovics et al. (1983) found blueshifted forbidden emission lines. UV spectra, taken by Appenzeller et al. (1980) with IUE, show emission lines superimposed on a weak continuum.

HR 5999

The unusual properties of the bright star HR 5999 (≡ HD 144668) were discovered by Bessell and Eggen (1972). HR 5999 is of spectral type A7 III-IV with hydrogen lines in emission and with a large rotational velocity $vsini = 180\,km\,s^{-1}$. Due to these properties, because of its location in an obscured region with many T Tauri stars, and because of its position in the HR diagram above the zero-age main sequence, HR 5999 is thought to belong to the group of Herbig Ae/Be stars, which are PMS stars of intermediate mass (e.g. Tjin A Djie et al., 1989 and references therein). HR 5999 and HR 6000, which are the two bright stars in the central part of the Lupus 3 dark cloud shown in Figure 2, form a common proper motion visual binary (Dunlop–199). HR 5999 is the more southern star of the two. Note that both stars have been confused in Bessell and Eggen (1972) and in several other earlier papers. The suggestion by Andersen and Nordström (1978) that HR 5999 could be a long period binary with mass exchange was not confirmed by speckle interferometry (Baier et al., 1985).

Since colour and brightness variations are correlated, the photometric variability has been interpreted in terms of variable obscuration by circumstellar dust (Bessell and Eggen, 1972; Thé and Tjin A Djie, 1978; Thé et al., 1978, 1981). Several studies found a variable ratio R of total to selective absorption ranging from 3 to more than 6 (e.g. Tjin A Djie and Thé, 1978; Thé et al., 1985). Baade and Stahl (1989) report a high $R \sim 5$ too, but they could not find any variability. The high value of R indicates that the composition of the circumstellar dust differs from the interstellar one (e.g. Andersen et al., 1982). Strong evidence for the presence of dust is also inferred by an IR excess found by e.g. Smyth et al. (1979) or by Thé et al. (1981), who also studied the overall flux distribution from 0.12 to 4.7 μm. The UV spectrum, that shows shell lines and many emission lines (e.g. Thé et al., 1985; Brown et al., 1986), is interpreted as due to chromospheric activity. It should be noted that no X-ray flux was detected by EXOSAT (Thé et al., 1985).

Baade and Stahl (1989) detected a modulation of the V-lightcurve with a period of 48.68 days and an amplitude of 0.25 mag which is superimposed on a random variability of about 1 mag. They interpret this behaviour in terms of dust associated with an orbiting more solid body. On the basis of high-resolution spectroscopy Baade and Stahl found indications for intrinsic variations due to nonradial oscillations.

Th 28

The association of a bipolar HH jet system with the emission-line object Th 28 has been discovered by Krautter (1986). Figure 7 shows a direct CCD-image of the Th 28 system taken through a narrow band Hα interference filter (from Krautter, 1986). Two oppositely directed jet-like structures (length 0.008 and 0.009 pc at a distance of 140 pc) are emanating ($v \simeq 320\,km\,s^{-1}$) from a central star-like source, and two HH objects (Th 28-HHE and Th 28-HHW) are located on both sides exactly on the axis defined by the bipolar jets at distances of 0.020 and 0.024 pc, respectively. The electron density decreases by about two orders of magnitude along the jet axis. Graham and Heyer (1988) found a third HH object 87″ SE

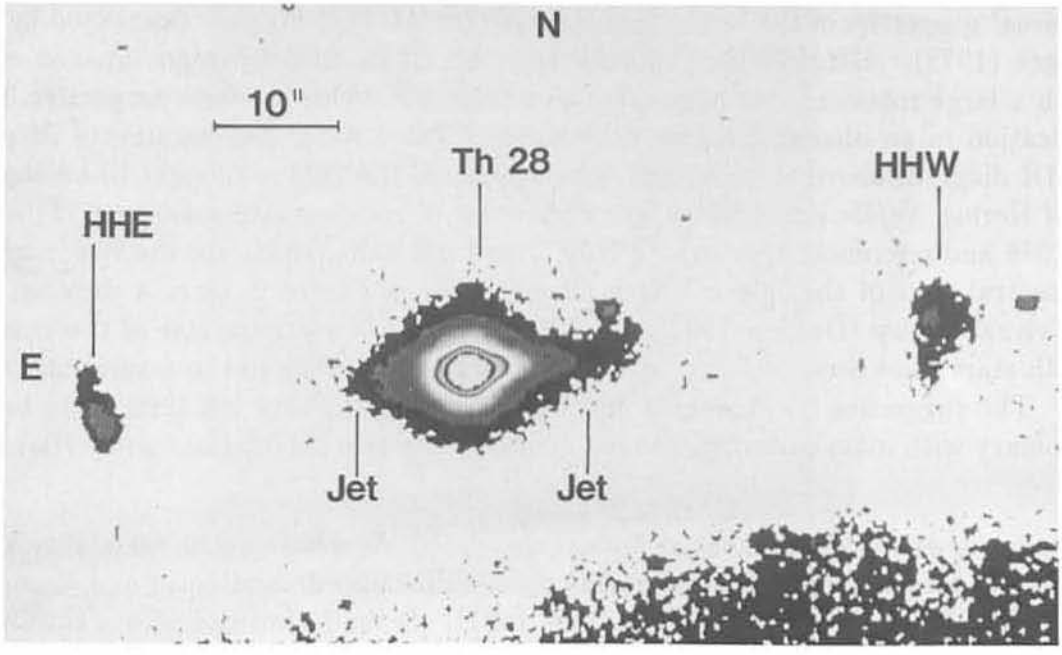

Figure 7: Central parts of the Th 28 Herbig-Haro jet system. (From Krautter, 1986).

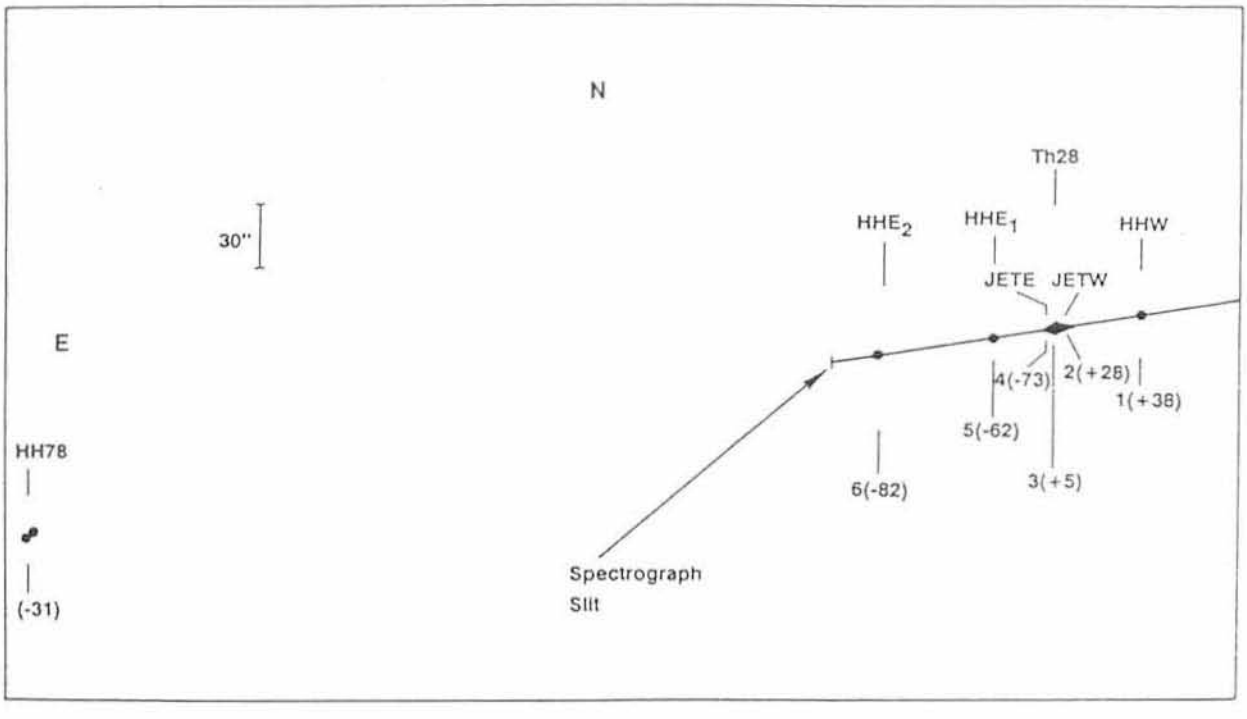

Figure 8: Schematic sketch showing relative positions of Th 28, the two jets, and the associated HH objects. The numbers in parentheses denote the observed heliocentric velocities at six different positions. (From Graham and Heyer, 1988).

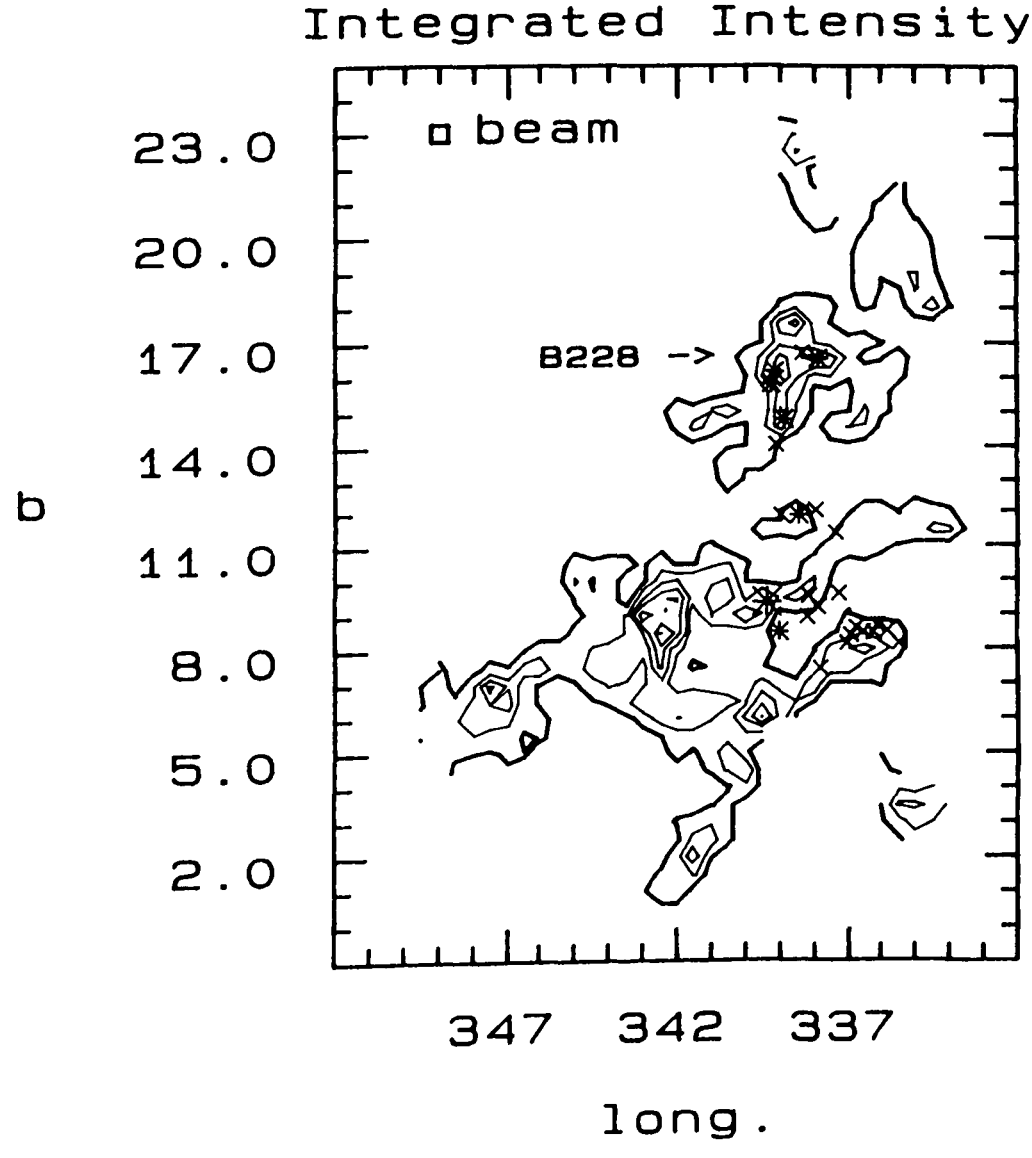

Figure 9: Map of integrated CO intensity in the Lupus dark cloud area. The positions of all Schwartz (1977) Hα stars are marked. The large cluster symbol at (339.0°,8.5°) represents the dense Lupus 3 subgroup. (From Murphy et al., 1986).

CoD -33° 10685 and suggest that energetic stellar winds are not necessarily associated with very active chromospheres. Reipurth and Zinnecker (1992) found a faint companion to CoD −33° 10685.

Several stars in Lupus (Sz 65, CoD -33° 10685, Sz 77, Th 12, Sz 98) are included in an extensive study by Finkenzeller and Basri (1987) on the atmospheres of low- and intermediate active T Tauri stars. Physical parameters (mass, radius surface gravity) of the investigated stars were determined. Finkenzeller and Basri's main conclusion is that the important features in T Tauri stars are clearly chromospheric. Th 12, a low-activity T Tauri star, is the only PMS star in Lupus of which soft X-rays have been detected yet (Gahm 1980). However, only very few X-ray observations have been carried out so far in the Lupus star forming region.

IV. Radio observations

^{12}CO observations covering 170 square degrees toward the Lupus dark cloud area were carried out by Murphy et al. (1986). Figure 9 shows their map of integrated ^{12}CO intensity $I_A = \int T_A^* \, dv$. The position of all Hα emission line stars of Schwartz's (1977) list are marked. The total CO emission has a large angular extent of about 23° along one axis. The maxima of the CO emission can be clearly identified with optically visible narrow filament like dust lanes. Several of these structures are included in the *Catalog of Dark Globular Filaments* by Schneider and Elmegreen (1979), who suggest that the dust lanes might eventually collapse into Bok globules. Two separate regions above and below $b \leq 12°$ can be distinguished. Since the kinetic gas temperatures and the FWHM of the velocity distribution are similar throughout Lupus, Murphy et al. conclude that the gas in the two separate areas is physically related and at the same distance. For the total mass of the cloud they derived from the empirical relationship between integrated CO brightness temperature and H_2 column density a 'CO mass' of $M_{CO} \sim 1.5\ 10^4\ M_\odot$. On the other hand, for the viral mass they derived $M_{Vir} \sim 4.5\ 10^4\ M_\odot$. The mean of both estimates gives a total mass $M_{tot} \sim 3\ 10^4\ M_\odot$. This is about of the same size as the mass of the Taurus-Auriga cloud which was estimated by Ungerechts and Thaddeus (1987) to be $\sim 3.5\ 10^4\ M_\odot$. In a formaldehyde survey in southern dark clouds Sandqvist and Lindroos (1976) detected this molecule in all nine clouds in Lupus investigated by them.

There is also a strong correlation between the projected positions of the T Tauri stars and the CO emission. The T Tauri stars therefore form compact centers of star formation in an extended group of physically related dark clouds. Murphy et al. suggest that the other CO maxima might be likely places of recent star formation as well, which might be in several cases in the mode of embedded sources. It should be noted, however, that up to now no embedded near IR sources, as for instance found in Chamaeleon (e.g. Schwartz, this volume) have been reported in the Lupus dark cloud region.

V. Distance to the Lupus star forming region

Published distance estimates to the Lupus cloud are in most cases based on distance estimates of individual stars. Several estimates are based on the binary stars HR 5999/HR 6000. With the assumption that both stars are members of the Local Association (Pleiades Group), Bessell and Eggen (1972) derived a distance of 300 pc. Eleven years later, Eggen (1983) derived with the same basic assumption, but in a more extensive study, a kinematic distance of 170 pc. Thé and Tjin A Djie (1978) determined from Walraven photometry a colour index of HR 6000 which corresponds to a B6 star. Under the assumption, that HR 6000 is a main sequence star, they find a distance 270 pc. However, HR 6000 is a peculiar B type object with weak helium and strong P II (Eggen 1983) which affects the colour index. Using high resolution spectroscopy, Andersen and Jaschek (1984) determined a spectral type A0Vp:. This implies that HR 6000, being intrinsically fainter than assumed by Thé and Tjin A Djie, is at a smaller distance.

Appenzeller et al. (1978) used the bright star HD 140748 that apparently illuminates matter belonging to Barnard 228, indicating a physical association. Since several conflicting spectral types are published in the literature (B6V, B7V, B9V), they obtained with a mean spectral type an approximate distance $\sim$ 125 pc. Schneider and Elmegreen (1979) obtained for the bright stars HD 143749, HD 193947, HD 144667/HD 144668, and HD 149447, of which they assume an association with the filaments in Lupus also on the basis of reflection nebulosity, distances of 160 pc, 220 pc, 150 pc, and 60 pc, respectively.

Murphy et al. (1986) found that the Lupus dark cloud complex is projected onto a gap between two subgroups of the Scorpius-Centaurus OB association. They discuss two possibilities, namely that the Lupus dark clouds are related to the Sco-Cen OB association or that the Lupus dark clouds are in front of the OB association, causing an apparent gap in the association. In the latter case, they derive a distance of 130 pc, in the former case the Lupus clouds would be at 170 pc, the mean distance of the Sco-Cen association.

Franco (1990) used colour excess distribution from uvbyβ photometry of stars towards the lower parts of the Lupus clouds to derive a distance of $\approx$ 165 $\pm$ 15 pc.

Considering all these different distance estimates, it seems rather safe to conclude that the distance to the Lupus dark cloud is between the limits 130 pc and 170 pc. However, within these limits, no clear decision can be made yet. For the time being, a mean distance of $\sim$ 150 pc seems the best choice. In any case, Lupus belongs among the most nearby star forming regions.

VI. Conclusions

The star forming region in Lupus is in several respects similar to those in Taurus-Auriga and in Chamaeleon (Schwartz, this volume). Only low-mass star formation is going on in all three star forming regions, no massive young OB stars have been found. All three clouds

contain major T associations with 70 or more members, and the mass of the molecular cloud material is about the same for at least Lupus and Taurus-Auriga (no mass determination has been published for Chamaeleon). Since the distances to the three clouds are roughly the same, comparative studies between them will not be affected by selection effects due to different distances. Moreover, all three belong to the nearest star forming regions known which makes them especially well suited for observational studies.

On the other hand, several of the properties of the Lupus star forming region differ significantly from those of the other clouds. The T Tauri stars in Lupus have an outstanding mass spectrum, since the relative amount of stars with $M \leq 0.5\ M_{\odot}$ is much higher than in any other comparable cloud. This indicates that the star formation in Lupus is controlled by magnetic forces. Contrary to other clouds, only very few embedded IR sources have been found yet in Lupus. As compared with e.g. the Taurus-Auriga cloud, the general level of PMS activity in Lupus seems to be lower. There are only few HH objects and jet sources, no molecular outflow has been reported yet, and there are certainly less T Tauri stars with strong forbidden lines which is believed to be an indicator of activity. This might lead to the conclusion that the star forming region in Lupus is relatively old.

In this paper the observational results on the Lupus star forming region have been reviewed. However, as compared with well studied regions at more northern declinations, far less observational studies have been carried out so far in Lupus. Future observations might reveal several of the above addressed 'missing' PMS phenomena; in any case, Lupus is a very attractive star forming region for future observations.

Acknowledgements

The author thanks Drs. Immo Appenzeller, Janos Kelemen, Bo Reipurth, and Bernhard Wolf for valuable discussions. For the preparation of this paper the SIMBAD data retrieval system, data base of the Strasbourg astronomical data center, has been used.

References

Andersen, J., Nordström, B.: 1978, *A&AS* **29**, 309

Andersen, J., Gahm, G.F., Krelowski, J.: 1982, *A&A* **113**, 176

Andersen, J., Jaschek, M.: 1984, *A&AS* **55**, 469

Appenzeller, I., Mundt, R., Wolf, B.: 1978, *A&A* **63**, 289

Appenzeller, I., Chavarria, C., Krautter, J. Mundt, R., Wolf, B.: 1980, *A&A* **90**, 184

Appenzeller, I., Jankovics, I., Krautter, J.: 1983, *A&AS* **53**, 291

Appenzeller, I., Wagner, S.: 1989, *A&A* **225**, 432

Baade, D., Stahl, O.: 1989, *A&A* **209** 255

Baier, G., Bastian, U., Keller, E., Mundt, R., Weigelt, G.: 1985, *A&A* **153**, 278

Bastien, P.: 1985, *ApJS* **59**, 277

Bastien, P., La Van Suu, A., Menard, F., Bertout, C., Bouvier, J., Boivin, L.: 1987, Poster presented at the *NATO ASI on Galactic and Extragalactic Star Formation*, Whistler, BC

Bertout, C., Carrasco, L., Mundt, R., Wolf, B.: 1982, *A&AS* **47**, 419

Bessel, M.S., Eggen, O.J.: 1972, *ApJ* **177**, 209

Bouvier, J., Bertout, C.: 1989, *A&A* **221**, 99

Brown, A., Tjin A Djie, H.R.E., Thé, P.S.: 1986, in *New Insights in Astrophysics, ESA SP-263*, p. 173

Cohen, M., Kuhi, L.V.: 1979 *ApJS* **41**, 743

Cohen, M., Dopita, M.A., Schwartz, R.D.: 1986 *ApJ* **307**, L21

Drissen, L., Bastien, P., St.-Louis, N.: 1989, *AJ* **97**, 814

Eggen, O.J.: 1983, *MNRAS* **204**, 377

Evans, A., Bode, M.F., Whittet, D.C.B., Davies, J.K., Kilkenny, D., Baines, D.W.T.: 1982, *MNRAS* **199**, 37p

Finkenzeller, U., Basri, G.: 1987, *ApJ* **318**, 823

Franco, G.A.P.: 1990, *A&A* **227**, 499

Gahm, G.F.: 1980, *ApJ* **242**, L163

Gahm, G.F., Nordh, H.L., Olofsson, S.G., Carlborg, N.C.J.: 1974, *A&A* **33**, 399

Gahm, G.F., Nordh, H.L., Olofsson, S.G.: 1975, *Icarus* **24**, 372

Gahm, G.F., Fredga, K., Liseau, R., Dravins, D.: 1979, *A&A* **73**, L4

Gahm, G.F., Lago, M.T.V.T., Penston, M.V.: 1981, *MNRAS* **195**, 59p

Gahm, G.F., Krautter, J.: 1982, *A&A* **106**, 25

Gahm, G.F., Fischerström, C., Liseau, R., Lindroos, K.P.: 1989, *A&A* **211**, 115

Giovanelli, F., Rossi, C., Covino, E., Errico, L., Vittone, A.A., Bisnovatyi-Kogan, G.S., Kurt, V.G., Sheffer, E.K., Lamzin, S.A.: 1988, in: *A Decade of UV Astronomy with the IUE Satellite, ESA SP-281*, vol. **2**, 101

Graham, J.A., Heyer, M.H.: 1988, *PASP* **100**, 1529

Henize, K.G.: 1954 *ApJ* **119**, 459

Henize, K.G.: 1976 *ApJS* **30**, 491

Herbig, G.H.: 1977, *ApJ* **214**, 747

Herbig, G.H., Rao, N.K.: 1972, *ApJ* **174**, 401

Herbig, G.H., Bell, K.R.: 1988, *Lick Obs. Bull.* no. **1111**

Heyer, M.H., Graham, J.A.: 1989, *PASP* **100**, 816

Heyer, M.H., Graham, J.A.: 1990, *PASP* **102**, 117

Hoffmeister, K.: 1965, *Veröff. Sternwarte Sonnenberg* **6**, 93

Hutchinson, M.G., Evans, A., Davies, J.K., Bode, M.F.: 1989, *MNRAS* **237**, 683

Jankovics, I., Appenzeller, I., Krautter, J.: 1983, *PASP* **95**, 883

Joy, A.H.: 1945, *ApJ* **102**, 168

Krautter, J.: 1986, *A&A* **161**, 195

Krautter, J., Reipurth, B., Eichendorf, W.: 1984, *A&A* **133**, 169

Krautter, J., Kelemen, J.: 1987, *Mitt. Astron. Ges.* **70**, 397

Krautter, J., Kelemen, J.: 1992, in preparation

Lago, M.T.V.T.: 1982, *MNRAS* **198**, 445

Lago, M.T.V.T.: 1984, *MNRAS* **210**, 323

Mundt, R.: 1984, *ApJ* **209**, 749

Murphy, D.C., Cohen, R., May, J.: 1986, *A&A* **167**, 234

Plagemann, S.: 1969, *Mem. Soc. Roy. Liege* 5^{th} Series **19**, 331

Reipurth, B., Wamsteker, W.: 1983, *A&A* **119**, 14

Reipurth, B., Graham, J.A.: 1988, *A&A* **202**, 219

Reipurth, B., Zinnecker, H.: 1992, in preparation

Sandqvist, A., Lindroos, K.P.: 1976, *A&A* **53**, 179

Schneider, S., Elmegreen, B.G.: 1979, *ApJS* **41**, 87

Schwartz, R.D.: 1977, *ApJS* **35**, 161

Schwartz, R.D., Noah, P.: 1978, *AJ* **83**, 785

Schwartz, R.D., Heuermann, R.W.: 1981, *AJ* **86**, 1526

Shu, F.C., Adams, F.C., Lizano, S.: 1987, *ARA&A* **25**, 23

Smyth, M.J., Dean, J.F., Robertson, B.S.C.: 1979, *MNRAS* **187**, 29p

Strom, S.E., Strom, K.M., Edwards, S.: 1988, in *Galactic and Extragalactic Star Formation*, eds. R. Pudritz and M. Fich, (Kluwer, Dordrecht), p. 53

Thé, P.S.: 1962, *Contr. Bosscha Obs.* No. **15**

Thé, P.S., Tjin A Djie, H.R.E.: 1978, *A&A* **62**, 439

Thé, P.S., Bakker, R., Wesselink, T.J.H., van der Linden, T.J.: 1978, *A&AS* **33**, 213

Thé, P.S., Tjin A Djie, H.R.E., Bakker, R., Bastiaansen, P.A., Burger, M., Cassatella, A., Fredga, K., Gahm, G.F., Liseau, R., Smyth, M.J., Viotti, R., Wamsteker, W., Zeuge, W.: 1981, *A&AS* **44**, 451

Thé, P.S., Tjin A Djie, H.R.E., Brown, A., Catala, C., Doazan, V., Linsky, J.L., Mewe, R., Praderie, F., Talavera, A., Zwaan, C.: 1985, *Irish Astron. J.* **17**, 79

Tjin A Djie, H.R.E., Thé, P.S., Andersen, J., Nordström, B., Finkenzeller, U., Jankovics, I.: 1989, *A&AS* **78**, 1

Ungerechts, H., Thaddeus, P.: 1987, *ApJS* **63**, 645

Young Low Mass Stars in the Norma Cloud

Bo Reipurth[1] and J. A. Graham[2]

[1] European Southern Observatory
Casilla 19001
Santiago 19, Chile

[2] Carnegie Institution of Washington
Department of Terrestrial Magnetism
5241 Broad Branch Rd., N.W.
Washington DC 20015, USA

Abstract

We review the low mass star formation activity in the Sa 187 cloud in Norma. The cloud contains the Herbig-Haro objects HH 56 and HH 57. We discuss in particular the FU Orionis star which recently appeared next to HH 57. HH 56 shows a clear bow shock shape on deep CCD images, and appears to originate from a young star embedded in the little nebula Re13. Both stellar energy sources drive major molecular outflows.

1. The Norma Cloud Sa 187

The southern constellation Norma contains a number of small dark clouds. One of these, Sa 187, is located around $\alpha \approx 16^h30$ $\delta \approx -45°$ (Sandqvist 1977). It has attracted considerable interest since Schwartz (1977) discovered two Herbig-Haro objects there, HH 56 and HH 57. The cloud consists of two main parts, a larger, structured "head" to the west and a narrow filamentary "tail" stretching to the east (see the red Schmidt plate in Fig. 1). The east-west extent of the whole cloud is a little more than half a degree. There is no direct determination of the distance of the cloud; Cohen et al. (1984) suggested 200 pc, Reipurth (1985) favored 300 pc, Graham and Frogel (1985) argued for 700 pc, and Cohen et al. (1986) used 940 pc. Re-examining the various arguments, a distance of 500–700 pc seems now most probable; for the purpose of discussion we will in the following adopt the Graham and Frogel distance of 700 pc, noting with these authors the considerable uncertainty in this estimate.

The large-scale extinction patterns in this part of the Milky Way have been discussed by Haug and Bredow (1977) and in more detail by Gregorio Hetem et al. (1988). CO observations were made of the cloud complex by Alvarez et al. (1986), which suggest a total mass of 500 $(d/700)^2$ solar masses.

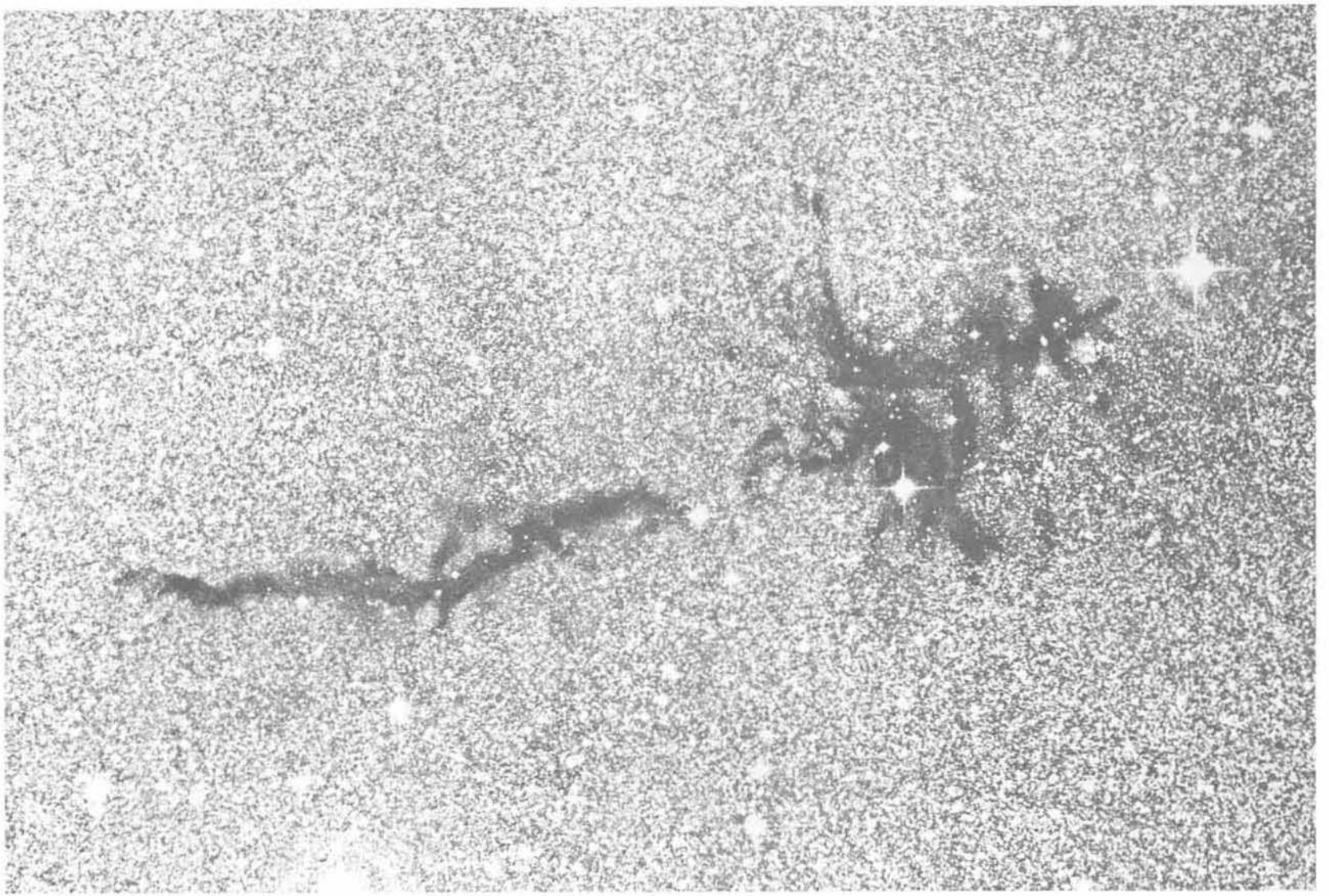

Figure 1. The molecular cloud Sa 187, as seen on a red ESO Schmidt plate

The eastern filament is also presently forming stars; a nebulous star is located in the middle of the filament, while two small reflection nebulae are found in each end of the filament (Reipurth et al. 1992a).

A few Hα emission stars in the general region of the Norma cloud have been reported by Schwartz (1977) and Schwartz et al. (1990).

2. HH 57 and the Associated FUor

HH 57 was discovered by Schwartz (1977) in a dense region of obscuration at the western edge of the Norma cloud complex. Red low resolution spectra of the HH object are presented by Schwartz and Dopita (1980). A proper motion study by Schwartz et al. (1984) showed that HH 57 has very low tangential velocity, and consequently there is a large uncertainty on the derived position angle of the proper motion vector. Molecular hydrogen emission was detected in HH 57 by Wilking et al. (1990).

The red CCD image in figure 2 shows HH 57 as a small knot next to a star and connected to this with small lobes of reflected light. Another reflection nebula is located at the opposite side of the star. Polarization measurements by Scarrott et al. (1987) confirm that the star is the illuminating source.

V346 Nor was first detected as an infrared source by Elias (1980) and Reipurth and Wamsteker (1983). Shortly after, Graham (1983) discovered that a visible star had appeared where nothing had been seen before, neither on the POSS print (1964) nor on the plates taken by Schwartz at the time of the discovery of HH 57 (Schwartz 1977). The star was clearly brightening already in 1980, as documented by SERC Schmidt plates. Soon after it was confirmed as an FU Ori star (Graham and Frogel 1985, Reipurth 1985). The star is a strong IRAS source (e.g. Cohen and Schwartz 1987). Far-infrared airborne observations are presented by Cohen et al. (1984, 1985). More recently sub-millimeter observations have revealed large amounts of cool circumstellar dust (Weintraub et al. 1991, Reipurth et al. 1992b). The 3μm water ice band was detected in absorption towards V346 Nor, together with a relatively sharp dip at 2.97μm likely due to ammonia ice (Graham and Chen 1991).

The spectrum of V346 Nor shows mostly a very red almost featureless continuum. In the early 1983 low-resolution spectrum by Reipurth (1985), Hα appears to be purely in absorption. Since early 1984, the star has had strong but variable Hα emission with a characteristic P Cygni profile showing a deep absorption trough extending bluewards to -450 km sec^{-1} (see Fig. 3). The very weak absorption spectrum was classified as type F8III by Cohen et al. (1986). In the last couple of years FeII lines have begun to become prominent in emission. The CaII triplet near λ8500 has been in emission since 1983. The NaI D lines are in absorption and are blueshifted. [OI]$\lambda\lambda$6300, 6363 have recently become prominent. Blue shifted [SII] lines have also been observed with a velocity ≈ -60 km sec^{-1}.

Table 1. *Photometry of V346 Nor*

Source	B	V	J	H	K	L	10μm	20μm
JHE 79-2			12.20	10.01	8.18			
RW 79-2			11.96	9.87	8.19	6.18		
BR 81-1				8.78	8.45	6.57		
JAG 83-3	19.49	17.23						
JAF 83-3					7.45	6.19	2.12	0.10
BR 83-4			10.17	8.74	7.64	5.86		
JAF 83-4			9.98	8.86	7.59	6.22		
BC 83-5			9.97	8.65	7.56			
JAG 83-5		16.81						
BC 83-9			10.08	8.67	7.66			
BC 83-9			10.12	8.73	7.70	6.34		
JAG 83-10	18.61	16.68						
JAF 83-10			9.99	8.68	7.61	6.25		
JAG 84-1		17.0						
JAG 84-3	18.48	16.61						
JAG 85-1			10.01	8.73	7.79	6.74	2.4	0.0
BR 85-2			10.24	8.79	7.73	6.07		
JAG 85-5			10.05	8.78	7.77	6.41		
BR 86-2			10.17	8.80	7.75	6.00		
BR 88-5			10.03	8.64	7.51	5.70		
JAG 88-6		(16.72)	9.88	8.57	7.48	6.08	2.04	
BR 89-2			10.51	8.75	7.31	5.25		
AUL 90-2	18.00	16.10						
AUL 90-6	18.23	16.35						
AUL 90-8	17.83	16.34						

JHE : J. H. Elias
RW : Reipurth and Wamsteker
BR : B. Reipurth
JAG : J. A. Graham
JAF : J. A. Frogel
BC : B. Carney
AUL : A. U. Landolt

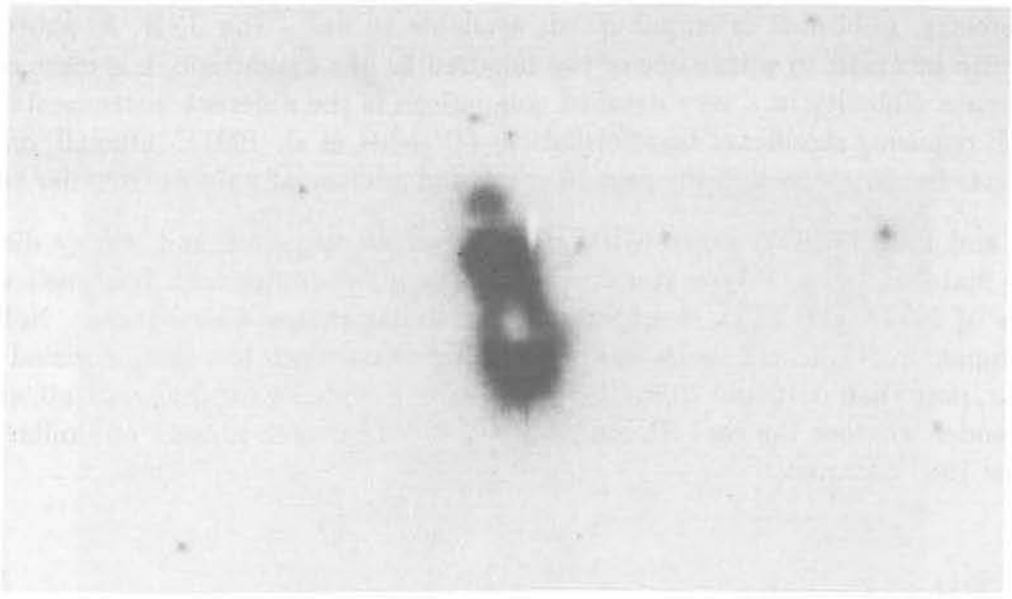

Figure 2. A CCD image of HH 57 and the associated FUor V346 Nor. Only the Herbig-Haro knot is in emission, other features are reflected light. The spike in the HH object is from a defect in the CCD detector.

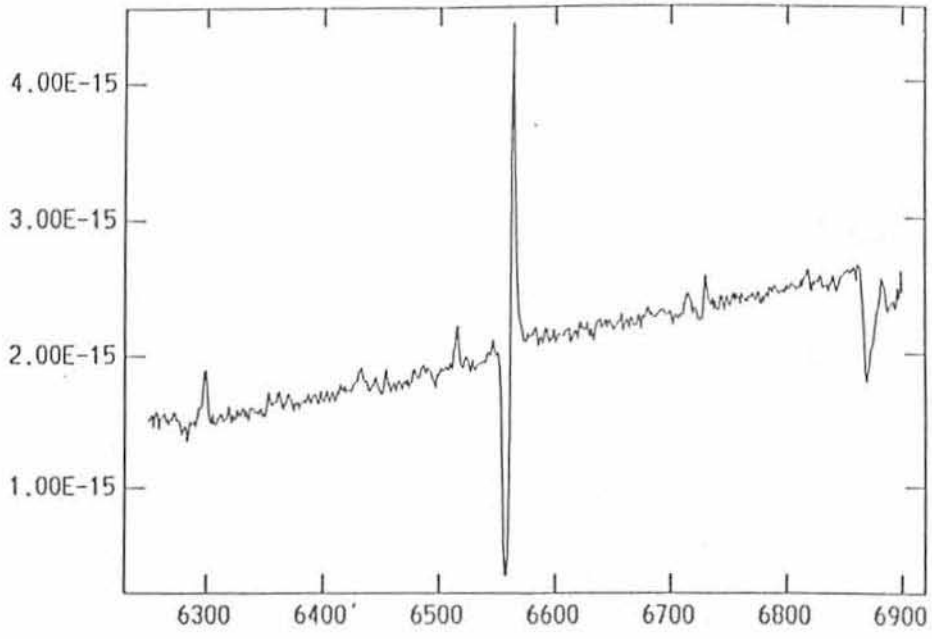

Figure 3. A red medium-resolution spectrum of V346 Nor taken on June 2, 1988 by Graham and Heyer (unpublished). Hα shows a strong P Cygni profile. Between Hα and the [OI] line at λ6300 there are three Fe II emission lines.

The spectral energy distribution has changed little since 1983 although variations of a few tenths of a magnitude in the visible light seem to be common. In Table 1 we have compiled all photometry, published or unpublished, available to us. The J, H, K photometry is mostly quite accurate, to within one or two hundredths of a magnitude, L is more uncertain. But the main difficulty in a very detailed comparison is the different instrumental systems employed, requiring significant transformations (Bouchet et al. 1991). Overall, one can see that the star has brightened in the past 10 years, and additionally shows irregular variability.

Graham and Frogel (1985) suggested that the observed spectrum and energy distribution could be matched by an F-type star surrounded by a two-component dust shell with temperatures of 2000K and 325K in addition to the stellar energy distribution. Note that in the accompanying table, the variations in the infrared are much less than in visual light. In particular, note that at 10 and 20μm there is no strong evidence for change at all, and we are led to wonder whether the cool IR component could have been present at similar intensity before the 1980 outburst.

3. The HH 56 Complex

Spectra of HH 56 were obtained by Schwartz and Dopita (1980), showing that its velocity is slightly redshifted to about +36 km sec^{-1}. Wilking et al. (1990) detected it in molecular hydrogen emission. On a Schmidt plate it looks perfectly stellar. But on deep interference filter CCD images it shows faint structure, revealing a morphology reminiscent of a bow shock like in HH 34 (Reipurth et al. 1986). The apparent bow shock faces to the north-east, in the same approximate direction as the proper motion vector, as determined by Schwartz et al. (1984). The HH object moves away from a little nebula, Re 13, which reflects light from a star apparently embedded in the cloud (Reipurth 1981). Spectra of Re 13 show Hα in emission (Alvarez et al. 1986, Cohen et al. 1986). No infrared source has so far been detected there, but recently the embedded star was detected as a weak 1300μm source (Reipurth et al. 1992b). Additional documentation of the association between HH 56 and Re 13 comes from a faint new HH knot, HH 56B, further to the north-east along the line defined by HH 56 and Re 13 (see Fig. 4). In the opposite direction and also along the well defined flow axis there is another HH knot, so that the HH 56 complex comprises a major well collimated HH flow (Reipurth et al. 1992a).

Observations in several molecular species made at the SEST at La Silla have revealed two large molecular outflows, one centered on Re 13 and another on the FU Ori star at HH 57. Both south-western lobes are blueshifted, and beautifully outline cavities at the edge of the cloud and seen on CCD images. The red-shifted lobes merge, because there is a slight difference between the angle of the axes of the two flows (Olberg et al. 1989, Reipurth et al. 1992a).

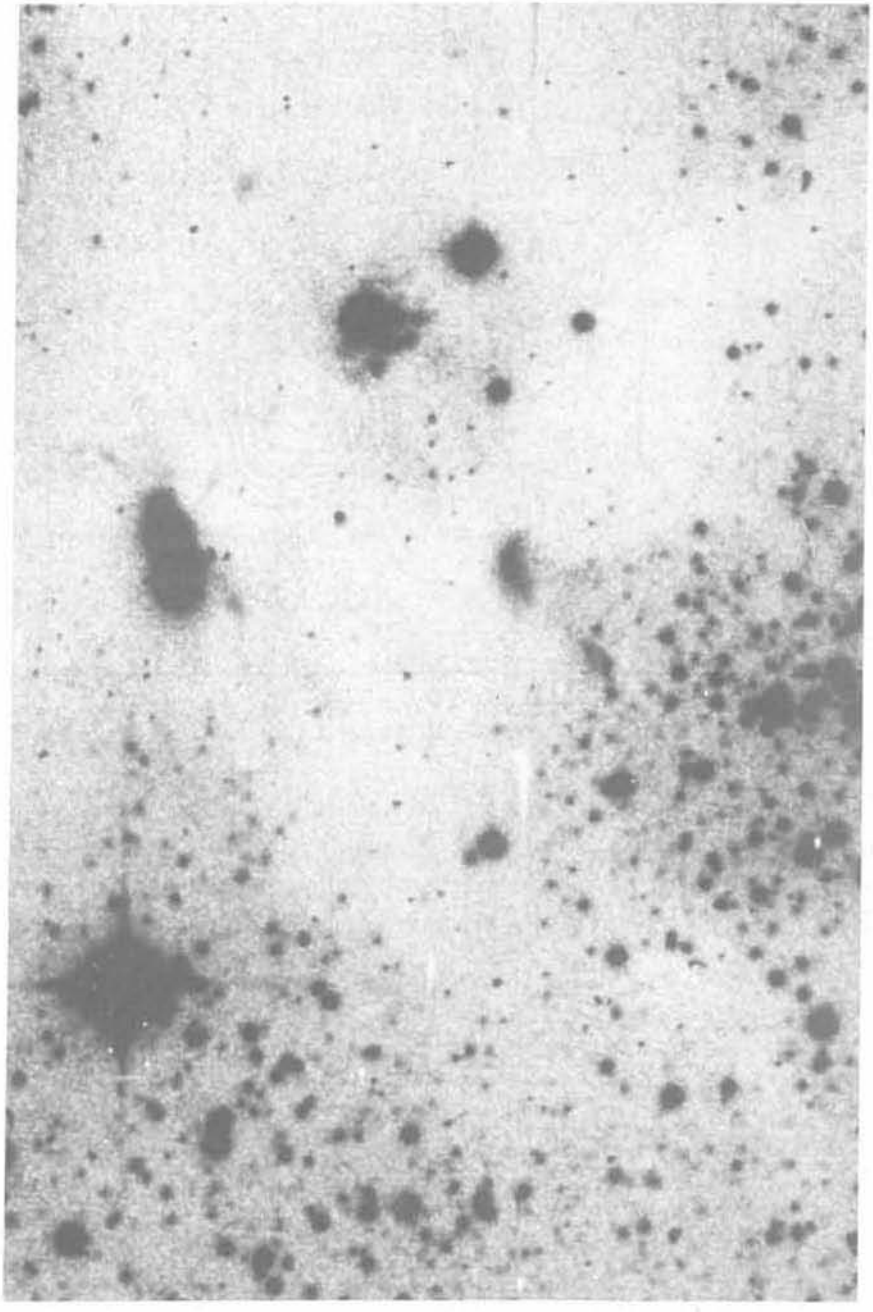

Figure 4. A [SII] interference filter CCD image showing HH 57 and its associated FUor, and part of the HH 56 complex and a small reflection nebula from its driving source, Re 13.

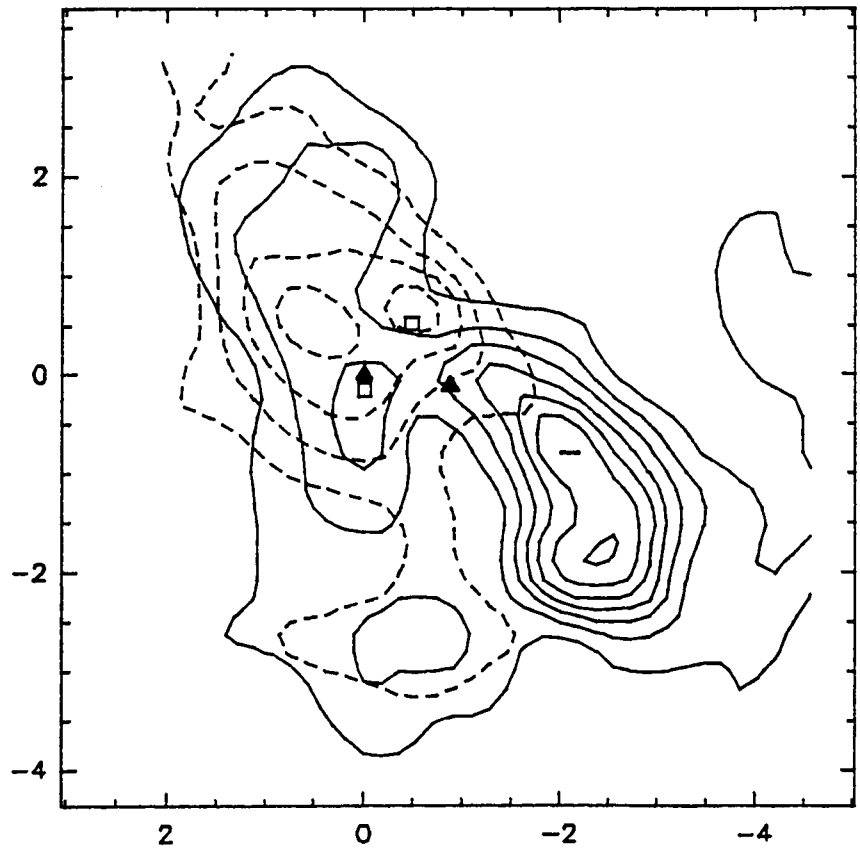

Figure 5. The molecular flows around HH 56 and HH 57, shown in a ^{12}CO contour plot. With red (short dash) and blue (solid line) wing emission. The positions of the HH 57 infrared source at (0,0) and of Re 13 are marked by filled triangles. The open squares mark HH 57 and HH 56, respectively. Offsets are given in arcminutes.

References

Alvarez, H., Bronfman, L., Cohen, R., Garay, G., Graham, J.A., Thaddeus, P.: 1986, *ApJ* **300**, 756

Bouchet, P., Manfroid, J., Schmider, F.: 1991, *A&A Suppl.* **91**, 409

Cohen, M., Schwartz, R.D.: 1987, *ApJ* **316**, 311

Cohen, M., Schwartz, R.D., Harvey, P.M., Wilking, B.A.: 1984, *ApJ* **281**, 250

Cohen, M., Harvey, P., Schwartz, R.D.: 1985, *ApJ* **296**, 633

Cohen, M., Dopita, M.A., Schwartz, R.D.: 1986, *ApJ* **302**, L55

Elias, J.H.: 1980, *ApJ* **241**, 728

Graham, J.A.: 1983, *IAU Circular* No. 3785

Graham, J.A., Frogel, J.A.: 1985, *ApJ* **289**, 331

Graham, J.A., Chen, W.P.: 1991, *AJ* **102**, 1405

Gregorio Hetem, J.C., Sanzovo, G.C., Lépine, J.R.D.: 1988, *A&AS* **76**, 347

Haug, U., Bredow, K.: 1977, *ApJS* **30**, 235

Olberg, M., Reipurth, B., Booth, R.S.: 1989, in *The Physics and Chemistry of Interstellar Molecular Clouds*, eds. G. Winnewisser and J.T. Armstrong, p. 120

Reipurth, B.: 1981, *A&AS* **44**, 379

Reipurth, B.: 1985, *A&A* **143**, 435

Reipurth, B., Wamsteker, W.: 1983, *A&A* **119**, 14

Reipurth, B., Bally J., Graham, J.A., Lane, A.P. Zealey, W.J.: 1986, *A&A* **164**, 51

Reipurth, B., Olberg, M., Booth, R.S.: 1992a, in press

Reipurth, B., Chini, R., Krügel, E., Kreysa, E., Sievers, A.: 1992b, in preparation

Sandqvist, Aa.: 1977, *A&A* **57**, 467

Scarrott, S.M., Gledhill, T.M., Warren-Smith, R.F.: 1987, *MNRAS* **227**, 701

Schwartz, R.D.: 1977, *ApJS* **35**, 161

Schwartz, R.D., Dopita, M.A.: 1980, *ApJ* **236**, 543

Schwartz, R.D., Jones, B.F., Sirk, M.: 1984, *AJ* **89**, 1735

Schwartz, R.D., Persson, S.E., Hamann, F.W.: 1990, *AJ* **100**, 793

Weintraub, D.A., Sandell, G., Duncan, W.: 1991, *ApJ* **382**, 270

Wilking, B.A., Schwartz, R.D., Mundy, L.G., Schultz, A.S.B.: 1990, *AJ* **99**, 344

Star Formation in the Ophiuchus Molecular Cloud Complex

Bruce A. Wilking

Department of Physics
University of Missouri St.-Louis
8001 Natural Bridge Road
St. Louis, MO 63121, USA

Abstract

The nearby Ophiuchus complex extends for tens of parsecs in the plane of the sky and is comprised of filamentary clouds of low density molecular gas interspersed with dense molecular cores. What distinguishes the Ophiuchus clouds from other dark cloud complexes is the large (550 $M_\odot$) centrally condensed core in the westernmost cloud and the associated high density of young stellar objects. The 1 pc × 2 pc core region is characterized by high gas column densities corresponding to visual extinctions of 50−100 mag. The relatively high efficiency of star formation in the core (SFE $\geq$20%) suggests it is the formation site of a gravitationally bound open cluster. The distribution of both high and low density molecular gas in the Ophiuchus complex will be reviewed with particular emphasis on the westernmost or ρ Ophiuchi cloud. The corresponding distribution of young stellar objects as revealed by infrared observations and Hα surveys of the complex will also be presented. Combining data from IRAS with ground-based infrared observations has led to the identification of 78 cluster members in the ρ Oph cloud. The evolutionary state of these objects inferred from their 1−100 μm spectral energy distributions and the luminosity function of the cluster will be discussed. A major conclusion from this analysis is that the duration of star formation in the ρ Oph core is less than 3.5×10^6 years, suggesting that stars have formed in a relatively efficient burst.

Most recently, attention has been turned to star formation in the L1689 cloud which lies about 1 degree east of the ρ Oph cloud. While displaying a lower density of star formation than the ρ Oph cloud, the cloud cores L1689N and L1689S host interesting examples of deeply embedded sources. The properties of a proposed protobinary system in L1689N, as revealed by interferometric observations, will be discussed.

I. Introduction

Lying in the Scorpius-Centaurus OB association, the filamentary system of dark clouds in Ophiuchus extends for tens of parsecs. Their distance from the Sun has been estimated to be about 160 pc (Bertiau 1958, Whittet 1974, Chini 1981), although a more recent evaluation suggests a somewhat lower value of 125±25 pc (de Geus, de Zeeuw, and Lub 1989). The westernmost cloud in the complex, or ρ Ophiuchi cloud, is comprised of the L1681, L1686,

and L1688 clouds and contains a large visually opaque core (Bok 1956). The core region lies adjacent to a reflection nebula illuminated by the B2 V star HD147889. The L1689 and L1709 clouds form the bases of two filamentary streamers which extend to the east (L1689, L1712, L1729) and northeast (L1709, L1740, L1744, L1755, and L1765) from the ρ Oph cloud. Early spectroscopic surveys of the area revealed numerous emission-line stars (Struve and Rudkjøbing 1949, Haro 1949); the realization that these were pre-main sequence stars pointed to the ρ Oph cloud as a region of recent star formation. This was confirmed by near infrared surveys which unveiled a large population of embedded objects (Grasdalen, Strom, and Strom 1973; Vrba et al. 1975).

This review will focus on star formation in the ρ Ophiuchi cloud but will discuss observations of other regions of the complex. It complements and expands upon a recent overview of the ρ Oph cloud by Klose (1986). In Section II, the distribution of low density molecular gas in the Ophiuchus complex, as traced by emission from CO and its isotopes, will be discussed. In Sec. III, observations of high density molecular gas are reviewed, focussing on cold cores revealed by a recent study of DCO^+ emission. The distribution of lightly obscured emission-line stars and embedded infrared sources and their relationship to the molecular gas is the topic of Sec. IV. Evidence for mass loss among the population of young objects and the cloud energetics is the subject of Sec. V. An analysis of star formation in the ρ Oph cloud which combines the molecular-line, near-infrared, and far-infrared data of the region is presented in Sec. VI. Finally in Sec. VII, star formation in the L1689 cloud and the proposed protobinary system IRAS 16293–2422 are discussed.

II. The Distribution of Low Density Molecular Gas

Widespread self-absorption and the high optical depths of ^{12}CO emission lines make ^{13}CO the best tracer of column density in the Ophiuchus clouds (e.g., Encrenaz, Falgarone, and Lucas 1975). The distribution of $^{13}CO(J=1\rightarrow0)$ emission, mapped with 2.4 arcmin resolution, is shown in Figs. 1a and 1b over a 30 square degree area which includes the ρ Oph cloud and the eastern filaments (Loren 1989a). The total mass of the complex is determined to be 3050 $M_\odot$ with about half of this contained in the ρ Oph cloud. These maps not only underscore the filamentary structure of the clouds, also evident in lower resolution maps of ^{12}CO emission (de Geus, Bronfman, and Thaddeus 1990), but also demonstrate the clumpy nature of the gas. From these data, Loren (1989a,b) identifies 89 molecular clumps which are either kinematically or spatially distinct. The overall cloud morphology is suggestive of the passage of a shock, however, the expected streaming motions of the gas are not well established (e.g., Vrba 1977; Loren and Wootten 1986; Loren 1989a,b; de Geus, Bronfman, and Thaddeus 1990, de Geus and Burton 1991).

In the core of the ρ Oph cloud, ^{13}CO (as well as ^{12}CO) emission lines are self-absorbed. Hence, emission from the rarer isotope $C^{18}O$ best delineates the column density distribution in the core (Lada and Wilking 1980). $C^{18}O(J=1\rightarrow0)$ observations with a resolution of 1.1 arcmin have revealed a 1 pc×2 pc ridge of high column density gas which forms a centrally condensed core containing about 550 $M_\odot$ (Wilking and Lada 1983). It is this

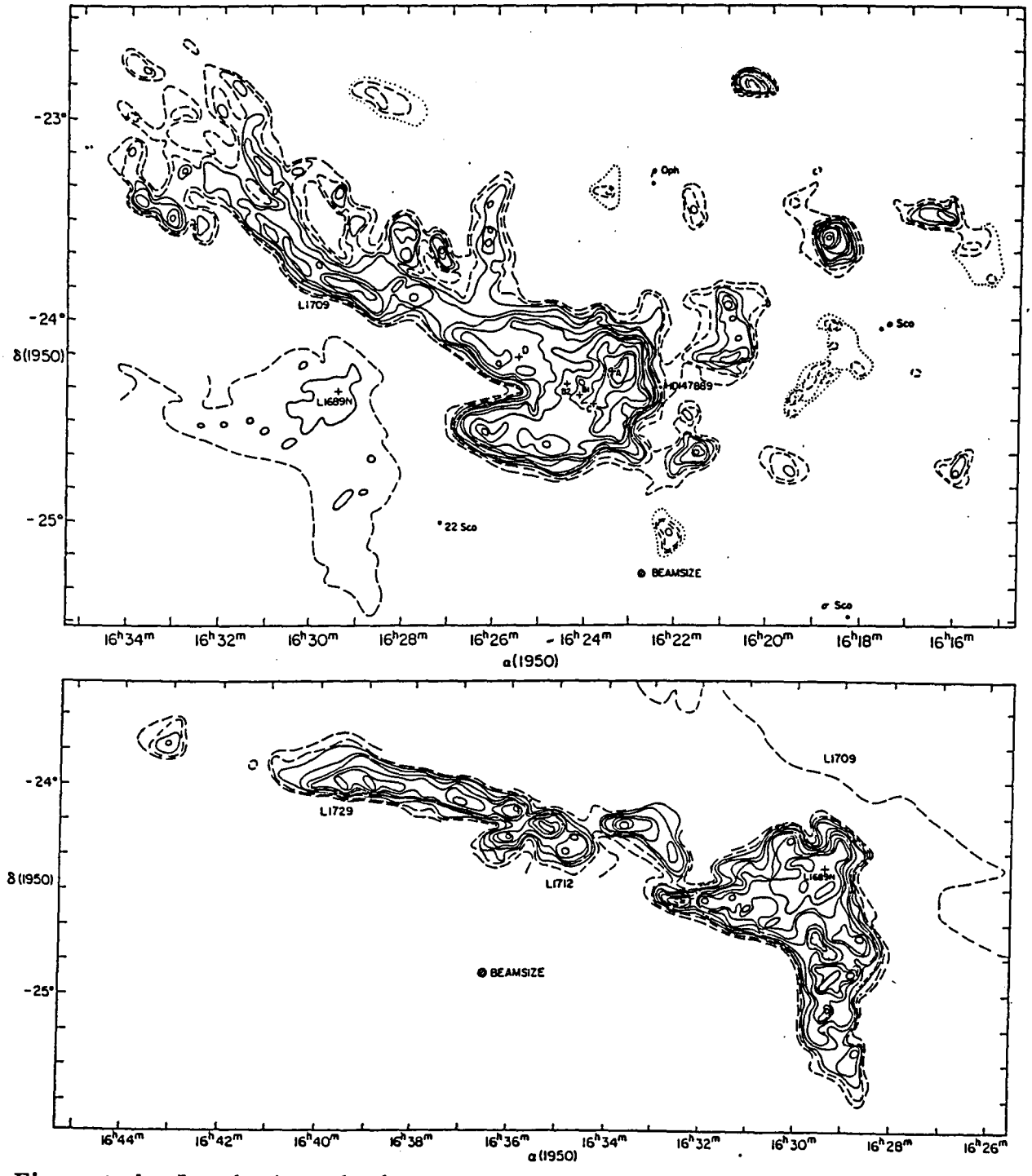

Figure 1a,b: Low density molecular gas over a 30 square degree area of the Ophiuchus complex as traced by 2.4 arcmin resolution observations of $^{13}CO(J=1–0)$ emission lines (Loren 1989a). The contours are in units of TR*; the lowest (dashed) contours represent values of 2 K and 3 K, followed by contours of 4, 5, 6, 7, 8, 10 (bold), 14, 16, 18, and 20 K (bold). Also shown for reference are the locations of several early B stars in the region.

core that distinguishes the Ophiuchus cloud from other dark clouds forming low mass stars such as those in Taurus-Auriga. Hydrogen column densities in the core are estimated to range from $0.4-1.4\times10^{23}$ cm^{-2} which corresponds to 25–100 mag of visual extinction. In Fig. 2, a previously unpublished 1.4 arcmin resolution map of the integrated intensity of $C^{18}O(J=2\rightarrow1)$ emission lines is shown. The distribution of high column density gas is similar to that revealed by the $C^{18}O(J=1\rightarrow0)$ maps, i.e., it lies in a northwest-southeast ridge with a very sharp column density gradient on the western edge.

A large velocity gradient (LVG) code has been used to model the observed $2-1$ and $1-0$ line intensities and suggests that the $C^{18}O$ emission in the ρ Oph cloud is not in local thermodynamic equilibrium (LTE). Moreover, the $C^{18}O$ emission lines are probably optically-thick in the 2–1 transition throughout the high column density core. We have considered three high column density regions which show little variation in integrated intensity over a $3' \times 3'$ area. Because of the similar beam sizes used to observed the 2–1 and 1–0 transitions (1.4′ vs 1.1′) and the uniformity of the emission, no corrections have been made for the different beam sizes. In the northwestern region of the ridge comprising the ρ Oph A core where the gas temperatures are believed to be 40–45 K, we derive peak densities of $3.5-4.5\times10^3$cm^{-3} and $C^{18}O$ column densities of $\sim 1\times10^{16}$ cm^{-2}. Due to subthermal excitation of the $C^{18}O$, the LTE approximation applied to 1–0 data yields estimates for the column density as much as 2.5 times greater than those from the LVG models. In the cooler central regions of the core and the northeastern periphery where gas temperatures are in the range of 20–30 K, the LVG column densities are in better agreement with those derived assuming LTE. As in ρ Oph A, subthermal excitation causes LTE column densities from 1–0 data to be consistently higher than those derived from the LVG code, but by only 50% or less. In addition, the 1–0 lines as well as the 2–1 lines from these regions are likely to be optically thick. The (2–1)/(1–0) line ratios are surprisingly low in central/southeastern regions of the core suggesting either the 2–1 lines are self-absorbed or there is a large amount of low density gas. This is the same region where $^{13}CO(1-0)$ emission lines were found to be self-absorbed (Lada and Wilking 1980). These data are best fit by LVG models with densities of 900-1600 cm^{-3} and column densities of $\sim 1.5\times10^{16}$ cm^{-2}. Similarly, in the northeastern periphery of the ridge (about 14 arcminutes west of the ρ Oph A core), we derive low values for the density ($1.3-1.7\times10^3$ cm^{-3}) and $C^{18}O$ column densities of $\sim 4\times10^{15}$ cm^{-2}.

In summary, single-temperature LVG models suggest non-LTE conditions in the ρ Oph core leading to possible overestimations of the $C^{18}O$ column densities derived from 1–0 data assuming LTE. Additionally, because of the substantial optical depth in the 2–1 transition, $C^{18}O$ (1–0) emission lines are better tracers of true column density in ρ Oph. Further multi-transition observations of the cloud in several isotopes of CO are needed to determine the temperature and column density structure of the cloud in more detail.

III. The Distribution of High Density Molecular Gas

Observations of density-sensitive molecules, such as SO, H_2CO, NH_3, HCO^+, and DCO^+, have shown that the high density gas is closely associated with the high column density

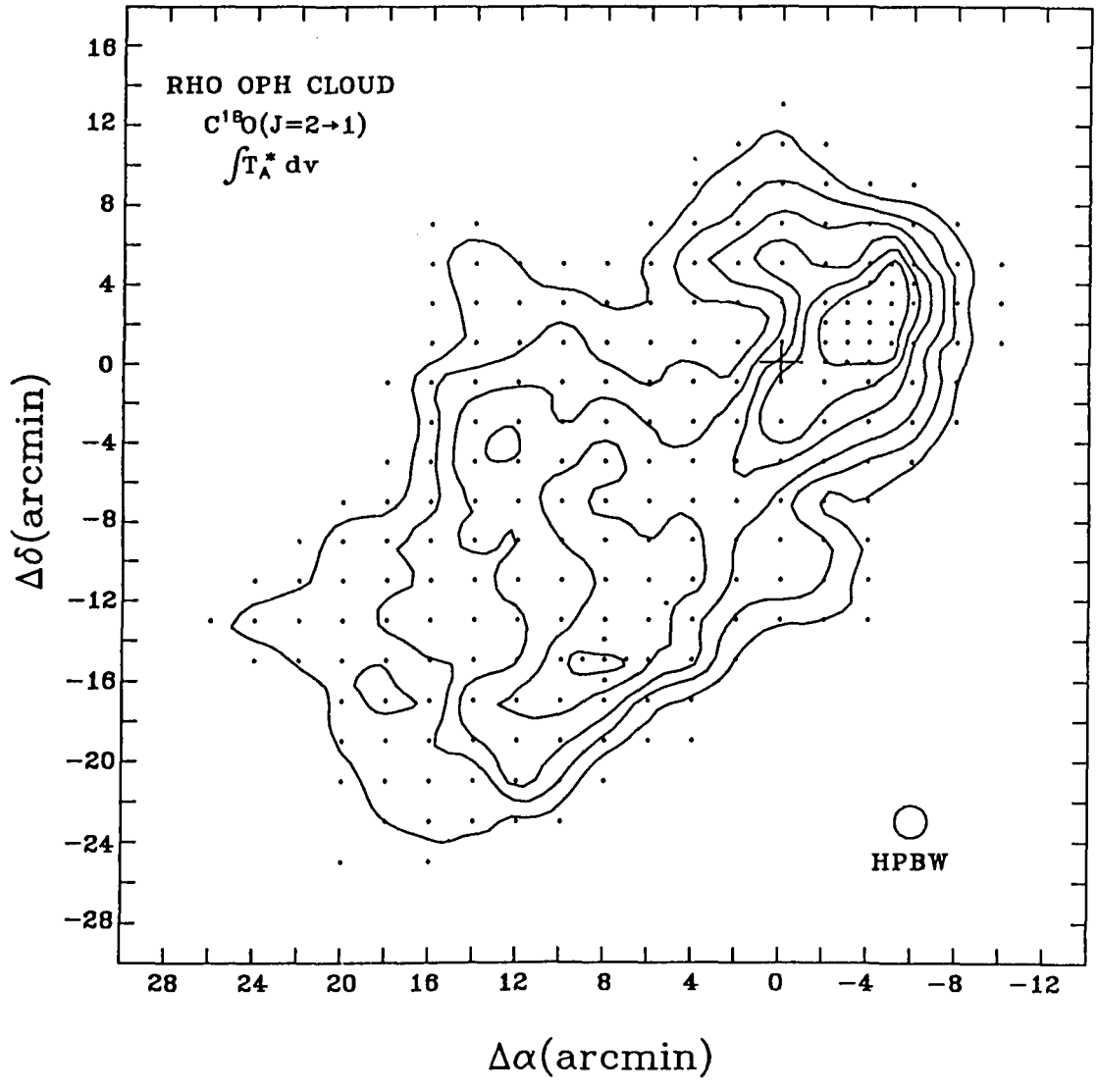

Figure 2: A previously unpublished map of $C^{18}O$(J=2–1) integrated intensity in the ρ Oph core. The 1.4 arcmin resolution observations were obtained with the University of Texas Millimeter-Wave Observatory. The contours levels are 2.5, 3.5, 4.5, 6, 7.5, and 9 K km s^{-1}. The 225 positions in the cloud observed to construct this map are shown by dots. A cross marks the (0,0) for the map which is the position of the YSO Source 1 (E25): $16^h23^m32\overset{s}{.}8$ $-24°16'44''$. The nominal locations of the high density regions ρ Oph A and B would be (–2,1) and (8,–5), respectively.

gas. In the core of the ρ Oph cloud, observations of SO and H_2CO (λ=2mm) emission have located two distinct concentrations of dense gas separated by about 0.6 pc and connected by a plateau of dense material: ρ Oph A at the northwestern end of the $C^{18}O$ ridge and ρ Oph B just northeast of the ridge center (Gottlieb et al. 1978; Loren, Sandqvist and Wootten 1983). Modeling of H_2CO emission lines at λ=2 mm and 2 cm imply peak densities of $n(H_2) = 3\times10^5$ cm^{-3} in the 50 $M_\odot$ ρ Oph A core, densities greater than 10^6 cm^{-3} in the 110 $M_\odot$ ρ Oph B core, and densities of about 5×10^4 cm^{-3} in the plateau (Loren, Sandqvist and Wootten 1983). The ρ Oph B core is unique in that it displays rare 2 cm H_2CO emission, originating in several rotating fragments (Loren et al. 1980; Martin-Pintado et al. 1983; Wadiak et al. 1985). In addition, the ρ Oph B core is colder than ρ Oph A; observations of NH_3 suggest kinetic temperatures of 19 K at ρ Oph B and 45 K for ρ Oph A (Zeng, Batrla, and Wilson 1984). This temperature difference is confirmed by the dearth of temperature-sensitive deuterated molecules in ρ Oph A relative to ρ Oph B (Loren and Wootten 1986).

The most extensive study of high density gas in the ρ Oph complex has been made using multi-transition observations of the DCO^+ molecule (Loren, Wootten, and Wilking 1990). The nature of the DCO^+ chemistry and excitation requires that the emitting regions be simultaneously dense and cold. Twelve dense cores have been observed, the majority in the ρ Oph cloud but several in L1709 and L1689. They range in mass from 8–44 $M_\odot$ and in density from $10^{4.5-6}$ cm^{-3}. The kinetic temperature is less than 15 K in most cores but may reach 25 K in the core associated with ρ Oph A. The distribution of dense gas (cores A-F) in the $C^{18}O$ ridge of the ρ Oph core is shown in Fig. 3. Submillimeter emission from cold dust (15±5 K) has been detected from a compact region (0.5′×1.0′) which coincides with the center of the ρ Oph A core (Ward-Thompson et al. 1989; see also Schwartz, Snell, and Schloerb 1989). The relationship of the cold DCO^+ cores with submillimeter emission and with heavily obscured IRAS sources on their periphery has led to the suggestion that they are future sites for star formation. It is interesting to note that the masses, temperatures, and velocity dispersions of these cores lie between those derived for cold cores in the Taurus-Auriga complex and for giant molecular cloud cores (e.g., Table 1, Wilking 1989). To the extent that we can compare core properties determined from different molecules, the implication is that cores in Ophiuchus may ultimately form stars of intermediate mass.

IV. The Embedded Population

A. Emission-Line Stars and X-Ray Sources

The presence of emission lines, notably Hα, in the spectrum of stars in regions of star formation is characteristic of objects in the T Tauri phase of pre-main-sequence evolution. Spectroscopic observations, and later objective prism surveys, identified about 75 emission-line stars in the complex, with the majority concentrated in the ρ Oph cloud (Struve and Rudkjøbing 1949, Haro 1949, Dolidze and Arakelyan 1959). More recently, an Hα objective prism survey of the complex by Wilking, Schwartz, and Blackwell (1987) has revealed a total of 65 emission-line stars; a table of accurate positions and relative Hα line strengths can be

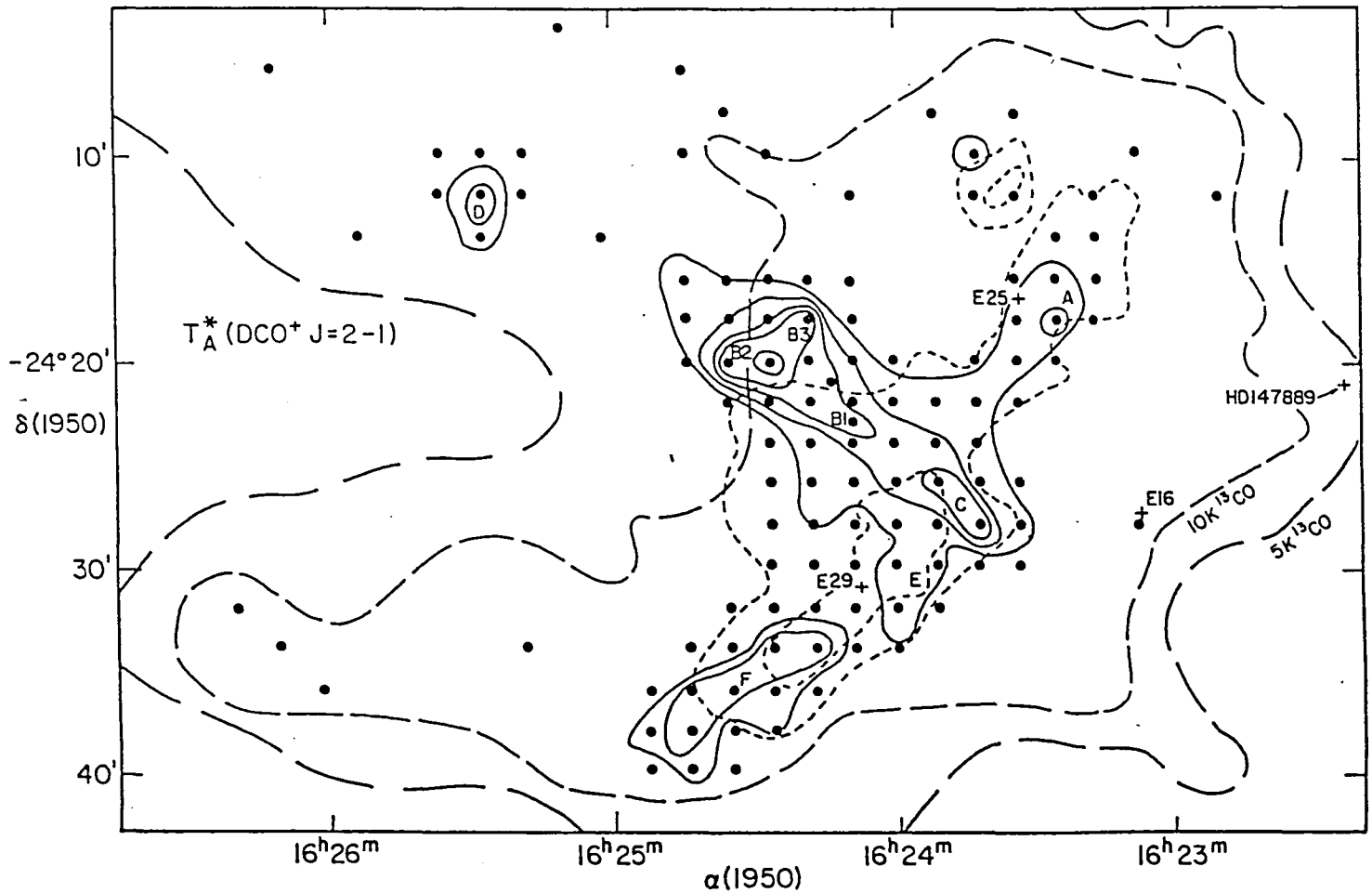

Figure 3: The distribution of DCO^+(J=2–1) in the core of the ρ Oph cloud (Loren, Wootten, and Wilking 1990). Solid contours show the intensity of T_A^* of DCO^+ at the levels of 0.4, 0.8, 1.2, 1.6, and 2.0 K. The positions sampled are shown by filled circles. The dense cores are labeled A–F. The ridge of lower density $C^{18}O$ gas is shown by short dashed contours. The boundaries of the ρ Oph cloud are outlined by two long dashed contours and are the 5 K and 10 K contours of T_R^* of ^{13}CO. The positions of the four most luminous objects in the cloud are labeled by crosses.

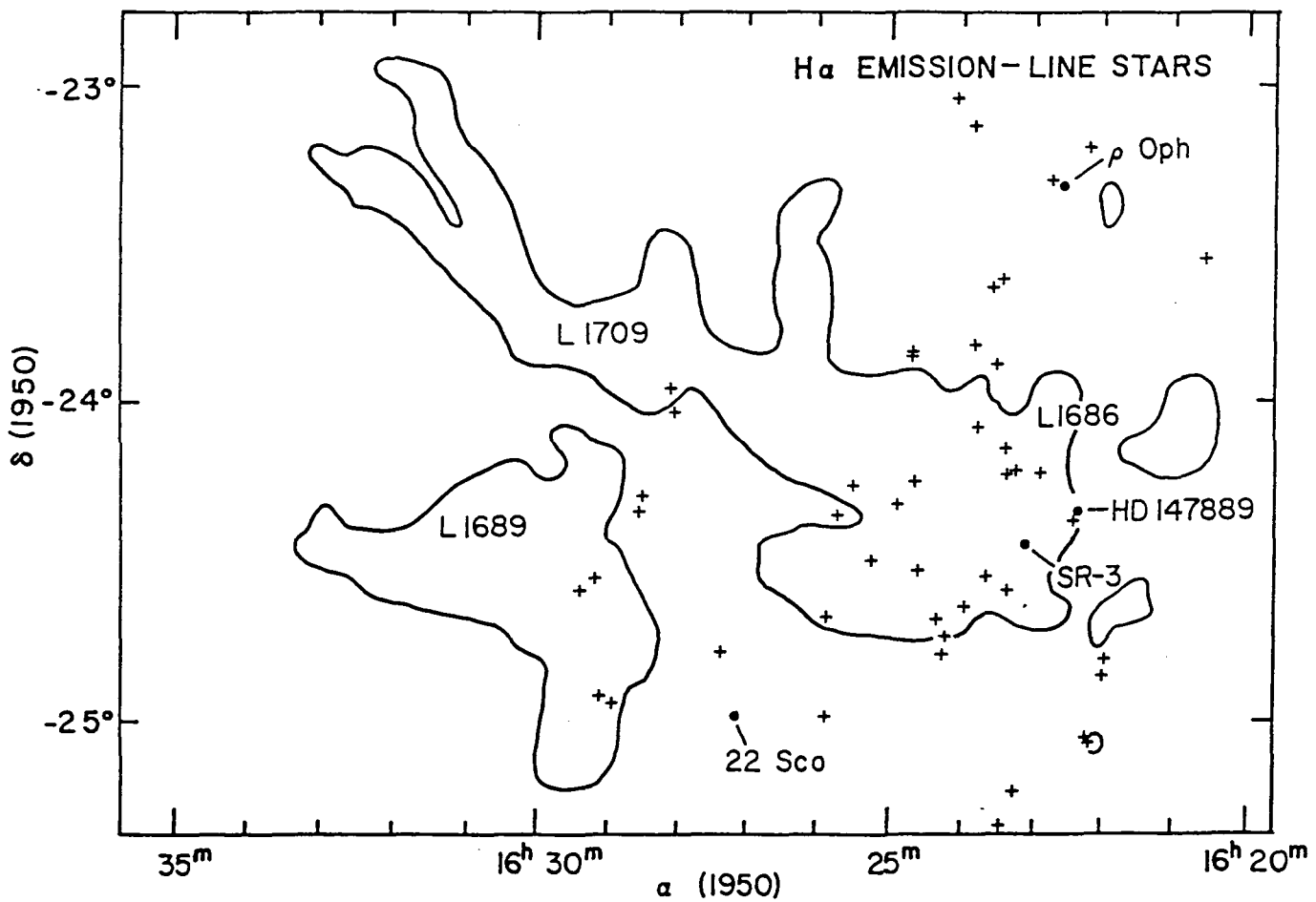

Figure 4: The distribution of Hα emission line stars relative to the major concentrations of molecular gas in the Ophiuchus complex (Wilking, Schwartz, and Blackwell 1987). The clouds are outlined by contours of ^{13}CO emission where $T_A^* = 3$ K (Loren and Wootten 1986).

found for these sources in their paper. Only 32 of these objects had been identified in previous Hα surveys, suggesting that variability may be a major factor in the detection of such objects. Among these 65 objects, 18 have thus far been confirmed as T Tauri stars (e.g., Rydgren, Strom, and Strom 1976, Cohen and Kuhi 1979, Rydgren 1980). The tendency for the remaining Hα objects to be associated with molecular gas, x-ray emission, and/or far-infrared emission implies many are young stellar objects in a T Tauri phase of evolution. Recently, Bouvier and Appenzeller (1991) have made a spectroscopic and photometric survey of optical counterpart candidates of X-ray sources in the ρ Oph cloud. They found 27 stars with Hα emission, 12 of which are new. These X-ray counterparts are mostly weak emission T Tauri stars.

The distribution of Hα emission-line stars relative to the ρ Oph, L1689, and L1709 molecular clouds is shown in Fig. 4. The majority of objects are associated with the western half of the ρ Oph cloud yet few are observed directly toward the densest gas, an effect created by the large visual extinctions. This concentration of emission-line stars near the large centrally condensed core may imply either a critical density for the formation of stars or a progression of star formation through the complex from west to east. The latter would be favored by proponents of a shock wave origin for the cloud morphology.

Highly variable soft x-ray emission is also associated with pre-main sequence stars which have dissipated most of their circumstellar envelopes. Thought to be connected with surface flare activity, the x-ray emission has also been found in a new class of young pre-main-sequence objects with virtually no circumstellar dust called the weak emission T Tauri stars (Walter et al. 1988). *Einstein* observations of the Ophiuchus region have revealed 50 x-ray sources with nearly half known to be pre-main sequence stars (Montmerle et al. 1983). A fraction of these also display variable radio continuum emission (e.g., Feigelson and Montmerle 1985, André, Montmerle, and Feigelson 1987; Stine et al. 1988, André et al. 1991). The distribution of x-ray sources is reminiscent of the Hα stars as they are found primarily at the periphery of the dense molecular gas.

B. The Embedded Population: Infrared Observations

The majority of young stellar objects (YSOs) which have formed in the ρ Oph cloud are rendered invisible both by extinction from circumstellar dust and from the dark cloud itself. The first infrared surveys of the ρ Oph cloud core unveiled a cluster of 2 μm sources with a stellar density higher than expected from background sources (Grasdalen, Strom, and Strom 1973; Vrba et al. 1975). Balloon-borne far-infrared observations provided evidence that most of the embedded objects were low-luminosity YSOs (Fazio et al. 1976, Cudlip et al. 1984). Subsequent near-infrared surveys expanded the range and sensitivity of previous work while attempting to distinguish between association members and background field stars (Elias 1978, Wilking and Lada 1983). Criteria to identify association members include the absence of 2.3 μm CO emission, a relationship with large columns of gas and dust, and the presence of an infrared excess in the 3.4–20 μm spectral region (e.g., Elias 1978, Lada and Wilking 1984). Tanaka et al. (1990) detected the three-micron ice-band feature in a number of embedded sources.

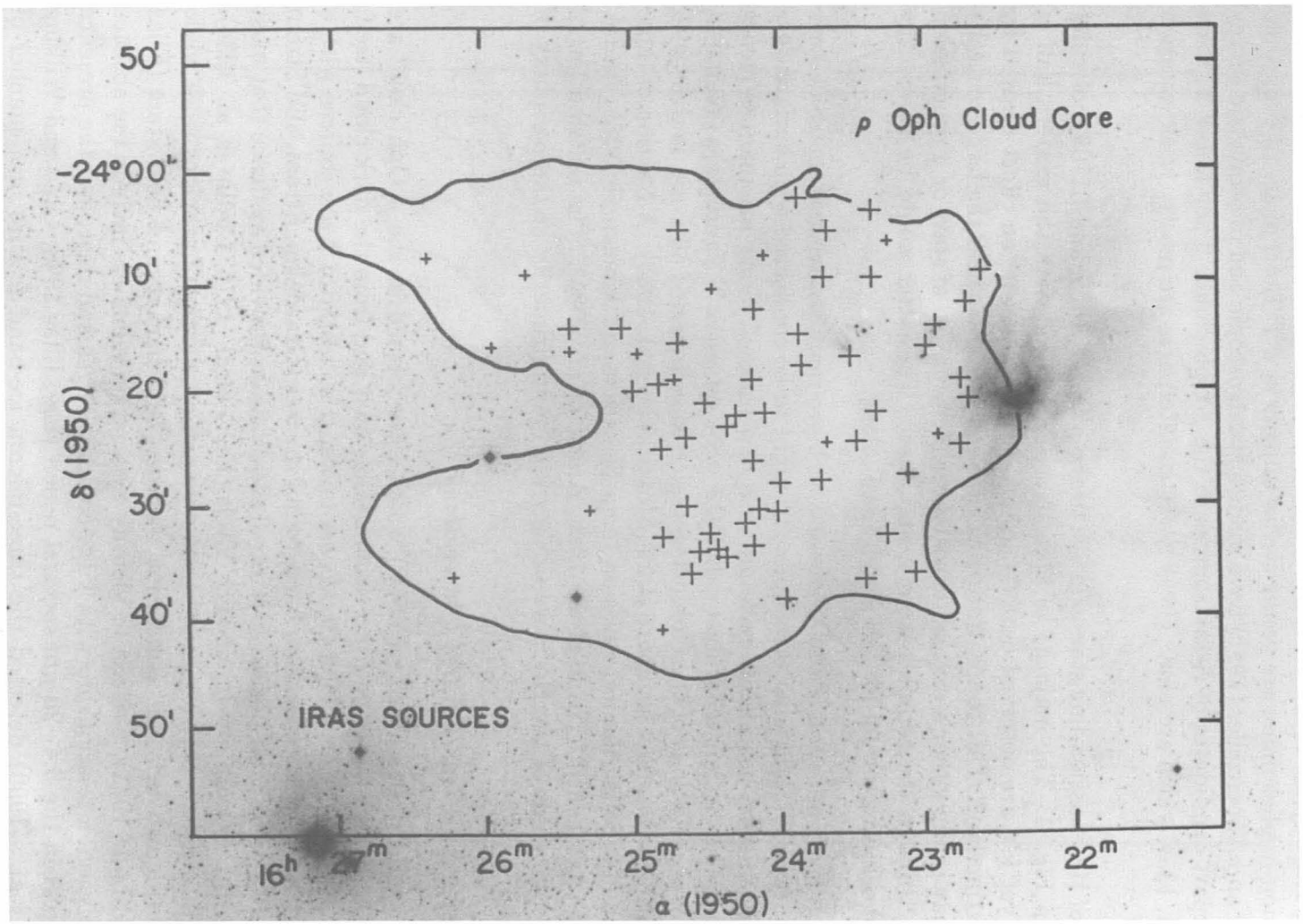

Figure 5: The locations of point and small extended 12μm sources in the ρ Oph cloud observed by IRAS, superposed on the red photograph from the Palomar Sky Survey (Wilking, Lada, and Young 1989). Large crosses mark the positions of sources with 12μm flux densities greater than 0.25 Jy and small crosses less than this value. The solid contour outlining the molecular cloud represents a ^{13}CO emission line strength of $T_R^* = 6$ K (Loren 1989a).

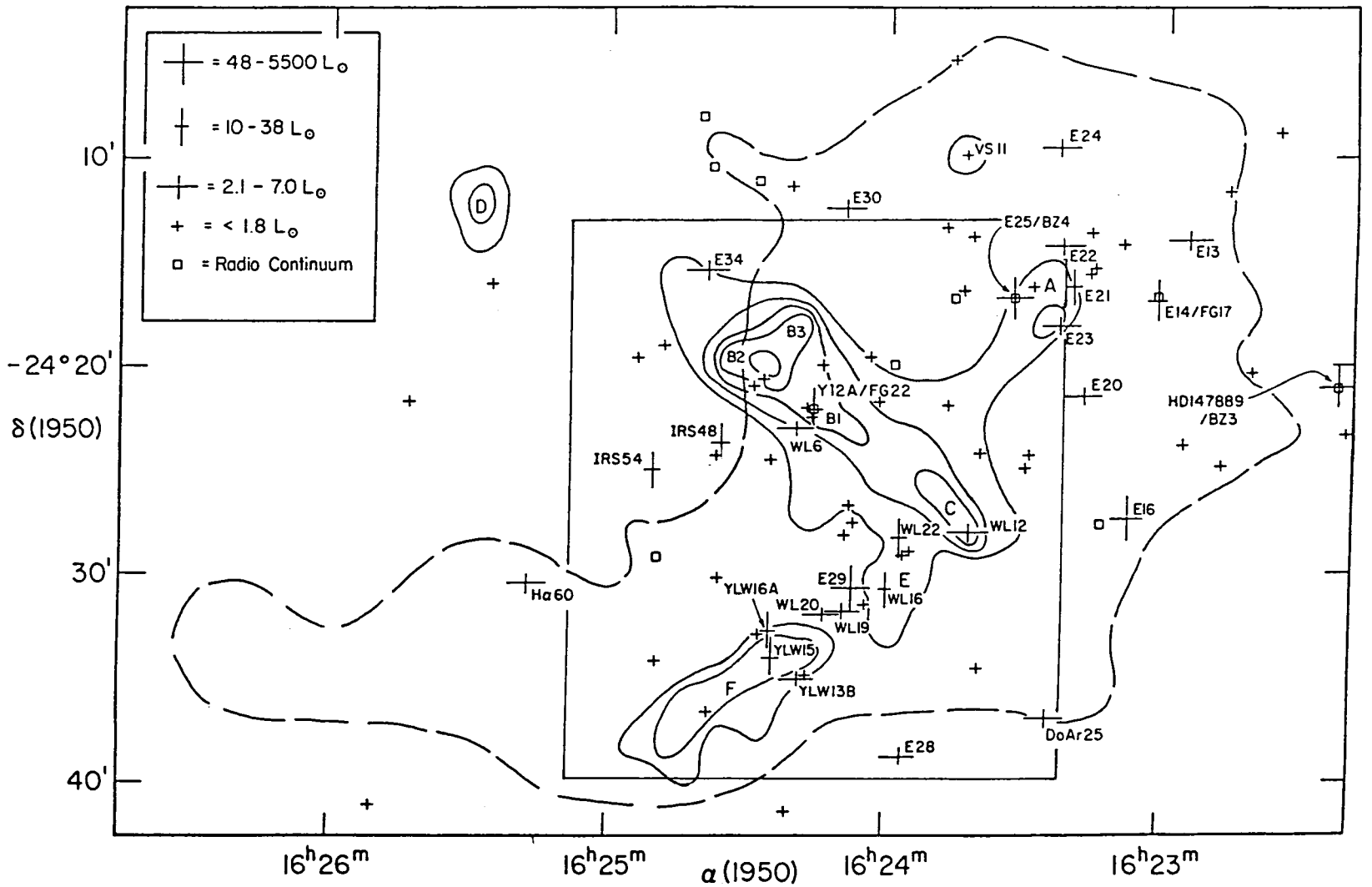

Figure 6: The distribution of 78 association members relative to the cold, dense gas in the ρ Oph core (adapted from Loren, Wootten, and Wilking 1990). Larger symbols correspond to the more luminous YSOs. The boundary of the molecular cloud is marked by the $T_R^* = 10$ K contour for ^{13}CO. This area of the cloud has been completely sampled by IRAS and Hα emission-line surveys but not near infrared surveys. The contours and labels for the DCO^+ emission are the same as Fig. 3. The large box outlines the area imaged by sensitive near-infrared camera observations which are presented in Fig. 7.

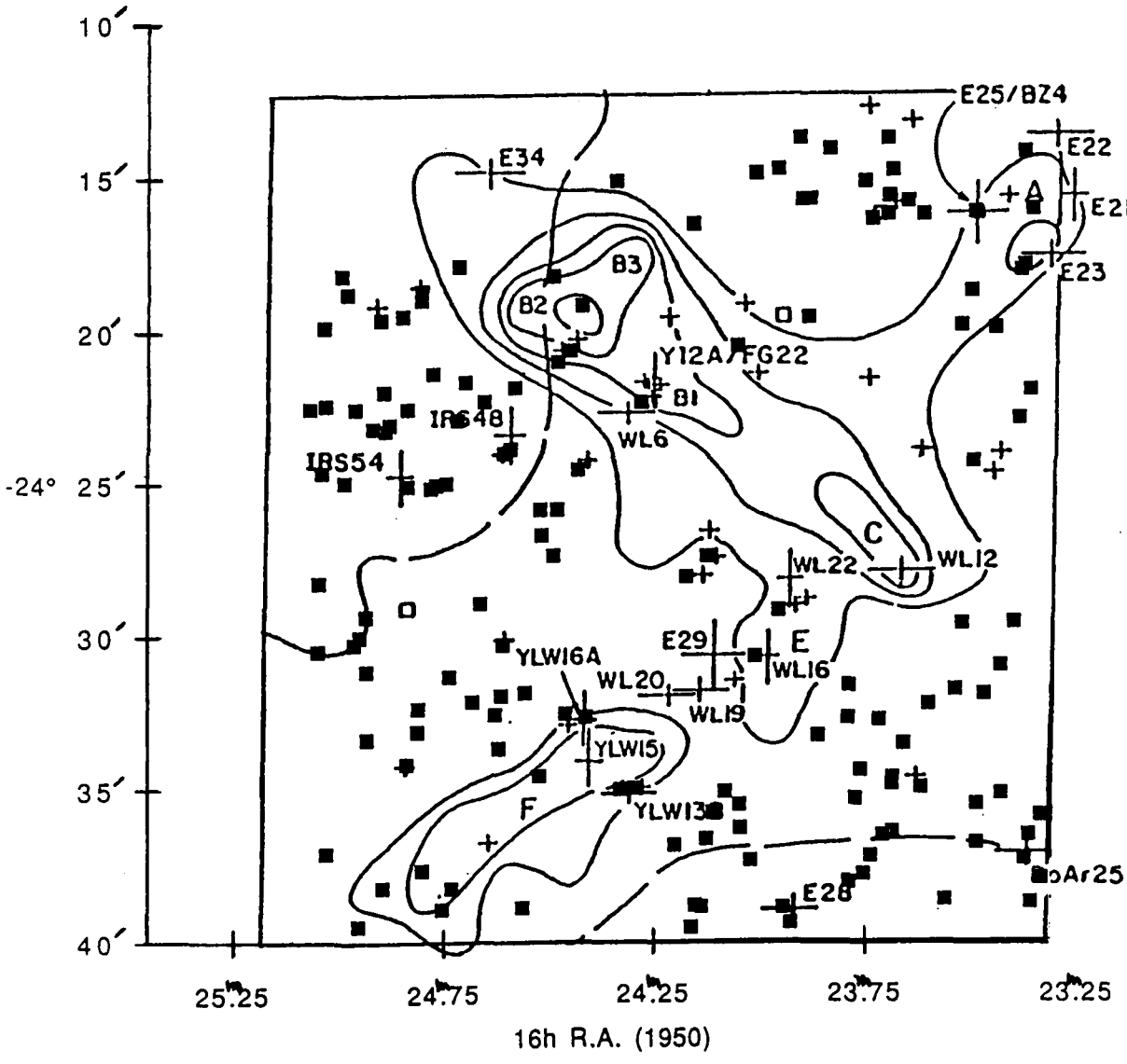

Figure 7: A plot showing the positions of near-infrared sources detected at J, H, and K (solid squares) by a infrared camera survey of a 645 square arcmin region of the ρ Oph core (Greene, Young, and Meyers-Rice 1990). The completeness limit for these data was J=16.4 mag, H=14.5 mag, and K=13.0 mag. For reference, the outline of DCO^+ emission (solid contours) and positions of 48 previously known cluster members (plus signs) from Fig. 6 are shown. The 144 sources plotted from this new survey are only a subset of the 481 sources detected at K. Some of the previously known cluster member sources are not among the 144 sources plotted because they were either too faint to be detected at J or in an area not observed at J (only 8% of the area covered at H and K).

V. Mass Loss and Cloud Energetics

Despite the fact that most YSOs probably undergo a phase of energetic mass loss during their pre-main-sequence evolution, few signposts for mass loss activity have been detected in the ρ Oph cloud. Such detections have no doubt been hindered by the high visual extinctions, complex self-absorbed ^{12}CO profiles and source confusion in millimeter-wave beams. Surprisingly few Herbig-Haro objects have been found in the ρ Oph clouds, the first one, HH 79, was identified by Reipurth and Graham (1988). New deep CCD images have confirmed that the candidate HH object WSB47 (Wilking, Schwartz and Blackwell 1987) is indeed a bona fide Herbig-Haro object (Reipurth 1992). Surveys for molecular outflows in Ophiuchus have been only moderately successful (Fukui et al. 1986, Walker et al. 1988, Fukui 1989). In the ρ Oph cloud where source confusion is a potential problem, four sources of moderate velocity CO have been reported. The most spectacular of these is a highly collimated outflow observed near ρ Oph A with a full velocity extent, $\Delta v = 28$ km s^{-1} (André et al. 1990a). The outflow is bipolar and orientated near the plane of the sky. The source which most likely drives the outflow is a strong millimeter-wave continuum and weak radio continuum source VLA 1623 which is undetected at near- to far-infrared wavelengths. Other suspected outflows include a bipolar outflow associated with GSS30 ($\Delta v = 9$ km s^{-1}; Tamura et al. 1990), a very extended bipolar outflow observed with low angular resolution toward the cold core ρ Oph B3 ($\Delta v = 17$ km s^{-1}; Loren 1989b, Armstrong 1989), and a monopolar outflow associated with IRAS 16244–2432 (YLW16) detected using millimeter-wave interferometry ($\Delta v = 11$ km s^{-1}; Terebey, Vogel, and Myers 1989). The latter source is a 16 $L_\odot$ embedded object coincident with several H_2O masers (Wilking and Claussen 1987).

Three outflows have been observed in the less confused cloud filaments and all are bipolar. The best-studied outflow is associated with a cold far-infrared source in L1689N, IRAS 16293–2422 (Wooten and Loren 1987; Walker et al. 1988, Mizuno et al. 1990, Walker et al. 1990). With a $\Delta v = 40$ km s^{-1}, the high velocity gas is distributed in two pairs of red and blue-shifted lobes, characteristic of outflows which lie nearly in the plane of the sky. Like YLW16A, this 27 $L_\odot$ source is associated with a group of H_2O masers, suggesting the maser emission from these sources is collisionally pumped as the stellar wind interacts with circumstellar material (Wilking and Claussen 1987, Wootten 1989). Outflows have also been reported in L1689S and L1709 (Fukui 1989; Terebey, Vogel, and Myers 1989) but no maps have been published to date. The L1689S outflow is associated with an IRAS source 16289–2450 and has a $\Delta v = 11$ km s^{-1} (Wootten et al. 1992). The driving sources for the L1689 outflows will be discussed further in Sec. VII.

The heating of the dust and molecular gas in ρ Oph is dominated by three early spectral-type stars which lie at the western edge of the cloud: HD147889 (B2 V), Source 1 (B3–B5 V), and SR–3 (B9–A0 V) (Garrison 1967, Elias 1978, Lada and Wilking 1984, Greene and Young 1989). This is demonstrated by the similar distributions of far-infrared emitting dust (T_d=30–60 K) and warm molecular gas along the western margin of the cloud (e.g., Cudlip et al. 1984). Yet there is strong evidence that external heating from HD147899 does not penetrate the entire depth of the cloud (Greene and Young 1989). While the dust optical

depth at 60 μm is well-correlated with the molecular column density (from $C^{18}O$ lines), the dust appears to be heated to only about 10–20% of the cloud's depth. Additionally, there is evidence that the gas and dust are not perfectly coupled ($T_{gas} > T_{dust}$) in the core, but this may be an effect caused by the presence of internal heat sources. This situation is in contrast to the L1689 cloud where the interstellar radiation field from the Sco OB2 association is probably the dominant heating source and the dust and gas are well-coupled in the outer cloud layers (Jarrett, Dickman, and Herbst 1989).

VI. Star Formation in the ρ Oph Cloud

A. The Utility of Spectral Energy Distributions

Clues to the evolutionary state and mass of a YSO can be deduced from its spectral energy distribution (SED). The shape of the emergent 1–100 μm SED of a young stellar object depends upon the distribution of circumstellar dust which, in turn, is determined by its evolutionary state. For example, we expect a protostar which is surrounded by large amounts of circumstellar material to have a different infrared signature than an optically visible T Tauri star whose main infall stage has ended. Indeed broad band infrared photometry of association members in ρ Oph show that their SEDs fall into well-defined classes with systematic variations in shape (Lada and Wilking 1984; Wilking, Lada, and Young 1989). Theoretical models have been successful in describing these variations in SED shapes and suggest they form a quasi-continuous evolutionary sequence (e.g., Adams and Shu 1986, Adams, Lada, and Shu 1987, Myers et al. 1987, Lada 1987). SEDs which rise steeply into far-infrared wavelengths (Class I) are associated with heavily obscured objects and are modeled as accreting protostars. SEDs with peaks in the near and far-infrared (Class IID) are modeled as objects which have developed a strong wind and cleared away significant amounts of original infalling material. SEDs with small infrared excesses (Class II) are associated with T Tauri stars surrounded by disks and those with no excess (Class III) with post T Tauri stars. As more observations become available, it may be necessary to modify this simple evolutionary scheme to include the fact that some weak emission T Tauri stars appear to be similar in age to classical T Tauri stars (e.g. Walter et al. 1988) and that not all Class I objects appear to have circumstellar disks (André et al. 1990b).

Theoretical evolutionary tracks for pre-main-sequence objects indicate they evolve toward the main sequence from a higher luminosity regime (e.g., Iben 1965, Stahler, Shu, and Taam 1980). Therefore, the bolometric luminosity of a YSO gives an upper limit to its ultimate main sequence luminosity and mass. Reliable estimates for the bolometric luminosity of a YSO which has been observed over a broad range of wavelengths can be obtained by simply integrating its SED provided the following assumptions are valid: (1) the source's luminosity is radiated isotropically and either (2) there is no extinction toward the source, or (3) all of the extinction is produced by a shell of circumstellar dust which reradiates the absorbed light in the near-to far-infrared spectral region. Modeling of Class I sources suggests that assumptions (1) and (3) are well satisfied. For Class II objects, however, the assumption of no extinction underestimates the true luminosity while the presence of an anisotropically

radiating disk will lead to overestimates (see Wilking, Lada, and Young 1989 for details). These two effects introduce at most a factor of two uncertainty but tend to cancel.

B. The Youth of the Ophiuchus Cluster

From the collection of over 50 SEDs for objects in the ρ Oph cloud, the duration of the Class I phase and the age of the infrared cluster have been estimated (Wilking, Lada, and Young 1989). Since the number of Class I and Class II objects are roughly equal, the duration of the Class I phase is estimated to be approximately equal to the average age of the ρ Oph T Tauri stars, or 4×10^5 years. This translates into a mass accretion rate of 2.5×10^{-6} $M_\odot$/yr for a 1 $M_\odot$ star. The estimate for the length of the embedded state would drop by a factor of 4 if allowances were made for the luminosity evolution of Class I objects and for a population of weak emission T Tauri stars equal in age and number to the Class II population. The resulting mass accretion rate of 10^{-5} $M_\odot$/yr is similar to that estimated for the ρ Oph cloud from protostar theory (Adams, Lada, and Shu 1987). The relative number of Class II to Class III objects in the cloud sets an upper limit to the duration of star formation of 3.5×10^6 years. This upper limit is consistent with the estimate of 1.5×10^6 years for both the age of the oldest ρ Oph T Tauri star (SR−22) and the contraction time for the least massive main sequence star, the B9−A0 V star SR−3.

C. A Deficiency of Intermediate Mass Stars?

Combining ground-based infrared photometry with IRAS observations, bolometric luminosities have been estimated for 58 association members and upper limits to L_{bol} for an additional 16 (Wilking, Lada, and Young 1989). The luminosity function, shown in Fig. 8, underscores the low-luminosity nature of the infrared cluster; nearly half of the objects have luminosities less than 1.8 $L_\odot$ and 76% less than 5.6 $L_\odot$. A remarkable feature of the luminosity function is that sources are segregated in luminosity by their SED class; 82% of the sources with $5.6\ L_\odot < L_{bol} < 56\ L_\odot$ are Class I while 67% of the lower luminosity sources are Class II. This segregation suggests that either low mass stars in ρ Oph are undergoing luminosity evolution as they progress from the Class I to Class II phase or that the most recent episode of star formation has produced predominantly intermediate mass stars. The former possibility would point to a deficiency of intermediate mass stars in the cloud relative to the Initial Luminosity Function.

D. The Search for Brown Dwarfs

The high density of low mass young stellar objects, the proximity of the cloud, and the high visual extinction in the core makes the ρ Oph cloud a prime target for surveys for brown dwarfs. In addition, brown dwarfs only a few million years in age are expected to be brighter in the infrared than those in the field. A recent deep H and K survey of the core has been performed by G. Rieke and M. Rieke (1990) using a HgCdTe infrared camera. They find at least three brown dwarf candidates over a 200 arcmin^{-2} area. Given the high sensitivity of this survey to brown dwarfs, one would conclude there is not a large population of such objects in the cloud (see also Rieke, Ashok, and Boyle 1989).

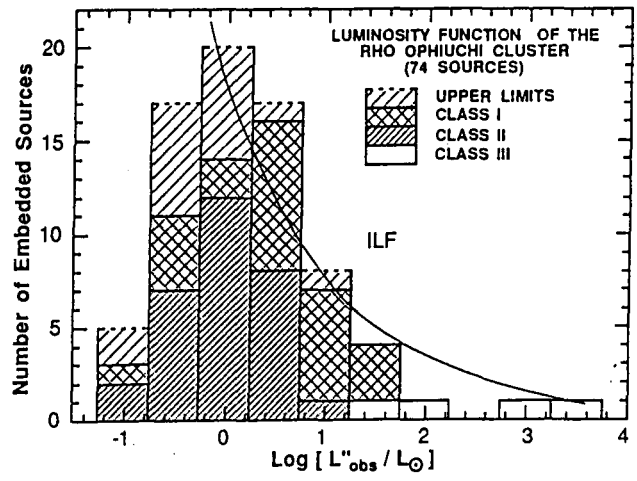

Figure 8: The luminosity function of 74 sources embedded in the Oph cloud (Wilking, Lada, and Young 1989). For comparison, the luminosity function derived from the Initial Mass Function (the ILF) is shown, normalized to the number of sources with well-determined luminosities in the $-0.25 < \log L < 0.75$ range. The YSOs in each luminosity bin are grouped according to the shapes of their SEDs. Luminosity estimates for sources with no detectable IRAS flux are shown as upper limits and are not included in the normalization of the ILF.

E. A Starburst in the ρ Oph Cloud

A high stellar density of YSOs in the large centrally-condensed core sets the ρ Oph cloud apart from other star-forming dark clouds. This feature has been quantified by estimations for the star formation efficiency (SFE): the ratio of total stellar mass to the total mass of stars plus gas. While determinations of the SFE are subject to large uncertainties, conservative estimates for the ρ Oph core imply a SFE > 20% (Wilking and Lada 1983; Wilking, Lada, and Young 1989). The absence of massive stars in the cloud, which maintains the quiescent conditions of the core gas, insures the continued conversion of gas into stars and the slow release of gas from the cluster. These factors will promote the emergence of a gravitationally bound cluster from the core (Wilking and Lada 1983; Lada, Margulis, and Dearborn 1984).

In principle, an extended episode of star formation could lead to the relatively high values observed for the SFE. However, the youth of the ρ Oph cluster precludes this scenario. Instead, it appears that the high SFE is the result of an efficient burst of star-forming activity which has occurred over the last few million years. It is not clear what could trigger such a burst, although several mechanisms have been proposed, including shock compression (Vrba 1977, Loren and Wootten 1986) and draining of angular momentum from the core by rotation of the filaments (Uchida et al. 1990).

VII. Star Formation in L1689

A smattering of Hα stars, x-ray sources, and IRAS sources give testimony to recent star formation in the L1689 cloud. Although near-infrared studies of the cloud are only beginning, array camera images suggest that the star formation process has not been as prolific as in the

ρ Oph cloud (Greene, Young, and Meyers-Rice 1990). The dense molecular cores L1689N and L1689S mark the most active centers of star formation. The 50 $M_\odot$ L1689S core is delineated by DCO^+ emission and contains several denser clumps (Loren, Wootten, and Wilking 1990; Wootten et al. 1992). The only IRAS source in the core, 16289–2450, is actually comprised of two heavily obscured infrared sources with a projected separation of 120″ (mostly east-west) and a combined luminosity of ~ 7 $L_\odot$. The easternmost of these sources lies nearest the center of the molecular outflow alluded to in Sec. V. Several arcminutes south of these objects may be the most recent site of star formation in L1689S: a 10 $M_\odot$ clump displaying rare 2cm H_2CO emission containing a radio continuum source and water maser emission (Wootten et al. 1992). In L1689N, a 15 $M_\odot$ core is defined by DCO^+ and NH_3 emission with the cold far-infrared source IRAS 16293–2422 lying on its westernmost edge (Wootten and Loren 1987; Loren, Wootten, and Wilking 1990). This source has yet to be detected with ground-based infrared telescopes; emission characteristic of 20–40 K dust is observed over the 25–2700μm spectral region, radiating a total luminosity of ~ 27 $L_\odot$ (Walker et al. 1986; Mundy, Wilking, and Myers 1986; Walker, Adams, and Lada 1990; Mezger, Sievers, and Zylka 1991). As discussed in Sec. V, IRAS 16293–2422 lies at the centroid of a complicated distribution of high velocity molecular gas.

Under the scrutiny of interferometric observations, IRAS 16293–2422 has displayed an increasing amount of complexity. Initial 6.3″ × 4.5″ observations with the Owens Valley Radio Observatory (OVRO) Millimeter-Wave Interferometer of $C^{18}O$ (J=1–0) emission and the 2.7mm continuum showed the IRAS source to be an elongated structure (1800 AU × < 800 AU) of gas and dust with a 2.4 km s^{-1} velocity shift along the major axis (Mundy, Wilking, and Myers 1986; Mundy, Wootten, and Wilking 1990). The orientation of the structure is roughly perpendicular to the axis of the molecular outflow and the direction of the local magnetic field. The gravitational influence of IRAS 16293–2422 evidently extends beyond the 1800 AU emission region as a flattened region of NH_3 emission has been observed with the VLA out to a radius of 4000 AU at the same position angle as the inner region (Mundy, Wootten, and Wilking 1990). The 0.9 km s^{-1} velocity shift of the NH_3 emission implies an included mass of 1.0–1.2 $M_\odot$ (Mundy et al. 1992).

VLA radio continuum observations led to the first suggestion that IRAS 16293–2422 was a protobinary system. Observations at λ = 2cm and 6cm detected two sources within the 2.7mm emission region, separated by $\sim$ 840 AU along its major axis (Wootten 1989; Estalella et al. 1991). As shown in Fig. 9, more recent OVRO observations at 2.7mm with 4.5″ × 2.5″ resolution have confirmed the duplicity of the source, resolving the elongated structure into two components coincident with the radio sources (Mundy et al. 1992). The compact nature of the millimeter-wave emission argues that this material is confined to two circumstellar disks, each containing about 0.5 $M_\odot$. Comparing this with the dynamical mass of the system constrains the central objects to be $\leq$ 0.5 $M_\odot$ and requires the luminosity of the system to be produced primarily through accretion. The properties of the southernmost radio/millimeter-wave source suggest it is the source of the CO outflow. It is associated with all of the H_2O maser emission, has extended emission from ionized gas at λ = 3.6 to 1.3 cm with a spectral index of 0.4, and displays an enhanced abundance of SO relative to its

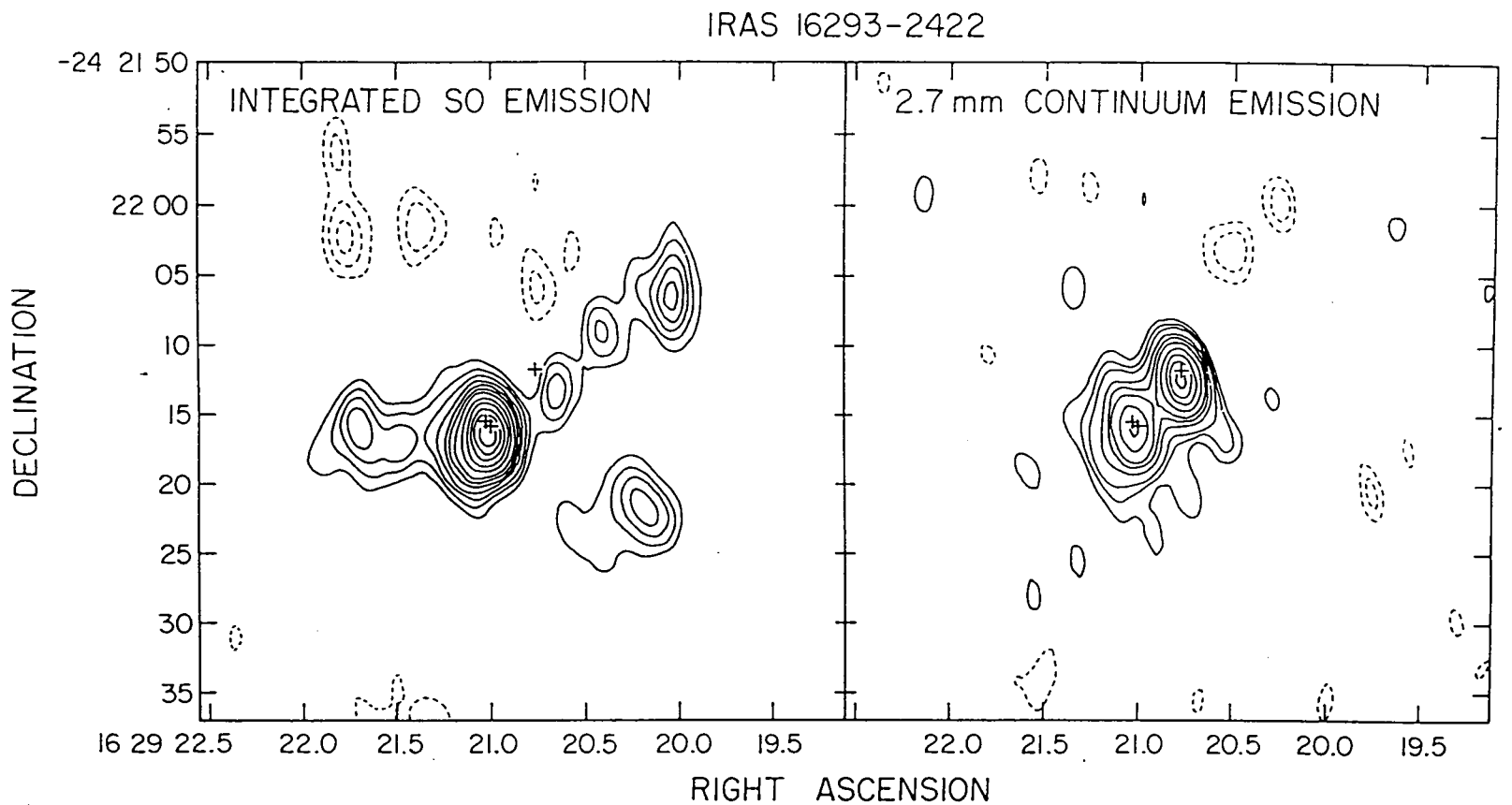

Figure 9: Interferometric observations of IRAS 16293–2422 in the SO J=2,3 – 2,1 line and the 2.7mm continuum (Mundy et al. 1990). These 4.5″×2.5″ observations were made with the OVRO millimeter-wave interferometer. The contour levels for the line map are –4, –3, –2, 2, 3, 4, 5, 6, 7, 8, 9, 10, 12, 14, 16 and 18 times 0.37 Jy beam^{-1} km s^{-1}. For the continuum map, the contour levels are –4, –2, 2, 4, 6, 8, 10, 12, 14, 18, 22, 26 and 30 times 7.5 mJy beam^{-1}. The plus signs mark the positions of the radio continuum sources observed by Wootten (1989).

northern counterpart (see Fig. 9). It will be most interesting to see if higher resolution molecular-line observations of IRAS 16293–2422 resolve the gas component into two sources or if the young binary system shares some circumstellar material.

VIII. Summary and Future Work

Throughout much of the Ophiuchus complex, the distribution of gas and young stars resembles most other dark clouds forming low mass stars (Fig. 10). What distinguishes the Ophiuchus complex is the large centrally condensed core in the ρ Oph cloud which appears to be the formation site of a gravitationally bound open cluster. The high stellar density of YSOs in the core has allowed us to look beyond the study of individual objects and to investigate the more global aspects of star formation. The population of YSOs in the core appears to have been formed by an efficient burst of star forming activity over the past few million years. The most heavily obscured, and presumably youngest, objects have higher luminosities than their more evolved counterparts, suggesting they may have an additional source of energy such as accretion. An outstanding question is whether the mass function of this infrared cluster varies significantly from the Initial Mass Function. Infrared array cameras which can probe more deeply into the dense cloud and sample the lowest luminosity YSOs and perhaps substellar objects may be able to address this problem with the help of a better theoretical understanding of how YSOs evolve in luminosity as they approach the main sequence. Another unresolved problem is the role of shocks in molding the present cloud morphology and triggering the formation of stars. Perhaps high resolution molecular-line observations will reveal the detailed kinematics expected from the passage of a shock.

Because of the large number of embedded sources with well-determined spectral energy distributions and luminosities, the ρ Oph infrared cluster can serve as a standard to which other regions of low mass star formation can be compared. Detailed studies of the embedded populations in adjacent clouds in the Ophiuchus complex, such as L1689, will provide important data for comparisons with the ρ Oph cluster and give us insight into how the star formation rate and mass function may vary over a given complex.

The proximity of the Ophiuchus complex and the large population of YSOs in a wide variety of evolutionary states makes the cloud an ideal target for high resolution infrared, millimeter, and radio wavelength observations. Infrared observations of YSOs with milliarcsecond to arcsecond resolution are possible using speckle interferometry, lunar occultations, and infrared array cameras. These observations have already begun to reveal the distribution of circumstellar dust and the presence of pre-main-sequence binary systems on size scales of 20–1000 AU (see Zinnecker (1989) for review). The dynamics and distribution of circumstellar gas and dust on scales of tens to hundreds of AU are within the reach of observations with the VLA, millimeter-wave interferometers, and submillimeter arrays planned for the future. These observations will yield important constraints to theoretical models for the early evolution of young stellar objects and ultimately lead to a better understanding of the role of accretion, circumstellar disks, and mass outflows in this evolution.

Figure 10: The main parts of the ρ Ophiuchi cloud complex is seen in this panoramic view based on a deep red Schmidt plate obtained at the ESO Schmidt telescope. A large ghost from a bright star is seen in the upper left corner.

Acknowledgements

I would like to thank Jim Blackwell and Lee Mundy for their assistance with the LVG calculations. I am also grateful to Tom Greene for communicating his infrared camera results prior to publication. Many thanks go to Tom Greene, Bo Reipurth, Al Wootten and Hans Zinnecker for helpful discussions and comments which have improved this manuscript. Partial support was received under the IRAS Data Analysis Program funded through NASA's Astrophysical Data Program.

References

Adams, F. C., Lada, C. J., and Shu F. H.: 1987, *ApJ* **312**, 788

Adams, F. C. and Shu, F. H.: 1986, *ApJ* **308**, 836

André, Ph., Martin-Pintado, J., Despois, D., and Montmerle, T.: 1990a, *A&A* **236**, 180

André, Ph., Montmerle, T., and Feigelson, E. D.: 1987, *AJ* **93**, 1182

André, Ph., Montmerle, T., Feigelson, E. D., and Steppe, H.: 1990b, *A&A* **240**, 321

André, Ph., Phillips, R. B., Lastrade, J. F., Klein, K. L.: 1991, *ApJ* **376**, 630

Armstrong, J. T.: 1989, in *Physics and Chemistry of Interstellar Molecular Clouds*, G. Winnewisser and J. T. Armstrong (Berlin: Springer-Verlag), p. 143

Barsony, M., Burton, M. G., Russell, A. P. G., Carlstrom, J. E., and and Garden, R.: 1989, *ApJ* **346**, L93

Bertiau, F. C.: 1958, *ApJ* **128**, 533

Bok, B. J.: 1956, *AJ* **61**, 309

Bouvier, J., Appenzeller, I.: 1991, *A&AS*, in press

Chini, R.: 1981, *A&A* **99**, 346

Cohen, M. and Kuhi, L. V.: 1979, *ApJS* **41**, 743

Cudlip, W., Emerson, J.P., Furniss, I., Glencross, W. M., Jennings, R. E., King, K. J., Lightfoot, J. F., and Towlson, W.A.: 1984, *MNRAS* **211**, 563

de Geus, E., de Zeeuw, P. T., and Lub, J.: 1989, *A&A* **216**, 44

de Geus, E., Bronfman, L., Thaddeus, P.: 1990, *A&A* **231**, 137

de Geus, E., Burton, W. B.: 1991, *A&A* **246**, 559

Dolidze, M. V., and Arakelyan, M. A.: 1959, *Soviet Astr.-AJ* **3**, 434

Elias, J. H.: 1978, *ApJ* **224**, 453

Encrenaz, P. J., Falgarone, E., and Lucas, R.: 1975, *A&A* **44**, 73

Estalella, R., Anglada, G., Rodríguez, L. F., Garay, G.: 1991, *ApJ* **371**, 626

Fazio, G. G., Wright, E. L., Zeilik, M., III, and Low, F. J.: 1976, *ApJ* **206**, L165

Feigelson, E. D., Montmerle, T.: 1985, *ApJ* **289**, L19

Fukui, Y.: 1989, in *Low Mass Star Formation and Pre-Main Sequence Objects*, ed. Bo Reipurth (Garching: ESO), p. 95

Fukui, Y., Sugitani, K., Takaba, H., Iwata, T., Mizuno, T., Ogawa, H., and Kawabata, K.: 1986, *ApJ* **311**, L85

Garrison, R. F.: 1967, *ApJ* **147**, 1003

Gottlieb, C., Gottlieb, E., Litvak, M., Ball, J., and Penfield, H.: 1978, *ApJ* **219**, 74

Grasdalen. G. L., Strom, K. M., and Strom, S.E.: 1973, *ApJ* **184**, L53

Greene, T. P. and Young, E. T.: 1989, *ApJ* **339**, 258

Greene, T. P., Young, E. T., and Meyers-Rice, B.: 1990, unpublished observations

Haro, G.: 1949, *AJ* **54**, 188

Iben, I., Jr.: 1965, *ApJ* **141**, 993

Ichikawa, T. and Nishida, M.: 1989, *AJ* **97**, 1074

Jarrett, T. H., Dickman, R. L., and Herbst, W.: 1989, *ApJ* **345**, 818

Klose, S.: 1986, *Ap&SS* **128**, 135

Lada, C. J.: 1987, *Star Forming Regions*, M. Peimbert and J. Jugaku, Dordrecht Reidel, 1

Lada, C. J., Margulis, M., and Dearborn, D.: 1984, *ApJ* **285**, 141

Lada, C. J., and Wilking, B. A.: 1980, *ApJ* **238**, 620

Lada, C. J., and Wilking, B. A.: 1984, *ApJ* **287**, 610

Loren, R. B.: 1989a, *ApJ* **338**, 902

Loren, R. B.: 1989b, *ApJ* **338**, 925

Loren, R. B., Sandqvist, Aa., and Wootten, H. A.: 1983, *ApJ* **270**, 620

Loren, R. B., Wootten, H. A., Sandqvist, Aa., and Bernes, C.: 1980, *ApJ* **240**, L165

Loren, R. B. and Wootten, H. A.: 1986, *ApJ* **306**, 142

Loren, R. B., Wootten, H. A., and Wilking, B. A.: 1990, *ApJ* **365**, 269

Martin-Pintado, J., Wilson, T. L., Gardner, F. F., and Henkel, C.: 1983, *A&A* **117**, 145

Mezger, P. G., Sievers, A., and Zylka, R.: 1991, IAU Symp. No. 147 on *Fragmentation of Molecular Clouds and Star Formation*, ed. E. Falgarone et al., p. 245

Mizuno, A., Fukui, Y., Iwata, T., and Nosawa, S.: 1990, *ApJ* **356**, 184

Montmerle, T., Koch-Miramonde, L., Falgarone, E., and Grindlay, J.: 1983, *ApJ* **269**, 182

Mundy, L. G., Wilking, B. A., and Myers, S. T.: 1986, *ApJ* **311**, L75

Mundy, L. G., Wilking, B. A., Blake, G., Sargent, A. I., and Wootten, H. A.: 1992, *ApJ*, in press

Mundy, L. G., Wootten, H. A., and Wilking, B. A.: 1990, *ApJ* **352**, 159

Myers, P. M., Fuller, G. A., Mathieu, R. D., Beichman, C. A., Benson, P. J., Schild, R. E., and Emerson, J. P.: 1987, *ApJ* **319**, 340

Reipurth, B.: 1992, in preparation

Reipurth, B., and Graham, J. A.: 1988, *A&A* **202**, 219

Rieke, G. H., Ashok, N. M., Boyle, R. P.: 1989, *ApJ* **339**, L71

Rieke, M., Montgomery, E., Blessinger, M., Kleinhans, W., Vural, K., *Proceedings of the Infrared Detector Array Workshop*, Feb. 7-9 1989, Ames Research Center, p. 321

Rieke, G.H. and Rieke, M. J.: 1990, *ApJ* **362**, L21

Rydgren, A. E.: 1980, *AJ* **85**, 438

Rydgren, A. E., Strom, S. E., and Strom, K.M.: 1976, *ApJS* **30**, 307

Schwartz, P. R., Snell, R. L., and Schloerb, F. P.: 1989, *ApJ* **336**, 519

Stahler, S. W., Shu, F. H., and Taam, R. E.: 1980, *ApJ* **241**, 637

Stine, P. C., Feigelson, E. D., André, P., and Montmerle, T.: 1988, *AJ* **96**, 1394

Struve, O. and Rudkjøbing, M.: 1949, *ApJ* **109**, 92

Tamura, M., Sato, S., Suzuki, H., Kaifu, N., and Hough, J. M.: 1990, *ApJ* **350**, 728

Tanaka, M., Sato, S., Nagata, T., Yamamoto, T.: 1990, *ApJ* **352**, 724

Terebey, S., Vogel, S. N., and Myers, P. C.: 1989, *ApJ* **340**, 472

Uchida, Y., Mizuno, A., Nosawa, S., and Fukui, Y.: 1990, *PASJ* **42**, 69

Vrba, F. J.: 1977, *AJ* **92**, 198

Vrba, F. J., Strom, K. M., Strom, S. E., and Grasdalen, G. L.: 1975, *ApJ* **197**, 77

Wadiak, E. J., Wilson, T. L., Rood, R. T., and Johnston, K. J.: 1985, *ApJ* **295**, L43

Walker, C. K., Lada, C., Young, E., Maloney, P., and Wilking, B.: 1986, *ApJ* **309**, L47

Walker, C. K., Lada, C. J., Young, E. T., and Margulis, M.: 1988, *ApJ* **332**, 335

Walker, C. K., Adams, F. C., and Lada, C. J.: 1990, *ApJ* **349**, 515

Walker, C. K., Carlstrom, J., Bieging, J., Lada, C., and Young, E.: 1990, *ApJ* **364**, 173

Walter, F., Brown, A., Mathieu, R., Myers, P., and Vrba, F.: 1988, *AJ* **96**, 297

Ward-Thompson, D., Robson, E. I., Whittet, D. C. B., Gordon, M. A., Walther, D. M., and Duncan, W. D.: 1989, *MNRAS* **241**, 119

Whittet, D. C. B.: 1974, *MNRAS* **168**, 371

Wilking, B. A.: 1989, *PASP* **101**, 229

Wilking, B. A., and Claussen, M. J.: 1987, *ApJ* **320**, L133

Wilking, B. A. and Lada, C. J.: 1983, *ApJ* **274**, 698

Wilking, B. A., Lada, C. J., and Young, E. T.: 1989, *ApJ* **340**, 823

Wilking, B. A., Schwartz, R. D., and Blackwell, J. H.: 1987, *AJ* **94**, 106

Wootten, H. A.: 1989, *ApJ* **337**, 858

Wootten, H. A., and Loren, R. B.: 1987, *ApJ* **317**, 220

Wootten, H. A., Loren, R. B., Mangum, J., and Butner, H.: 1992, in preparation

Young, E. T., Lada, C. J., and Wilking, B. A.: 1986, *ApJ* **304**, L45

Zeng, Q., Batrla, W., and Wilson, T. L.: 1984, *A&A* **141** 127

Zinnecker, H.: 1989, in ESO Workshop on *Low Mass Star Formation and Pre-Main Sequence Objects*, ed. Bo Reipurth, p. 447

Star Formation in the Corona Australis Region

J.A. Graham

Carnegie Institution of Washington
Dept. of Terrestrial Magnetism
5241 Broad Branch Rd, N.W.
Washington, DC 20015, USA

Abstract

An overview is provided of star formation in the Corona Australis region as we understand it at present. The most active area is that centered on the variable star R CrA and the Herbig-Haro object HH 100. This is coincident with the densest molecular cloud core in the region. Both objects are likely to be the centers of major material outflows. Perhaps the most exciting breakthrough in recent years has been the recognition here of many heavily obscured low-mass stars making up a loose association known as "the coronet" (Taylor and Storey 1984). Other bright stars in the area which still qualify as pre-main sequence objects are S CrA, T CrA, VV CrA and TY CrA. Each of these is associated with an outflowing stellar wind. All are likely close double stars. As each star varies, there is a need to obtain spectra at different apparent magnitude levels.

I. Introduction

The Corona Australis region has a special place in a survey of centers of star formation in the southern hemisphere. It is close; at a distance of approximately 130 pc (e.g. Knacke et al. 1973, Marraco and Rydgren 1981); but it also contains many examples of young stars, covering a range of masses; some embedded, some associated with material outflows, others which have apparently cleared most of the dusty environment associated with their birth. Their proximity makes it possible to observe features on a smaller linear scale than is feasible in the study of similar regions 3 or 4 times more distant. The contrast between this area, with its several variable stars involved in reflection nebulosity and the neighboring Milky Way fields approximately 20° away has always been a striking one but its southern location has delayed detailed study. In recent years, interest has intensified following the discovery of strong concentrations of molecular material (Loren 1979), bright infrared sources and several Herbig-Haro (HH) objects (Knacke *et al.* 1973; Strom, Grasdalen and Strom 1974; Schwartz, Jones and Sirk 1984; Hartigan and Graham 1987). An exciting event has been the recognition of several very heavily obscured low-mass stars in the area making up a small association which has been named "the coronet" (Taylor and Storey 1984; Wilking, Taylor and Storey 1986). One of these stars, R1 (IRS 7) has two small radio lobes which may arise from wind shocks on a toroidal structure around it (Brown 1987).

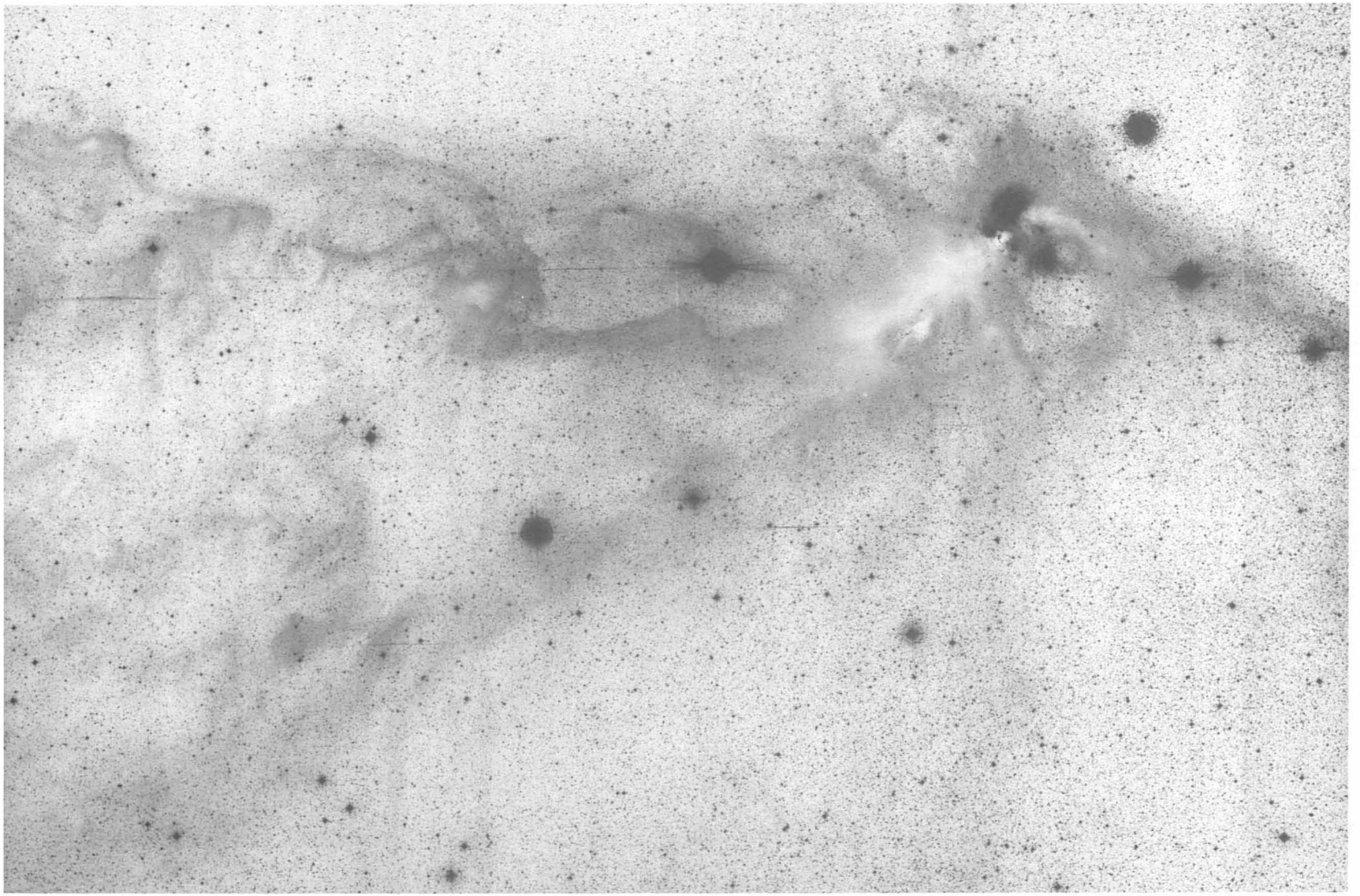

Figure 1. The windswept appearance of the Corona Australis cloud complex is striking in this contrast-enhanced print by C. Madsen from a deep red ESO Schmidt plate.

associated with HH objects or outflows. R CrA resembles much more strongly an early T Tauri star. The FeII and [SII] lines in the spectrum support a T Tauri classification. FeI lines are weak, presumably because of high excitation temperature. Heavy veiling inhibits observation of a photospheric absorption spectrum. The Hα line shows significant night-to-night variations (Graham and Phillips 1987). There is a weak 3.1μm ice band (Chen and Graham 1990).

T CrA is close to R CrA and illuminates a small radial plume which is directed away from R CrA. The spectral type of T CrA is approximately F0. OI λ7773 is strong in absorption. Hα is in emission with a sharp absorption core. The CaII λ8500 triplet can be distinguished in absorption over moderately strong Paschen lines also in absorption. The star is unusually red for its spectral type. This could be due to interstellar or circumstellar reddening or to the presence of a red companion. Images occasionally appear elongated in position angle 90°. [OI] and weak [SII] lines are in emission and are blue shifted by -22 km s^{-1} (heliocentric), LiI λ6708 is not present. These spectroscopic data come from a paper by Graham, Finkenzeller and Heyer (in preparation). The star has an appreciable infrared excess out to 2μm so that a disk and accompanying wind may be still present if the star is in fact single. The possible multiplicity should be checked.

HH 100-IRS is not seen directly in visible light and was one of the first "protostellar" infrared sources to be identified (Strom, Strom and Grasdalen 1974; Strom, Grasdalen and Strom 1974). The IR spectrum shows both 3.1μm ice and 9.7μm silicate absorption bands (Whittet and Blades 1980; Aitken and Roach, quoted by Axon *et al.* 1982; Graham and Chen 1991). The continuum flux is highly variable at all wavelengths (Axon *et al.* 1982; Reipurth and Wamsteker 1983). This appears to be partly due to variable dust extinction, but there is also a component from a changing infrared excess. HH 100-IRS excites HH 100 and probably also HH 96, 97, 99 and 101 (Schwartz, Jones and Sirk 1984, Hartigan and Graham 1987). Several of the HH objects have been detected in molecular hydrogen (Brown et al. 1983, Wilking et al. 1990). HH 100 itself is partly reflection nebulosity (itself slightly variable (Strom and Graham, unpublished)). Scattered light from the embedded source enables a chromospheric T Tauri-like spectrum to be studied which is almost certainly that of the embedded star (Cohen, Dopita and Schwartz 1986). Graham, Finkenzeller and Heyer (in preparation) will describe another short exposure spectrum which shows that the CaII triplet at λ8500 is strongly in emission and that the lines are of approximately equal intensity. HH 100-IRS should be watched for change.

R1(IRS 7) is the most unusual of the newly discovered IR sources. The radio lobes and the weak extended emission discovered by Brown (1987) are remarkably similar to those found around the IRS 5 source in L 1551 (Rodríguez *et al.* 1986). The bolometric magnitude of the object is modest but one cannot escape the impression that a bipolar flow has formed here or is in the process of being formed.

All of these objects thus appear to be responsible for some wind activity in the area and may together be clearing away much of the remaining dust in the cloud core. R CrA in particular

II. Centers of Star Formation; Present and Past

R CrA — T CrA — HH 100-IRS — R1(IRS 7)

These 4 objects are in the same part of the CrA cloud but are apparently the result of separate star forming events.

R CrA varies in brightness between 10^m and 14^m and illuminates the reflection nebula NGC 6729. The surface brightness of the nebula varies but this does not correlate with the brightness of the star (Graham and Phillips 1987). The spectral type of R CrA has been suggested as A or F but it is not well established because of the difficulty in distinguishing photospheric absorption features from those which are formed in a shell which, in the blue at least, dominates the spectrum (Mendoza, Jaschek, and Jaschek 1969; Greenstein and Aller 1947). R CrA is the probable source of HH 104 (Schwartz, Jones, and Sirk 1984). Apart from the strong Balmer line absorption in the blue, its spectrum shows in emission FeII, CaII λ8500 and HeI (with an inverse P Cygni profile). [OI] and [SII] are present with heliocentric velocities -25 and -45 km s^{-1} with respect to the star. As the star brightens and fades, the FeII and CaII lines brighten and fade along with the continuum while the [OI] and [SII] lines stay at approximately the same level of intensity. The photometric and spectroscopic variability is best explained by appreciable veiling of the star by thick clouds close to it. The forbidden lines are produced outside the obscuring region at distances of $10 - 100$ AU from the star and do not vary along with the light of the star (Graham 1989; Graham, Finkenzeller and Heyer, in preparation). A similar arrangement (with the clouds inside 1 AU) is required to explain the rapidly changing shadow patterns which are observed on the reflection nebula (Graham and Phillips 1987 and references therein).

R Cra has a strong infrared excess and a bolometric luminosity of $130 M_\odot$. Examination of available photometry shows that most of the light variation occurs at wavelengths shorter than 5μm. At visual wavelengths there is no correlation between magnitude and B-V color over a magnitude range of at least 2 indicating substantial neutral absorption probably by large dust particles. In the near infrared, $1.2 - 3.5\mu$m, the radiation comes mostly from dust heated close to the star. There is a correlation between visual flux and the IR color gradient but not with the IR flux itself. At brighter magnitudes, the near IR flux is more peaked towards the blue. Interpreted as a dust temperature, values between 1800 and 800K with an average close to 1000K are suggested. Measurements at 10 and 20μm vary remarkably little in this star. An extended source at 60μm and 100μm (Cruz-González, McBreen, and Fazio 1984; Wilking et al. 1985) is centered on R CrA and is due to substantial amounts of warm dust being heated by the star or its outflowing wind. R CrA is the dominant member of the coronet cluster. Polarization measurements (Ward-Thompson *et al.* 1985) show evidence for scattering material in the form of a disk around the star. Molecular hydrogen emission was detected by Wilking et al. (1990) around R CrA.

Although R CrA is often referred to as a Herbig Ae star, it is atypical in several respects (Catala 1989). Catala points out that Herbig Ae and Be stars are in the radiative phase, with radiative envelopes. As a class, the [OI] blueshift is weak or absent and they are rarely

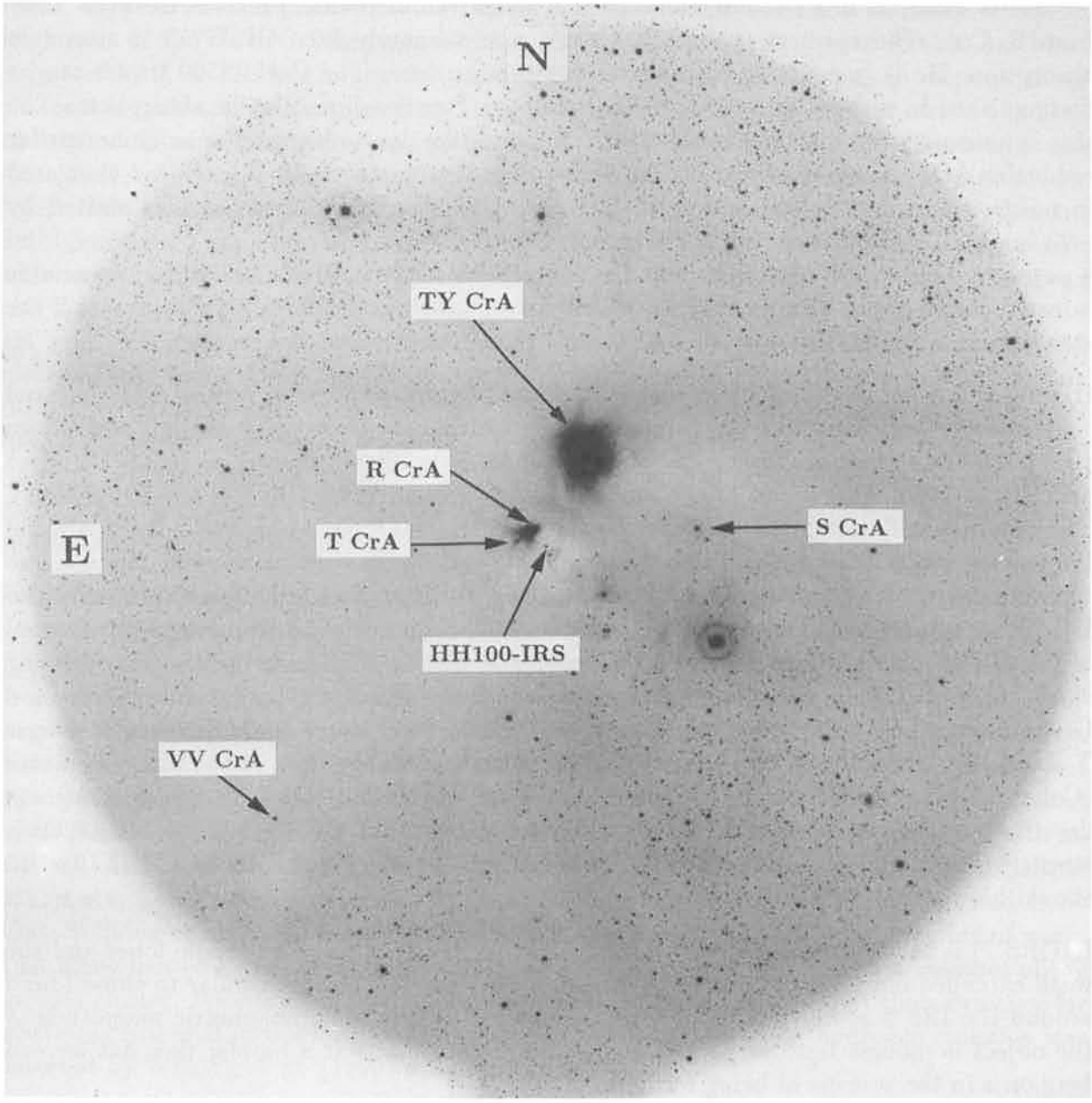

Figure 2: Star Forming Regions in Corona Australis. The photograph was taken through a red filter with the Cerro Tololo 4-meter telescope. The size of the circular field is 50 arc min.

promises to provide important data about the distribution of circumstellar matter within a few AU of a young, active star.

S CrA

We list this star separately as it is distant from the group discussed in the previous section and it has unique features of its own. S CrA is one of the best spectroscopically studied T Tauri stars. Apart from early work by Joy(1945), and Rydgren(1977), most of the work has been done by the Heidelberg group (Appenzeller and Wolf 1977; Wolf, Appenzeller and Bertout 1977; Bertout *et al.* 1982; Appenzeller, Jankovics and Krautter 1983; Appenzeller, Jankovics and Östreicher 1984; Appenzeller, Jankovics and Jetter 1986). Imaging reveals associated HH objects and a faint reflection nebula (Strom *et al.* 1986, Reipurth and Graham 1988). The star is a close visual double with separation 1.″4, p.a. 147°, $\Delta m = 1^m$ which was discovered by Joy and van Biesbrock (1944) and more recently remeasured by Baier *et al.* (1985).

The spectrum of S CrA, described in most detail by Appenzeller, Jankovics and Jetter (1986), shows strong FeI, FeII, CaII and HeI emission lines along with [OI], [SII] and Balmer and Paschen hydrogen lines. It is one of the best examples of the YY Orionis subtype in which some emission lines have distinct red-displaced absorption features (Appenzeller and Wolf, 1977; Rydgren, 1977). Absorption lines are in general very weak and there is apparently strong veiling in the spectrum. Emission lines are seen through into the ultraviolet (there is no dominating shell spectrum as we see in R CrA). FeI emission is stronger in the 5000Å region than in R CrA. As in R CrA, significant night-to-night variations occur in the line profiles, most conspicuously in the Balmer lines (Bertout *et al.* 1982). The spectral type of the companion star is still unknown. If it is a very red star, it may contaminate the observed photometry and spectra of S CrA in a minor way in the red and infrared.

Velocities have now been measured for the two HH objects HH 82a,b which are located approximately 45″ and 90″ E of the star (Graham, Finkenzeller and Heyer, in preparation). Based on observed Hα and [SII] wavelengths, heliocentric velocities of –50 and –34 km s^{-1} are found. In S CrA itself, the data published by Appenzeller, Jankovics and Östreicher(1984) and by Bertout *et al.* (1982) show that higher negative velocities are measured from the forbidden lines (–111 km s^{-1}) while 12 permitted emission lines in the spectrum give –2 km s^{-1}. There are thus strong grounds for believing in a moderate mass outflow from around this star despite the evidence shown for infall by the red-displaced absorption features and we await with interest high resolution molecular maps of the region.

VV CrA

This star is even more isolated from the main center of star formation but it is still well within the molecular cloud and is a very active star. Unlike other young stellar objects discussed here, it does not illuminate a reflection nebula and it is not associated with HH objects. The spectrum shows very strong FeI and FeII lines in emission with large blue displacements in the forbidden lines which indicate again the presence of strong outflowing

winds. Balmer and Paschen lines are strong in emission. It is generally believed, largely because of the red color, that the star has late spectral type. Appenzeller *et al.* (1986) discussed a high resolution spectrum of this star along with their more extensive S CrA data. They proposed that the spectra of the two stars could be explained by the same basic physical model and that the prime difference is one of inclination. Graham, Finkenzeller and Heyer have a low resolution spectrum which covers the range λ5600 – 8900Å. Like the Appenzeller *et al.* spectrum it shows in emission many FeII lines, as well as those of HeI $\lambda\lambda$ 5876, 6678, 7065, NaI $\lambda\lambda$ 5890, 5896 and the CaI λ8500 triplet. Also seen near λ8500 are members of the FeI(60) multiplet. The FeI lines are much stronger in VV CrA than in R CrA or S CrA. Forbidden lines of [OI], [SII] and [FeII] can be identified. There is a moderately strong 3.1μm ice feature (Chen and Graham 1990).

Infrared photometry (e.g. Glass and Penston 1975) points to a strong IR excess for this star. However, a major complication to the interpretation comes from the discovery by Frogel (private communication) that the IR peak is 2″ to the NE of VV CrA and is definitely not coincident with VV CrA as observed visually. Subsequent examination of lightly exposed Las Campanas plates confirms Frogel's discovery. CCD images through various filters show that the companion is a very red object (Reipurth and Zinnecker 1992). The companion star dominates the observed flux between 1 and 4μm. Examination of all available IR photometry indicates that both stars are variable. IRAS fluxes are high showing the presence of abundant warm dust associated with one or both stars. More photometry and spectroscopy covering both the visual and the infrared are required to clarify the situation with VV CrA.

TY CrA

This is the brightest of the CrA variables, and it is important to include it as an example of a star which has almost arrived at the main sequence. It is a good example of a Herbig Be star with spectral type B9 but only very weak emission (Finkenzeller and Mundt 1984). Listed in the CoD as −37° 13024 it forms a visual pair with CoD −37° 13023. Both stars illuminate the reflection nebula NGC 6726/7. TY CrA has been found by Kardopolov, Sahanionok and Filip'ev (1981) and more recently by I. Heyer (unpublished, communicated by G. Herbig) to be an eclipsing variable with period 2.89 days. With reasonable parameters this corresponds to a separation of about 0.05 AU. Cardelli and Wallerstein (1989) have observed interstellar molecular lines in the direction of the star and find further evidence of a large grain size in the cloud. Whittet et al. (1983) detected strong 3.3μm emission towards TY CrA. This emission is spatially extended (Chen and Graham 1990). The neighboring star CoD −37° 13023 has a close visual companion discovered by Hubble (quoted by Herbig and Bell 1988).

TY CrA is the least active of the stars discussed here. It is coincident with a strong 100μm source (Cruz-González, McBreen and Fazio 1984) but compared to other similar sources, there is an absence of radiation at shorter wavelengths. There is a weak outflowing wind (Finkenzeller and Mundt 1984). Evidently most of the dust within a few AU of the star has been cleared away by winds or by the companion star leaving only the more distant cooler dust with the temperature of about 30 – 50°.

III. Material Outflows

Outflowing stellar winds are characteristic of all young stars. The winds are stronger by many orders of magnitude than those presently around the Sun. They are associated with much more massive, slower moving flows of cold molecular material which can be detected by the observation at mm-wavelengths of CO radiation. From the previous discussion, it is clear that there are many likely sources in the area for driving such material outflows and it is not surprising that, with the limited spatial resolution available until recently, the picture has been a rather confused one.

As part of an extended survey of 71 young stellar objects, Levreault(1988) has provided the best mapping up to the present of CO flows in CrA. High velocity wings were first noticed in Loren's(1979) work but no detailed survey was made. Levreault concluded that his new map could be best understood as the superposition of two bipolar outflows, one with symmetry axis EW, probably centered on R CrA and the other in position angle 30° centered on HH 100-IRS. These source identifications are not completely certain because of the limited resolution of the survey. For example, R1(IRS 7) could be an important contributor. The optical data point to these two pre-main sequence stars as being among the youngest and most luminous in the region. S CrA and VV CrA are less luminous but are still likely to be responsible for more modest outflows. S CrA has apparently carved a small cavity out of the surrounding cloud material. Its boundary can be seen as it scatters light from the star. On its eastern side, the cavity is broken and it is here that we see the two HH objects which indicate the direction of a probable bipolar outflow. Note that it is approximately parallel to the suggested outflow from R CrA.

IV. Concluding Remarks

The CrA region is one of the most attractive for more detailed and extended study of low-mass star formation. We view close by several discrete star forming events which are at different evolutionary stages ranging from HH 100 -IRS, which is still deeply embedded within the cloud core, to TY CrA which has cleared away most of the dust in its immediate surroundings and is now almost on the main sequence. All the stars we have discussed are still highly variable. All carry signatures of stellar youth. It is notable that of the 5 stars discussed here that we can view directly, all but one show evidence for multiplicity. Even the exception, R CrA, is a member of the coronet cluster and has an infrared source 15″ away. Is this a general characteristic or does the CrA cloud produce an unusually large fraction of multiple stars? Stellar duplicity, even on the 100 AU scale (and it is unlikely that the stellar orbits are circular), must have an important effect on the evolution of disk-like structures which are currently thought to form almost routinely about recently condensed stars. As Wilking, Taylor and Storey(1986) point out, star formation in this part of the CrA cloud does seem to be unusually efficient, at least in the dense core near R CrA and HH 100-IRS.

The sources of the variability of the CrA stars must be many, including such factors as occultation by nearby clouds, star spots, stellar flares, and accretion from the surrounding

interstellar medium. Surprisingly, few spectra have been taken which cover the major fraction of the known light range. With the little data available, it is already clear that the line emission source regions are very stratified and extend out from the star through many AU. Sorting these out will lead to a better picture of the young central star itself, its evolutionary state and of the way that it is interacting with its surroundings where planetary systems may be in the process of formation.

References

Alvarez, H., Bronfman, L., Cohen, R., Garay, G., Graham, J., and Thaddeus, P.: 1986, *ApJ* **300**, 756

Appenzeller, I., and Wolf, B.: 1977, *A&A* **54**, 713

Appenzeller, I., Jankovics, I., and Krautter, J.: 1983, *A&AS* **53**, 291

Appenzeller, I., Jankovics, I., Östreicher, R.: 1984, *A&A* **141**, 108

Appenzeller, I., Jankovics, I., and Jetter, R.: 1984, *A&AS* **64**, 65

Axon, D.J., Allen, D.A., Bailey, J., Hough, J.H., Ward, M.J., Jameson, R.F.: 1982, *MNRAS* **200**, 239

Baier, G., Bastian, U., Keller, E., Mundt, R., and Weigelt, G.: 1985, *A&A* **153**, 278

Bertout, C., Carrasco, L., Mundt, R., and Wolf, B.: 1982, *A&AS* **47**, 419

Brown, A.: 1987, *ApJ* **322**, L31

Brown, A., Millar, T.J., Williams, P.M., Zealey, W.J.: 1983, *MNRAS* **203**, 785

Cappa de Nicolau, C.E., Pöppel, W.G.L.: 1991, *A&AS* **88**, 615

Cardelli, J.I., and Wallerstein, G.: 1989, *AJ* **97**, 1099

Catala, C.: 1989, in *Low Mass Star Formation and Pre-Main Sequence objects*, ESO Workshop Proceedings, ed B. Reipurth, p. 471

Chen, W.P., and Graham, J.A.: 1990, *BAAS* **22**, 1248

Cohen, M., Dopita, M.A., and Schwartz, R.D.: 1986, *ApJ* **307**, L21

Cruz-González, I., McBreen, B., and Fazio, G.C.: 1984, *ApJ* **279**, 679

Finkenzeller, U., and Mundt, R.: 1984, *A&AS* **55**, 109

Glass, I.S., and Penston, M.V.: 1975, *MNRAS* **172**, 227

Graham, J.A.: 1989, *PASP* **101**, 880

Graham, J.A., and Phillips, A.C.: 1987, *PASP* **99**, 91

Graham, J.A., and Chen, W.P.: 1991, *AJ* **102**, 1405

Hartigan, P., and Graham, J.A.: 1987, *AJ* **93**, 913

Hartigan, P., and Lada, C.J.: 1985, *ApJS* **59**, 383

Herbig, G.H.: 1960, *ApJS* **4**, 337

Herbig, G.H., and Bell, K.R.: 1988, *Lick Obs. Bull.* 1111

Joy, A.H.: 1945, *ApJ* **102**, 168

Joy, A.H., and van Biesbrock, G.: 1944, *PASP* **56**, 123

Kardopolov, V.I., Sahanionok, V.V., and Filip'ev, G.K.: 1981, *Perem. Zvdz.* **21**, 589

Knacke, R.F., Strom, K.M., Strom, S.E., Young, E., and Kunkel, W.: 1973, *ApJ* **179**, 847

Levreault, R.M.: 1988, *ApJS* **67**, 283

Llewellyn, R., Payne, P., Sakellis, S., and Taylor, K.N.R.: 1981, *MNRAS* **196**, 29P

Loren, R.B.: 1979, *ApJ* **227**, 832

Loren, R.B., Sandqvist, Aa., and Wootten, A.: 1983, *ApJ* **270**, 620

Marraco, H.G., and Rydgren, A.E.: 1981, *AJ* **86**, 62

Mendoza V., E.E., Jaschek, M., and Jaschek, C.: 1969, *Bol. Obs. Ton. y Tacubaya* **5**, 107

Reipurth, B., and Graham, J.A.: 1988, *A&A* **202**, 219

Reipurth, B., and Sandell, G.: 1985, *A&A* **150**, 307

Reipurth, B., and Wamsteker, W.: 1983, *A&A* **119**, 14

Reipurth, B., and Zinnecker, H.: 1992, in preparation

Rodríguez, L.F., Cantó, J., Torrelles, J.M., and Ho, P.T.P.: 1986, *ApJ* **301**, L25

Rossano, G.S.: 1978, *AJ* **83**, 234

Rydgren, A.E.: 1977, *PASP* **89**, 557

Schwartz, R.D.: 1977, *ApJS* **35**, 161

Schwartz, R.D., Jones, B.F., and Sirk, M.: 1984, *AJ* **89**, 1735

Strom, K.M., Strom, S.E., and Grasdalen, G.L.: 1974, *ApJ* **187**, 83

Strom, S.E., Grasdalen, G.L., and Strom, K.M.: 1974, *ApJ* **191**, 111

Strom, K.M., Strom, S.E., Wolff, S.C., Morgan, J., Wenz, M.: 1986, *ApJS* **62**, 39

Taylor, K.N.R., and Storey, J.W.V.: 1984, *MNRAS* **196**, 29P

Vrba, F.J, Coyne, G.V., and Tapia, S.: 1981, *ApJ* **243**, 489

Vrba, F.J., Strom, S.E., and Strom, K.M.: 1976, *AJ* **81**, 317

Ward-Thompson, D., Warren-Smith, R.F., Scarrott, S.M., and Wolstencroft, R.D.: 1985, *MNRAS* **215**, 537

Whittet, D.C.B., and Blades, J.C.: 1980, *MNRAS* **191**, 309

Whittet, D.C.B., Williams, P.M., Bode, M.F., Davies, J.K., Zealey, W.J: 1983, *A&A* **123**, 301

Wilking, B.A., Harvey, P.M., Joy, M., Hyland, A.R., Jones, T.J.: 1985, *ApJ* **293**, 165

Wilking, B.A., Taylor, K.N.R., and Storey, J.W.V.: 1986, *AJ* **92**, 103

Wilking, B.A., Schwartz, R.D., Mundy, L.G., Schultz, A.S.B.: 1990, *AJ* **99**, 344

Wolf, B., Appenzeller, I., and Bertout, C.: 1977, *A&A* **58**, 163

The Serpens Molecular Cloud

C. Eiroa

Observatorio Astronómico-IGN
c/ Alfonso XII, 3
28014 Madrid, Spain

1. Introduction

The work of Strom *et al.* (1974) was the first of a long series of studies related to the Serpens molecular cloud. Since then many optical, infrared and radio observations have been devoted to studying the characteristics of this active star-forming region. Attention has mainly been drawn to the so-called Serpens core, due to the large number of phenomena concerning star formation and related topics taking place there. In this contribution, I summarize the most relevant observational aspects of Serpens we know about at present. In section 2 some large scale characteristics are described. Section 3 is dedicated to the cloud core, presenting the optical, IR, and radio data separately. Section 4 briefly addresses some individual interesting sources and the core as a whole. Finally, in Section 5 some future work is suggested.

2. The large-scale molecular cloud

The region known as the Serpens molecular cloud is seen on optical photographs as a large obscured area of about $1° \times 2°$ in size, located to the north of the young variable star VV Ser (Figure 1). Several reflection nebulae are seen in the region, the most prominent of which are S68 (=DG152), DG153 (Sharpless, 1959; Dorschner and Gürtler, 1963) and a bright bipolar nebula normally referred to as the Serpens bipolar reflection nebula (hereafter SRN).

There are only few works devoted to the analysis of the large-scale properties of the cloud. The two most extensive optical studies have been done by Cohen and Kuhi (1979) and Chavarría *et al.* (1988, see also references therein), in which several young stars are identified. Cohen and Kuhi provided information about 9 stars showing Hα emission, including SRN. Chavarría *et al.* studied VV Ser and another 12 stars associated with reflection nebulae by means of Strömgren and IR photometry and optical spectroscopy; they also proposed 13 new candidate Hα emission line stars. In all cases, the stars are intermediate B or A or later spectral type stars. Table 1 gives a summary of the optical stars studied by Cohen and Kuhi (1979) and Chavarría *et al.* (1988). More recently, Reipurth and Eiroa (1991) have identified a new Hα emission line star and, in addition, they found four Herbig-Haro nebulae, HH 106–HH 109, which are the first, unambiguously identified HH objects in Serpens.

Zhang *et al.* (1988b) have presented IRAS maps of a $3° \times 3°$ region centered on the Serpens core. The cloud core, marginally resolved at 60 and 100 μm, and various point sources

are detected. Several of these IRAS point sources are identified with or are close to PMS stars and reflection nebulae: e.g. IRAS 18282+0006 (VV Ser), IRAS 18263+0027 (Ser G3-G6), IRAS 18278+0111 (S68). IRAS 18273+0059, identified with several red stars and a reflection nebula, is the most luminous point source in the cloud, $540L_{\odot}$ (Zhang *et al.* assume a distance of 700 pc, but see below). Large-scale extended emission is seen in all four IRAS bands. The 60/100 μm colour temperature varies between $\approx$ 20 to 30 K, the total emission of the extended structure is $\approx$ 3200 $L_{\odot}$ and the total mass inferred from the IR data is $\approx$ 300 $M_{\odot}$. Relying on the analysis of the energetics and temperature distribution, Zhang *et al.* conclude that both stellar and interstellar radiation fields contribute to the heating of the extended emission.

The 2.6 mm line of CO over an area of around 300 square arc minutes has been mapped by Loren *et al.* (1979). Two broad maxima of T_A^* are found: one coinciding with the core and the other one located to the north of the reflection nebula S68. CO is self-reversed in many positions of the cloud. Kinetic temperatures are around 20 K, reaching a maximum of 27 K approximately at the position of the near-IR source SVS4.

Palla and Giovanardi (1989) have recently surveyed three fields and six point sources for H_2O maser emission. Only the source FIRS1 in the core was positively detected.

The distance to the cloud is still a matter of controversy. The kinematic distance calculated from CO data is $\approx$ 600 pc (Zhang *et al.*, 1988b). Photometric values between 250 and 700 pc are given in the literature (Chavarría *et al.*, 1988; Zhang *et al.*, 1988b and references therein). The different estimates of the photometric distance are generally based on the same stars, the discrepancy coming from the assumption of different luminosity classes. De Lara *et al.* (1991) have reobserved several Serpens stars. The new value they find is 311$\pm$38 pc and is based on five well-observed stars.

3. The cloud core

3.1. Optical observations

Optical studies of the Serpens core have mainly been concentrated around SRN and to a lesser extent around the nebulosity GGD 29 (Gyulbudaghian *et al.*, 1978).

Extensive CCD images up to wavelengths around 0.9μm have been carried out by Hartigan and Lada (1985) and Gómez de Castro *et al.* (1988). Around 20-25 stars are observed in the I (0.9 μm) CCD images. 7 nebulae are found among them: 5 showing a cometary-like morphology and the other two a bipolar one. 3 out of the 5 cometaries are also seen in the optical photographs; one of the bipolars is SNR itself. The second bipolar is very faint and is associated with a radio source and one of the stars in the SVS4 PMS stellar group (see below). Figure 2 shows the 0.9 μm image centered on SRN taken by Gómez de Castro *et al.* (1988). In that figure two cometary nebulae and the young double source SVS20 are also seen.

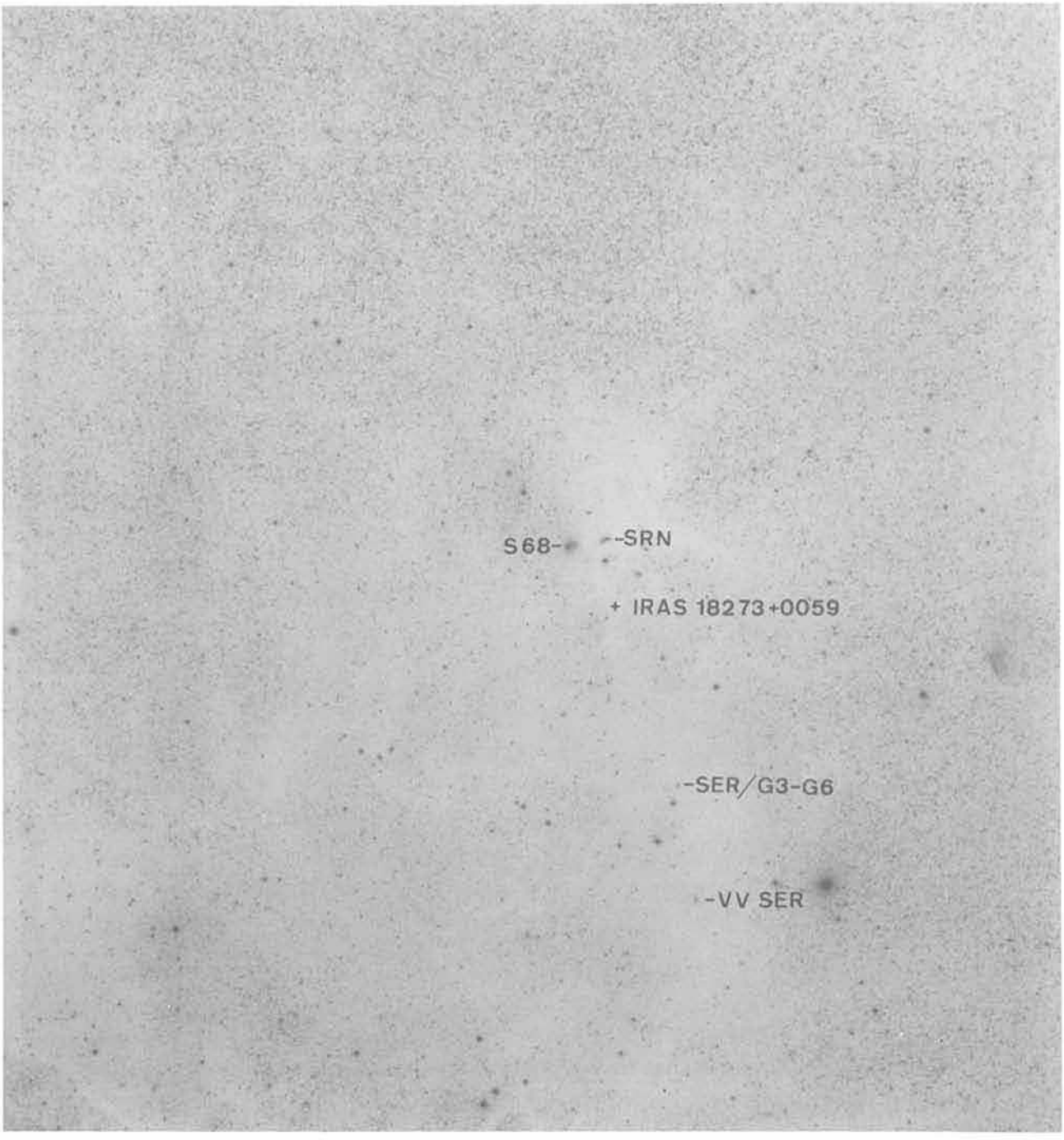

Figure 1: The Serpens molecular cloud as seen on the POSS red plate. Large scale structure is clearly visible on this photograph. Some prominent objects are indicated.

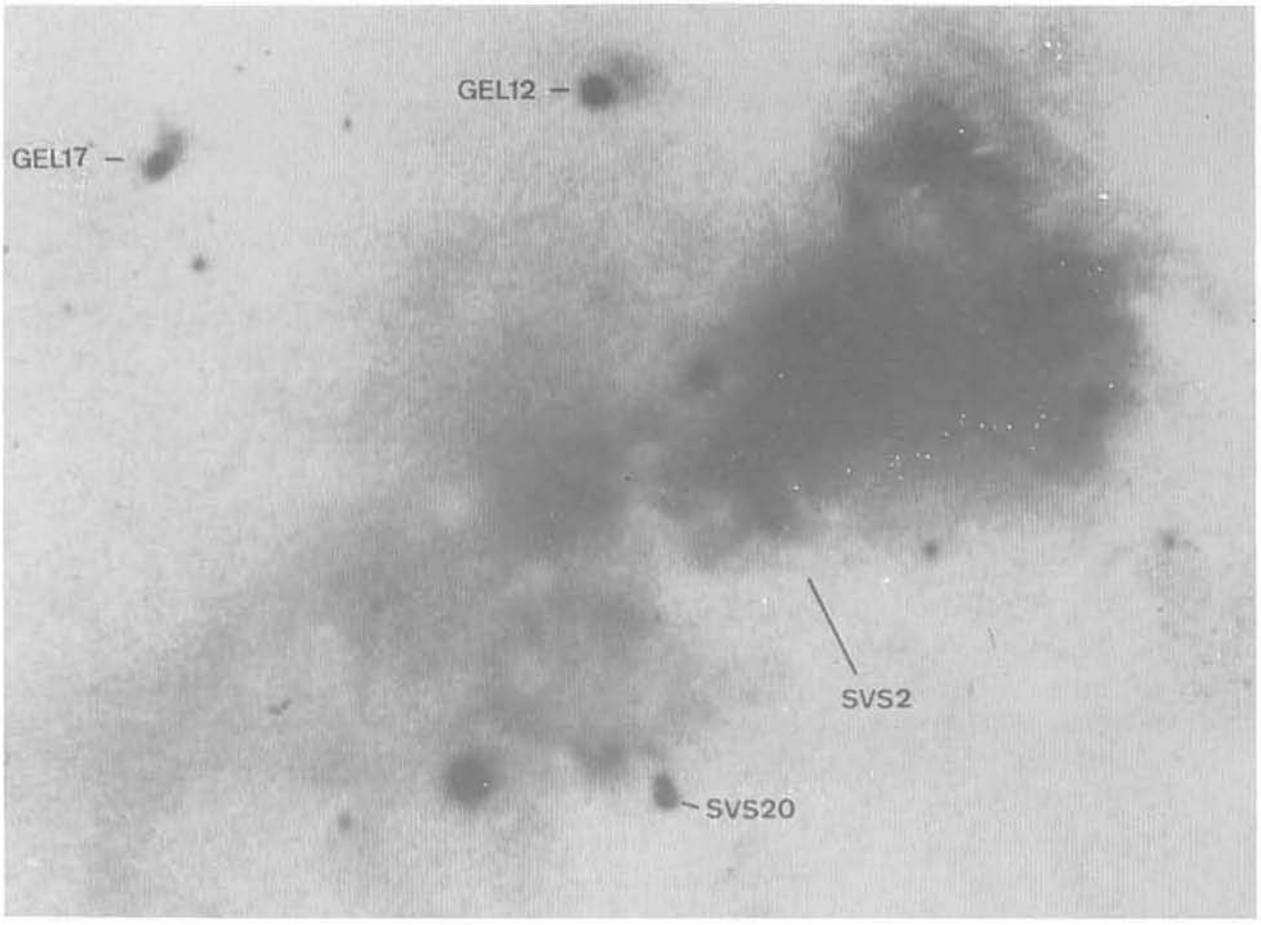

Figure 2: 0.9 μm image of SRN taken with the Calar Alto Observatory 3.5 m telescope. SVS2, the star illuminating SRN, is hidden by the nebulosity on this picture; its approximate position is indicated. Two cometary nebulae and the young double PMS star SVS20 are also shown.

Polarimetric measurements of SRN have been carried out by Worden and Grasdalen (1974), King *et al.*, (1983), Warren-Smith *et al.* (1987) and Gómez de Castro *et al.* (1988). Two distinct polarization patterns are seen: the typical centro-symmetric orientation of the electric vectors in bipolar nebulae, and a non-centro symmetric band around the illuminating star, perpendicular to the main axis of the nebula, where the polarization grade goes down. The exciting star, SVS2 (Strom *et al.* 1976), is seen at the apex of the northwestern bipolar lobe.

Spectroscopy of SRN has been carried out by Strom *et al.* (1974), Cohen and Kuhi (1979), and Gómez de Castro (1990). Hα is seen in emission and presents a complex spatial structure close to the star SVS2. The hydrogen line is split in a blueshifted and a redshifted component covering a velocity range from ≈ -250 to 320 km s^{-1}; in addition, there seems to be a compact ($< 3''$) shocked emission knot, located $\approx 1.5'$ west of SVS2, embedded in SRN (Gómez de Castro, 1990, and private communication). We also have an Hα spectrum of GGD29. In this case a broad Hα emission of ≈ 200 km s^{-1} is seen (Eiroa, unpublished observations).

3.2. Infrared observations

Strom *et al.* (1976) studied at near-IR wavelengths a region of around 95 arcmin^2 approximately centered on SRN. They found 20 sources, of which at least six were not associated with visible objects. Churchwell and Koornneef (1986) mapped the central 10 arcmin^2 of the core at 2.2μm and found 13 sources, most of them being new detections and only three identified with optical counterparts. Eiroa *et al.* (1987) and Gómez de Castro *et al.* (1988) observed the regions around SRN, SVS20 and SVS4. They found extended emission associated with SVS2 (the illuminating star of SRN) and with SVS20, as well as several individual infrared sources at the position of SVS4. As a whole, a total amount of around 30 near-IR sources have been detected in the works mentioned, many of them presenting the characteristics of low-mass PMS objects.

Eiroa and Casali (1991) have carried out a very detailed study in the near-IR of the Serpens cloud core. We have obtained high sensitivity near-IR images of a region of 30 arcmin^2 centered on SRN, thus practically covering the whole cloud core. The observations have been done with IRCAM at the United Kingdom Infrared Telescope (Mauna Kea); data have been obtained through the filters J, H, K, L'(narrow) and ice (narrow 3.1μm filter). The main results are as follows. (a): Around 160 near-IR sources are observed in the field; most of them are new detections. (b): Several new stars associated with cometary-like nebulae are found. In particular, a near-IR counterpart of the far-IR/radio source Serpens-FIRS1 has been detected for the first time. The source has the appearance of a jet-like nebulosity with a point-like source (see also Eiroa and Casali, 1989). (c): The images reveal new nebular structures associated with known Serpens embedded sources; in addition, a large-scale, very diffuse nebulosity extending from the north of SRN towards SVS4 is obvious in the K-image; its size is $2' \times 3'$. (d): The data show that around 50 young low-mass stars are embedded in the Serpens core. This figure increases considerably the previous estimate by Gómez de

Castro *et al.* (1988).

Observations of the 3.1 μm absorption due to H_2O ice-coated dust grains in the line of sight of several Serpens sources have been reported by Churchwell and Koornneef (1986), Eiroa *et al.* (1987), Eiroa and Leinert (1987), Eiroa and Hodapp (1989a) (these latter authors also observed the 4.67μm absorption of solid CO) and Eiroa and Casali (1991). They used photometric, spectroscopic and speckle techniques. The observations demonstrate that the icy grains are widespread in the Serpens intracloud medium and are not strictly limited to circumstellar PMS environments. A relationship seems to exist between the optical depth of the 3.1 μm absorption and the optical extinction. In this sense, Serpens is similar to the Taurus complex, although in Serpens the A_v-threshold to detect the ice absorption is likely to be higher than in Taurus.

Far-IR observations have been carried out by Nordh *et al.* (1982) and Harvey *et al.* (1984). In addition, Zhang *et al.* (1988a) have presented IRAS maps of the core. Morphologically, it presents a "double-peaked" structure. One peak is located towards the NW of SRN in the more optically obscured part of the cloud. This peak, normally called Serpens-FIRS1, is well defined displaying a clear point-like appearance and is associated with a triple radio source, H_2O masers, and a recently discovered near-IR jet-like nebulosity. The second peak is located near SRN and is not point-like; it is a source extending from the north of SRN to the south in the direction of SVS4. This far-IR emission overlaps quite well with the diffuse nebulosity detected in the near-IR images. The estimated total luminosity of the Serpens core differs considerably among the three aforementioned works (for an explanation see the discussion of Zhang *et al.*, 1988a). However, they do have in common the relatively low luminosity derived from the far-IR data, which indicates that only intermediate or low-mass stars are present. The dominant far-IR source is FIRS1 with a total luminosity of $L \approx 1.2 \times 10^{-3}$ D^2(pc) $L_\odot$. Colour temperature and optical depth maps have been derived by Zhang *et al.* (1988a) from the IRAS data. The colour temperature exhibits a hot ridge extending from the SE towards the NW through SRN. The temperature in the ridge achieves values of $\approx$ 34 K in some locations; outside the ridge the temperature decreases down to $\approx$ 23 K. In addition, the 100μm optical depth map presents an appearance similar to the brightness distribution. Thus, the far-infrared peaks could be produced by dust density effects.

3.3. Radio observations

CO, OH, NH_3, HCO and H_2CO molecular radio observations of the core have been carried out by a variety of groups (Loren *et al.*, 1979, 1981; Loren and Wooten, 1980, Ho and Barret, 1980, Rodríguez *et al.*, 1980; Little *et al.*, 1980; Ungerechts and Güsten, 1984; Takano, 1986; Torrelles *el al.*, 1989). The LSR velocity of the molecular lines is $\approx$8 km/s and the widths are suprathermal (e.g. v(NH_3)$\approx$1 km s^{-1}, Ungerechts and Güsten, 1984). Kinetic temperatures deduced from CO are higher than those deduced from NH_3 and similar to the dust temperatures deduced from IRAS. Loren *et al.* (1979) observed a high density core ($n(H_2) \approx 7 \times 10^4 cm^{-3}$) of radius 3.3 arcmin and mass 1200 $M_\odot$ (at their assumed distance of 440 pc). The relatively low resolution NH_3 observations of Little *et al.* (beamwidth 2.2')

show an ammonia distribution similar to the far-IR emitting region, likely indicating a high density gas-dust mixture. The NH_3 map of Ungerechts and Güsten (resolution 40″) shows two subclouds. The NW cloud approximately coincides with Serpens-FIRS1 and the SE cloud is located close to SRN and coincides with the K-diffuse large-scale nebulosity. Gas densities from NH_3 and H_2CO line measurements estimated by the latter authors are in the range $1\text{–}2\times10^4$ cm^{-3}. The total mass of the high density clouds is 20 $M_\odot$ (assumed distance of 440 pc) and they are virialized. In addition, a SE-NW velocity gradient of $\approx$ 1.3 km s^{-1} pc^{-1} has been noticed by Ho and Barret (1980) and Ungerechts and Güsten (1984).

CO and OH molecular outflows in the direction of Serpens have been detected by Loren *et al.* (1981), Bally and Lada (1983), Mirabel (1987), Mirabel *et al.* (1987), and Clark and Turner (1987). In addition, Nordh *et al.* (1982) reported high velocity CO-wings at the position of SVS4. Bally and Lada (1983) mapped the CO outflow, its size is very large, around $12'\times17'$. The blueshifted and redshifted components are centered close to SRN on the diffuse K-nebulosity. A total velocity extent of $\approx$ 28 km s^{-1} is seen in CO and OH. The outflows cannot be ascribed to a single driving source. In fact, the morphology of the CO outflow and the K IRCAM image suggest that the molecular gas of Serpens is somehow being pushed away by the common action of the PMS objects embedded in the cloud core (Eiroa and Casali, 1991). In this sense, new high-resolution CO observations carried out with the Nobeyama 45-m telescope show very different CO wing profiles towards the sources FIRS1 and SVS4 (Eiroa *et al.*, 1992, unpublished observations).

Two radio continuum sources were discovered by Rodríguez *et al.* (1980). Further radio continuum measurements have been carried out by Ungerechts and Güsten (1984), Snell and Bally (1986) and Rodríguez *et al.* (1989). One of the sources is located at the position of SVS4 and the second is associated with FIRS1. In both cases the luminosity deduced from the radio continuum is much larger than the total IR luminosity (Snell and Bally, 1986). I refer to the following section for some more details concerning the radio sources.

H_2O maser emission has been detected by Blair *et al.* (1978), Rodríguez *et al.* (1978, 1980), Dinger and Dickinson (1980) and Palla and Giovanardi (1989). Ungerechts and Güsten (1984) failed to detect any H_2O masers. The maser source seems to be associated with FIRS1 and shows a remarkable variability in its velocity structure and flux (see e.g. Palla and Giovanardi, 1989). In addition, OH maser emission has recently been detected by Rodríguez *et al.* (1989) and coincides in position with the radio source associated with FIRS1.

Mirabel *et al.* (1989) have found extended, weak anomalous OH emission in the direction of several galactic star-forming regions, including Serpens. This emission with a 1667/1665 line ratio close to 4 is similar to that produced by extragalactic megamasers; Mirabel *et al.* suggest that this result could help to understand the extragalactic megamaser phenomenon.

JCMT continuum observations between 0.8 and 2mm have been carried out at Mauna Kea (Casali *et al.*, 1992). The extended 1.1mm emission shows a morphology quite different

from that detected in NH_3 and in the far-IR. Few known Serpens stars are detected in this wavelength range. In addition, two new submillimeter sources have been found.

4. Short discussion

4.1. PMS objects in the cloud core

Table 2 gives a list of confirmed young objects in the Serpens core, which can be found in published works (Churchwell and Koornneef, 1986; Gómez de Castro *et al.*, 1988; Eiroa and Casali, 1989). Gómez de Castro *et al.* estimated lower limits of 6% and 240 $M_\odot$ pc^{-3} for the star formation efficiency and the stellar density respectively. In fact, the near-IR images (Eiroa and Casali, 1991) demonstrate that $\approx$50 young objects are embedded in the cloud core. Thus, both figures are increased considerably with respect to the previous estimate, and the conclusion of Gómez de Castro *et al.* about the formation of a gravitationally bounded cluster after the removal of the gas cloud is reinforced. On the other hand, the argumentation is based on an assumed distance of 250 pc (Chavarría *et al.*, 1988). If the distance of 700 pc is considered (Zhang *et al.*, 1988b), the conclusion of GEL must be regarded with caution for the star formation efficiency and the stellar density would be considerably lower.

Additionally, the young objects present a remarkable alignment of their projected symmetry axes in the SE-NW direction, which is approximately parallel to the large-scale helical component of the local magnetic field (Mathewson and Ford, 1970; Gómez de Castro *et al.*, 1988). The new cometary nebulae found in the near-IR images are also oriented in the same direction. Such alignments are found in various clouds (e.g. Strom *et al.*, 1986) and are interpreted in terms of the role played by the magnetic field in the formation of outflows and, in general, in the star formation processes. This interpretation is in conflict with that of Warren-Smith *et al.* (1987), who suggest a magnetic field perpendicular to the main axis of the nebulae. The interpretation of Gómez de Castro *et al.* seems also to be in contradiction to that of Zhang *et al.* (1988a), who suggest a flattened dust ring rotating on an axis perpendicular to the main axis of the nebulae. They base their interpretation on the SE-NW velocity gradient of NH_3 (Ungerechts and Güsten, 1984) and on the far-IR and NH_3 morphology.

4.2. Individual objects

SRN. The Serpens reflection nebula is the most outstanding optical object of the cloud core (Figure 2). SRN is illuminated by the PMS source SVS2 as the centrosymmetric pattern of the polarization shows (e.g. Worden and Grasdalen, 1974). This pattern is distorted in some regions of the SE nebular lobe due to the presence of other PMS Serpens stars (e.g. SVS20). SVS2 has been classified as late B or early A (Worden and Grasdalen, 1974), although a M0 spectral type has also been proposed (Cohen and Kuhi, 1979). Assuming a distance of 250 pc, Gómez de Castro *et al.* estimated a bolometric luminosity in the range 0.6–20 $L_\odot$; this range should be increased to 5–160 $L_\odot$ if the distance of 700 pc is taken. In any case, an intermediate/low luminosity PMS star is implied. The Hα spectrum of SVS2 shows that

the star is losing mass (Gómez de Castro, 1990), and she suggests that the magnetic field could play a significant role. The direct images and the polarization measurements in SRN indicate the presence of a dust disk around SVS2; its apparent size is $\approx 5''-8''$ and produces an optical extinction of around 7 mag. Eiroa and Hodapp (1989b) have carried out high spatial resolution infrared images of a field $9''\times 9''$ around SVS2; the infrared morphology is similar to that observed at shorter wavelengths and the dust disk is also evident. The band of low polarization associated with the disk is probably produced by multiple scattering in the optically thick dust disk (Bastien, 1987).

GGD29. This object was initially proposed as a suspected HH object (Gyulbudaghian *et al.*, 1978). However, polarization measurements show that the object is in fact a reflection nebulosity, the illuminating star being the brightest of the two optically visible stars (Warren-Smith *et al.*, 1987); this star suffers low foreground extinction (Gómez de Castro *et al.*, 1988). As mentioned in 3.1. there is a broad Hα line emission. On the infrared images of Eiroa and Casali (1991) GGD29 seems to be the latest member of a chain of stars going from the east to the northwest, although at present we do not know if this is accidental or if those stars are related indeed.

CK2. It is one of the redder objects observed in the core (Churchwell and Koornneef, 1986) and shows the deepest observed ice feature in Serpens (Eiroa and Hodapp, 1989a). Wolfire and Churchwell (1987) have fitted the CK2 energy distribution, the best-fit model being a PMS star of $M\approx 2\ M_\odot$ and $L\approx 27\ L_\odot$, and suffering a foreground optical extinction of ≈ 32 mag.

SVS20. The object was first found by Strom *et al.* (1974). SVS20 is the brightest near-IR source in Serpens and is, in fact, a double source. The separation between both components is $1.6''$ and the brightness ratio remains practically constant from 0.9μm to 5μm (Eiroa *et al.*, 1987; Eiroa and Leinert, 1987; Leinert, private communication). The depth of the ice feature appears to be the same for both stars, which suggests that they suffer similar optical extinction and, consequently, have similar intrinsic energy distribution, in spite of their different luminosities. Relying on luminosity and temperature constraints Eiroa and Leinert (1987) suggest that the SVS20 stars are 1-2 $M_\odot$ PMS objects which have not achieved the T Tauri stage yet. A qualitatively similar result for SVS20 as a single source is found by Wolfire and Churchwell (1987) on the basis of their energy distribution models.

SVS4. This is the IR source south of SRN where a radio continuum source is detected (Rodríguez *et al.*, 1980). The ice band is very pronounced at this position of the cloud (Eiroa and Hodapp, 1989a). CCD images show the presence of a very faint bipolar-like object. This is the only object departing from the common orientation of the Serpens nebulae (Gómez de Castro *et al.*, 1988). Deep near-IR images show 11 objects surrounded by a tenuous nebulosity of $\approx 50''$ in size (Eiroa and Casali, 1989). One of the IR stars coincides with the bipolar-like nebula; a second one is the cometary nebula GEL5. The total luminosity lies in the range 22.5–175 $L_\odot$, depending on the assumed distance; thus, the stars constitute a group of low luminosity objects, likely solar-type stars. Assuming that the stars are of 1 $M_\odot$ and that they are grouped in a volume of diameter equal to the observed angular size, the

mass stellar density exceeds the value of 10^3 $M_\odot$ pc^{-3}, even for the distance of 700 pc. This means that the PMS SVS4 stellar group is really very dense.

FIRS1. This object is the most luminous source embedded in the cloud core, L$\approx$ 115 $L_\odot$ (for d=310 pc), and it is the only location where H_2O maser emission has been detected. The 6cm radio continuum source has a triple structure consisting of a central object, and two lobes with spectral indices characteristic of nonthermal emission. These outer components show proper motions (Rodríguez *et al.*, 1989). A jet-like nebulosity with a point source at its SE apex is detected in the near-IR; the nebulosity mainly consists of H_2 emission (Eiroa and Casali, 1989). FIRS1 is the only spot in the Serpens core where shock excited emission is detected. In addition, the nonthermal emission of the radio source makes FIRS1 a very unusual object (Rodríguez *et al.*, 1989); theoretical studies of the object have been made by Crusius-Wätzel (1990) and Henriksen et al. (1991). Very recently, Torrelles et al. (1992) have performed sensitive VLA observations in NH_3 of the object.

5. Future work

The proximity of the Serpens region and the richness of observed phenomena make Serpens a good laboratory for studying the processes involved in the formation of stars in molecular clouds using high quality observational data. In addition, Serpens appears to be suited for comparing the predictions of theoretical models with observational results.

A non-exhaustive list of future observational work to be done in Serpens should include the following aspects:

- The distance to the cloud should be determined precisely. This is a key parameter for aspects like the luminosity of the sources and figures as important for the theories of star formation in molecular clouds as the star formation efficiency and the stellar density. The distance estimate of 310 pc given by de Lara *et al.* (1991) is probably the best one for the Serpens dark cloud at present. Nevertheless, an independent estimate confirming their value would be extremely useful.

- A reliable determination of the total cloud core mass is also necessary. The estimates that have been done using different mass indicators – which, in fact, sample different parts of the cloud (H_2CO, NH_3, far-IR) – differ in factors larger than one order of magnitude.

- The total luminosity of individual sources should be estimated in order to constrain better the mass of the Serpens PMS objects. This could probably be done by means of mid- and far-IR observations (ISO) and by using submillimeter telescopes.

- The magnetic field seems to play a key role in Serpens. However, there are no measurements of the field within the cloud and its immediate surroundings.

- The molecular outflows have been observed with poor spatial resolution. Higher spatial resolution observations should be carried out to study the outflow of cloud material close to several PMS sources (e.g., FIRS1).
- The near-IR source in FIRS1 does not seem to coincide with the radio source. In addition, the 2.2μm position significantly differs in the works of Eiroa and Casali (1989) and Rodríguez *et al.* (1989). New observations are necessary to elucidate this point since they might be useful to understand the young stellar activity in this part of the cloud core.
- New very deep observations of the tiny nebulosity in SVS4 should investigate if it is a bipolar nebulosity indeed, and why it departs from the common alignment of other objects in Serpens.
- More observations of the large-scale Serpens molecular cloud characteristics are necessary to achieve a complete picture of this interesting star formation region. In particular, infrared and radio observations of the field around the objects HH106–HH109 should be undertaken.

Acknowledgements

My work in Serpens would have been impossible without the collaboration of M. Casali, A. I. Gómez de Castro, K. -W. Hodapp, Ch. Leinert and R. Lenzen. This work has been supported in part by grant DGICY PB87-0167.

References

Bally, J., Lada, C. J.: 1983, *ApJ* **265**, 824

Bastien, P.: *ApJ* **317**, 231

Blair, G. N., Davis, J. H., Dickinson, D. F.: 1978, *ApJ* **226**, 435

Casali, M. M., Duncan, W., Eiroa, C.: 1992, in preparation

Chavarría-K., C., de Lara, E., Finkenzeller, U., Mendoza, E. E., Ocegueda, J.: 1988, *A&A* **197**, 151

Churchwell, E. , Koornneef, J.: 1986, *ApJ* **300**, 729

Clark, F. O., Turner, B. E.: 1987, *A&A* **176**, 114

Cohen, M., Kuhi, L. V.: 1979, *ApJS* **41**, 743

Crusius-Wätzel, A. R.: 1990, *ApJ* **361**, L49

De Lara, E., Chavarría-K., C., López Molina, G.: 1991, *A&A* **243**, 139

Dinger, A. St. C., Dickinson, D. F.: 1980, *AJ* **85**, 1247

Dorschner, J., Gütler, J.: 1963, *Astron. Nachr.* **287**, 257

Eiroa, C., Casali, M. M.: 1989, *A&A* **223**, L17

Eiroa, C., Casali, M. M.: 1991, submitted to *A&A*

Eiroa, C., Hodapp, K. -W.: 1989a, *A&A* **210**, 345

Eiroa, C., Hodapp, K. -W.: 1989b, *A&A* **236**, 217

Eiroa, C., Leinert, Ch.: 1987, *A&A* **188**, 46

Eiroa, C., Lenzen, R., Leinert, Ch., Hodapp, K. -W.: 1987, *Astrophys.* **179**, 171

Gómez de Castro, A. I.: 1990, in *Galactic and Intergalactic Magnetic Fields*, IAU Symp. **140**, Kluwer, p. 318

Gómez de Castro, A. I., Eiroa, C., Lenzen, R.: 1988, *A&A* **201**, 299

Gyulbudaghian, A. L., Glushkov, Yu. I., Denisyuk, E. K.: 1978, *ApJ* **224**, L 137

Hartigan, P., Lada, C. J.: 1985, *ApJS* **59**, 383

Harvey, P. M., Wilking, B. A., Joy, M.: 1984, *ApJ* **278**, 156

Henriksen, R. N., Ptuskin, V. S., Mirabel, I. F.: 1991, *A&A* **248**, 221

Ho,, P. T. P., Barret, A. H.: 1980, *ApJ* **237**, 38

King, D. J., Scarrott, S. M., Taylor, K.N.R.: 1983, *MNRAS* **202**,1087

Little, L. J., Brown, A. T., McDonalds, G. H., Riley, P. W., Matheson, D. N.: 1980, *MNRAS* **193**, 115

Loren, R. B., Evans, II, N. J., Knapp, G. R.: 1979, *ApJ* **234**, 932

Loren, R. B., Plambeck, R. L., Davis, J. H., Snell, R. L.: 1981, *ApJ* **245**, 495

Loren, R. B., Wooten, A.: 1980, *ApJ* **242**, 568

Mathewson, D. S., Ford, V. l.: 1970, *Mem. R. Astron. Soc.* **74**, 139

Mirabel, I. F.: 1987, in *Star Forming Regions*, IAU Symp. **115** (Reidel), p. 315.

Mirabel, I. F., Ruiz, A., Rodríguez, L. F., Canto, J.: 1987, *ApJ* **318**, 729

Mirabel, I. F., Rodríguez, L. F., Ruiz, A.: 1989, *ApJ* **346**, 180

Nordh, H. L., Van Duinen, R. J., Sargent, A. I., Fridlund, C. V. M., Alladers, J. W. G., Beintema, D.: 1982, *A&A* **115**, 308

Palla, F., Giovanardi, C.: 1989, *A&A* **223**, 267

Reipurth, B., Eiroa, C.: 1992, *A&A* in press

Rodríguez, L. F., Curiel, S., Moran, J. M., Mirabel, I. F., Roth, M., Garay, G.: 1989, *ApJ* **346**, L85

Rodríguez, L. F., Moran, J. M., Dickinson, D. F., Gyulbudaghian, A. L.: 1978, *ApJ* **226**, 115

Rodríguez, L. F., Moran, J. H., Ho, P.T.P., Gottlieb, E. W.: 1980, *ApJ* **235**, 845

Sharpless, S.: 1959, *ApJ Ser.* **4**, 257

Snell, R. L., Bally, J.: 1986, *ApJ* **303**, 683

Strom, S. E., Grasdalen, G. L., Strom, K. M.: 1974, *ApJ* **191**, 111

Strom, K. M., Strom, S. E., Wolff, S. C., Morgan, J., Wenz, M.: 1986, *ApJS* **62**, 39

Strom, S. E., Vrba, F. J., Strom, K. M.: 1976, *AJ* **81**, 638

Takano, T.: 1986, *ApJ* **303**, 349

Torrelles, J. M., Ho, P. T. P., Rodríguez, L. F., Canto, J., Verdes-Montenegro, L.: 1989, *ApJ* **346**, 756

Torrelles, J. M., Gomez, J. F., Curiel, S., Eiroa, C., Rodríguez, L. F., Ho, P. T. P.: 1992, *ApJ Letters*, in press

Ungerechts, H., Güsten, R.: 1984, *A&A* **131**, 177

Warren-Smith, R. F., Draper, P. W., Scarrott, S. M.: 1987, *MNRAS* **227**, 749

Wolfire, M. G., Churchwell, E.: 1987, *ApJ* **315**, 315

Worden, S. P., Grasdalen, G. L.: 1974, *A&A* **34**, 37

Zhang, C. Y., Laureijs, R. J., Clark, F. O.: 1988a, *A&A* **196**, 236

Zhang, C. Y., Laureijs, R. J., Clark, F. O., Wesselius, P. R.: 1988b, *A&A* **199**, 170

Table 1. Visible young stars associated with the Serpens molecular cloud.

Object	α (1950)	δ (1950)	V(mag)	Sp.T.	Notes
1 BD-2°4607	$18^h\ 18^m\ 57^s$	−2° 04′ 02″	10.44	A2V:	1
3 VV Ser	$18^h\ 26^m\ 15^s$	+0° 06′ 34″	12.67	A2eβ	1
4	$18^h\ 26^m\ 59^s$	−0° 15′ 35″	9.55	.	1
5	$18^h\ 27^m\ 00^s$	+1° 06′ 13″		K0:	1
6	$18^h\ 27^m\ 01^s$	+1° 06′ 20″	8.2	A0V	1
7	$18^h\ 27^m\ 25^s$:	+0° 58′ 35″:	12.42		1
9	$18^h\ 27^m\ 35^s$	+1° 01′ 17″	11.86	>G9	1,a
10 BD+1°3694	$18^h\ 27^m\ 52^s$	+1° 11′ 26″	9.92	A1V	1
12 SAO 123590	$18^h\ 28^m\ 17^s$	+1° 21′ 22″	8.45	B4V	1
13 SAO 123595	$18^h\ 28^m\ 37^s$	+1° 25′ 14″	8.57	B3V	1
14	$18^h\ 28^m\ 40^s$	−2° 22′ 54″	14.12	Beβ	1
15 SAO 123661	$18^h\ 32^m\ 35^s$	+0° 00′ 03″	7.99	B3V	1
16	$18^h\ 34^m\ 24^s$	+0° 17′ 36″	10.75	<A0V	1
17	$18^h\ 29.3^m$:	−2° 05.4′ :	14.17		1
Ser groups/G1	$18^h\ 25.7^m$:	−0° 05′ :	17.3	K7	2
/G1/c			19.6		2
/G2			15.1	K1	2
/G3			18.4	K7	2
Ser groups/G4	$18^h\ 26^m\ 31^s$:	+0° 27′ 08″:	19.7		2
/G5			17.5	M1	2
/G6			16.8	K3	2
ESO Hα 279	$18^h\ 26^m\ 59^s$	+1° 16′ 39″			3

1: The numbering corresponds to Chavarría *et al.*(1988)
2: Cohen and Kuhi (1979)
3: Reipurth and Eiroa (1992)
a: double star

Table 2. Positions and K magnitude of confirmed young objects in the Serpens cloud core.

Object	Other Name	α (1950)	δ (1950)	K(mag)	Notes
FIRS1		$18^h\ 27^m\ 17.3^s$	1° 13′ 23″	14.76	3
SVS4/1		$18^h\ 27^m\ 24.0^s$	1° 10′ 09″	13.65	3
SVS4/2	GEL5	$18^h\ 27^m\ 24.2^s$	1° 10′ 51″	11.26	2,3
SVS4/3		$18^h\ 27^m\ 24.3^s$	1° 10′ 30″	13.42	3
SVS2	CK3,GEL6	$18^h\ 27^m\ 24.5^s$	1° 12′ 41″	8.80	1,2,3
SVS4/4	GEL7	$18^h\ 27^m\ 24.6^s$	1° 10′ 39″	11.01	2,3
SVS4/5		$18^h\ 27^m\ 25.1^s$	1° 10′ 52″	11.44	3
SVS4/6	CK5,GEL9	$18^h\ 27^m\ 25.3^s$	1° 10′ 56″	11.89	1,2,3
SVS20	CK1,GEL10	$18^h\ 27^m\ 25.4^s$	1° 11′ 59″	6.97	1,2,3
SVS4/10	GEL11	$18^h\ 27^m\ 25.4^s$	1° 10′ 43″	10.35	2,3
SVS4/7		$18^h\ 27^m\ 25.5^s$	1° 10′ 20″	13.02	3
SVS4/8		$18^h\ 27^m\ 25.5^s$	1° 10′ 29″	11.37	3
SVS4/9		$18^h\ 27^m\ 25.5^s$	1° 10′ 38″	9.81	3
CK4	GEL12	$18^h\ 27^m\ 25.9^s$	1° 13′ 17″	9.3	1,2
SVS4/11		$18^h\ 27^m\ 26.0^s$	1° 10′ 42″	12.24	3
CK2		$18^h\ 27^m\ 28.2^s$	1° 13′ 17″	8.86	1
CK6	GEL15	$18^h\ 27^m\ 28.4^s$	1° 11′ 33″	9.95	1,2
CK7		$18^h\ 27^m\ 29.3^s$	1° 11′ 54″	12.74	1,2
SVS1	GEL17	$18^h\ 27^m\ 29.3^s$	1° 13′ 10″	9.62	2
GEL18	GGD29	$18^h\ 27^m\ 31.3^s$	1° 14′ 16″		2

1: Churchwell and Koornneef (1986)
2: Gómez de Castro *et al.* (1988)
3: Eiroa and Casali (1989)